

**Superoxide reactions in seawater:
evaluating the impact of superoxide
on trace metal redox cycles and dust
dissolution in the open ocean**

DISSERTATION

**Zur Erlangung des Doktorgrades
der Mathematisch-Naturwissenschaftlichen Fakultät
der Christian-Albrechts-Universität zu Kiel**

vorgelegt von:

Maija Iris Heller

Kiel, 2009

Referent: Prof. Dr. Douglas W. R. Wallace

Koreferent: Prof. Dr. Arne Körtzinger

Tag der mündlichen Prüfung: March 12, 2010

Zum Druck genehmigt: May 25, 2010

Prof. Dr. rer. nat. Lutz Kipp

Dekan

“Nullius in verba”

This thesis comprises the following manuscripts:

Manuscript 1: *Application of a Superoxide (O_2^-) thermal source (SOTS-1) for the determination and calibration of O_2^- fluxes in seawater*

Published in *Analytica Chimica Acta*, 2010

Contribution: Maija I. Heller developed the analytical methods and planned and performed all the experiments, evaluated the data and wrote the paper. The underlying theory for the mathematical description of the data was developed in cooperation with Peter L. Croot who also assisted with the interpretation of the data and the writing of the paper.

Manuscript 2: *The kinetics of Superoxide reactions with CDOM in Tropical Atlantic surface waters near Cape Verde*

Revised manuscript submitted to *Journal of Geophysical Research - Oceans*

Contribution: Maija I. Heller collected the samples, performed the experiments, evaluated the data and wrote the paper. Peter L. Croot performed the modeling work on the quinone reactions, developed the data analysis tools and contributed to the interpretation of the data and the writing of the paper.

Manuscript 3: *Superoxide decay as a probe for speciation changes during dust dissolution in Tropical Atlantic surface waters near Cape Verde*

Submitted to *Marine Chemistry*

Contribution: Maija I. Heller collected the samples while on *Islandia*, set up and run the incubation experiments, evaluated the data and wrote the paper. Peter L. Croot assisted in the design of the experiments and in the interpretation of the data and helped write the paper.

Manuscript 4: *Superoxide decay kinetics in the Southern Ocean*

Published in *Environmental Science and Technology*, 2009.

Contribution: Maija I. Heller performed the experiments, evaluated the data and wrote the paper. Peter L. Croot designed the experiment and helped in the interpretation of the results and contributed to the writing of the paper.

Contents:

Summary

Zusammenfassung

Chapter I: Introduction

What is superoxide?

Why is superoxide important?

Sources of Superoxide in the Open Ocean

Sink terms for Superoxide in the Open Ocean

Relevance of superoxide to trace metal biogeochemistry

Previous studies on dust dissolution regarding the potential effect of superoxide on this process

Study regions

Materials and Methods

Analytical Measurements

Participation in Scientific Expeditions during this work

Thesis Outline

Glossary

References

Chapter II: Application of a Superoxide (O_2^-) thermal source

(SOTS-1) for the determination and calibration of O_2^- fluxes in seawater

Chapter III: The kinetics of Superoxide reactions with CDOM in

Tropical Atlantic surface waters near Cape Verde (TENATSO)

Chapter IV: Superoxide decay as a probe for speciation changes during

dust dissolution in Tropical Atlantic surface waters near Cape Verde

Chapter V: Superoxide Decay Kinetics in the Southern Ocean

ES&T Environmental News: Redox effects of superoxide in polar waters

Chapter VI: Conclusions and future outlook

Acknowledgements

Summary

The major external source of iron (Fe), which is an essential nutrient for all aquatic organisms, to the Ocean is through aeolian deposition of dust. The Superoxide radical (O_2^-) is a key species affecting metal redox speciation and has been shown to cycle Fe between the thermodynamically favoured, but poorly soluble, Fe(III) species and the more bioavailable reduced Fe(II) form.

The primary hypothesis that this thesis examines is whether there is significant dissolution of recently deposited aeolian dust by O_2^- in the surface waters around Cape Verde in the Atlantic Ocean. A secondary goal was to fully identify and determine the significance of all reactions involving O_2^- in the open ocean. Due to problems with the methods in the existing published literature I was compelled to develop and evaluate new techniques and methods which could be successfully used for the field expeditions in this work. This includes a new theoretical basis for the interpretation of the data as in many cases the existing theory was too simplistic giving rise to serious artifacts.

The first manuscript describes the optimized methodology I developed for the calibration and determination of O_2^- fluxes in seawater which avoids most of all the discrepancies found in previous works. This was achieved through the application of an O_2^- thermal source for use as calibration source for both concentration and flux measurements.

O_2^- reactions with dissolved organic matter is the subject of my 2nd manuscript as little is known about these reactions which may be important for the cycling and oxidation of organic matter. This work found in waters close to Cape Verde a relative small but significant contribution from organic material to the O_2^- decay.

The 3rd manuscript examines the question of which processes control dust dissolution in seawater. My results indicate that while ligand promoted and thermal dissolution appeared to be clearly important, the experiments in natural waters were highly variable and most of this variability was apparently related to dynamic factors attributed to changes in surface seawater chemistry occurring over both spatial and temporal scales. Key amongst these factors was most likely the abundance of colloidal metal species and ligands.

The last manuscript describes work on superoxide decay kinetics in the Southern Ocean where measurements of O_2^- decay kinetics throughout the water column were performed. In this work Cu was found to be the major sink of O_2^- in the Southern Ocean despite being strongly organically complexed. This indicates that the Cu organic complexes react directly with O_2^- . Contrastingly the reaction with Fe was relatively slow throughout the water column suggesting that organic complexes of iron do not react significantly with O_2^- .

Zusammenfassung

Es ist bekannt, dass der Eintrag von Staub in das Oberflächenwasser der Ozeane eine der wichtigsten externen Quellen für Eisen ist, dass für alle im Wasser vorkommenden Organismen essentiell ist. Gerade in Regionen mit hohem regelmäßigem Staubeintrag (z.B. subtropischer Atlantik) spielen daher die mit dem eingetragenen Material zusammenhängenden Stoffflüsse eine zentrale Rolle. Das Superoxid Radikal (O_2^-) gilt als Mediator zwischen verschiedenen Redox Stufen wichtiger Spurenmetalle (z.B. Fe, Cu). In dem Fall von Eisen vermittelt O_2^- zwischen dem thermodynamisch begünstigten, allerdings schlecht löslichen Fe(III) Spezies und der besser bioverfügbaren Form Fe(II).

Grundlegend für die vorliegende Dissertation war daher die Frage, ob O_2^- signifikant die Auflösung von Saharastaub beeinflussen kann, welcher durch Wind in das Oberflächenwasser um die Kapverdischen Inseln eingetragen wird. Ein weiteres Ziel dieser Arbeit war die Identifizierung sowie Quantifizierung aller Reaktionen in die das Superoxid Radikal im offenen Ozean involviert ist. Bisher publizierte Methoden zur Messung von O_2^- fanden in dieser Arbeit aufgrund von Inkonsistenzen der Detektionsmethoden und Auswertungen keine Anwendung. Nach eingehender praktischer sowie theoretischer Analyse der bereits existierenden Analysen stellte sich heraus, dass es nötig war, eine neue Methode zur Bestimmung von O_2^- im Seewasser zu entwickeln. Diese Methode wurde zuerst in Laborversuchen etabliert und evaluiert und im weiteren Verlauf dieser Arbeit auch erfolgreich bei den Feldexpeditionen im offenen Ozean (Kapverdischen Inseln, Südpolarmeer) genutzt. Die Etablierung dieser Methode beinhaltet darüber hinaus eine neue theoretische Basis für die Interpretation der Daten, in welcher –im Gegensatz zu früher publizierten Datenanalysen– den verschiedenen komplexen Reaktionsmechanismen des Superoxides Rechnung getragen wird.

Das erste Manuskript dieser Arbeit beschreibt die optimierte Methodik, welche für die Kalibrierung und Ermittlung von Superoxid-Stoffflüssen in Seewasser entwickelt wurde. Dieses wurde durch den Einsatz einer thermischen O_2^- -Quelle erreicht, die einerseits zur Kalibrierung des Systems und andererseits sowohl für die Bestimmung der Konzentration als auch für die Stofffluss-Messungen verwendet werden kann.

Reaktionen von O_2^- mit gelöstem organischem Material im offenen Ozean sind das Thema des zweiten Manuskripts. Bisher ist wenig über diese Reaktionen bekannt, die möglicherweise eine zentrale Rolle im Kreislauf und bei der Oxidation von organischem Material spielen. In dieser Arbeit wurde im subtropischen Atlantik nahe der Kapverdischen Inseln ein kleiner aber signifikanter Beitrag von organischem Material für die Reaktionen von O_2^- gefunden.

Das dritte Manuskript untersucht in einem experimentellen Ansatz welche Prozesse die Auflösung von Staub in Seewasser kontrollieren. Die Ergebnisse deuten darauf hin, dass die Auflösung von Staub durch das Vorhandensein von Liganden und durch thermische Reaktionen gefördert wird. Die Experimente in natürliche vorkommenden Wasser zeigen allerdings variable Ergebnisse und der größte Teil dieser Variabilität ist offenbar mit dynamischen Faktoren verbunden die mit Änderungen der chemischen Zusammensetzung des Oberflächenwassers zusammenhängen welche sowohl auf einer räumlichen als auch zeitlichen Skala ablaufen. Der bestimmende Faktor ist hierbei höchst wahrscheinlich das Vorhandensein von kolloidalen Spezies und Liganden.

Das vierte Manuskript beschreibt die Arbeit über die Zerfallskinetik von O_2^- im Südpolarmeer wobei hierfür Messungen in der gesamten Wassersäule durchgeführt wurden. Hierbei wurde eine neue Versuchsstrategie angewandt um die Reaktionswege von O_2^- in polaren Gewässern zu klären. Diese Arbeit zeigt, dass Kupfer die Hauptsenke von O_2^- im Südpolarmeer darstellt, obwohl dieses stark durch organische Liganden komplexiert ist. Die Ergebnisse deuten darauf hin, dass organische Cu-Komplexe direkt mit O_2^- reagieren. Die Reaktion mit Eisen hingegen war in allen untersuchten Tiefen relativ gering, was darauf hinweist, dass organische Fe-Komplexe nicht signifikant mit O_2^- reagieren.

Introduction

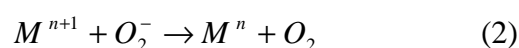
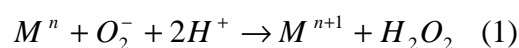
What is superoxide?

Superoxide (O_2^- , IUPAC name: dioxide ($\bullet O_2^-$)) was named in 1934 by Neuman after his investigation of the paramagnetic properties of KO_2 [Neuman, 1934]. The conjugate acid of superoxide, hydroperoxyl (HO_2 , IUPAC name: hydroperoxy(\bullet)) is in pH-dependent equilibrium with O_2^- ($pK_a = 4.8$) [Bielski *et al.*, 1985; Christensen and Sehested, 1988] and both species are known as especially strong oxidants and as initiators of radical reactions but for many years were considered to be little more than an interesting chemical curiosity [Sawyer and Valentine, 1981]. In 1969 it was observed that an enzymatic reaction involving O_2 produced superoxide and that metalloproteins catalysed the disproportion of superoxide, these proteins were thus given the name “superoxide dismutase” or SOD for short [McCord and Fridovic, 1969]. The possibility that superoxide might be an important intermediate in aerobic life provided a new impetus to studies of superoxide reactivity and its role in shaping biology and the environment.

Why is superoxide important?

Superoxide can be produced via a number of enzymatic processes [Marshall *et al.*, 2005b] and in particular through photosynthesis via the Mehler reaction [Mehler, 1951]. In phytoplankton cells, O_2^- concentrations are regulated through the action of SODs [Asada *et al.*, 1977; Marta *et al.*, 1989], to eliminate detrimental reactions including lipid peroxidation [Kellogg and Fridovich, 1975] and the inhibition of nitrogen fixation in the marine cyanobacterium *Trichodesmium* [Cunningham and Capone, 1992]. Superoxide has also been implicated in fish kills due to enhanced production by toxic phytoplankton [Oda *et al.*, 1997].

In geochemical processes, although O_2^- is a transient species it is suspected of involvement in the redox cycling of metal ions in natural waters through its ability to act as both a reductant and oxidant (see reactions 1 and 2 below) [Rose and Waite, 2006; Voelker and Sedlak, 1995; Voelker *et al.*, 2000; Zafiriou *et al.*, 1998].



Thus O_2^- is potentially a key transient species in the biogeochemical cycling of iron (Fe) and copper (Cu) with implications for their speciation and hence bioavailability. However little is currently known about O_2^- chemistry in seawater and research is clearly required in order to improve our understanding of its role in oceanic trace metal biogeochemical processes.

Sources of Superoxide in the Open Ocean

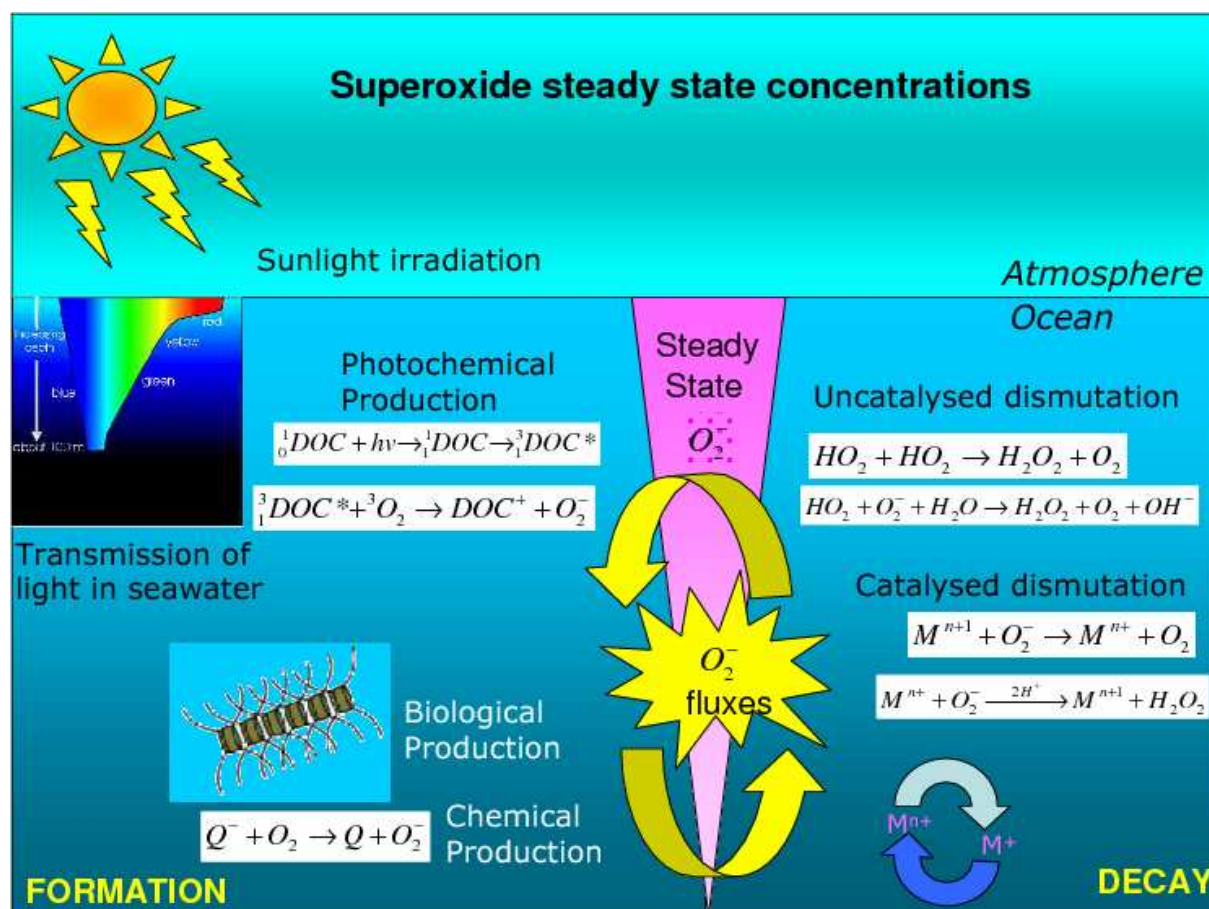
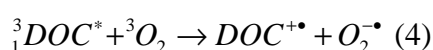


Figure 1: Schematic showing the cycling of superoxide in the open ocean.

Photochemical sources of superoxide

In sunlit surface waters O_2^- is a product of the photo-oxidation of coloured dissolved organic matter (CDOM) [Micinski *et al.*, 1993]. The main mechanism for the production of O_2^- is believed to be via the absorption of a photon by DOC (dissolved organic carbon) leading to an excited triplet state which subsequently reacts with O_2 , which occurs naturally in the triplet state, to form O_2^- and a carbocation of DOC [O'Sullivan *et al.*, 2005] (Reactions 3 and 4 below). The apparent quantum yield of this process is low as the photon energy absorbed by CDOM is mostly dissipated by heat loss (95-98%) or by fluorescence (1%) and only a small percentage reaches the triplet state through intersystem crossing (1-4%). Triplet CDOM can also form other reactive oxygen species (ROS) such as singlet oxygen and the hydroxyl radical [Blough and Zepp, 1995].



Estimates of the apparent quantum yield (AQY) exist for the combination of reactions 3 and 4 based on the absorbance of CDOM and H₂O₂ formation rates [O'Sullivan *et al.*, 2005; Yocis *et al.*, 2000]. Wavelength specific AQY based on H₂O₂ production show highest values (1 x 10⁻³) in the UV-B range (280-320 nm) and decrease logarithmically with increasing wavelength through the UV-A region (320-400 nm), while in the visible region of the spectrum (400-700 nm) the AQY is essentially zero. Most estimates of the photochemical production of O₂⁻ in seawater have been based on measurements of H₂O₂ *in situ* formation fluxes [Obernosterer *et al.*, 2001; Yocis *et al.*, 2000; Yuan and Shiller, 2001] and indicate rates in surface waters of 9 (Antarctic) to 17 nM h⁻¹ (Tropical Atlantic), assuming the rate of O₂⁻ production is twice that of H₂O₂. In sunlit seawater O₂⁻ quasi-steady concentrations of ~10-100 nM were initially estimated based on the assumption that only the uncatalysed dismutation pathway was occurring [Millero, 1987; Petasne and Zika, 1987]. Later research included other important reactions with O₂⁻, such as with Fe and Cu [Voelker and Sedlak, 1995; Voelker *et al.*, 2000; Zafiriou *et al.*, 1998] or organic matter [Goldstone and Voelker, 2000] and suggest that under a midday tropical sun, steady state concentrations of O₂⁻ in seawater are in the pM range.

Nature of sunlight in seawater

The majority of the photons from the sun which enter the sea are absorbed, while a small fraction may be scattered back in the upwards direction (albedo effect) [Kirk, 1994]. The solar spectrum at the surface of the ocean is made up predominantly of visible (400-700 nm) and infrared (700 – 2000 nm) radiation as ultraviolet (UV) light is attenuated in the atmosphere by the presence of trace gases and in particular O₃ which prevents light of below 280 nm wavelength from reaching the surface. Infrared light is rapidly absorbed by water itself and is responsible for the solar heating of the surface ocean (Figure 2). While UV light is the most energetic part of the sunlight spectrum and is capable of breaking many types of chemical bonds, it is however strongly absorbed by CDOM in seawater leading to its rapid attenuation in the upper water column (Figure 2). Visible wavelengths (400 – 700 nm) are attenuated the least in the ocean resulting in the typical blue colour of open ocean waters. The presence of small particles such as phytoplankton leads to increased scattering of the light which affects shorter wavelengths more than longer ones resulting in the 'greener' waters of the coastal ocean and in particle laden estuarine systems a 'yellow-green' colour. Thus the photochemical production of O₂⁻ is limited to the near surface waters where UV light penetrates.

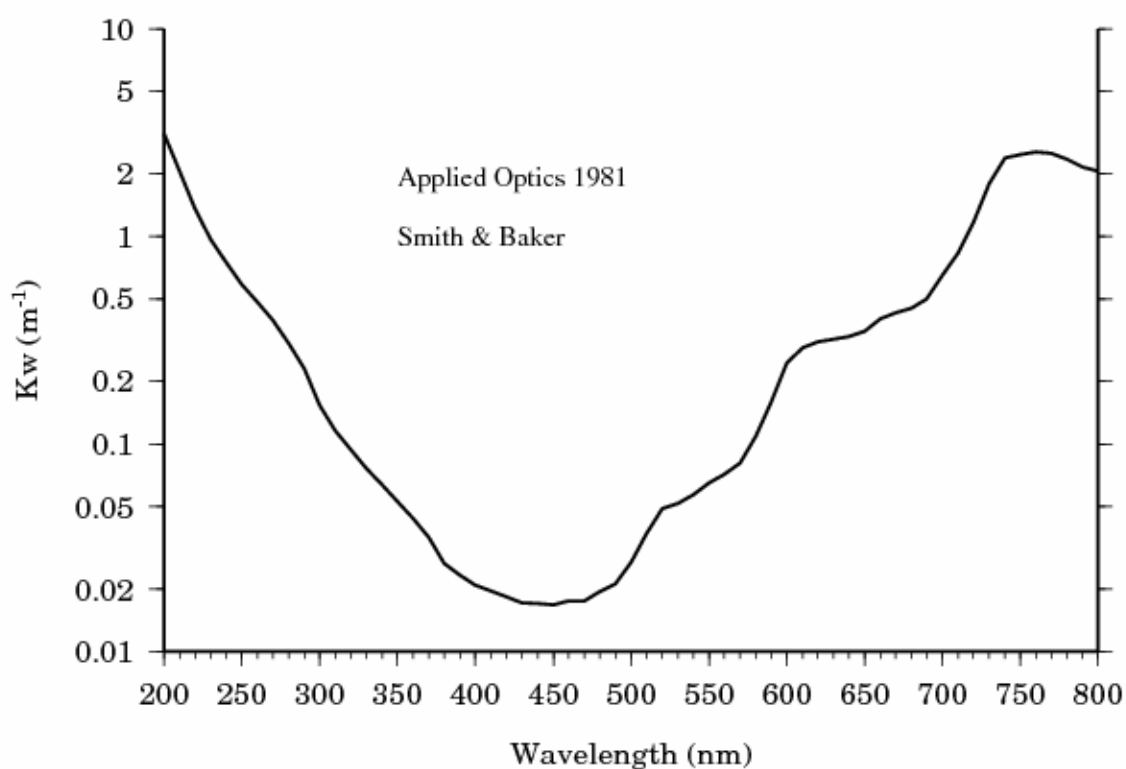


Figure 2: Diffuse attenuation coefficient for light in optically clear seawater as a function of wavelength (data from Smith and Baker [1981]).

Biological sources of superoxide

Superoxide is also produced by metabolic processes in bacteria and phytoplankton [Kim *et al.*, 2000; Marshall *et al.*, 2002] and is suspected to also occur in photosynthetic organisms through the Mehler reaction [Mehler, 1951]. As O_2^- is an intermediate oxygen species in the pathway from O_2 to H_2O it can be produced by both photosynthetic and respiratory processes (Figure 3).

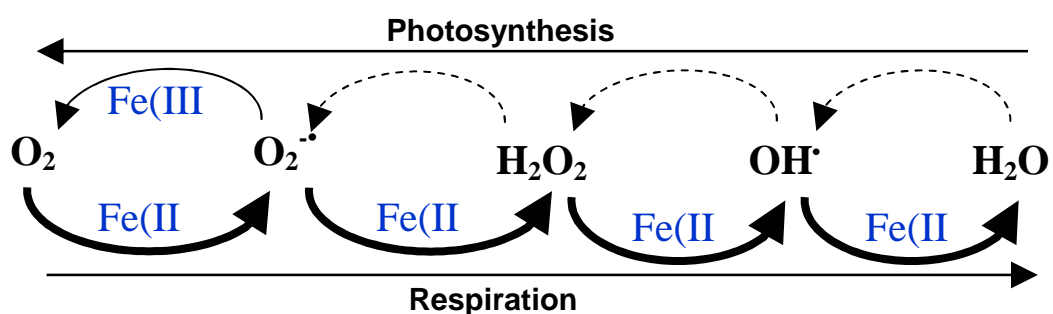


Figure 3: Reaction pathway of oxygen to water (Respiration) and the reverse reaction (Photosynthesis) and the resulting reaction intermediates.

In laboratory experiments O_2^- production has been observed in cultures of some toxic marine phytoplankton [Marshall *et al.*, 2002; Oda *et al.*, 1997], diatoms [Kustka *et al.*, 2005] or in cyanobacteria [Rose *et al.*, 2005]. Superoxide production rates have been estimated at $8.4 \times 10^{-16} \text{ mol cell}^{-1} \text{ h}^{-1}$ for the diatom *T. weissflogii* [Kustka *et al.*, 2005] with higher rates for 4 toxic species $0.45\text{-}4 \times 10^{-12} \text{ mol cell}^{-1} \text{ h}^{-1}$ [Oda *et al.*, 1997]. Superoxide production by phytoplankton has been suggested to occur in order to enhance the toxicity of algal exudates or serve as an allelopathic agent against bacterial fouling [Marshall *et al.*, 2005a]. An alternative hypothesis suggested for open ocean species is that O_2^- is produced in response to iron limitation as a mechanism to reduce Fe(III) to the more bioavailable Fe(II) [Rose *et al.*, 2005] though other researchers suggest that this is a ‘futile’ exercise as the Fe(II) is rapidly oxidized back to Fe(III) [Kustka *et al.*, 2005].

Sink terms for Superoxide in the Open Ocean

Measurements of superoxide decay in the ocean are rare as earlier studies were hampered due to technical limitations related to O_2^- sources and detection systems [Zafiriou, 1990]. Recent studies in the Tropical Pacific found values for the pseudo first order decay of O_2^- of $9.7 \times 10^{-3} \text{ s}^{-1} > k > 1 \times 10^{-4} \text{ s}^{-1}$ [Rose *et al.*, 2008], though these values are most likely underestimates as these authors added the chelating agent DTPA immediately prior to their measurements. Higher rates ($0.02 - 1.4 \text{ s}^{-1}$) have been found in estuarine and coastal waters [Goldstone and Voelker, 2000; Voelker *et al.*, 2000; Zafiriou *et al.*, 1998] where reactions with Cu species was suggested to be the major sink term for superoxide. Workers in this field have developed the following reactivity scheme for O_2^- :

$$\frac{\partial[O_2^-]}{\partial t} = 2k_D[O_2^-]^2 + \sum k_M[M]_X[O_2^-] + k_{org}[O_2^-] \quad (5)$$

where the metal reactions (k_M) include both the Cu(II)/Cu(I) and Fe(III)/Fe(II) redox pairs, the reaction with organic substances is described by the first order rate k_{org} . k_D is the second order dismutation rate (unit: $M^{-1}s^{-1}$) which has been described by Zafiriou [1990].

$$\sum k_M[M]_X = (k_{Cu(I)}[Cu(I)] + k_{Cu(II)}[Cu(II)] + k_{Fe(II)}[Fe(II)] + k_{Fe(III)}[Fe(III)]) \quad (6)$$

The observed rate of superoxide decay can then be written as follows with only a single term each for the first order and second order rate components

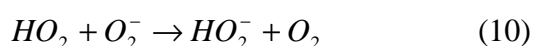
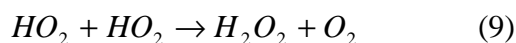
$$\frac{\partial[O_2^-]}{\partial t} = 2k_D[O_2^-]^2 + k_{obs}[O_2^-] \quad (7)$$

where k_{obs} is described as the sum of the first order reaction rates.

$$k_{obs} = \sum k_M [M]_X + k_{org} \quad (8)$$

Uncatalysed dismutation reaction of superoxide

The second order uncatalysed dismutation reaction of superoxide was initially postulated to be the main source of hydrogen peroxide in the ocean ([*Moffett and Zafiriou, 1990; Petasne and Zika, 1987*] via reactions 9 and 10 shown below:



The kinetics of the uncatalysed dismutation reaction in seawater was investigated by Zafiriou [1990] who found that sea salts had only a minor influence on this reaction when compared to pure water. This reaction is strongly pH dependent in the pH range 5-11 with an increasing decay rate with decreasing pH. Measurements in the seawater pH range can be described by the following equation: $k_D = 5 \pm 1 \times 10^{12} [H^+]$ [*Zafiriou, 1990*].

Reaction of superoxide with organic molecules

CDOM is the main absorbing substance in the ocean and plays an important role in light availability for primary production [*Del Vecchio and Blough, 2002*] and for photochemical reactions where it is critical to the production of free radical species [*Dister and Zafiriou, 1993*]. CDOM is comprised of a number of potential chromophores but overall forms a small part of the Dissolved Organic Carbon (DOC) pool in the ocean [*Nelson et al., 2007*]. In seawater CDOM is believed to be produced by heterotrophic processes in the upper water column [*Steinberg et al., 2004*] and is destroyed by solar bleaching. The distribution of CDOM is also dependent on terrestrial inputs and from the decomposition of organic matter where humic and fulvic acids contribute greatly [*Del Vecchio and Blough, 2004*]. As CDOM is also found in deep waters it has been suggested to be actively transported globally through large-scale processes including upwelling [*Nelson et al., 2004*]. The redox active fraction of CDOM, which can easily exchange electrons, has been attributed to quinone moieties which can shuttle between different redox states [*Scott et al., 1998*]. Quinones react rapidly with superoxide [*Bielski et al., 1985*] and have been suggested to be the potential reactants in seawater [*Goldstone and Voelker, 2000*].

Reactivity of superoxide with trace metals in the open ocean

Inorganic complexes of Cu(II)/Cu(I) and Fe(II)/Fe(III) can react rapidly with superoxide leading to a catalytic cycle for O_2^- decay [Voelker *et al.*, 2000]. Reactions of metals with O_2^- are critical because of their potential to keep metals in thermodynamically unfavoured oxidation states under ambient seawater conditions. In seawater reactions with O_2^- are suggested to be the source of Cu(I) and Fe(II) in sun lit open ocean surface waters [Miller *et al.*, 1995; Millero *et al.*, 1987; Voelker and Sedlak, 1995]. More recently reactions with O_2^- were invoked as a contributing cause for the persistence of Fe(II) during Southern Ocean iron enrichment experiments [Croot *et al.*, 2008; Croot *et al.*, 2001; Croot *et al.*, 2005].

Relevance of superoxide to trace metal biogeochemistry

Marine Biogeochemistry of Iron

Iron is an essential nutrient for all aquatic organisms and has been subject of extensive investigations over the last few decades due to its role in limiting primary productivity in the High Nutrient Low Chlorophyll (HNLC) regions of the ocean [Behrenfeld and Kolber, 1999; Hutchins *et al.*, 1998; Martin and Fitzwater, 1988; Martin *et al.*, 1991; Martin *et al.*, 1994]. Studies on iron limitation have increased our understanding of the speciation of the Fe(III) and Fe(II) redox states in seawater, the mechanisms of transformation between these two species and their bioavailability. Fe(III) is the thermodynamically favored form of iron under seawater conditions but undergoes rapid precipitation or particle scavenging in the formation of various Fe(III) oxyhydroxide phases with differing chemical reactivities [Kuma *et al.*, 1996]. It is for this reason that the growth of phytoplankton is limited due to the low concentrations of dissolved iron and the slow kinetics of exchange of iron from particles. Dissolved Fe(III) has been shown to be complexed by strong ligands, produced by bacteria or phytoplankton, which help to increase the solubility of iron in seawater [Rue and Bruland, 1995].

The reduced form of iron, Fe(II), is highly soluble in seawater but is rapid oxidized to Fe(III) through oxidation via H_2O_2 or O_2 [González-Dávila *et al.*, 2006]. The reduction of Fe(III) to Fe(II) by photochemical [Kuma *et al.*, 1992] or other processes, including direct reduction by O_2^- , are possible mechanisms by which particulate or complexed iron can be made more bioavailable. In the warm surface waters of tropical regions, Fe(II) is expected to be a short lived intermediate in the iron cycling due to the fast kinetics of oxidation with H_2O_2 and O_2 . Laboratory studies however have indicated that reactions with O_2^- may help to

maintain a significant steady state Fe(II) concentration in surface waters [Voelker and Sedlak, 1995].

The supply of iron to the productive surface waters of the open ocean is predominantly through two main pathways: (I) Aeolian deposition [Jickells *et al.*, 2005] and (II) upwelling of deep waters [de Baar *et al.*, 1995] including mixing of iron rich water from the benthos [Blain *et al.*, 2007; Pollard *et al.*, 2009]. Iron has a relatively short residence time in the surface ocean due to combination of low solubility and high biological demand [Croot *et al.*, 2004; Jickells, 1999].

Marine Biogeochemistry of Copper

Copper is also an essential micronutrient in the ocean but it is also toxic for most marine organisms [Brand *et al.*, 1986]. The dominant phytoplankton species in oligotrophic tropical waters, *Synechococcus* [Waterbury *et al.*, 1979; Waterbury *et al.*, 1986] and *Prochlorococcus* [Olson *et al.*, 1990] have been found to be extremely sensitive to free Cu(II) concentrations above 1-10 pmol L⁻¹ [Brand *et al.*, 1986; Mann *et al.*, 2002]. In seawater dissolved copper is strongly complexed by organic ligands resulting in low free Cu concentrations [Moffett, 1995]. These copper complexing ligands are believed to be of biological origin as they are produced either passively or actively by organisms in response to Cu stress [Croot *et al.*, 2000; Moffett and Brand, 1996].

In oxygenated seawater the thermodynamically favored redox state of Cu is Cu(II), significant concentrations (pM) of Cu(I) may be present in surface waters [Moffett and Zika, 1988]. In general Cu(I) oxidation in the open ocean is believed to be controlled through oxidation by O₂ as the reaction with H₂O₂ is significantly slower under typical open ocean conditions [Moffett and Zika, 1988].

Copper can be supplied to the surface waters of the open ocean by a variety of natural pathways: (1) Atmospheric deposition. (2) Advection of suspended material from coastal regions. (3) Upwelling and mixing from deep water. Residence time estimates for copper in the ocean range from 2-50 years for surface waters and 1500-5000 years for deep waters [Boyle and Edmond, 1975].

Aeolian supply of trace metals to the ocean

The main external input of trace elements to the ocean is through aeolian dust transport from the great deserts of the world [Jickells *et al.*, 2005] in concert with the global wind regime (Figure 4). Importantly the average particle size decreases with distance from the

desert source of the aeolian minerals although some large particles ($>20 \mu\text{m}$) can be transported over long distances [Mahowald *et al.*, 2005]. Studies of Saharan dust have shown that the particle diameter decreased from $\sim 7\text{-}28 \mu\text{m}$ at the coast of West Africa [Stuut *et al.*, 2005] to $1\text{-}3 \mu\text{m}$ in Caribbean waters [Talbot *et al.*, 1986].

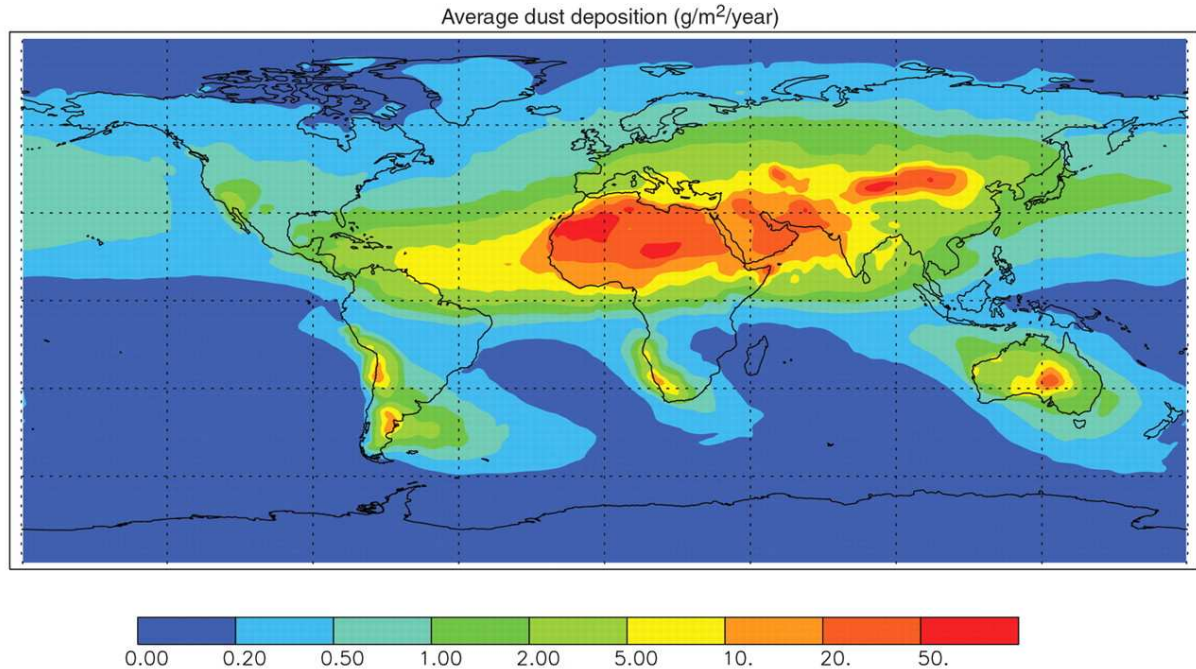


Figure 4: Dust fluxes to the world oceans based on a composite of three published modeling studies [Jickells *et al.*, 2005].

The total aeolian flux of desert dust to the surface waters of the oceans is relatively well constrained but the fraction which subsequently dissolves for metals like iron or copper and which is then available for the growth of phytoplankton is not well known at present. Global models assume that only 1-2% of the aerosols which are transported to the ocean are converted into dissolved iron in seawater. However field measurements show a much wider range of values depending on the dust loading and source [Baker and Jickells, 2006; Baker and Croot, 2008].

Observations of temporal changes in the concentration of dissolved iron show that the input through dust must be significantly higher than the model results [Sedwick *et al.*, 2007]. In the Southern Hemisphere the dust deposition is significantly lower than in the Northern hemisphere due to the lack of land masses to act as source regions. In the tropical Atlantic which receives high dust fluxes, iron is found in relatively high concentrations in the surface waters, and the particle fluxes to the deep waters are also dominated by dust inputs [Croot *et al.*, 2004; Kremling and Streu, 1993].

Photoreduction of particulate iron

The conversion of different iron phases to labile and bioavailable iron through photoreductive mechanisms has been proposed from a combination of field and laboratory studies [Johnson *et al.*, 1994; Waite and Morel, 1984; Wells and Mayer, 1991]. Most notably the photoreductive dissolution of poorly soluble iron(III) minerals such as goethite or hematite has been observed [Borer *et al.*, 2009b; Siffert and Sulzberger, 1991]. These experiments found a light induced reduction of surface Fe(III) at the hydr(oxide) surface and a consequent oxidation of surface coordinated water or hydroxyl groups which lead to the production of Fe(II) and OH radicals, finally yielding H₂O₂ [Cunningham *et al.*, 1988; Waite and Morel, 1984]. Further studies have shown that strong iron binding ligands, including siderophores such as desferrioxamine B, enhanced the photoreductive dissolution [Borer *et al.*, 2009a; Borer *et al.*, 2009b]. It is generally accepted that organic ligands which may contain humic or fulvic substances or hydroxycarboxylic and carboxylic acids efficiently promote the photoreductive dissolution of Fe(III) phases [Kuma *et al.*, 1995; Voelker *et al.*, 1997].

Using published and experimental data for iron oxy(hydr)oxides, Sherman [2005] showed it is possible to predict the electrochemical bands in aqueous solution as a function of pH. Under seawater pH (8.3) the direct photoreduction of colloidal iron results in nanomolar concentrations of dissolved and free Fe(II). This study states that organic ligands may promote the photochemical dissolution simply because they prevent the recombination at the oxide surface caused by an electron hole. These electron holes appear through excitement caused for example by sunlight and the resultant skip of electrons from the valence into the conduction band. To understand thermodynamic driving forces for photochemical reductive dissolution processes it is important to know the electrochemical potentials of the valence and conduction bands relative to the standard electrochemical potentials of the for example Fe(II)/FeOOH redox couple. However complexation of dissolved Fe(II) by strong ligands like siderophores is required to allow the further dissolution of colloidal iron. Currently however, it is unclear how ROS species such as O₂⁻ and H₂O₂ may affect this process.

The role of Organic Complexes in solubilizing Iron in Seawater

It is well known that siderophores play an important role in the acquisition of iron by bacteria [Neilands, 1981]. Siderophores are low-molecular-weight organic ligands with a high affinity for iron [Neilands, 1995]. The iron binding groups are mostly hydroxamate or catecholate but also α -hydroxycarboxylate and carboxylate groups [Sayed and Chincholkar,

2006]. Hydroxamate functional groups form solution complexes with Fe(III) by a loss of a proton from the hydroxylamine (-NOH) group whereas catecholate groups bind via the phenolic oxygen after the loss of two protons. Both forms end up in five membered rings [Crumbliss, 1990] and most of the siderophores are hexadentate ligands and form 1:1 complexes with iron [Kraemer, 2004]. The concentration of siderophores in most natural systems is low and it has been calculated that the production by marine cyanobacteria is a costly strategy in terms of cellular nutrient and energy budgets [Volker and Wolf-Gladrow, 1999]. The most well studied siderophore is Desferrioxamine B (DFO) because of its commercial availability. The widespread use of DFO makes it to a useful reference but it is difficult to estimate how well DFO represents the full spectrum of the approximately 500 known siderophore structures [Kraemer, 2004]. It has been shown that siderophores have a strong kinetic effect on the dissolution of iron containing minerals [Carrasco *et al.*, 2007; Kraemer *et al.*, 2005]. The iron oxide dissolution initiated by siderophores is a surface controlled mechanism via a proton- or ligand- promoted mechanism [Kraemer *et al.*, 2005]. The absorption of the siderophore on the mineral surface is the first necessary step but also lowers the concentration of siderophores in the solution what may therefore decrease the effect on iron solubility. Borer *et al.* [2007; 2009a] showed that more iron was dissolved when a combination of siderophore and oxalate was used. The addition of surface-active agents (surfactants), which may be produced by bacteria, has also been shown to enhance dissolution of iron oxides [Carrasco *et al.*, 2007].

Photoreduction of Iron Organic Complexes in Seawater

High Fe(II) concentrations in oxic seawater observed during phytoplankton blooms have been suggested to arise from the photoreduction of Fe(III) organic compounds [Kuma *et al.*, 1992; Öztürk *et al.*, 2004]. Several laboratory studies have tested various dissolved organic substances like gluconic or citric acid or humate and fulvic compounds which are known to be released from phytoplankton or present in seawater [Kuma *et al.*, 1992; Voelker and Sulzberger, 1996; Voelker *et al.*, 1997]. Photoreduction of Fe(III)-fulvic acid and citrate are strongly influenced by pH, and although Fe(III)-humate and Fe(III)-oxalate are easily photoreduced in acidic waters this process is not expected to occur at the normal pH of seawater. It has been found that Fe(III) is rapidly photoreduced by sunlight in the presence of hydroxycarboxylic acids like glyceric, gluconic, glucuronic, glucaric and tartaric acids which are oxidation products of sugars [Kuma *et al.*, 1995]. The oxidation of glucose for example forms gluconic and glucuronic acid and these substances have been found in high

concentrations in surface waters during a spring bloom in Funka Bay (Japan) with a coincident elevated Fe(II) concentration [Kuma *et al.*, 1992].

Processes involved in the dissolution of Saharan dust in seawater

Figure 5 below summarizes the major pathways and iron species identified in the solubilization of Saharan dust to dissolved iron in seawater as described above. Superoxide is suspected to play a role in converting both particulate and soluble Fe(III) to the more bioavailable Fe(II).

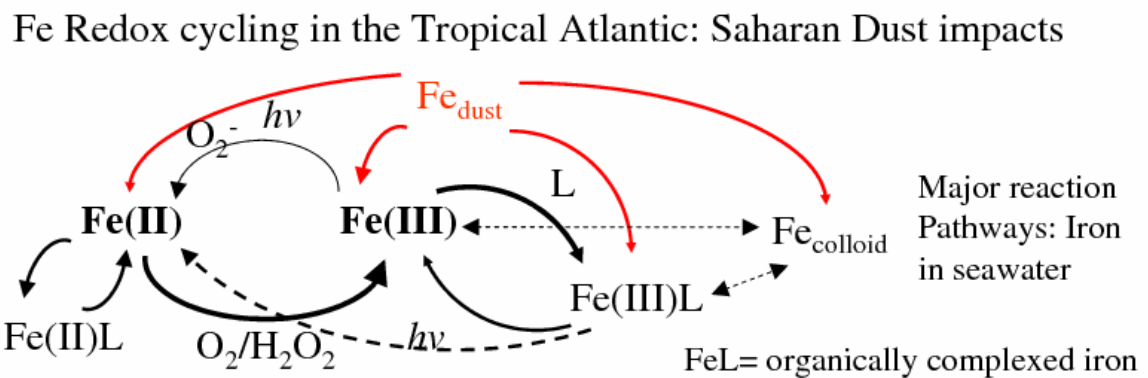


Figure 5: Main reaction pathways for superoxide with dust, iron (Fe) and ligands (L) considered in this work

Previous studies on dust dissolution regarding the potential effect of superoxide on this process

Laboratory studies

Recently Fujii *et al.* [2006] conducted a study on the kinetics of the O₂⁻ mediated dissolution of amorphous ferric oxyhydroxides (AFO) in seawater. They followed the rate of formation of Fe(II) by complexing it with the strong Fe(II) complexing agent Ferrozine [Stookey, 1970]. Fujii *et al.* gave particular attention to the effect of aging and concentration of the AFO on the rate of the O₂⁻ mediated dissolution process. They observed that the ferrous production rates decreased with aging which they suggested occurred because of changes in the chemical and physical properties of the AFO which affected the reactivity of inorganic ferric species with O₂⁻. From modeling work they indicated that thermal dissolution of the AFO was an important aspect of this process. They suggested that O₂⁻ plays a role in the

dissolution of newly formed AFO but they could not clearly demonstrate what its significance is in the natural environment.

Kustka et al. [2005] reported in their laboratory studies using cultures of marine diatoms, that in their EDTA-buffered media, which contained about 45 pM of inorganic Fe(III), that over half the Fe(III) reduction was mediated by extracellular O_2^- production. Surprisingly they found no effect by either the addition of an O_2^- sink (Superoxide dismutase, SOD) or source (Xanthine/Xanthine oxidase) on the Fe uptake in these cultures. Interestingly they also found no effect of the enzyme SOD on the uptake of Fe from either ferrihydrite or from a Fe-labeled porphyrin. They concluded from their data that the Fe(II) formed in their experiments by O_2^- proceeded via the reduction of Fe(III) rather than by the reduction and dissociation of FeEDTA complexes. They also noted that the newly formed Fe(II) by O_2^- is rapidly reoxidized to Fe(III) in pH 8 oxygenated seawater and that the majority of the iron was reoxidized before uptake by the diatoms.

Dust dissolution experiments in the Mediterranean

Wagener et al. [2008] showed in a field study conducted over one year in the Mediterranean Sea that natural iron binding ligands affect the dissolution rates of dust particles when they enter the sea surface. This study also claimed that the determination of the concentration of iron binding ligands by voltammetry [*Croot and Johansson, 2000*] was no better than using DOC as a parameter to follow this process. This study also suggested that photochemistry seemed to play a significant role in the bioavailability of the organically complexed Fe as suggested previously [*Barbeau et al., 2001*].

Model studies

A model study by Weber et al. [2005] tried to analyze the redox cycle of Fe between its various physical (dissolved, colloidal, particulate) and chemical (redox state and organic complexation) forms in the top 500 m of the water column. This model implied dust deposition rates, mixed layer depth and solar radiation measurements from the Bermuda Atlantic Time-series Study (BATS) and proposed to give a quantitative assessment how the cycling of iron influences its uptake by phytoplankton. This study proposed that the cycling of iron mostly occurs in the mixed layer due to light dependency on the photoreduction processes and the seasonal variation of primary production. It was concluded that O_2^- is responsible for driving the photochemical cycle and in turn its availability was assumed to be dependent on the concentration and speciation of copper in the water column. This model of

biogeochemistry and speciation of Fe was coupled with the General Ocean Turbulence Model (GOTM) and a NPZD-type (Nutrient-Phytoplankton-Zooplankton-Detritus) ecosystem model to improve the knowledge of the temporal patterns and vertical profiles of dissolved Fe [Weber *et al.*, 2007]. This one-dimensional model of Fe biogeochemistry was later extended for use at the Tropical Eastern North Atlantic Time Series Observatory (TENATSO) with a more complex description of the origin and fate of organic ligands and inclusion of particle aggregation and sinking [Ye *et al.*, 2009]. The profile of dissolved iron was found to strongly be influenced by the abundance of organic ligands. This study also suggested that the high dust deposition at the TENATSO site delivers on the one hand a high input of Fe into surface waters, while on the other hand it provides inorganic particles which might be responsible for Fe scavenging and particle aggregation.

STUDY REGIONS

SOPRAN in Cape Verde and the TENATSO site

The eastern tropical and subtropical Atlantic Ocean is considered to be a key region for observations of global climate and environmental changes. The Cape Verde archipelago (Figure 6) is situated in the middle of this region adjacent to the West African coast and the upwelling region that is located there but also it lies directly below the path of Saharan dust that is transported from Africa to the Atlantic Ocean. This high input of Saharan dust has a crucial impact on marine microorganisms, CO₂ fixation and the production of climate and radiatively relevant trace gases. Atmospheric dust has long been identified as a source of nutrients to the ocean (Figure 4) and is likely the dominant source of iron to this region [Jickells *et al.*, 2005]. Additionally the spectral energy of the solar radiation is also influenced by dust and aerosols which can have an impact on light dependent processes in the euphotic zone with resulting effects on biological productivity and photochemical reactions.

Primary productivity in the oligotrophic eastern tropical Atlantic is strongly limited by the availability of fixed nitrogen, with the exception of the Mauritanian upwelling zone close to the West African coast [Pradhan *et al.*, 2006]. In the absence of upwelled sources of nitrogen, much of the primary productivity of the oligotrophic North East Atlantic is apparently driven by nitrogen fixing cyanobacteria [Voss *et al.*, 2004], including the well known species *Trichodesmium* [Tyrrell *et al.*, 2003], which utilize the enzyme nitrogenase [Chen *et al.*, 1998]. Indeed recent work has shown that the *nifH* gene, which can be used as marker for nitrogenase using species, is widespread in this region [Langlois *et al.*, 2005]. Nitrogen fixation in this region has been shown via bioassay experiments to be limited by

phosphorous [Sañudo-Wilhelmy *et al.*, 2001], iron [Moore *et al.*, 2009] and both iron and phosphorous [Mills *et al.*, 2004].

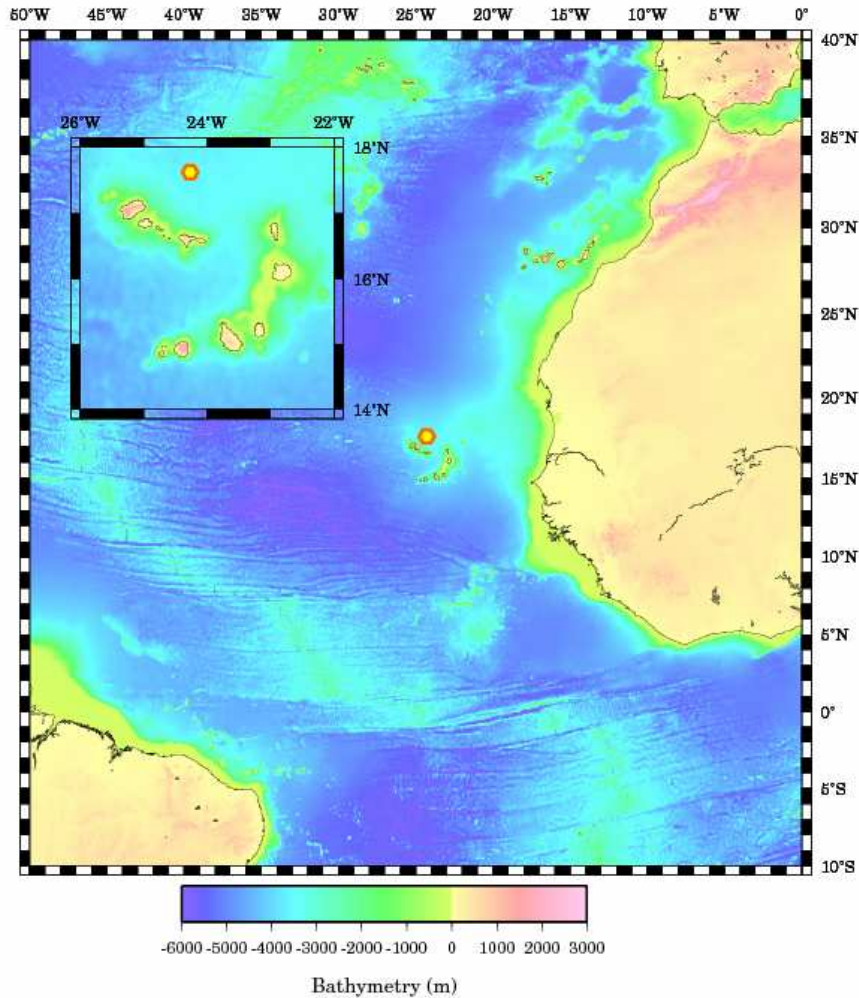


Figure 6: Bathymetric map of the Tropical North Atlantic showing the location of the Cape Verde archipelago and the TENATSO site (orange/yellow hexagon). (insert) The Cape Verde archipelago and the location of the TENATSO site (orange/yellow hexagon).

The Cape Verde Islands are particularly interesting as their location is under the main dust transporting pathway but they are close enough to the African continent to identify the dust source regions in the Sahara desert and Sahel. Chiapello [1995] measured dust fluxes at an aerosol monitoring station on Sal, Cape Verde, between December 1991 and December 1994 in order to assess the transport processes of the African dust over the North-Eastern Tropical Atlantic. This study found a distinct seasonal pattern which showed maximum dust input during December and January (Figure 7). The meteorological analysis at this time suggested that the dust transport occurred in the trade winds and at low altitudes. The

capacious amount of dust was carried out of North-Western Africa, in particular from the Sahel.

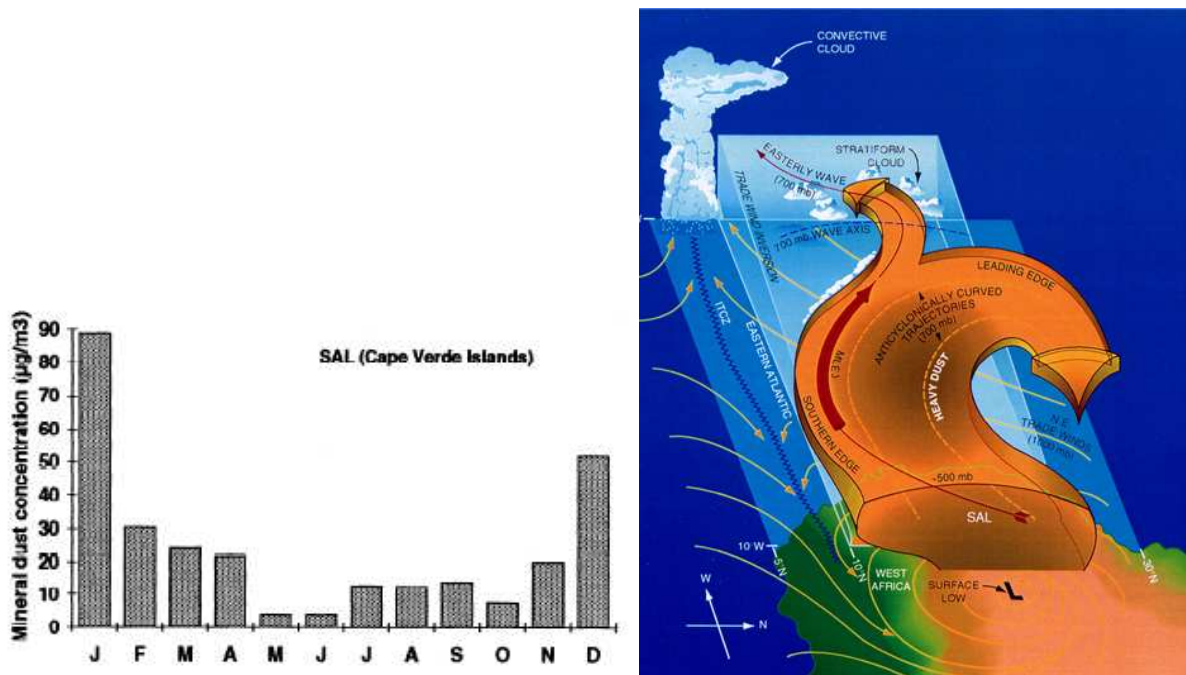


Figure 7: (left) Monthly arithmetic mean of mineral dust concentration at the surface level at Sal, Cape Verde [Chiapello *et al.*, 1995], (right) The formation of the Saharan Air Layer (SAL) over Western Africa [Karyampudi *et al.*, 1999].

A later study examining Saharan aerosols, via their effect on the aerosol optical depth (AOD), across West Africa and the Eastern Atlantic regions [Karyampudi *et al.*, 1999] was able to use back trajectory calculations to show a characteristic anti-cyclonic rotation of the dust plume over the eastern Atlantic as it moved from its source regions in West Africa. Backscattering profiles and optical depth were analysed to investigate the general feature of the dust plume and its geographic variation in optical thickness. This analysis was used to develop aspects of a conceptual Saharan dust plume model (Figure 7) in which a warm dry air mass, known as the Saharan Air Layer (SAL), uplifts dust and transports it over the Eastern Atlantic. The presence of the SAL has been suggested to hinder the formation of hurricanes in this region [Karyampudi and Pierce, 2002].

The Cape Verde islands represent a unique location to observe these processes. Despite the scientific relevance of this region, logistical factors have previously handicapped, or prevented, a sustained high quality research and measurement program. In the last few years a considerable effort has been invested into the establishment of a long term observatory, TENATSO (Tropical Eastern North Atlantic Time Series Observatory), with continuous and comprehensive measurements of important biological, chemical and physical processes in both the atmosphere and the ocean. To answer complex scientific questions

requires long term studies which in turn demand strong local support and the oceanographic work in this thesis and other SOPRAN work has benefitted from cooperation with the Instituto Nacional de Desenvolvimento das Pescas (INDP) in Mindelo on Sao Vicente (Cape Verde).

The Southern Ocean at Drake Passage

During the course of this thesis work the opportunity arose to participate in the IPY-GEOTRACES Polarstern expedition, ANTXXIV-3, along the Zero meridian and across the Weddell Sea and Drake Passage (Figure 8). On this expedition Cu speciation and hydrogen peroxide measurements were performed (Manuscripts in preparation) and superoxide decay rate experiments were made in the Drake Passage (Chapter 5).

The Southern Ocean is an important component of the global climate system, particularly in its role in buffering heat and atmospheric CO₂ and in the formation of Antarctic Bottom water. The Southern Ocean is the largest of the HNLC regions on the globe; the high levels of nitrate (and phosphate) south of the Polar Front that persist have suggested many potential limiting processes for the low biomass maintained [Smetacek *et al.*, 1997], with iron limitation the most likely as was demonstrated during expeditions such as SOIREE [Boyd *et al.*, 2000]. In the Southern Ocean, the complex relationships between iron, light and mixed layer depth create a dynamic environment, which control phytoplankton biomass, upon which the presence of grazers exert a further influence.

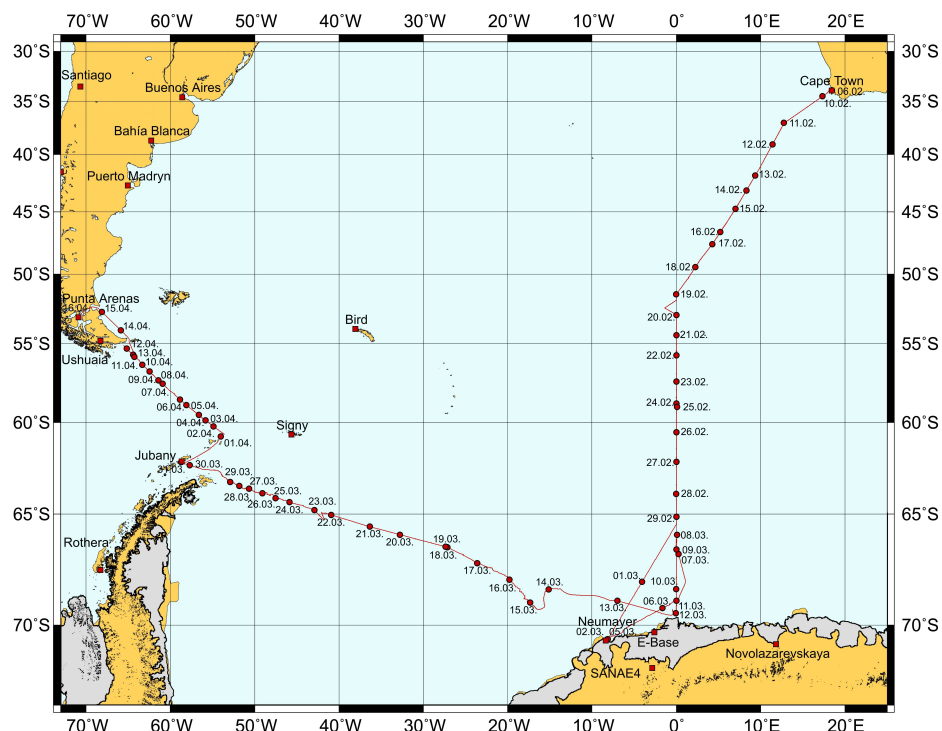


Figure 8: Cruise Track of ANTXXIV-3

As explained previously the Southern Ocean is a region of low dust supply (Figure 4) and is an HNLC region and thus provides a contrast to the main study region of the Tropical Atlantic with which to observe regional effects on O_2^- reactivity in the global ocean.

Materials and Methods

Sampling Platforms at Sea

For the Cape Verde work all sampling was performed using the INDP research vessel *R.V. Islandia* (Figure 9). The *Islandia* was originally a fishing vessel but has over the course of this thesis work been slowly converted into a modern oceanographic research vessel. Southern Ocean work was performed using the German research ice breaker *R.V. Polarstern* (Figure 9) which is administered by the AWI (Alfred Wegener Institut in Bremerhaven).



Figure 9: (left) The *RV Islandia* in the Tropical waters near Sao Vicente, Cape Verde (right) and the *R.V. Polarstern* breaking ice in the Weddell Sea

Trace Metal Clean Sampling at Sea

Sampling for trace metals at sea from any platform is complicated by the risk of contamination, particularly for iron, due to the steel constructions of shipping vessels and the ever presence of rust particles. In order to eliminate contamination during sampling, most notably for the work on the *Islandia*, a number of different sampling systems were employed in this thesis work and a brief description is provided in the following section.

MITESS – Moored In-situ Trace Element Serial Sampler

Due to the difficulties of obtaining trace metal clean samples from such a small research vessel as the *Islandia* for this work two Automated Trace Element (ATE) samplers

were purchased from Dr Ed Boyle at Massachusetts Institute of Technology (MIT). The ATE is a single-sample module of MITESS [Bell *et al.*, 2002] that was developed to allow personnel at the Bermuda Atlantic Time Series (BATS) and Hawaii Ocean Time Series (HOTS) to collect uncontaminated mixed-layer trace metal samples. The ATE (Figure 10) is constructed from Teflon and contains a stepper motor that can be programmed, via an IR wand, to open and close the sampler at different times. A 500 mL high density polyethylene (HDPE) (Nalgene) wide mouth sampling bottle is contained within the ATE and this is filled with seawater once the sampler is opened underwater. The ATE was deployed from the *Islandia's* J-frame using a Kevlar line, weighted down by 40 kg of plastic encased lead weights, to the required sampling depth prior to the pre-programmed opening time and then recovered after the time the sampler should have closed. Once returned to the laboratory at the INDP in Mindelo the sampler was placed in a laminar flow hood (Air-Clean 600), the sampling bottle was removed from the ATE, filtered into another 500 mL HDPE sampling bottle and acidified for later analysis in the laboratory in Kiel.

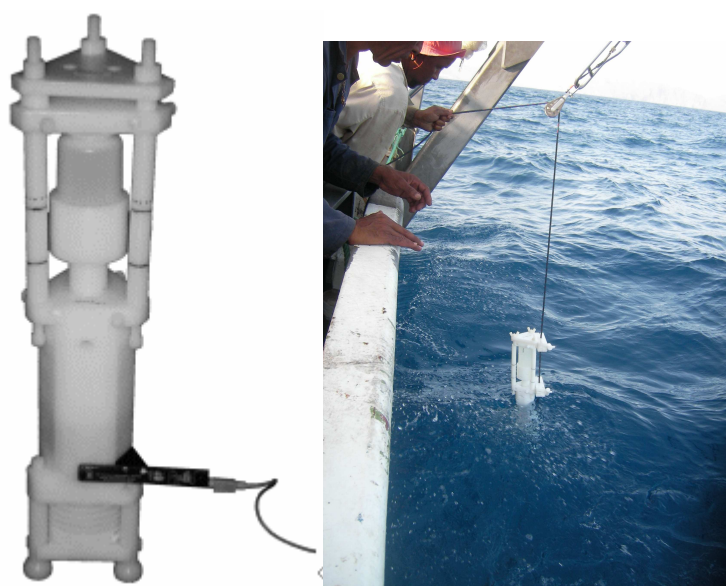


Figure 10: MITESS sampler (left) in the laboratory and (right) being deployed from the *R.V. Islandia*.

FISH

Large volume trace metal clean surface water samples were obtained when working on the *Islandia* using a towed fish sampling system (Figure 11). Surface sampling was performed by pumping seawater into the shipboard container through a tube attached to a towed fish. Contamination from the ship was minimized by towing the fish at ~ 5m distance alongside the ship with the crane arm of a hydrographic winch (J-frame), keeping it outside the ship's wake

as far as possible. The fish is a 1m long solid stainless steel, epoxy coated torpedo of 50 kg with three fins at the tail. The sample tubing consisted of 15m of Bev-a-line IV (Excelon) tubing (1/2 inch outside diameter) which was connected to the fish at one end and to an Almatec A-15 Teflon diaphragm pump at the other. The diaphragm pump was driven by compressed air supplied by a Jun-Air 300 compressor. Collection of all samples took place within the 10' research container that is located on the trawl deck of the *Islandia*. The walls of the research container were lined with clean plastic bags in order to turn it into a pseudo clean room as no HEPA filtered laminar flow cabinets are available onboard the *Islandia*. The tubing was attached with tape and tie-wraps to the fish and the stainless steel hydrowire deployed from the J-frame. Prior to deployment the tubing had been extensively cleaned with 0.1M HCl and rinsed with MQ water. Filtered seawater was obtained in-line at a flow rate of 2-3 L min⁻¹ through a Sartorius Sartobran PH filter cartridge (0.4µm prefilter and 0.2 µm final filter). Unfiltered seawater was obtained directly from the outlet of the diaphragm pump.



Figure 11: The FISH sampler deployed from the *R. V. Meteor* during M71-3 in the Mediterranean.

GO-FLO samplers

During the work performed on the *Islandia* in May 2009, seawater samples from the upper water column (0-100 m) were obtained using trace metal clean Teflon lined GO-FLO samplers (General Oceanics, Miami, USA) deployed on a Kevlar line (identical to the one used for the MITESS sampling above). On larger research ships the GO-FLOs would be transferred into a class 100 clean container prior to sampling. As this is not possible presently on the *Islandia*, samples were maintained in the GO-FLOs until the ship returned to Mindelo

where they could be transferred to the IFM-GEOMAR 20' clean container that was deployed at the INDP during this period. The collected seawater was filtered through an 0.2 μm membrane filter (Sartorius) under nitrogen overpressure (0.2 – 0.3 bar) into 125 or 1000 mL acid cleaned LDPE bottles (Nalgene) for later analysis for trace metals or into 1000 mL acid cleaned Teflon bottles (Nalgene) for superoxide experiments.

The TITAN Sampling System of the NIOZ

For the work performed during ANTXXIV-3 trace metal clean water samples were obtained using the TITAN system (Figure 12) belonging to the NIOZ (Netherlands Institute for Sea Research) [de Baar *et al.*, 2008]. In brief this is a complete trace metal clean CTD constructed from titanium with a standard Seabird CTD system and using 24 trace metal clean GO-FLO samplers for the water collection. The NIOZ system also includes a separate trace metal clean container which is solely used for collecting water samples from the sampling frame once it is back onboard the ship.

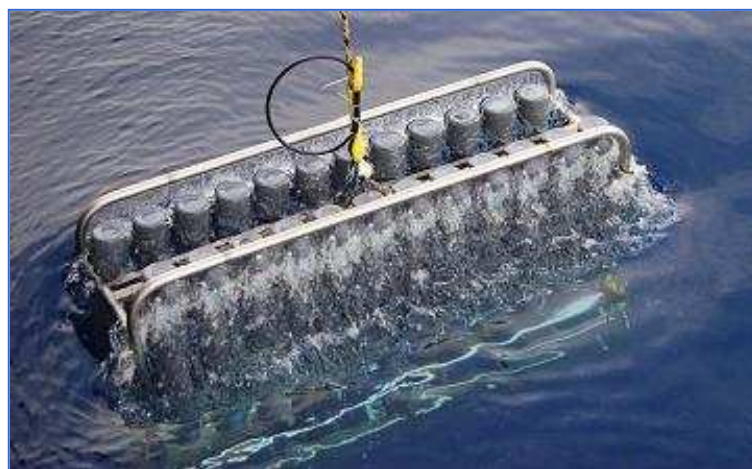


Figure 12: The TITAN sampler with a full complement of 24 GO-FLO bottles deployed from the *R.V. Polarstern* during ANTXXIV-3.

Analytical Measurements

Measuring Superoxide

ROS (Reactive Oxygen Species) are present at very low concentrations in the open ocean. The lifetimes of ROS, with the exception of hydrogen peroxide and organic peroxides, are very short (μsec to sec). Moreover, the measurements of ROS in the field require

sensitive, rapid, robust, simple and transportable instruments. Flow injection methods are typically best suited for work at sea, either in a discrete mode (sample injection loop of sample into reagent flow) or as a continuous signal (continuous mixing of reagent and sample). Quantitative work on O_2^- in seawater has been seriously handicapped by the lack of a simple and reliable method to produce the radical at a constant and accurately known rate. Manuscript I of this thesis presents information on both sources and detection methods currently being used for seawater measurements of O_2^- and their strengths and weaknesses.

For O_2^- measurements in this thesis I adapted an existing chemiluminescence analysis method which utilizes the reagent [2-methyl-6-(4-methoxyphenyl)-3,7-dihydroimidazo[1,2-a]pyrazin-3-one HCl] (MCLA) [Nakano, 1998; Oosthuizen *et al.*, 1997; Pronai *et al.*, 1992; Tambo *et al.*, 1998]. The mechanism and specificity for the reaction of MCLA and O_2^- is well described [Kambayashi *et al.*, 2003] and for the present work MCLA was found to be the best analytical technique currently available.

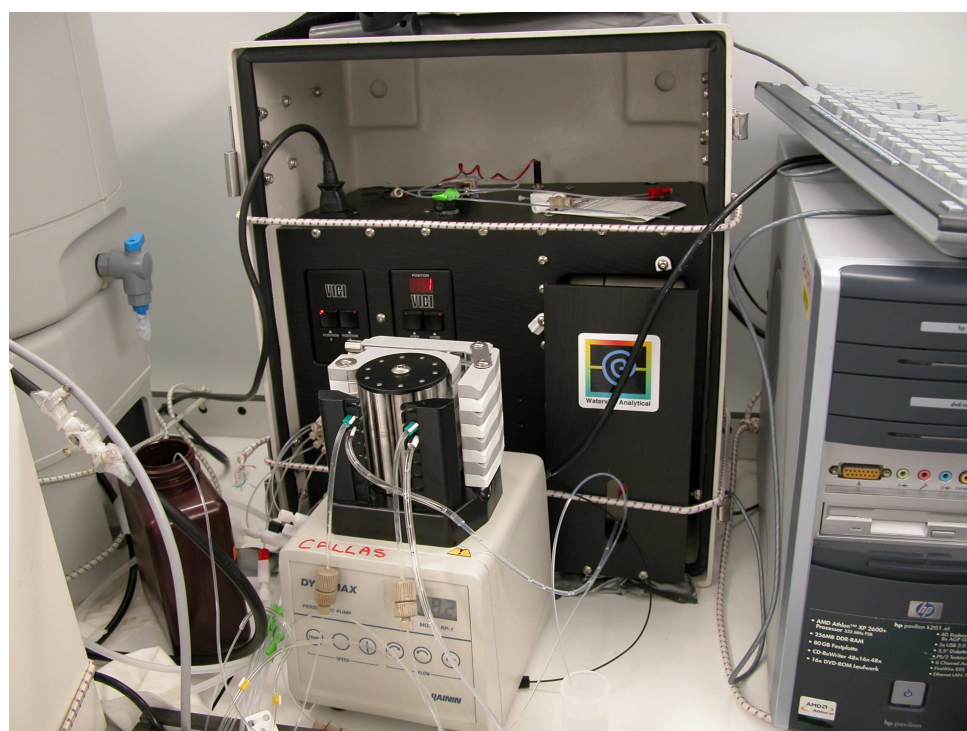


Figure 13: Chemiluminescence flow injection analysis (FIA) system as used for superoxide decay rate experiments during ANTXXIV-3. The same equipment is also used for the analysis of Fe(III), Fe(II) and H_2O_2 (see below).

In brief, for O_2^- determination the sample and the MCLA reagent were applied directly into the flow cell of an FeLume chemiluminescence analyzer (Waterville Analytical, Maine, USA) using a peristaltic pump (Gilson Minipuls 3, operating at 18 rpm,) with the sample line

being pulled through the flow cell as this leads to the smallest amount of dead time in the system (typically 2-3 s). The typical setup for the instrument is shown in Figure 13. Two new FeLume instruments were purchased for work in Cape Verde. We adapted our existing Labview™ (National Instruments) software to make new programs to specifically run the equipment for real time analysis of O_2^- .

Calibrating Superoxide concentrations and fluxes

As superoxide is a transient species and highly reactive it is not a trivial task to accurately quantify in seawater. In this study the appropriate numerical tools were developed and a number of superoxide sources and methods for the purposes of calibrating O_2^- concentrations and/or fluxes specifically in seawater were investigated. The superoxide thermal source bis(4-carboxybenzyl)hyponitrite (SOTS)-1 was found easy to employ as a reliable source of O_2^- which could be successfully applied in seawater. More information about the work with this superoxide thermal source and also on the findings with already existing sources and methods can be found in the first manuscript of this thesis which summarizes the laboratory work which was conducted during this thesis.

Measuring Superoxide decay rates

The approach performed in this study is based on measuring the decay rate of known quantities of added O_2^- (as KO_2) to seawater. O_2^- is detected via its chemiluminescence reaction with MCLA (see above). For the present work an experimental setup similar to that used in nutrient bioassay experiments [Mills *et al.*, 2004] was adopted by which a number of experimental treatments are utilized: (i) Control – reaction with unmodified seawater. (ii) Metal free reaction – this is achieved by complexation of trace metals in solution with DTPA, (iii & iv) addition of Cu(II) to the seawater to form a titration series with the control (this approach was also used in a previous study [Voelker *et al.*, 2000]) and (v & vi) addition of Fe(III) to the seawater to form a titration series with the control.

Coloured Dissolved Organic Matter Absorbance

CDOM measurements were performed using a LWCC-2100 100 cm pathlength liquid waveguide cell (World Precision Instruments, Sarasota, FL, USA) and an Ocean Optics USB4000 UV-VIS spectrophotometer in conjunction with an Ocean Optics DT-MINI-2-GS light source. Samples were syringe filtered through 0.2 μ m filters (Sarstedt), the first 10 mL were discarded and the absorbance measured by direct injection into the LWCC. Absorbance

measurements were made relative to MQ water and corrected for the refractive index of seawater based on the procedure outlined in Nelson *et al.* [2007]. The resulting dimensionless 6 optical density spectra were converted to absorption coefficient (m^{-1}): $a\text{CDOM}(\lambda) = 2.303 A_\lambda/l$, where 2.303 converts decadal logarithmic absorbance to base e, and l is the effective optical pathlength of the waveguide (here 103.8 ± 0.5 cm as determined by the manufacturer).

Determination of H₂O₂ by Flow Injection Analysis (FIA)

In the present work H₂O₂ was measured using a flow injection chemiluminescence (FIA-CL) reagent injection method [Yuan and Shiller, 1999]. In brief, the chemiluminescence of luminol is catalysed by the reaction of H₂O₂ present in the sample with Co²⁺ at alkaline pH. H₂O₂ standards were made by serial dilution from a primary stock solution (30% Fluka - Trace Select). The concentration of the primary standard was determined by direct spectrophotometry of the solution ($\epsilon = 40.9 \text{ mol L}^{-1} \text{ cm}^{-1}$, [Hwang and Dasgupta, 1985]). Secondary standards (~100 μM) were also analysed spectrophotometrically using Cu(II) and 2,9-dimethyl-1,10-phenanthroline [Kosaka *et al.*, 1998]. Sample concentrations were corrected daily for the reagent blank [Yuan and Shiller, 1999] and for H₂O₂ in the ultrapure water (20-60 nmol L^{-1}). Samples were analysed using 5 replicates: typical precision was 2-3% through the concentration range 1-300 nM, the detection limit (3σ) was typically 0.2 nmol L^{-1} .

Determination of Dissolved Iron by FIA

The dissolved Fe concentration was measured in the laboratory in Kiel with an established luminol chemiluminescence flow injection analysis (FIA) method [de Jong *et al.*, 2000; Obata *et al.*, 1993]. Discrete samples for dissolved iron were taken in 100 mL clean polyethylene bottles (Kartell) and acidified to pH 1.8 with triple quartz distilled (3QD) concentrated hydrochloric acid (1 ml l^{-1}). All sample bottles had been cleaned by leaching in hot (60° C) 6M HCl for at least 24 hours followed by ample rinsing with Milli-Q (MQ) water.

Determination of Trace Metals by Graphite Furnace Atomic Absorption Spectrophotometry (GFAA)

Samples were analysed according to the method described in Grasshoff [1999] and Kremling and Streu [2001]. For the analysis of Cd, Co, Cu, Fe, Ni, Pb and Zn, 300–500 g portions of the samples were subjected to a simultaneous dithiocarbamate–Freon extraction modified from the procedure by Danielsson *et al.* [1978] implying maximum concentration factors of 500. The final extracts with the metals were measured by electrothermal atomic

absorption spectrometry with Zeeman background correction (ETAAS; Perkin-Elmer Model 4100 ZL). Accuracy and precision was evaluated using both the certified reference material NASS-5 or the SAFe intercalibration sample [Johnson *et al.*, 2007].

Iron Solubility Measurements using ^{55}Fe

The radioisotope ^{55}Fe is a weak beta emitter with a half-life of 2.7 years. Fe solubility measurements were performed using the radioisotope, ^{55}Fe (Hartmann Analytics, Braunschweig, Germany). The experimental setup was adapted from Nakabayashi *et al.* [2002] and Kuma *et al.* [1996]. The ^{55}Fe isotope had a specific activity of 157.6 MBq/mg Fe, a total activity of 75MBq, and was dissolved in 0.1 M HCl. ^{55}Fe dilution standards were produced with MQ water and acidified with quartz distilled (QD) HCl to a pH below 2.

After the addition of ^{55}Fe ($t_0 = 0\text{h}$; total Fe $\text{Fe}_T = 20 \text{ nmol L}^{-1}$; pH 7.9) to each sample, a small subsample was immediately filtered through a 0.02 μm Anotop syringe filter (Whatman) and acidified with (QD) HCl, to keep the Fe from adsorbing to the bottle walls [Fischer *et al.*, 2007; Schlosser and Croot, 2008]. Duplicates of the unfiltered and 0.02 μm filtered samples (400 μL) were transferred into 6 mL vials to which 4.5 mL of scintillation fluid (Lumagel Plus[®]) were then added. This procedure was repeated for subsamples taken at later times. Sample storage, treatment and measurement were performed at room temperature (20°C). The activity of the ^{55}Fe solutions was determined by scintillation counting (Packard, Tri-Carb 2900TR) and then converted to soluble Fe concentrations, taking into account the activity of the added isotope solution and the *in-situ* dissolved Fe concentration of each sample.

Aerosol Optical Thickness – Microtops and Aerosol Robotic Network (AERONET) measurements

The Maritime Aerosol Network (MAN) [Smirnov *et al.*, 2009] has been developed as a component of the Aerosol Robotic Network (AERONET). MAN deploys Microtops Sun photometers and utilises the calibration procedure and data processing traceable to AERONET. The Microtops Sun photometer is a handheld device specifically designed to measure columnar aerosol optical depth and water vapor content [Morys *et al.*, 2001]. The direct Sun measurements are acquired in five spectral channels within the spectral range 340–1020 nm. The bandwidths of the interference filters vary from 2 to 4 nm (UV channels) to 10 nm for visible and near infrared channels. During the course of this work I undertook Microtops measurements on *Islandia* and *Polarstern* expeditions (Figure 14).



Figure 14: The Author performing Microtops measurements for the MAN during an *Islandia* expedition in July 2008.

Airmass back Trajectories and Satellite Chlorophyll Estimates

Satellite data was routinely used in this work to determine the sources of dust to the study sites via back trajectory analysis (HYSPLIT), and to examine changes in surface ocean chlorophyll (NASA Ocean Color: using MODIS TERRA and AQUA and SEAWIFs satellites). For back trajectory analysis, the air masses sampled were classified according to 5-day back trajectories calculated for arrival heights of 10, 500 and 1000 m above the ship's position (NOAA Air Resources Laboratory HYSPLIT model, FNL data set). Ocean Color data was accessed via the Ocean Color Time-Series Online Visualization and Analysis System (<http://reason.gsfc.nasa.gov/Giovanni/>), based on the GES-DISC Interactive Online Visualization and Analysis Infrastructure (Giovanni) which was developed by GES DISC to provide users with an easy-to-use, web-based interface for the visualization and analysis of the Earth Science data.

Participation in Scientific Expeditions during this work

At the start of SOPRAN phase I it was hoped that we would be able to conduct studies at the TENATSO time series station at three different times, the dry, rainy and high dust input (January) season, during the first three years of the fund of this project. Unfortunately, in 2007 the research vessel, *R. V. Islandia*, which was key to achieving this goal, was still under going major repairs and at the time of our first trip to Cape Verde in July 2007 the ship was in the dry dock and lacked an interior. The purpose of this visit then became an exercise in building up and fitting out the interior of the new TENATSO laboratory at the INDP. At this time we were able to obtain a first idea of the logistical challenges that arise with working in the Cape Verde islands and importantly we made the first social contacts and could test and obtain the first data for ROS from water close to the shore of Sao Vicente while simultaneously conducting light measurements over the course of the day.

As the *Islandia* was still not seaworthy at the beginning of 2008 I had the opportunity to participate in the IPY-GEOTRACES expedition ANTXXIV-3 to the Antarctica with the German icebreaker *R.V. Polarstern* along the zero Meridian, to the Neumayer station, through the Weddell Sea and Drake Passage to Punta Arenas in Chile. During this cruise my role was to measure the concentration of H₂O₂ throughout the water column and to help determining Titanium and Copper speciation while also testing a new sampling strategy we had set up to follow superoxide kinetics in the Southern Ocean.

In July 2008 finally we were able to obtain our first real field trips with the *Islandia* to a station in the south west of Sao Vicente and 3 further stations which were located on a diagonal between Mindelo, Sao Vicente and the TENATSO time series station. As our work was combined with that of the bioassay group at IFM-GEOMAR we did not at this time go out the entire distance to the TENATSO site. This was because it became quickly apparent that for the bioassays, the travel time between TENATSO and Mindelo was too long (over 6 hours) to guarantee optimal cell viability. At this time I conducted dust dissolution experiments in parallel with the bioassays to examine the possible role of superoxide in this process.

As part of my PhD thesis work, two further trips were undertaken to the Cape Verde archipelago in November 2008 and May 2009, and each time a visit to the TENATSO station was accomplished. During May 2009 I performed further dust dissolution experiments in parallel with the bioassay work being performed at that time, for the November 2008 work no bioassay work was carried out and only abiotic dust dissolution experiments were undertaken.

Thesis Outline

The primary hypothesis that this thesis examines is whether there is significant dissolution of recently deposited aeolian dust by superoxide in the open ocean with a particular focus on the TENATSO site. In order to fully understand the significance of all the reactions involving superoxide in the open ocean to assess the importance of the potential reaction with dust it was necessary to examine and evaluate the existing literature for methods of superoxide determination and the potential fluxes of superoxide in seawater. Unfortunately already at the beginning of this work, which was conducted in the laboratory in Kiel to configure a detection system for superoxide, I found with both sources of superoxide and detection methods serious problems for use in seawater that had not been adequately addressed by previous researchers on this topic. Thus I was compelled to develop and evaluate new methods and techniques that could be used for the field expeditions to Cape Verde and the Southern Ocean for the present work. This included the development of a new theoretical basis for the interpretation of the data obtained from my experimental approach as in many cases the existing theory was too simple for application to seawater studies. The approach that is used in this thesis was optimised for application to the understanding of environmental processes involving superoxide in the ocean.

Thus the first paper of this thesis introduces a methodology for the calibration and determination of superoxide fluxes in seawater and introduces the reader into the problems of making accurate measurements of a transient reactive species such as O_2^- . Further information is supplied about the reactivity of O_2^- and on the existing information regarding sources and detection methods which have previously been applied in seawater. Most importantly this paper shows the successful application of the superoxide thermal source SOTS-1 as a O_2^- source in seawater for use as a calibration source for both concentration and flux measurements. A theoretical framework for interpretation of the results is developed and compared to laboratory data obtained using 3 different superoxide detection systems.

The second paper describes an investigation of the decay kinetics of O_2^- with organic matter in the oligotrophic waters at and nearby the TENATSO ocean observatory adjacent to the Cape Verde archipelago. A number of reactions have been identified in seawater that affect O_2^- decay rates; including the 2nd order uncatalysed dismutation reaction of superoxide, or reactions with trace metals species, which have been examined in a few studies. However little is known about the possible reaction of O_2^- with organic matter which may be important for the cycling and oxidation of organic matter in surface waters and as a non-trace metal sink for superoxide. In this work I found a small but significant contribution from organic material

to the superoxide decay rate but this had no statistically significant relationship to the measured CDOM absorbance, suggesting it was a minor component of the CDOM that was reacting with superoxide. Indeed comparison of the data for deep waters below the euphotic zone with H_2O_2 concentrations suggests that this reaction may be due to the presence of quinone moieties which make up only a small part of the CDOM but help to regulate the deep water H_2O_2 concentration.

Paper 3 examines the primary hypothesis directly through a series of observations of O_2^- decay kinetics from the waters around Sao Vicente, Cape Verde. This work was performed as an integral part of SOPRAN (German SOLAS) activities in Cape Verde. It is well known that the major source of trace metals to the Tropical Atlantic is through aeolian deposition of Saharan dust. In the sunlight waters of the Tropics, where relatively high fluxes of O_2^- potentially exist due to photochemical reactions of DOM, there exists the possibility of a kinetically controlled reduction of Fe from aerosol derived colloids and particles to the more soluble and bioavailable Fe(II). The method applied in this work allows an assessment of changes in both the organic reactivity with O_2^- simultaneously with changes in the free metal speciation of Fe and/or Cu. This is an important breakthrough as it allows the evaluation of the importance of the different reaction pathways for O_2^- and thus the factors which control metal redox speciation in seawater. Through this approach we can ascertain relatively rapidly whether dust dissolution has altered the *in situ* iron speciation in seawater and hence if any changes in bioavailability may have occurred. The results gained from this work indicate that overall Cu dominates superoxide decay in the study region and that the reaction between dust and O_2^- is apparently a minor sink term.

The fourth paper in this thesis describes work on O_2^- decay kinetics in the Southern Ocean waters during the Polarstern expedition (ANTXXIV-3). Measurements of O_2^- decay kinetics throughout the water column were performed at 3 stations during a transect through the Drake Passage in the austral autumn of 2008. A new sampling strategy was used here, based on existing bioassay protocols, designed to elucidate the sinks of O_2^- in polar waters throughout the water column. The titration of the samples with Fe or Cu revealed that Cu was the major sink of O_2^- in the Southern Ocean despite it being strongly organically complexed and indicates that the Cu organic complexes react directly with O_2^- . Contrastingly the reaction with iron was slowly overall and suggests that organic complexes of iron do not react with superoxide appreciably. This work has then direct implications for the redox cycling and bioavailability of Cu and Fe in the Southern Ocean and was thus featured in the Environmental News section of ES&T upon publication.

Glossary of commonly used Abbreviations and Terminology used in this Thesis

AERONET Aerosol Robotic Network

AFO Amorphous Ferric Oxyhydroxides

ATE Automated Trace Element

AQUA is a multi-national NASA scientific research satellite studying the precipitation evaporation and cycling of water. It is the second major component of the Earth Observing System

AQY Apparent Quantum Yield

BATS Bermuda Atlantic Time Series

CDOM Coloured Dissolved Organic Matter

Cu Copper

CTD Conductivity Temperature Density

DFO Desferrioxamine B

DMSO Dimethylsulfoxide

DOC Dissolved Organic carbon

DOM Dissolved Organic Matter

DTPA Diethylenetriaminopentaacetic acid

EDTA Ethylenediaminetetraacetic acid

ETAAS Electrothermal atomic absorption spectrometry

ESR Electron Spin Resonance

FC Ferricytochrome c

FIA Flow Injection Analyzer

Fe Iron

Fz Ferrozine

GFAA Graphite Furnace Atomic Absorption Spectrophotometry

Giovanni GES-DISC Interactive Online Visualization and Analysis Infrastructure

Glu Gluconic Acid

GOTM General Ocean Turbulence Model

H₂O₂ Hydrogen peroxide

HCl Hydrochloric acid

HDPE High Density Poly Ethylene

HEPA High Efficiency Particle Arresting – an air filter that removes particles from the air allowing samples to be manipulated without risk of contamination from the air.

HNLC High Nutrient Low Chlorophyll

HOTS Hawaii Ocean Time Series
HX Hypoxanthine
IGBP International Global Biosphere Program
INDP Instituto Nacional para Desenvolvimento das Pescas
MAN Maritime Aerosol Network
MCLA [2-methyl-6-(4-methoxyphenyl)-3,7-dihydroimidazo[1,2-a]pyrazin-3-one HCl]
M.I.T Massachusetts Institute of Technology
MITESS Moored In-situ Trace Element Serial Sampler
MODIS Moderate Resolution Imaging Spectroradiometer
N₂ Nitrogen gas
NBD-Cl 7-Chloro-4-nitrobenzo-2-oxa-1,3-diazole
NBS National Bureau of Standards (USA)
NBT Nitroblue Tetrazolium
NIOZ Royal Netherlands Institute for Sea research
NOAA National Oceanic and Atmospheric Administration
NPZD Nutrient-Phytoplankton-Zooplankton-Detritus
MQ 18MΩ cm resistivity water
KO₂ Potassium superoxide
LWCC Liquid Waveguide Capillary Cell
NaOH Sodium hydroxide
O₂ Oxygen
O₂⁻ Superoxide
PBS Phosphate Buffered Solution
PC Polycarbonate
PR Production Rate
PVC Polyvinylcarbonate
ROS Reactive Oxygen Species
RPM Rotations per Minute
QD Quartz distilled
Q Quinone
QH₂ Hydroquinone
Q• Semiquinone radical
SAL Saharan Air Layer
SeaWiFS Sea-viewing Wide Field-of-view Sensor

Sec Second

SOD Superoxide Dismutase

SOLAS Surface Ocean Lower Atmosphere Studies – SOLAS is an IGBP international research initiative comprising of over 1500 scientists in 23 countries. The primary objective is *"To achieve quantitative understanding of the key biogeochemical-physical interactions and feedbacks between the ocean and atmosphere, and of how this coupled system affects and is affected by climate and environmental change."*

SOPRAN Surface Ocean Processes in the Anthropocene – The BMBF Verbundprojekt which carries out SOLAS research in Germany.

SOTS Superoxide Thermal Source

SW Seawater

Terra (EOS AM-1) is a multi-national NASA scientific research satellite in a sun-synchronous orbit around the Earth. It is the flagship of the Earth Observing System

TENATSO Tropical Eastern North Atlantic Time Series Observatory – An European Union funded project which combines atmospheric and oceanographic observations from Cape Verde.

UV Ultraviolet

X Xanthine

XO Xanthine Oxidase

REFERENCES

- Asada, K., S. Kanematsu, and K. Uchida (1977), Superoxide dismutases in photosynthetic organisms: Absence of the cuprozinc enzyme in eukaryotic algae, *Archives of Biochemistry and Biophysics*, 179(1), 243.
- Baker, A. R., and T. D. Jickells (2006), Mineral particle size as a control on aerosol iron solubility, *Geophysical Research Letters*, 33(17).
- Baker, A. R., and P. L. Croot (2008), Atmospheric and marine controls on aerosol iron solubility in seawater, *Marine Chemistry*, doi:10.1016/j.marchem.2008.1009.1003.
- Barbeau, K., E. L. Rue, K. W. Bruland, and A. Butler (2001), Photochemical cycling of iron in the surface ocean mediated by microbial iron(III)-binding ligands, *Nature*, 413(6854), 409-413.
- Behrenfeld, M. J., and Z. S. Kolber (1999), Widespread Iron Limitation of Phytoplankton in the South Pacific Ocean, *Science*, 283, 840-843.
- Bell, J., J. Betts, and E. Boyle (2002), MITESS: a moored in situ trace element serial sampler for deep-sea moorings, *Deep-Sea Research*, 49, 2103-2118.
- Bielski, B. H. J., D. E. Cabelli, R. L. Arudi, and A. B. Ross (1985), Reactivity of HO₂/O₂⁻ Radicals in Aqueous-Solution, *Journal of Physical and Chemical Reference Data*, 14(4), 1041-1100.
- Blain, S., et al. (2007), Effect of natural iron fertilization on carbon sequestration in the Southern Ocean, *Nature*, 446(7139), 1070-U1071.
- Blough, N. V., and R. G. Zepp (1995), Reactive oxygen species in natural waters, *Published by Blackie Academic and Professional, an Imprint of Chapman & Hall, Western Cleddens Road, Bishopbriggs Glasgow G64 2NZ*, 280-286.
- Borer, P., S. J. Hug, B. Sulzberger, S. M. Kraemer, and R. Kretzschmar (2007), Photolysis of citrate on the surface of lepidocrocite: An in situ attenuated total reflection infrared spectroscopy study, *J. Phys. Chem. C*, 111(28), 10560-10569.
- Borer, P., S. M. Kraemer, B. Sulzberger, S. J. Hug, and R. Kretzschmar (2009a), Photodissolution of lepidocrocite (gamma-FeOOH) in the presence of desferrioxamine B and aerobactin, *Geochimica Et Cosmochimica Acta*, 73(16), 4673-4687.
- Borer, P., B. Sulzberger, S. J. Hug, S. M. Kraemer, and R. Kretzschmar (2009b), Photoreductive Dissolution of Iron(III) (Hydr)oxides in the Absence and Presence of Organic ligands: Experimental Studies and Kinetic Modeling, *Environmental Science & Technology*, 43(6), 1864-1870.
- Boyd, P. W., et al. (2000), Mesoscale iron fertilisation elevates phytoplankton stocks in the polar Southern Ocean, *Nature*, 407, 695-702.
- Boyle, E., and J. M. Edmond (1975), Copper in surface waters south of New Zealand, *Nature*, 253, 107-109.
- Brand, L. E., W. G. Sunda, and R. R. L. Guillard (1986), Reduction of Marine Phytoplankton Reproduction Rates by Copper and Cadmium, *Journal of Experimental Marine Biology and Ecology*, 96, 225-250.
- Carrasco, N., R. Kretzschmar, M. L. Pesch, and S. M. Kraemer (2007), Low concentrations of surfactants enhance siderophore-promoted dissolution of goethite, *Environmental Science & Technology*, 41(10), 3633-3638.
- Chen, Y.-B., B. Dominic, M. T. Mellon, and J. P. Zehr (1998), Circadian Rhythm of Nitrogenase Gene Expression in the Diazotrophic Filamentous Nonheterocystous Cyanobacterium *Trichodesmium* sp. Strain IMS 101, *J. Bacteriol.*, 180(14), 3598-3605.
- Chiapello, I., G. Bergametti, L. Gomes, B. Chatenet, F. Dulac, J. Pimenta, and E. S. Soares (1995), An Additional Low Layer Transport of Sahelian and Saharan Dust over the North-Eastern Tropical Atlantic, *Geophysical Research Letters*, 22(23), 3191-3194.

- Christensen, H., and K. Sehested (1988), HO₂ and O₂⁻-Radicals at Elevated-Temperatures, *Journal of Physical Chemistry*, 92(10), 3007-3011.
- Croot, P. L., and M. Johansson (2000), Determination of iron speciation by cathodic stripping voltammetry in seawater using the competing ligand 2-(2-Thiazolylazo)-p-cresol (TAC), *Electroanalysis*, 12(8), 565-576.
- Croot, P. L., J. W. Moffett, and L. E. Brand (2000), Production of extracellular Cu complexing ligands by eucaryotic phytoplankton in response to Cu stress, *Limnol. Oceanogr.*, 45(3), 619-627.
- Croot, P. L., P. Streu, and A. R. Baker (2004), Short residence time for iron in surface seawater impacted by atmospheric dry deposition from Saharan dust events, *Geophys. Res. Lett.*, 31(23), 4.
- Croot, P. L., K. Bluhm, C. Schlosser, P. Streu, E. Breitbarth, R. Frew, and M. Van Ardelan (2008), Regeneration of Fe(II) during EIFeX and SOFeX, *Geophys. Res. Lett.*, 35(19), L19606, doi:10.1029/2008GL035063.
- Croot, P. L., A. R. Bowie, R. D. Frew, M. Maldonado, J. A. Hall, K. A. Safi, J. La Roche, P. W. Boyd, and C. S. Law (2001), Retention of dissolved iron and Fe^{II} in an iron induced Southern Ocean phytoplankton bloom, *Geophys. Res. Lett.*, 28, 3425-3428.
- Croot, P. L., P. Laan, J. Nishioka, V. Strass, B. Cisewski, M. Boye, K. Timmermans, R. Bellerby, L. Goldson, and H. J. W. de Baar (2005), Spatial and Temporal distribution of Fe(II) and H₂O₂ during EISENEX, an open ocean mesoscale iron enrichment, *Marine Chemistry* 95, 65-88.
- Crumbliss, A. L. (1990), Iron Bioavailability and the Coordination Chemistry of Hydroxamic Acids, Elsevier Science Sa Lausanne.
- Cunningham, K. A., and D. G. Capone (1992), Superoxide dismutase as a protective enzyme against oxygen toxicity: An overview and initial studies in *Trichodesmium*. , in *Marine Pelagic Cyanobacteria: Trichodesmium and other Diazotrophs.*, edited by E. J. Carpenter, D. G. Capone and J. G. Rueter, pp. 331-341. , Kluwer Academic Publishers, Dordrecht/Boston/London.
- Cunningham, K. M., M. C. Goldberg, and E. R. Weiner (1988), Mechanisms for Aqueous Photolysis of Adsorbed Benzoate, Oxalate, and Succinate on Iron Oxyhydroxide (Goethite) Surfaces, *Environmental Science & Technology*, 22(9), 1090-1097.
- Danielsson, L. G., B. Magnusson, and S. Westerlund (1978), Improved Metal Extraction Procedure for Determination of Trace-Metals in Sea-Water by Atomic-Absorption Spectrometry with Electrothermal Atomization, *Analytica Chimica Acta*, 98(1), 47-57.
- de Baar, H. J. W., J. T. M. de Jong, D. C. E. Bakker, B. M. Löscher, C. Veth, U. Bathmann, and V. Smetacek (1995), Importance of iron for plankton blooms and carbon dioxide drawdown in the Southern Ocean, *Nature*, 373, 412-415.
- de Baar, H. J. W., et al. (2008), Titan: A new facility for ultraclean sampling of trace elements and isotopes in the deep oceans in the international Geotraces program, *Marine Chemistry*, 111(1-2), 4-21.
- de Jong, J. T. M., M. Boye, V. Schoemann, R. F. Nolting, and H. J. W. de Baar (2000), Shipboard techniques based on flow injection analysis for measuring dissolved Fe, Mn and Al in seawater *J. Environ. Monit.*, 2, 496-502.
- Del Vecchio, R., and N. V. Blough (2002), Photobleaching of chromophoric dissolved organic matter in natural waters: kinetics and modeling, *Marine Chemistry*, 78(4), 231-253.
- Del Vecchio, R., and N. V. Blough (2004), Spatial and seasonal distribution of chromophoric dissolved organic matter and dissolved organic carbon in the Middle Atlantic Bight.
- Dister, B., and O. C. Zafiriou (1993), Photochemical Free-Radical Production-Rates in the Eastern Caribbean, *J. Geophys. Res.-Oceans*, 98(C2), 2341-2352.

- Fischer, A. C., J. J. Kroon, T. G. Verburg, T. Teunissen, and H. T. Wolterbeek (2007), On the relevance of iron adsorption to container materials in small-volume experiments on iron marine chemistry: 55Fe-aided assessment of capacity, affinity and kinetics, *Marine Chemistry*, 107(4), 533-546.
- Fujii, M., A. L. Rose, T. D. Waite, and T. Omura (2006), Superoxide-Mediated Dissolution of Amorphous Ferric Oxyhydroxide in Seawater, *Environ. Sci. Technol.*, 40, 880-887.
- Goldstone, J. V., and B. M. Voelker (2000), Chemistry of superoxide radical in seawater: CDOM associated sink of superoxide in coastal waters, *Environmental Science & Technology*, 34(6), 1043-1048.
- González-Dávila, M., J. Santana-Casiano, and F. Millero (2006), Competition Between O₂ and H₂O₂ in the Oxidation of Fe(II) in Natural Waters, *Journal of Solution Chemistry*, 35(1), 95.
- Grasshoff, K., K. Kremling, and M. Ehrhardt (1999), *Methods of Seawater analysis*, Wiley-VCH Verlag, Weinheim (FRG).
- Hutchins, D. A., G. R. DiTullio, Y. Zhang, and K. W. Bruland (1998), An iron limitation mosaic in the California upwelling system, *Limnol. Oceanogr.*, 43, 1037-1054.
- Hwang, H., and P. K. Dasgupta (1985), Thermodynamics of the Hydrogen Peroxide-Water System, *Environmental Science and Technology*, 19, 255-258.
- Jickells, T. D. (1999), The inputs of dust derived elements to the Sargasso Sea; a synthesis, *Marine Chemistry*, 68, 5-14.
- Jickells, T. D., et al. (2005), Global Iron Connections Between Desert Dust, Ocean Biogeochemistry, and Climate, *Science*, 308(5718), 67-71.
- Johnson, K. S., K. H. Coale, V. A. Elrod, and T. Neil W (1994), Iron photochemistry in seawater from the equatorial Pacific, *Marine Chemistry* 46, 319-334.
- Johnson, K. S., et al. (2007), Developing Standards for Dissolved Iron in Seawater, *EOS, Transactions of the American Geophysical Union*, 88(11), 131-132.
- Kambayashi, Y., S. Tero-Kubota, Y. Yamamoto, M. Kato, M. Nakano, K. Yagi, and K. Ogino (2003), Formation of Superoxide Anion during Ferrous Ion-Induced Decomposition of Linoleic Acid Hydroperoxide under Aerobic Conditions, *J Biochem*, 134(6), 903-909.
- Karyampudi, V. M., and H. F. Pierce (2002), Synoptic-scale influence of the Saharan air layer on tropical cyclogenesis over the eastern Atlantic, *Monthly Weather Review*, 130(12), 3100-3128.
- Karyampudi, V. M., et al. (1999), Validation of the Saharan dust plume conceptual model using lidar, Meteosat, and ECMWF data, *Bulletin of the American Meteorological Society*, 80(6), 1045-1075.
- Kellogg, E. W., and I. Fridovich (1975), Superoxide, Hydrogen-Peroxide, And Singlet Oxygen In Lipid Peroxidation By A Xanthine-Oxidase System, *Journal Of Biological Chemistry*, 250(22), 8812-8817.
- Kim, D., T. Oda, A. Ishimatsu, and T. Muramatsu (2000), Galacturonic acid-induced Increase of Superoxide Production in Red Tide Phytoplankton *Chattonella marina* and *Heterosigma akashiwo*, *Biosci. Biotechnol. Biochem.*, 64, 911-914.
- Kirk, J. T. O. (1994), *Light and Photosynthesis in Aquatic Ecosystems*, 2nd ed., 525 pp., Cambridge University Press, Cambridge.
- Kosaka, K., H. Yamada, S. Matsui, S. Echigo, and K. Shishida (1998), Comparison among the methods for hydrogen peroxide measurements to evaluate advanced oxidation processes: Application of a spectrophotometric method using copper(II) ion and 2,9-dimethyl-1,10-phenanthroline, *Environmental Science & Technology*, 32(23), 3821-3824.
- Kraemer, S. M. (2004), Iron oxide dissolution and solubility in the presence of siderophores, Birkhauser Verlag Ag.

- Kraemer, S. M., A. Butler, P. Borer, and J. Cervini-Silva (2005), Siderophores and the dissolution of iron-bearing minerals in marine systems, in *Molecular Geomicrobiology*, edited, pp. 53-84, Mineralogical Soc America, Chantilly.
- Kremling, K., and P. Streu (1993), Saharan Dust Influenced Trace-Element Fluxes in Deep North-Atlantic Subtropical Waters, *Deep-Sea Research Part I-Oceanographic Research Papers*, 40(6), 1155-1168.
- Kremling, K., and P. Streu (2001), The behaviour of dissolved Cd, Co, Zn, and Pb in North Atlantic near-surface waters (30 degrees N/60 degrees W-60 degrees N/2 degrees W), *Deep-Sea Research Part I-Oceanographic Research Papers*, 48(12), 2541-2567.
- Kuma, K., S. Nakabayashi, and K. Matsunaga (1995), Photoreduction of Fe(III) by hydrocarboxylic acids in seawater, *Mar. Res.*, 29(6), 1559-1569.
- Kuma, K., J. Nishioka, and K. Matsunaga (1996), Controls on iron(III) hydroxide solubility in seawater: The influence of pH and natural organic chelators, *Limnol. Oceanogr.*, 41(3), 396-407.
- Kuma, K., S. Nakabayashi, Y. Suzuki, I. Kudo, and K. Matsunaga (1992), Photo-reduction of Fe(III) by dissolved organic substances and existence of Fe(II) in seawater during spring blooms, *Marine Chemistry*, 37, 15-27.
- Kustka, A. B., Y. Shaked, A. J. Milligan, D. W. King, and F. M. M. Morel (2005), Extracellular production of superoxide by marine diatoms: Contrasting effects on iron redox chemistry and bioavailability, *Limnology and Oceanography*, 50(4), 1172-1180.
- Langlois, R. J., J. LaRoche, and P. A. Raab (2005), Diazotrophic Diversity and Distribution in the Tropical and Subtropical Atlantic Ocean, *Appl. Environ. Microbiol.*, 71(12), 7910-7919.
- Mahowald, N. M., A. R. Baker, G. Bergametti, N. Brooks, R. A. Duce, T. D. Jickells, N. Kubilay, J. M. Prospero, and I. Tegen (2005), Atmospheric global dust cycle and iron inputs to the ocean, *Glob. Biogeochem. Cycle*, 19(4), 17.
- Mann, E. L., N. Ahlgren, J. W. Moffett, and S. W. Chisholm (2002), Copper toxicity and cyanobacteria ecology in the Sargasso Sea, *Limnol. Oceanogr.*, 47, 976-988.
- Marshall, J.-A., M. Hovenden, T. Oda, and G. M. Hallegraeff (2002), Photosynthesis does influence superoxide production in the ichthyotoxic alga *Chattonella marina* (Raphidophyceae), *J. Plankton Res.*, 24(11), 1231-1236.
- Marshall, J. A., T. Ross, S. Pyecroft, and G. Hallegraeff (2005a), Superoxide production by marine microalgae - II. Towards understanding ecological consequences and possible functions, *Marine Biology*, 147(2), 541-549.
- Marshall, J. A., M. de Salas, T. Oda, and G. Hallegraeff (2005b), Superoxide production by marine microalgae, *Marine Biology*, 147(2), 533-540.
- Marta, D. J., T. Farinaz, and J. C. David (1989), Taxonomic distribution of copper-zinc superoxide dismutase in green algae and its phylogenetic importance, *Journal of Phycology*, 25(4), 767-772.
- Martin, J. H., and S. E. Fitzwater (1988), Iron-Deficiency Limits Phytoplankton Growth in the Northeast Pacific Subarctic, *Nature*, 331(6154), 341-343.
- Martin, J. H., R. M. Gordon, and S. E. Fitzwater (1991), The case for iron., *Limnol. Oceanogr.*, 36, 1793-1802.
- Martin, J. H., et al. (1994), Testing the iron hypothesis in ecosystems of the equatorial Pacific Ocean, *Nature*, 371, 123-129.
- McCord, J. M., and I. Fridovic (1969), Superoxide Dismutase, *J. Biol. Chem.*, 244(22), 6049-6055.
- Mehler, A. H. (1951), Studies on reactions of illuminated chloroplasts : I. Mechanism of the reduction of oxygen and other hill reagents, *Archives of Biochemistry and Biophysics*, 33(1), 65-77.

- Micinski, E., L. A. Ball, and O. C. Zafiriou (1993), Photochemical Oxygen Activation - Superoxide Radical Detection and Production-Rates in the Eastern Caribbean, *Journal of Geophysical Research-Oceans*, 98(C2), 2299-2306.
- Miller, W. L., D. W. King, J. Lin, and D. R. Kester (1995), Photochemical redox cycling of iron in coastal seawater, *Marine Chemistry* 50, 63-77.
- Millero, F. J. (1987), Estimate of the life time of superoxide in seawater, *Geochimica et Cosmochimica Acta*, 51, 351-353.
- Millero, F. J., S. Sotolongo, and M. Izaguirre (1987), The Oxidation-Kinetics of Fe(II) in Seawater, *Geochimica Et Cosmochimica Acta*, 51(4), 793-801.
- Mills, M. M., C. Ridame, M. Davey, J. La Roche, and R. J. Geider (2004), Iron and phosphorus co-limit nitrogen fixation in the eastern tropical North Atlantic, *Nature*, 429, 292-294.
- Moffett, J. W. (1995), Temporal and Spatial Variability of Copper Complexation by Strong Chelators in the Sargasso Sea, *Deep Sea Research*, 42, 1273-1295.
- Moffett, J. W., and R. G. Zika (1988), Measurement of copper(I) in surface waters of the subtropical Atlantic and Gulf of Mexico, *Geochimica et Cosmochimica Acta*, 52, 1849-1857.
- Moffett, J. W., and O. C. Zafiriou (1990), An Investigation of Hydrogen-Peroxide Chemistry in Surface Waters of Vineyard Sound with (H-2)-O-18(2) and O-18(2), *Limnology and Oceanography*, 35(6), 1221-1229.
- Moffett, J. W., and L. E. Brand (1996), Production of strong, extracellular Cu chelators by marine cyanobacteria in response to Cu stress, *Limnol. Oceanogr.*, 41(3), 388-395.
- Moore, M. C., et al. (2009), Large-scale distribution of Atlantic nitrogen fixation controlled by iron availability, *Nature Geosci*, advance online publication.
- Morys, M., F. M. Mims, S. Hagerup, S. E. Anderson, A. Baker, J. Kia, and T. Walkup (2001), Design, calibration, and performance of MICROTOPS II handheld ozone monitor and Sun photometer, *J. Geophys. Res.-Atmos.*, 106(D13), 14573-14582.
- Nakabayashi, S., K. Kuma, K. Sasaoka, S. Saitoh, M. Mochizuki, N. Shiga, and M. Kusakabe (2002), Variation in iron(III) solubility and iron concentration in the northwestern North Pacific Ocean, *Limnology and Oceanography*, 47(3), 885-892.
- Nakano, M. (1998), Detection of active oxygen species in biological systems, *Cellular And Molecular Neurobiology*, 18(6), 565-579.
- Neilands, J. B. (1981), Microbial Iron Compounds, *Annual Reviews of Biochemistry*, 50, 715.
- Neilands, J. B. (1995), Siderophores - Structure And Function Of Microbial Iron Transport Compounds, *Journal Of Biological Chemistry*, 270(45), 26723-26726.
- Nelson, N. B., C. A. Carlson, and D. K. Steinberg (2004), Production of chromophoric dissolved organic matter by Sargasso Sea microbes, Elsevier Science Bv.
- Nelson, N. B., D. A. Siegel, C. A. Carlson, C. Swan, W. M. Smethie, and S. Khatiwala (2007), Hydrography of chromophoric dissolved organic matter in the North Atlantic, *Deep-Sea Research Part I-Oceanographic Research Papers*, 54(5), 710-731.
- Neuman, E. W. (1934), Potassium Superoxide and the Three-Electron Bond, *The Journal of Chemical Physics*, 2(1), 31-33.
- O'Sullivan, D. W., P. J. Neale, R. B. Coffin, J. B. Boyd, and C. L. Osburn (2005), Photochemical production of hydrogen peroxide and methylhydroperoxide in coastal waters, *Marine Chemistry*, 97, 14-33.
- Obata, H., H. Karatani, and E. Nakayama (1993), Automated Determination of Iron in Seawater by Chelating Resin Concentration and Chemiluminescence Detection, *Analytical Chemistry*, 65, 1524-1528.
- Obernosterer, I., P. Ruardij, and G. J. Herndl (2001), Spatial and diurnal dynamics of dissolved organic matter (DOM) fluorescence and H₂O₂ and the photochemical

- oxygen demand of surface water DOM across the subtropical Atlantic Ocean, *Limnol. Oceanogr.*, *46*(3), 632-643.
- Oda, T., A. Nakamura, M. Shikayama, I. Kawano, A. Ishimatsu, and T. Muramatsu (1997), Generation of Reactive Oxygen Species by Raphidophycean Phytoplankton, *Biosci. Biotechnol. Biochem.*, *61*, 1658-1662.
- Olson, R. J., S. W. Chisholm, E. R. Zettler, M. A. Altabet, and J. A. Dusenberry (1990), Spatial and temporal distributions of prochlorophyte picoplankton in the North Atlantic Ocean, *Deep-Sea Research*, *37*, 1033-1051.
- Oosthuizen, M. M. J., M. E. Engelbrecht, H. Lambrechts, D. Greyling, and R. D. Levy (1997), The effect of pH on chemiluminescence of different probes exposed to superoxide and singlet oxygen generators, *Journal of Bioluminescence and Chemiluminescence*, *12*(6), 277-284.
- Öztürk, M., P. Croot, S. Bertilsson, K. Abrahamsson, B. Karlson, R. Davis, M. Chierici, and E. Sakshaug (2004), Iron enrichment and photoreduction of iron under PAR and UV in the presence of hydrocarboxylic acid: Implications for phytoplankton growth in the Southern Ocean., *Deep-Sea Research II*, *51*(22-24), 2841-2856.
- Petasne, R. G., and R. G. Zika (1987), Fate of Superoxide in Coastal Sea-Water, *Nature*, *325*(6104), 516-518.
- Pollard, R. T., et al. (2009), Southern Ocean deep-water carbon export enhanced by natural iron fertilization, *Nature*, *457*(7229), 577-U581.
- Pradhan, Y., S. J. Lavender, N. J. Hardman-Mountford, and J. Aiken (2006), Seasonal and inter-annual variability of chlorophyll-a concentration in the Mauritanian upwelling: Observation of an anomalous event during 1998-1999, *Deep Sea Research Part II: Topical Studies in Oceanography*, *53*(14-16), 1548-1559.
- Pronai, L., H. Nakazawa, K. Ichimori, Y. Sagusa, T. Ohkubo, K. Hiramatsu, S. arimori, and J. Fehrer (1992), Time Course Of Superoxide Generation By Leukocytes-The MCLA Chemiluminescence System, *Inflammation*, *16*(5), 437-449.
- Rose, A. L., and D. Waite (2006), Role of superoxide in the photochemical reduction of iron in seawater, *Geochimica et Cosmochimica Acta*, *70*(15), 3869-3882.
- Rose, A. L., J. W. Moffett, and T. D. Waite (2008), Determination of Superoxide in Seawater Using 2-Methyl-6-(4-methoxyphenyl)-3,7- dihydroimidazo[1,2-a]pyrazin-3(7H)-one Chemiluminescence, *Anal. Chem.*, *80*(4), 1215-1227.
- Rose, A. L., T. P. Salmon, T. Lukondeh, B. A. Neilan, and T. D. Waite (2005), Use of superoxide as an electron shuttle for iron acquisition by the marine cyanobacterium *Lyngbya majuscula*, *Environmental Science & Technology*, *39*(10), 3708-3715.
- Rue, E. L., and K. W. Bruland (1995), Complexation of iron(III) by natural organic ligands in the Central North Pacific as determined by a new competitive ligand equilibration/adsorptive cathodic stripping voltammetric method, *Marine Chemistry* *50*, 117-138.
- Sañudo-Wilhelmy, S. A., A. B. Kustka, C. J. Gobler, D. A. Hutchins, M. Yang, K. Lwiza, J. Burns, D. G. Capone, J. A. Raven, and E. J. Carpenter (2001), Phosphorus limitation of nitrogen fixation by *Trichodesmium* in the central Atlantic Ocean, *Nature*, *411*(6833), 66-69.
- Sawyer, D. T., and J. S. Valentine (1981), How Super Is Superoxide, *Accounts of Chemical Research*, *14*(12), 393-400.
- Sayyed, R. Z., and S. B. Chincholkar (2006), Purification of siderophores of *Alcaligenes faecalis* on amberlite XAD, *Bioresource Technology*, *97*(8), 1026-1029.
- Schlosser, C., and P. L. Croot (2008), Application of cross-flow filtration for determining the solubility of iron species in open ocean seawater, *Limnology and Oceanography: Methods*, *6*, 630-642.

- Scott, D. T., D. M. McKnight, E. L. Blunt-Harris, S. E. Kolesar, and D. R. Lovley (1998), Quinone moieties act as electron acceptors in the reduction of humic substances by humics-reducing microorganisms, *Environmental Science & Technology*, 32(19), 2984-2989.
- Sedwick, P. N., E. R. Sholkovitz, and T. M. Church (2007), Impact of anthropogenic combustion emissions on the fractional solubility of aerosol iron: Evidence from the Sargasso Sea, *Geochem. Geophys. Geosyst.*, 8, 21.
- Sherman (2005), Electronic structures of iron(III) and manganese(IV) (hydr)oxide minerals: Thermodynamics of photochemical reductive dissolution in aquatic environments, *Geochimica et Cosmochimica Acta*, 69(13), 3249–3255.
- Siffert, C., and B. Sulzberger (1991), Light-Induced Dissolution of Hematite in the Presence of Oxalate - a Case-Study, *Langmuir*, 7(8), 1627-1634.
- Smetacek, V., H. J. W. DeBaar, U. V. Bathmann, K. Lochte, and M. M. R. VanderLoeff (1997), Ecology and biogeochemistry of the Antarctic Circumpolar Current during austral spring: A summary of Southern Ocean JGOFS cruise ANT X/6 of RV Polarstern, *Deep-Sea Res. Part II-Top. Stud. Oceanogr.*, 44(1-2), 1-21.
- Smirnov, A., et al. (2009), Maritime Aerosol Network as a component of Aerosol Robotic Network, *J. Geophys. Res.-Atmos.*, 114.
- Smith, R. C., and K. S. Baker (1981), Optical-Properties Of The Clearest Natural-Waters (200-800 Nm), *Appl. Optics*, 20(2), 177-184.
- Steinberg, D. K., N. B. Nelson, C. A. Carlson, and A. C. Prusak (2004), Production of chromophoric dissolved organic matter (CDOM) in the open ocean by zooplankton and the colonial cyanobacterium *Trichodesmium* spp, *Mar. Ecol.-Prog. Ser.*, 267, 45-56.
- Stookey, L. L. (1970), Ferrozine - A New Spectrophotometric Reagent for Iron, *Analytical Chemistry*, 42, 779-781.
- Stuut, J. B., M. Zabel, V. Ratmeyer, P. Helmke, E. Schefuss, G. Lavik, and R. Schneider (2005), Provenance of present-day eolian dust collected off NW Africa, *J. Geophys. Res.-Atmos.*, 110(D4), 14.
- Talbot, R. W., R. C. Harriss, E. V. Browell, G. L. Gregory, D. I. Sebacher, and S. M. Beck (1986), Distribution and Geochemistry of Aerosols in the Tropical North-Atlantic Troposphere - Relationship to Saharan Dust, *J. Geophys. Res.-Atmos.*, 91(D4), 5173-5182.
- Tampo, Y., M. Tsukamoto, and M. Yonaha (1998), The antioxidant action of 2-methyl-6-(p-methoxyphenyl)-3,7-dihydroimidazo[1,2-K]pyrazin-3-one (MCLA), a chemiluminescence probe to detect superoxide anions, *FEBS Letters* 430, 348-352.
- Tyrrell, T., E. Maranon, A. J. Poulton, A. R. Bowie, D. S. Harbour, and E. M. S. Woodward (2003), Large-scale latitudinal distribution of *Trichodesmium* spp. in the Atlantic Ocean, *J. Plankton Res.*, 25(4), 405-416.
- Voelker, B. M., and D. L. Sedlak (1995), Iron Reduction by Photoproduced Superoxide in Seawater, *Marine Chemistry*, 50(1-4), 93-102.
- Voelker, B. M., and B. Sulzberger (1996), Effects of fulvic acid on Fe(II) oxidation by hydrogen peroxide, *Environmental Science & Technology*, 30(4), 1106-1114.
- Voelker, B. M., F. M. M. Morel, and B. Sulzberger (1997), Iron redox cycling in surface waters: Effects of humic substances and light, *Environmental Science & Technology*, 31(4), 1004-1011.
- Voelker, B. M., D. L. Sedlak, and O. C. Zafiriou (2000), Chemistry of superoxide radical in seawater: Reactions with organic Cu complexes, *Environ. Sci. Technol.*, 34(6), 1036-1042.
- Volker, C., and D. A. Wolf-Gladrow (1999), Physical limits on iron uptake mediated by siderophores or surface reductases, *Marine Chemistry*, 65(3-4), 227-244.

- Voss, M., P. Croot, K. Lochte, M. Mills, and I. Peeken (2004), Patterns of Nitrogen Fixation along 10°N in the Tropical Atlantic, *Geophys. Res. Lett.*, *31*, L23S09, doi:10.1029/2004GL020127.
- Wagener, T., E. Pulido-Villena, and C. Guieu (2008), Dust iron dissolution in seawater: Results from a one-year time-series in the Mediterranean Sea, *Geophysical Research Letters*, *35*(16), 6.
- Weite, T. D., and F. M. M. Morel (1984), Photoreductive Dissolution of Colloidal Iron-Oxide - Effect of Citrate, *Journal of Colloid and Interface Science*, *102*(1), 121-137.
- Waterbury, J. B., S. W. Watson, R. R. L. Guillard, and L. E. Brand (1979), Widespread Occurrence of a Unicellular, Marine, Planktonic, Cyanobacterium, *Nature*, *277*(5694), 293-294.
- Waterbury, J. B., S. W. Watson, F. W. Valois, and D. G. Franks (1986), Biological and Ecological Characterization of the Marine Unicellular Cyanobacterium *Synechococcus*, *Canadian Bulletin of Fisheries and Aquatic Science*, *214*, 74-120.
- Weber, L., C. Volker, M. Schartau, and D. A. Wolf-Gladrow (2005), Modeling the speciation and biogeochemistry of iron at the Bermuda Atlantic Time-series Study site, *Glob. Biogeochem. Cycle*, *19*(1), 26.
- Weber, L., C. Volker, A. Oschlies, and H. Burchard (2007), Iron profiles and speciation of the upper water column at the Bermuda Atlantic Time-series Study site: a model based sensitivity study, *Biogeosciences*, *4*(4), 689-706.
- Wells, M. L., and L. M. Mayer (1991), The Photoconversion of Colloidal Iron Oxyhydroxides in Seawater, *Deep-Sea Research Part a-Oceanographic Research Papers*, *38*(11), 1379-1395.
- Ye, Y., C. Völker, and D. A. Wolf-Gladrow (2009), Impact of dust deposition on Fe biogeochemistry at the Tropical Eastern North Atlantic Time Series-series Observatory, *Biogeosciences Discuss.*, *6*, 4305-4359.
- Yocis, B. H., D. J. Kieber, and K. Mopper (2000), Photochemical production of hydrogen peroxide in Antarctic Waters, *Deep Sea Research Part I : Oceanographic Research*, *47*(6), 1077-1099.
- Yuan, J., and A. M. Shiller (1999), Determination of Subnanomolar Levels of Hydrogen Peroxide in Seawater by Reagent-Injection Chemiluminescence Detection, *Analytical Chemistry*, *71*, 1975-1980.
- Yuan, J., and A. M. Shiller (2001), The distribution of hydrogen peroxide in the southern and central Atlantic ocean, *Deep-Sea Research II*, *48*, 2947-2970.
- Zafiriou, O. C. (1990), Chemistry of superoxide ion (O_2^-) in seawater. I. pK_{asw}^* (HOO) and uncatalysed dismutation kinetics studied by pulse radiolysis, *Marine Chemistry*, *30*, 31-43.
- Zafiriou, O. C., B. M. Voelker, and D. L. Sedlak (1998), Chemistry of the superoxide radical (O_2^-) in seawater: Reactions with inorganic copper complexes, *Journal of Physical Chemistry A*, *102*(28), 5693-5700.

**Application of a Superoxide (O_2^-) thermal source (SOTS-1)
for the determination and calibration of O_2^- fluxes in
seawater**

Heller, M.I. and Croot, P.L.



Application of a superoxide (O_2^-) thermal source (SOTS-1) for the determination and calibration of O_2^- fluxes in seawater

M.I. Heller, P.L. Croot*

FB2 Marine Biogeochemie, Leibniz-Institut für Meereswissenschaften (IfM-Geomar), Dienstgebäude Westufer, Düsternbrooker Weg 20, 24105 Kiel, Germany

ARTICLE INFO

Article history:

Received 9 December 2009

Received in revised form 17 March 2010

Accepted 25 March 2010

Available online 1 April 2010

Keywords:

Superoxide

Seawater

Hydrogen peroxide

Chemiluminescence

Spectrophotometry

ABSTRACT

Superoxide (O_2^-) is an important short lived transient reactive oxygen species (ROS) in seawater. The main source of O_2^- in the ocean is believed to be through photochemical reactions though biological processes may also be important. Sink terms for O_2^- include redox reactions with bioactive trace metals, including Cu and Fe, and to a lesser extent dissolved organic matter (DOM). Information on the source fluxes, sinks and concentration of superoxide in the open ocean are crucial to improving our understanding of the biogeochemical cycling of redox active species. As O_2^- is a highly reactive transient species present at low concentrations it is not a trivial task to make accurate and precise measurements in seawater. In this study we developed the appropriate numerical analysis tools and investigated a number of superoxide sources and methods for the purposes of calibrating O_2^- concentrations and/or fluxes specifically in seawater. We found the superoxide thermal source bis(4-carboxybenzyl)hyponitrite (SOTS)-1 easy to employ as a reliable source of O_2^- which could be successfully applied in seawater. The thermal decomposition of SOTS-1 in seawater was evaluated over a range of seawater temperatures using both a flux based detection scheme developed using two spectrophotometric methods: (i) 7-chloro-4-nitrobenzo-2-oxa-1,3-diazole (NBD-Cl) and (ii) ferricytochrome c (FC), or a concentration based detection scheme using a chemiluminescence flow injection method based on the *Cypridina luciferin* analog 2-methyl-6-(p-methoxyphenyl)3-7-dihydroimidazol[1,2- α]pyrazin-3-one (MCLA) as reagent. Our results suggest SOTS-1 is the best available O_2^- source for determining concentrations and fluxes, all detection systems tested have their pros and cons and the choice of which to use depends more on the duration and type of experiment that is required.

© 2010 Elsevier B.V. All rights reserved.

1. Introduction

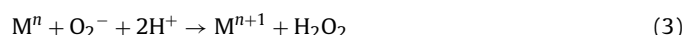
1.1. The reactivity of the superoxide anion radical (O_2^-) and its conjugated acid perhydroxyl radical (HO_2)

Superoxide (O_2^- : IUPAC name dioxide(\bullet 1-)) is a reactive intermediate in the redox cycling of water to oxygen, through both photosynthesis and respiration processes. In natural waters superoxide is predominantly a product of photochemical processes with organic chromophores (dissolved organic matter (DOM)) [1], though biological pathways also exist [2–3]. Superoxide and its conjugated acid (HO_2 the hydroperoxyl radical: IUPAC name hydridodioxigen(\bullet)), with a pK_a in seawater of 4.60 ± 0.15 [4], are known to mediate many transformations in biological and chemical systems in the ocean. The perhydroxyl radical reacts with itself or with superoxide to form hydrogen peroxide (H_2O_2) and oxygen

(O_2) via the uncatalysed dismutation reaction:



The observed rate constant k_D (combing reactions (1) and (2) above) for the uncatalysed disproportionation of O_2^- has been measured in seawater as a function of pH [4,5]. Superoxide can also act both as a reductant and oxidant and in seawater it is suggested [5–7] to play an important role in mediating redox changes between various chemical species and in with the bio-relevant trace metals Fe and Cu:



Combined together reactions (3) and (4) result in a catalytic cycle for superoxide dismutation, (catalyzed dismutation pathway). Typically reactions with the free metal species of Cu and Fe are extremely fast [8] and so only a small amount of metal is required to catalyze superoxide dismutation. In nature this is exploited in the design of Cu, Zn, Mn or Fe centered superoxide dismutases (SOD)

* Corresponding author. Tel.: +49 431 600 4207; fax: +49 431 600 4202.

E-mail address: pcroot@ifm-geomar.de (P.L. Croot).

which act within the cell to remove O_2^- produced by photosynthesis or other cellular processes [9]. Reactions with DOM can also be described by equations (3) and (4) and were found to be significant to the overall O_2^- decay in coastal seawater [10] but not so in the open ocean waters of the Southern Ocean [5]. Little is currently known on either the sources or products of superoxide reactions with DOM but it is clear that it is a major pathway for the oxidation of organic matter in the euphotic zone.

Assessing changes in metal redox speciation is critical to developing our understanding of metal biogeochemistry in the ocean. For example the O_2^- mediated cycling between the thermodynamically favoured, but poorly soluble, Fe(III) species and the more soluble reduced Fe(II) form could simultaneously increase the bioavailability of iron and prolong its residence time in the open ocean as suggested by recent modeling studies [11–13]. Information regarding O_2^- fluxes is also important for balancing the sources and sinks of the daughter product of O_2^- , H_2O_2 . In seawater H_2O_2 also plays an important role in redox reactions which involve biogeochemical relevant trace metals [14,15].

Thus in order to improve our present understanding of redox cycles in the ocean it is critical that we can accurately determine the production, instantaneous concentration ($[O_2^-]_i$) and decay of ROS like O_2^- and H_2O_2 in seawater under normal environmental conditions. Quantitative work on O_2^- in seawater has been seriously handicapped by the lack of a simple method to produce the radical at a constant and known rate. The present paper summarizes previous work on this topic of relevance to seawater and our own findings as we tested different sources and detection methods in an effort to determine O_2^- accurately. Our work suggests that the O_2^- thermal source SOTS-1 can be successfully used as a calibration source for O_2^- fluxes in seawater.

1.1.1. Reaction kinetics of superoxide

Based on previous research on O_2^- reactions in seawater with metal complexes [5–7,16] and organic matter [10] workers in this field have developed the following reactivity scheme for O_2^- :

$$\frac{\partial [O_2^-]}{\partial t} = 2k_D [O_2^-]^2 + \sum k_M [M]_X [O_2^-] + k_{org} [O_2^-] \quad (5)$$

where the metal reactions (k_M) include both the Cu(II)/Cu(I) and Fe(III)/Fe(II) redox pairs (equation (6)), the reaction with organic substances is described by the first order rate k_{org} .

$$\sum k_M [M]_X = (k_{Cu(I)} [Cu(I)] + k_{Cu(II)} [Cu(II)] + k_{Fe(II)} [Fe(II)] + k_{Fe(III)} [Fe(III)]) \quad (6)$$

The observed rate of superoxide decay can then be written as follows with only a single term each for the first order and second order rate components

$$\frac{\partial [O_2^-]}{\partial t} = 2k_D [O_2^-]^2 + k_{obs} [O_2^-] \quad (7)$$

where k_{obs} is described as the sum of the first order reaction rates.

$$k_{obs} = \sum k_M [M]_X + k_{org} \quad (8)$$

The complexing agent diethylenetriaminepentaacetic acid (DTPA) can be added to complex all the trace metals in solution and in this case $k_{obs} = k_{org}$ [10].

In the following sections we provide an overview about the impact of superoxide in the environment, and its sources and existing detection methods which are currently used in research. This section is important as in the course of this work we came across several inconsistencies regarding the production and detection methods for superoxide which forced us to invest a considerable

amount of time to read and conduct laboratory studies to recognize and understand these inconsistencies. The availability of aqueous O_2^- solutions, free from interfering materials or metal impurities is one of the most essential requirements for the study of HO_2/O_2^- chemistry. In the experimental section of this work we report the first results obtained using the superoxide thermal source SOTS-1 in seawater, a reagent that produces O_2^- without apparently many of the limitations found in other sources.

1.2. Sources of superoxide in natural waters

There are several sources for O_2^- that are known in seawater and they are discussed in turn below. Fig. 1 provides a schematic overview of the known sources and sinks for superoxide in the ocean.

1.2.1. Photochemistry

The existence of O_2^- in seawater was first proposed by Swallow [17] who suggested that O_2^- could be formed by reactions of the hydrated electron with O_2 dissolved in seawater. Later researchers provided qualitative or indirect evidence for the photochemical production of O_2^- in aqueous solutions based on the assumption that its decomposition is the major source for H_2O_2 [18–19]. In sunlit seawater O_2^- quasi-steady concentrations of ~10–100 nM were estimated based on the assumption that only the uncatalysed dismutation pathway was occurring [18,20].

Measurements of O_2^- fluxes in seawater were obtained from Caribbean waters [1] illuminated with a solar simulator and the fluxes determined by using isotopically labelled ^{15}NO gas to react with O_2^- [21] to form peroxyntirite which rearranges to form nitrate. Using this approach photochemical production rates for O_2^- in surface waters followed a seasonal cycle with 0.1–6 nM min⁻¹ sun⁻¹ (where sun⁻¹ is the intensity of the solar simulator used [22]) in spring- and 0.2–8 nM min⁻¹ sun⁻¹ in the autumn. Overall it was found that approximately 35% of the total radical flux was present as O_2^- .

The main mechanism for the production of O_2^- is thought to be from the absorption of a photon by DOM which excites this molecule into a triplet state which subsequently reacts with O_2 (naturally occurring in the triplet state) to form O_2^- and a carbocation [23]. Direct measurements of the apparent quantum yield for O_2^- are not available, however related data does exist for the formation of the reaction product H_2O_2 [23,24] and indicates that UV wavelengths, 300–400 nm, are the major source of O_2^- in seawater. Photochemical production of O_2^- in seawater based on measurements of H_2O_2 *in situ* formation fluxes [24–26] indicate rates in surface waters of 9 (Antarctic) to 17 nM h⁻¹ (Tropical Atlantic), assuming the rate of O_2^- production is twice that of H_2O_2 .

1.2.2. Reactions with O_2 and H_2O_2

Superoxide can also be produced throughout the water column via reactions between O_2 and reduced species and to a lesser extent between H_2O_2 and oxidized species. In seawater this may include the oxidation of free or complexed, Fe(II) or Cu(I) in the water column [14,15,27,28], or alternatively with reduced organic species such as semiquinone radicals [29,30] produced from the reduction of quinone compounds present in DOM [31] and in bacterial cells [32].

1.2.3. Biological production

Superoxide can be formed directly or through side reactions in various enzymatic processes [33,34] and by the auto-oxidation of a number of biologically significant compounds (see above). In laboratory experiments O_2^- production has been observed in phytoplankton cultures (see the review by Marshall et al. [35]) and is suggested to enhance the toxicity of algal exudates or to serve as

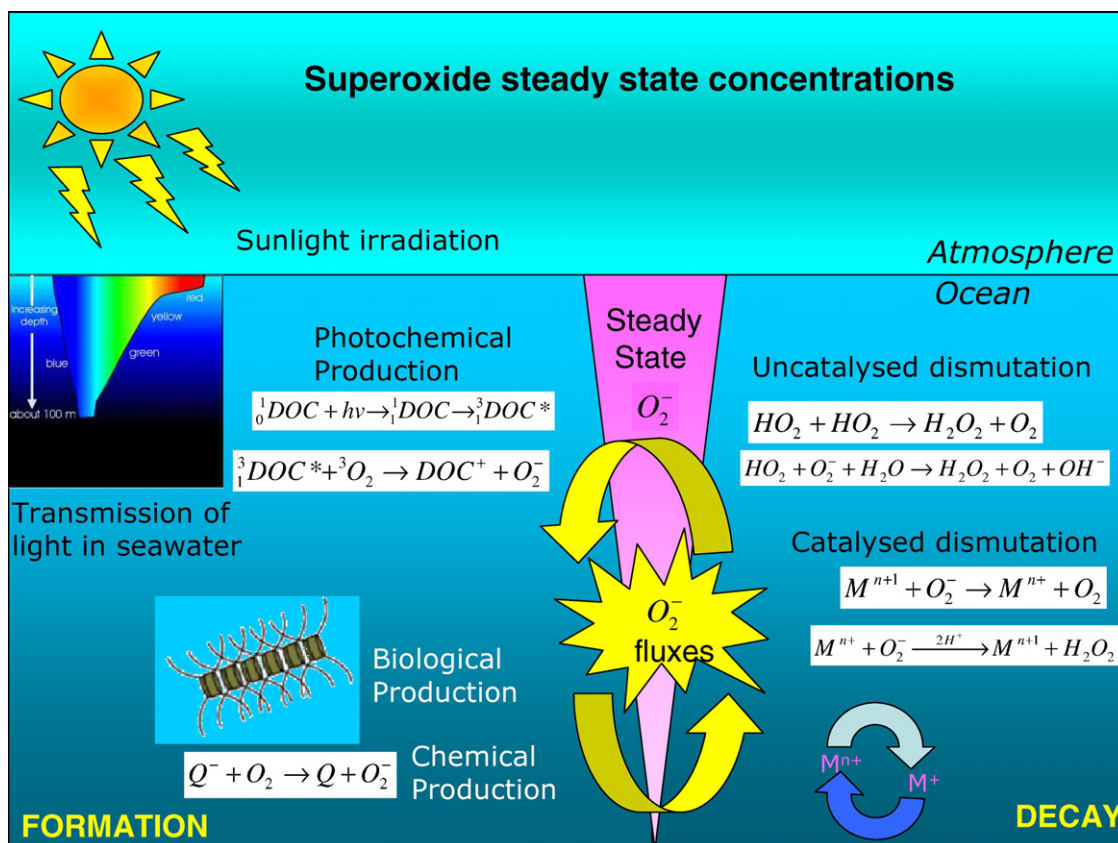


Fig. 1. Schematic of superoxide production and decay pathways in the ocean.

an allelopathic agent against bacterial fouling [36]. An alternative hypothesis suggested for open ocean species is that O_2^- is produced in response to iron limitation as a mechanism to reduce Fe(III) to the more bioavailable Fe(II) [37] though other researchers suggest that this is a 'futile' exercise as the Fe(II) is rapidly oxidized back to Fe(III) [38].

1.3. Salt effects and problems with the use of Good's buffers

Most published studies on O_2^- were conducted in simple solutions and not in a complex media such as seawater. This is important as the chemistry of HO_2/O_2^- is affected by several aspects in seawater. For example the effect of salts on the stability of HO_2 showed different values for NaCl, CaCl_2 and BaCl_2 and these observations can be interpreted as changes in the ionization of HO_2 due to ionic interactions [4]. The effect of this is to cause the lifetime of HO_2 and O_2^- to be 2–5 times longer than in pure water, if only the uncatalysed dismutation pathway exists, due to the interactions of Mg^{2+} and Ca^{2+} with O_2^- and the effect of ionic strength on the dissociation of HO_2 . Zafiriou [4] made the first direct measurements of K_{HO_2} in seawater ($\text{p}K_a^* = 4.60 \pm 0.15$) and measured the dismutation rate k_D to be $5 \pm 1 \times 10^{12} [\text{H}^+] \text{M}^{-2} \text{s}^{-1}$.

It is common practice for experiments in seawater where the pH needs to be controlled to use one of the Good's buffers [39], such as EPPS, HEPES, TRIS or PIPES. This is particularly the case for experiments where the trace metal speciation needs to be controlled as these buffers do not form complexes with the metals of interest. However for experiments with O_2^- it has been found that the amine containing buffers react with H_2O_2 or O_2^- to result in reactive buffer radicals or that even those buffers react with further oxidative compounds resulting in the formation of buffer radicals which react with oxygen to form ROS. Piperazine ring based

buffers like HEPES, EPPS and PIPES were found to produce radical species which have half-lives around 10 min [40]. It was also proposed that H_2O_2 oxidizes not only morpholine ring containing buffers like MOPS and MES but also piperazine ring buffers (PIPES, HEPES, EPPS) [41]. Kirsch et al. [42] suggested a mechanism where oxidative compounds (in their case peroxynitrite or any strong oxidant derived from it) oxidize amine buffers like HEPES and form radicals which further react with O_2 and leads to the formation of O_2^- and subsequently H_2O_2 . Thus they proposed that HEPES or similar organic buffers should be avoided in studies which work with oxidative substances. This finding was confirmed by Hodges and Ingold [43], who whilst working on O_2^- quantification using tetranitromethane (TNM) found that TRIS, HEPES and MOPS react with TNM and the radicals formed through this reactions undergo rapid radical chain processes. They concluded from their work that any compound which contains the N-CH chemical functionality will result in these reactions and should so be avoided in systems used for O_2^- quantification. In the present work we did not use Good's buffers for the reasons outlined above.

1.4. Superoxide sources for use with seawater

While O_2^- is stable in aprotic solvents like DMSO, for studies in seawater the difficulty in preparing a standard solution for calibration of detection methods is a major problem. The use of standards prepared in aprotic solvents may cause interferences due to the introduction of high concentrations of organic solvent. Similarly standards prepared in aqueous solution must be maintained at high pH to reduce the loss due to the uncatalysed dismutation reaction. In the case of solution with appreciable metal contaminants, complexing agents such as DTPA, are typically added to slow the loss rate of O_2^- .

Table 1

Compilation of extinction coefficients (ϵ , $\text{L mol}^{-1} \text{cm}^{-1}$) for O_2^- and $\text{H}_2\text{O}_2/\text{HO}_2^-$ at pH 13 for selected wavelengths as used in this study for spectrophotometric determination of the O_2^- concentration in KO_2 preparations. Data is drawn from Bielski and Allen [50] for $\text{H}_2\text{O}_2/\text{HO}_2^-$ and from Bielski et al. [8] for O_2^- .

λ (nm)	Extinction coefficient ϵ ($\text{L mol}^{-1} \text{cm}^{-1}$) (aqueous Solution pH 13)	
	$\text{H}_2\text{O}_2/\text{HO}_2^-$	O_2^-
	230	440
240	340	2345
250	260	2260
260	180	1940

1.4.1. Photochemical production in ketone/alcohol solutions

McDowell [44] proposed that O_2^- can be produced in air or O_2 saturated aqueous solution by the irradiation of a solution containing a ketone (acetone or benzophenone) with a primary or secondary alcohol (ethanol or 2-propanol). This approach has been used extensively over the intervening years for work in artificial seawater (NaHCO_3 2 mM, NaCl 10 mM) in combination with DTPA [10,45,46].

In the course of this work we applied the method of McDowell in order to generate O_2^- for the purposes of a calibrated standard solution, however our investigations revealed a number of factors apparently overlooked in previous works: (1) Ketones absorb in the same UV region as O_2^- , between 200 and 340 nm [47] and for most of the published protocols the majority of the absorbance at the wavelengths for quantification of O_2^- was in fact due to acetone and the assumption that it was solely due to O_2^- was false. Simply taking the absorption difference between the solution prior to the irradiation and after also is problematic as photochemical work suggests that for the reaction system containing 2-propanol and ketones (e.g. acetophenone or benzophenone) the overall reaction pathway is the oxidation of 2-propanol to acetone [48]. (2) The photogeneration of O_2^- will also generate $\text{H}_2\text{O}_2/\text{HO}_2^-$ [49] which also absorbs, although weakly, in the same region as O_2^- [50] (Table 1) and this must be corrected for. (3) Also alarmingly several studies using this method added DTPA to their reaction solution prior to irradiation in an effort to complex potential trace metal impurities. However it is well known that DTPA itself and in particular its ferric complexes, degrade under UV irradiance [51,52] or even sunlight [53]. Thus it is obvious that DTPA should only be added after irradiation.

1.4.2. Xanthine/xanthine oxidase

Xanthine oxidase (XO) catalyzes the oxidation of xanthine (X) or hypoxanthine (HX) in the presence of O_2 to form uric acid with the production of O_2^- or H_2O_2 . The XO/X method is used frequently due to the commercial availability of the reactants and the ease of use. Recently several papers have been published using XO/X as O_2^- source in seawater [37,54–56]. The flux of O_2^- varies as a function of pH and other conditions, at a pH of 7 there is believed to be a production of 20% O_2^- and 80% H_2O_2 [57]. Other radicals, such as carbonate radicals [58], may also be produced. The flux of the univalent pathway to O_2^- increases at alkaline pH, up to approximately pH 8, and under high pO_2 or low substrate (X or HX) conditions [57,59]. Calibration of the XO/X source is complicated in seawater by the need to accurately control and measure the pH during the experiment, something which is not a trivial task [60] and the source strength of XO/X may vary between samples. For quantitative work where a steady rate of O_2^- formation is required, the X/XO system was found to be unsuitable as XO becomes deactivated during its turnover decreasing the rate of O_2^- formation [61]. Additionally TNM reacts with O_2^- directly formed in the enzyme while Ferricytochrome c (FC) only reacts with free diffusible O_2^- [58,61]. Many researchers have also observed that commercial XO prepa-

Table 2

Experimentally determined values of the thermal production of superoxide by SOTS-1 in seawater.

	Thermal degradation rate k (s^{-1}) for SOTS-1 in Antarctic Seawater	
	NBD	FC
37.0 °C	$3.0 \pm 1.2 \times 10^{-5}$	$1.7 \pm 0.3 \times 10^{-4}$
30.0 °C	$4.3 \pm 0.4 \times 10^{-5}$	$7.0 \pm 1.3 \times 10^{-5}$
25.0 °C	$2.0 \pm 1.4 \times 10^{-5}$	$2.2 \pm 0.6 \times 10^{-5}$
20.0 °C	–	$1.7 \pm 0.4 \times 10^{-5}$
10.0 °C	$6.1 \pm 11 \times 10^{-6}$	$1.7 \pm 0.8 \times 10^{-5}$

rations are contaminated with iron or other trace metals [61–63]. This limits the use of XO only to experiments where trace metals are buffered with the use of DTPA or desferal and thus reactions between trace metals and O_2^- cannot be studied.

Table 2.

1.4.3. Pulse radiolysis

Initial research on O_2^- chemistry in aqueous solutions utilized pulse radiolysis to generate O_2^- by ionizing radiation under controlled conditions with determination of reaction products by UV-Vis spectroscopy [64]. The primary radicals generated by pulse radiolysis (e^- , H and OH) react rapidly with O_2 to form O_2^- , however in seawater OH reacts rapidly with bromide, requiring formate or methanol to be added to convert OH into O_2^- via borate or carbonate catalysis [4]. The use of pulse radiolysis for fieldwork is not practical as it requires the use of a linear accelerator or ^{60}Co source [65].

1.4.4. KO_2

Previously KO_2 was widely used to examine the reactivity of O_2^- as it was found to be a cheap direct source of O_2^- . The main problem with using KO_2 is the relatively low final yield [66] (~15%) and the generation of high concentrations of H_2O_2 which must be corrected for (see earlier). KO_2 was previously perceived to be contaminated with metals based on work performed during the 1970s and 1980s, however the observed contamination may have been related to the use of non trace metal free equipment and reagents [67]. Recently we reexamined the metal content of commercial KO_2 and found that trace metal impurities were low and KO_2 could be successfully used as a calibration source for O_2^- decay experiments in seawater [5]. Due to the nature of KO_2 it can only be used for pulse experiments and not as a source for flux measurements.

1.4.5. Superoxide thermal source SOTS-1

Current methods which generate O_2^- in relative high concentrations will favor the uncatalysed dismutation resulting in a high H_2O_2 production also. In order to mimic the *in vivo* situation where O_2^- is produced very slowly but continuously over a long duration Ingold et al. [68] synthesized a series of suitable azo compounds (superoxide thermal sources—SOTS) which decompose thermally to yield either directly or indirectly electron rich carbon-centered radicals. Many of those primary radicals are known to react with O_2 to yield carbocations and O_2^- [69].

The first of this novel family of compounds was di(4-carboxybenzyl)hyponitrite (SOTS-1). The decomposition of SOTS-1 in water at 37 °C and a pH of 7 was shown to follow first order decay (half-life 4900 s) and yield a O_2^- formation of 40 mol%. The critical step in the overall reaction involves a 1,2-H-atom shift [70] which converts the primary alkoxy radical into the desired electron rich carbon-centered radical (Fig. 2). This kind of radical rearrangement occurs only in the presence of water or alcohols and represents a pathway to produce O_2^- without direct or enzymatic formation of H_2O_2 [71]. SOTS-1 is reasonably soluble in water (1.5 mM)

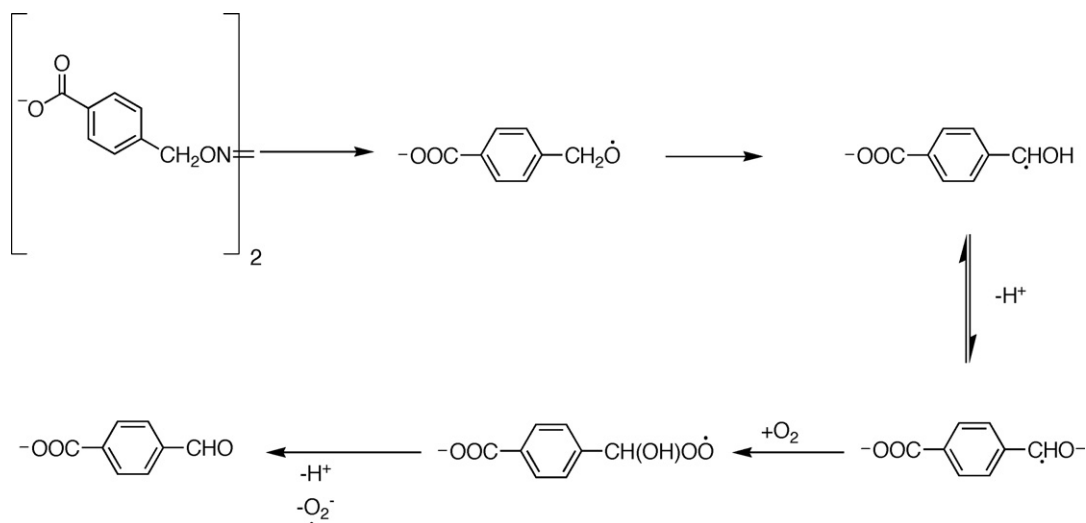


Fig. 2. The decomposition pathway of SOTS-1 and its reaction with oxygen with subsequent release of superoxide (Figure adapted from Ingold et al., 1997).

and the decay rate is independent of pH over the pH range 6.5–8 [68,72].

1.4.6. Ultrasonication of water

It is often overlooked in studies with phytoplankton that ultrasonication of samples either for cleaning cell or breaking them, does produce both O_2^- and subsequently H_2O_2 [73].

1.4.7. Alkaline DMSO

O_2^- can also be generated in alkaline air saturated DMSO solutions from the reaction between DMSO and OH^- to produce a methyl sulphanyl carbanion which reacts with O_2 to produce O_2^- [74,75]. Alternatively the direct reaction between hydroxide anions and oxygen can occur:



In the DMSO case the OH^\bullet radical is scavenged quickly by DMSO. This reaction can also occur in water under the high OH^- concentrations typically used to preserve O_2^- [76] and has been proposed as a source for O_2^- in experiments.

1.5. Superoxide detection methods used in seawater

1.5.1. Spectrophotometry

The spectrometric detection of O_2^- can be achieved by the direct measurement of the absorbance of O_2^- itself (direct method) or through the reaction with a specific chemical (indirect method) which results in an absorption change. Superoxide absorbs moderately in the UV (Table 1) [8]. Calibration of the O_2^- concentration by the direct method is complicated as H_2O_2 [50] and many organic molecules also absorb at these wavelengths and must be corrected for. This presence of H_2O_2 in O_2^- solutions is difficult to avoid as along with O_2 it is a major byproduct from the reactions of O_2^- in aqueous solutions. This complication has driven research into finding reagents that react specifically with O_2^- to form distinct and easy detectable species. In the following sections we examine the most frequently used reagents for this purpose and assess their applicability to seawater work (For more information on other reagents see recent reviews by Soh [77] and Bartosz [78]).

1.5.1.1. Ferricytochrome c (FC). The reduction of ferricytochrome c (Fe(III)) to ferrocyanochrome c (Fe(I)) by O_2^- is a rapid single electron process which can be monitored via spectrophotometry at 555 nm [33]. The rate constant for the reaction between O_2^- and FC has

been observed to be sufficiently high ($10^6 \text{ M}^{-1} \text{ s}^{-1}$) [79–81] to compete at μM concentrations of FC with the uncatalysed dismutation reaction at neutral pH [54,81]. Additionally the reaction of H_2O_2 with FC is insignificant when $[H_2O_2] < 0.1 \text{ mM}$ [86]. If FC is present in significant concentrations there will be no extra H_2O_2 production as O_2^- is oxidized back to O_2 . FC can however be reduced by molecules other than O_2^- [83] most notably Cu(I) complexes [84], alternatively reduced FC may be reoxidized to FC by Cu and Mn redox species [85–86].

1.5.1.2. Nitroblue tetrazolium (NBT). The ditetrazolium ion NBT^{2+} can be reversibly reduced to diformazan by the stepwise addition of four electrons with the formation of the transient NBT^+ (MF) and one stable intermediate consisting of one tetrazolium and one formazan center [87]. NBT has become a widely used *in situ* reagent for the detection of O_2^- although its use as a quantitative reagent has been less successful because of its complex chemistry and complicated acid-base properties [88]. One major problem with NBT is that the reaction products (mono- and diformazans) are only slightly soluble in aqueous solution. NBT can also be reduced by CO_2^- [88] and Glucose oxidase [89]. When used with X/XO NBT may react directly with XO [90] and in combination with detergents such as Triton X-100 marked increases in the reduction of NBT were observed [91], similarly in O_2^- DMSO solutions NBT was found to react with the methyl sulphanyl carbanion while FC did not [92]. The production of O_2^- itself by the oxidation of NBT^+ with O_2 can also be significant under certain conditions [65,93].

1.5.1.3. NBD-CL (7-chloro-4-nitrobenzo-2-oxa-1,3-diazole). NBD-CL was originally synthesized as a fluorescence reagent for amino acids and amines [94,95] and thiols [96]. In a recent work it was shown [97] that NBD-CL can also be used for the detection of O_2^- through the formation of a reaction product by either absorbance spectroscopy (at 470 nm) or via fluorescence (excitation 470 nm, emission 550 nm). NBD-CL reacts with nucleophiles [98] to form reversible Meisenheimer adducts [99].

1.5.2. Chemiluminescence detection methods

Several compounds have been used previously for the chemiluminescence detection of O_2^- . Luminol, which is frequently used for other chemiluminescence applications, does react with O_2^- but is not a specific indicator for O_2^- [100,101]. Similarly lucigenin was originally proposed to be useful for the detection of low levels of O_2^- [102,103], but later work showed an auto-oxidation reaction

leading to an overestimate of the O_2^- concentration and its use as a O_2^- probe was not recommended [104].

The most widely used chemiluminescence probe for O_2^- has been the *Cypridina luciferin* analog, 2-methyl-6-(p-methoxyphenyl)3-7-dihydroimidazol[1,2- α]pyrazin-3-one (MCLA) [105]. The chemiluminescence of MCLA by reaction with O_2^- involves the production of an unstable dioxetane, whose decomposition emits light [106] and the reaction is highly specific as shown by Kambayashi and Ogino [107] who tested several different ROS (O_2^- , 1O_2 , OH, Fe(II), alkyl peroxy radical and H_2O_2) and found only O_2^- and 1O_2 were able to induce MCLA chemiluminescence. Background chemiluminescence due to the auto-oxidation of the conjugated base of MCLA with O_2 [108] is reduced when the analytical pH < pK_a for MCLA ($pK_a = 7.75$) [109] and with lower MCLA concentrations [107]. MCLA shows overlapping maxima for chemiluminescence at pH 6 and pH 8.7 using XO/X, while a further maxima exists at pH 9.5 when using KO_2 [110].

1.6. Determining superoxide fluxes or concentrations

1.6.1. Goal of a reagent for superoxide flux determinations

In the present work we were searching for an analytical procedure that could determine O_2^- production fluxes in seawater under both conditions of photochemical and/or biological production. Leaving aside issues related to the chemical specificity of reagents for O_2^- (see recent reviews by Bartosz [78] and Soh [77]) we focus here on the numerical tools required for interpretation of the data. There are two possible analytical approaches; the first by measuring over time the “integrated production” of O_2^- while the second approach is to measure the instantaneous concentration of O_2^- .

1.6.2. Integrated production

For spectrophotometric or fluorometric reagents which react with O_2^- in solution the “integrated production” rate of O_2^- in seawater can be determined by a simple method in which the time rate of change of the absorption/fluorescence of the reagent is used to calculate the O_2^- production rate. The instantaneous production rate is thus a modified version of eq. (7).

$$\frac{\partial[O_2^-]}{\partial t} = PR - 2k_D[O_2^-]^2 - k_{obs}[O_2^-] - k_R[R][O_2^-] \quad (10)$$

where PR is the instantaneous production rate of O_2^- from all sources, k_R is the rate constant for the reaction between the reagent and O_2^- and [R] is the concentration of the reagent. Assuming that the reagent R is converted into the observable species A by only reactions with O_2^- the time dependent formation of A is then:

$$\frac{\partial A}{\partial t} = k_R[R][O_2^-] \quad (11)$$

If the reagent is the dominant sink term for superoxide ($k_R[R] \gg (2k_D[O_2^-] + k_{obs})$) and pseudo steady state conditions are assumed then eq. (10) further simplifies to the following:

$$PR = \frac{\partial A}{\partial t} \quad (12)$$

In our work using SOTS-1 as a O_2^- source, the first order thermal decomposition of the reagent permits the calculation of the time dependence of the concentration of SOTS-1 under conditions of constant temperature:

$$[SOTS]_t = [SOTS]_0 e^{-kt} \quad (13)$$

where k is the temperature dependent decay rate of the SOTS-1. In the absence of other O_2^- sources the PR from SOTS-1 can be described as follows, assuming a 0.4 stoichiometry for the reactions

between the SOTS-1 radical and O_2 [68]:

$$PR = 0.4k[SOTS]_t \quad (14)$$

If the analytical reagent reacting with O_2^- is present in high enough concentration so that it can be considered the only reaction affecting O_2^- concentrations then by equation (12) we have:

$$\frac{\partial A}{\partial t} = 0.4k[SOTS]_t \quad (15)$$

the solution to the time dependent concentration of A (for reagents such as NBD, NBT or FC) is then:

$$A_t = A_{SOTS}(1 - e^{-kt}) + A_0 \quad (16)$$

where A_t is the concentration of A at time t , A_0 is the concentration of A at time $t=0$ and A_{SOTS} is the maximum yield of A when the SOTS-1 has completely reacted ($A_{SOTS} = 0.4[SOTS]_0$). This equation can be rearranged to solve for k as a function of t .

$$-kt = \ln \left(1 - \frac{(A_t - A_0)}{A_{SOTS}} \right) \quad (17)$$

If there is an additional source of O_2^- (e.g. thermal or photochemical) that is produced at a constant rate m (mol s^{-1}) the equation then becomes:

$$PR = 0.4k[SOTS]_t + m = \frac{\partial A}{\partial t} \quad (18)$$

which has the following solution:

$$A_t = A_{SOTS}(1 - e^{-kt}) + A_0 + mt \quad (19)$$

The values of k , m and A_{SOTS} in equation (19) can be solved by least squares minimization of the time dependent results for A. Alternatively blank samples without SOTS-1 but with the same reagent concentration can be run to solve for m independently.

1.6.3. Steady state solutions: (For MCLA determination)

Flow injection methods using MCLA measure the O_2^- concentration, either in a discrete mode (sample injection loop of sample into reagent flow) or as a continuous signal (continuous mixing of MCLA reagent and sample). Using this approach to determine the instantaneous production rate leads to equation (20) and indicates that the decay rates for O_2^- must also be known or determined.

$$\frac{\partial[O_2^-]}{\partial t} = PR - 2k_D[O_2^-]^2 - k_{obs}[O_2^-] \quad (20)$$

In the case of a constant production rate of O_2^- either from a biological source or a steady photochemical source, equation (20) can easily be solved. A typical application could be the use of low concentrations of XO with a large excess of X resulting in a constant rate of O_2^- production. We assume here that the constant production rate is P ($\text{mol L}^{-1} \text{s}^{-1}$), and the initial O_2^- concentration is zero. In the specific case of DTPA amended seawater, where the pH is known, the value of k_D can be estimated from previous work in seawater [5,111]. If there is no appreciable organic reaction in samples with DTPA then equation (20) has the following analytical solution:

$$[O_2^-]_i = \frac{\sqrt{P}}{\sqrt{2k_D}} \tanh \left(t \sqrt{2k_D} \sqrt{P} \right) \quad (21a)$$

After some time the production rate comes into pseudo equilibrium with the decay rate and the equation reduces to the more practical version seen below:

$$P = 2k_D[O_2^-]_i^2 \quad (21b)$$

Similarly for seawater samples without DTPA, where the uncatalysed dismutation pathway is not significant

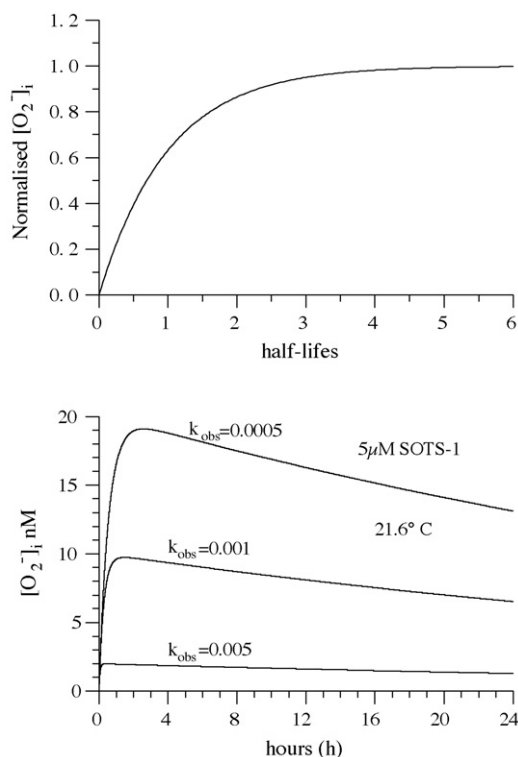


Fig. 3. (top) Normalised $[O_2^-]_i$ as a function of the half-life of the first-order decay rate for superoxide in seawater for a superoxide source with a constant production rate. (bottom) Instantaneous $[O_2^-]_i$ as a function of time for 3 different first-order decay rates of superoxide in seawater. The data here is modeled using the SOTS-1 decay rate determined in this work at 21.6 °C.

($k_{obs} \gg k_D [O_2^-]_i$), the production rate at any time t after equilibrium is established has the analytical solution shown below:

$$[O_2^-]_i = \frac{P}{k_{obs}} (1 - e^{-k_{obs}t}) \quad (22a)$$

After sufficient time (see below) a pseudo steady state is established and the relationship between the production rate and the O_2^- concentrations simplifies to:

$$P = k_{obs}[O_2^-]_i \quad (22b)$$

The time required (Equation (22a)) to achieve this apparent steady state is related to the half-life of the decay rate (k_{obs}) of O_2^- (Fig. 3) and after 1 half-life the observed $[O_2^-]_i$ is equal to half the value at steady state. This is an important point as the time to reach >95% of the maximal signal is at least 5 half-lives and for a value of $k_{obs} = 0.001 \text{ s}^{-1}$ ($t_{1/2} = 693 \text{ s}$) this implies it takes approximately 1 h to reach steady state.

1.6.3.1. Case (I) SOTS-1 and only uncatalysed dismutation. In the case of SOTS-1 at any time after the pseudo equilibrium is established the following equations holds for DTPA amended samples where the dismutation reaction is the only sink term for superoxide.

$$0.4k[SOTS]_0 e^{-kt} = 2k_D [O_2^-]_i^2 \quad (23)$$

Rearranging and taking the logarithm of both sides results in:

$$-kt = 2 \ln [O_2^-]_i + \ln \frac{2k_D}{0.4k[SOTS]_0} \quad (24)$$

Thus a plot of $\ln [O_2^-]_i$ versus time will have a slope of $k/2$. The value of k_D can also be determined here from the value of the intercept.

1.6.3.2. Case (II) SOTS-1 and first order decay of superoxide. In this case it is assumed that there is a fast first order reaction occurring with O_2^- and that the uncatalysed dismutation reaction is not important, this would most likely be the case in natural seawater. Combining equations (13), (14) and (20) leads to the rate equation below:

$$\frac{\partial [O_2^-]}{\partial t} = 0.4k[SOTS]_0 e^{-kt} - k_{obs}[O_2^-] \quad (25)$$

If the initial concentration of O_2^- is zero, then equation (25) has the exact solution [112]:

$$[O_2^-]_i = 0.4k[SOTS]_0 \left\{ \frac{e^{-kt} - e^{-k_{obs}t}}{k_{obs} - k} \right\} \quad (26a)$$

when $k_{obs} \gg k$, as would be expected under most circumstances in seawater, equation (26a) reduces to:

$$0.4k[SOTS]_0 e^{-kt} = k_{obs}[O_2^-]_i \quad (26b)$$

Taking the natural logarithm of both sides then gives:

$$-kt = \ln [O_2^-]_i + \ln \frac{k_{obs}}{0.4k[SOTS]_0} \quad (27)$$

Thus in this case a plot of $\ln [O_2^-]_i$ versus time will have a slope of k . Note that the value of k_{obs} can also be determined here from the value of the intercept as the value for $[SOTS]_0$ is known. The time to reach the maximum $[O_2^-]_i$ is given by the following relationship:

$$t = \frac{\ln (k/k_{obs})}{(k - k_{obs})} \quad (28)$$

Fig. 3 presents example solution of equation (26) with different values of k_{obs} showing the dependence on both the maximum $[O_2^-]_i$ and the time to reach this concentration on k_{obs} when using SOTS-1.

2. Experimental

2.1. pH measurements

In the present work we report seawater pH values using the total hydrogen scale (pH_{TOT}) [113] while we use the NBS scale, pH_{NBS} , for pH measurements of buffers and other low ionic strength solutions. All pH measurements were made using a WTW pH meter 330i calibrated with Tris buffers [114].

2.2. Reagents

All reagents were prepared using 18 MΩ cm resistivity water (hereafter MQ water) supplied by a combination of an ELIX-3 and Synergy 185 water systems (Millipore). High purity HCl (6 M, hereafter abbreviated to Q-HCl) was made by redistillation of Merck trace-metal grade acids in a quartz sub-boiling still. A pH 7, 50 mM phosphate buffer solution (PBS) was prepared by the dissolution of K_2HPO_4 and KH_2PO_4 . Catalase from bovine liver (Sigma Aldrich) was (23,000 units mg^{-1} , 31 mg protein mL^{-1} (Biuret)) cleaned according to the manufacturers instructions in order to remove the thymol preservative solution, as thymol reacts rapidly with superoxide [115]. The clean catalase was then resuspended in pH 7 phosphate buffer prior to use. A 3.8 mM stock solution of DTPA was prepared by dissolving 0.6 g in 400 mL MQ water. Trace metal clean surface seawater collected from the Drake Passage in the Southern Ocean during Polarstern expedition ANTXXIV-3 [5] was used as seawater throughout this work. All plasticware used in this work was extensively acid cleaned before use. During the laboratory work of this study we found only samples which were in Teflon bottles, syringes or filters to give reproducible

data. Preliminary experiments with samples stored in LDPE bottles were irreproducible and had higher background chemiluminescence signal and so the use of this type of bottle was discontinued in our work.

2.2.1. SOTS-1

500 μg aliquots of SOTS-1 (di(4-carboxybenzyl)hyponitrite) (Molecular weight 330.3 g mol^{-1}) was used as received (Cayman Chemicals) and stored at -80°C . Immediately prior to the start of any experiment the 500 μg SOTS-1 aliquots were dissolved in 200 μL DMSO (Fluka, puriss p.a. $\geq 99.9\%$) before further dilution in either pH 7 PBS or seawater. Typical final concentrations for SOTS-1 in this study were between 1.9 and 15.1 μM .

2.2.2. NBD-Cl

A 10 mM stock solution of NBD-Cl (4-chloro-7-nitrobenzo-2-oxa-1,3-diazole) was prepared by the dissolution of 0.1 g in 50 mL ethanol. For the experiments a final concentration of 100 μM NBD-Cl was used. A fresh NBD stock was prepared every 2–3 days. NBD-Cl has a characteristic absorbance at 343 nm and upon the reaction with O_2^- an absorbance peak at 470 nm can be detected. The value of the molar absorption coefficient $\epsilon = 4000 \text{ M}^{-1} \text{ cm}^{-1}$ previously determined [97] was confirmed in our own work, although we found the stoichiometry to be 1:1 and not 1:3 as suggested previously.

2.2.3. FC

FC (Molecular Mass 12,327 Da) from bovine heart muscle, purchased from Sigma–Aldrich was stored at -20°C until use. 100 mg of the protein were dissolved in 2 mL MQ water and primary stocks of this solution ($\sim 4 \text{ mM}$) were also kept at -20°C before further dilution to $\sim 40 \mu\text{M}$ in the experiments. FC exhibits a strong absorbance at 410 and a second band at 530 nm, while the reduced form Ferrocycytochrome c shows three absorption bands at 415, 520 and an acute peak at 550 nm. Through the reaction with O_2^- the reduction of the iron center converts FC to Ferrocycytochrome c and the reaction can be followed by the change of absorbance at 550 nm [116]. For FC the peak at 555 nm was used with the molar extinction coefficient of $\epsilon = 19600 \text{ M}^{-1} \text{ cm}^{-1}$ recommended by Sigma–Aldrich.

2.2.4. MCLA

MCLA([2-methyl-6-(4-methoxyphenyl)-3,7-dihydroimidazo[1,2-a]pyrazin-3-one, HCl]) (Fluka) was used as received. A primary 1 mM MCLA standard was prepared by dissolving 10 mg MCLA in 34.5 mL MQ water, where upon 1 mL aliquots of this solution were then pipetted into 2 mL polyethylene vials and frozen at -80°C until required for use. The working MCLA standard, 1 μM , was prepared from a thawed vial of the primary stock by dilution into a 1 L solution of 0.05 M sodium acetate (Sigma Ultra) buffered (4.1 g) in MQ water adjusted to pH_{NBS} 6. The experiments with MCLA were performed in either 50 mM PBS (pH_{NBS} 7.5) or in seawater collected from the Drake Passage during Polarstern expedition ANTXXIV-3 (pH_{TOT} 8.14).

2.3. Calibration of superoxide standards for use with MCLA

We had previously [5] adapted an existing chemiluminescence analysis methods for O_2^- which utilizes the reagent MCLA [110,117,118]. The mechanism and specificity for the reaction of MCLA and O_2^- is well described [119]. We used a commercially available analysis system (Waterville Analytical) which consists of a light tight box equipped with a Plexiglas spiral flow cell mounted below a photon counter (Hamamatsu HC-135-01) linked to a laptop computer via a Bluetooth™ connection controlled through our own purpose built Labview™ (National Instruments) software. For O_2^- determination we ran the sample and the MCLA reagent

directly into the flow cell using a peristaltic pump (Gilson Minipuls 3, operating at 18 rpm) with the sample line being pulled through the flow cell as this leads to the smallest amount of dead time in the system (typically 2–3 s). The overall flow rate through the cell was 8.25 mL min^{-1} , comprising 5.0 mL min^{-1} from the MCLA and 3.25 mL min^{-1} from the sample. The transit time through the optical cell (300 μL) was therefore 2.18 s. All experiments were conducted in an over pressurized trace metal clean laboratory at the IFM-GEOMAR in Kiel. The detection limit for O_2^- using this system is $\sim 50 \text{ pM}$ based on the analysis of the signal to noise ratio in the background chemiluminescence relative to the sensitivity determined by standard additions in seawater.

In the present work we used KO_2 as our O_2^- source for the calibration of the MCLA method as previously described [5]. In brief, a small amount of KO_2 (8–10 mg) was weighed out in a previously acid washed brown glass bottle containing 2 mL of 1 M NaOH and then further diluted with MQ water to a final volume of 15 mL. UV spectrophotometry was performed on the sample using either a 1 m LWCC-2100 100 cm pathlength liquid waveguide cell (World Precision Instruments, Sarasota, FL, USA), or a 10 cm Quartz-cuvette (Hellma), coupled to an Ocean Optics USB4000 UV-Vis spectrophotometer in combination with an Ocean Optics DT-MINI-2-GS light source. The concentration of both O_2^- and HO_2^- in the standard solution were determined by least squares solution to the measured absorbance, at multiple wavelengths, using published molar extinction coefficients for H_2O_2 [50] and O_2^- [8] (Table 1). Mean initial concentrations in the primary KO_2 solution assessed in this way were $900 \pm 50 \mu\text{M}$ for H_2O_2 and $90 \pm 10 \mu\text{M}$ O_2^- .

2.4. Determination of O_2^- fluxes and the thermal dissociation rate (k) of SOTS-1 in seawater and PBS by spectrophotometry

The decomposition rate (k) of SOTS-1 in seawater and in PBS was measured by following the O_2^- promoted change in absorbance of either FC or NBD-Cl. Each experiment was performed at a set temperature ($\pm 0.1^\circ\text{C}$) using a thermostated water bath (Fisher Scientific: FBC720). The complete experimental set covered a range of (10–37 $^\circ\text{C}$) temperatures relevant to seawater studies and for comparison to previous results. The experiment was initiated with the addition of 500 μg of SOTS-1 to a known volume (typically 100 or 500 mL) of seawater, or PBS, that had been previously equilibrated with DTPA (3.8 μM) for 24 h in a 1 L Teflon bottle. Aliquots of the SOTS-1 solution were poured into 60 mL Teflon bottles and the appropriate volumes of the reagents added to give the appropriate final concentrations: FC (40 μM) or NBD-Cl (100 μM). Samples were run in triplicate and were shielded from the light where possible. Absorbance measurements were performed using the same apparatus as described in section 2.3 with either a 1 cm quartz cuvette or the LWCC-2100. The time evolution of the absorbance signal was followed by taking frequent measurements of the sample solutions over the course of the experiment (1–5 days).

2.5. Determination of O_2^- fluxes from SOTS-1 in seawater and PBS by chemiluminescence

Experiments were performed in Teflon bottles and initiated by the addition of 500 μg of SOTS-1 to a known volume (typically 250 or 500 mL) of seawater, or PBS, that had been left to equilibrate with DTPA (3.8 μM) for 24 h. All reagents and samples were kept at a constant temperature ($21.5 \pm 0.2^\circ\text{C}$) throughout the course of the experiment in a temperature controlled class 100 clean laboratory. Samples were drawn directly into the flow cell of the chemiluminescence detector as described in Section 2.3.

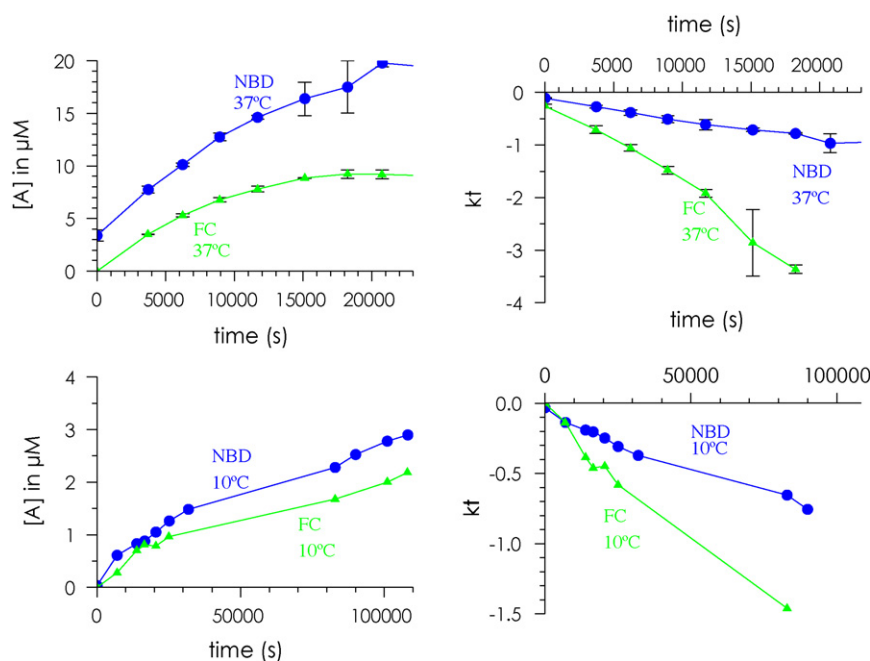


Fig. 4. Example plots of the apparent O_2^- release from SOTS-1 in Antarctic seawater using two spectrophotometric detection schemes. (Top, left): Integrated O_2^- concentrations determined by NBD and FC at 37 °C using a 1 cm cuvette. (Top, right) Plot of kt versus time using equation 17 for the data at 37 °C. (Bottom, left): Integrated O_2^- concentrations determined by NBD and FC at 10 °C using a 100 cm LWCC. (Bottom, right) Plot of kt versus time using equation 17 for the data at 10 °C.

3. Results and discussion

3.1. Superoxide production by SOTS-1 in seawater

3.1.1. Detection of the superoxide flux using NBD-Cl or FC

In seawater solutions containing SOTS-1 and NBD-Cl or FC the concentration of the absorbing species of the reaction product with O_2^- increased with time (Fig. 4) over all the temperatures ranges examined as expected. The data obtained using FC and NBD-Cl was fitted with equation (17), using either the expected value for A_{SOTS} (based on the expected stoichiometry of O_2^- production, 0.4, and the concentration of SOTS-1) or the measured absorbance (A_∞) obtained after all the SOTS-1 has decayed. Typical results are shown in Fig. 4 for experiments at 10 and 37 °C. In all experiments the integrated concentration of O_2^- as determined by reaction with NBD-Cl was always greater than that with FC (Fig. 4) and the absorbance of the NBD-Cl reaction product did not reach a plateau as predicted by equation (16) and was observed for FC. This indicates that there were one or more interfering reactions that were ongoing with NBD-Cl after the complete decomposition of the SOTS-1 O_2^- source. Thus in the case of NBD-Cl, the use of equation (17) leads to an underestimation of the decay rate of SOTS-1 as the yield is overestimated due to the interfering reaction. For FC equations (16) and (17) appear to describe the data reasonably well allowing good estimates of the SOTS-1 decay rate to be made as a function of temperature (Table 1).

In nearly all experiments with NBD-Cl the expected final yield of O_2^- , based on the SOTS-1 concentration added, was exceeded (Fig. 5) and the yield apparently increased with increasing temperature. However at high temperatures the apparent yield of O_2^- using NBD-Cl was greatly in excess of the expected yield from SOTS-1 (Fig. 5) indicating a chemical interference. This was not unexpected with NBD-Cl as it is well known that it reacts with amines and thiols to form species which absorb at similar wavelengths. As the reactions between NBD-Cl and amines [120] or thiols [96] are strongly temperature dependent and the total concentration of these species in our Antarctic seawater would have been expected to be low ($<1 \mu\text{M}$), another reaction must be occurring. It

is possible that NBD-Cl may react with the ketyl or alkoxy radicals produced by SOTS-1 as it has been shown [121] that a related benzofuran reacts with peroxy radicals produced from the thermal decomposition of 2,2'-azobis(2-amidinopropane) dihydrochloride (AAPH) [122,123] a compound related to SOTS-1. While reactions with carbon centered radicals produced by SOTS-1 is possible it could not explain yields above 250% which were measured at temperatures above 30 °C. A more likely source of interference is from the hydrolysis of NBD-Cl to form NBD-OH which also absorbs at 470 nm [120,124] and published hydrolysis rate data at 50 °C for NBD-Cl [125] and at 30 °C for the more reactive NBD-F [120] indicate that this could be a significant interference in this study. More work is obviously required on the exact mechanism of the reaction between NBD-Cl and O_2^- .

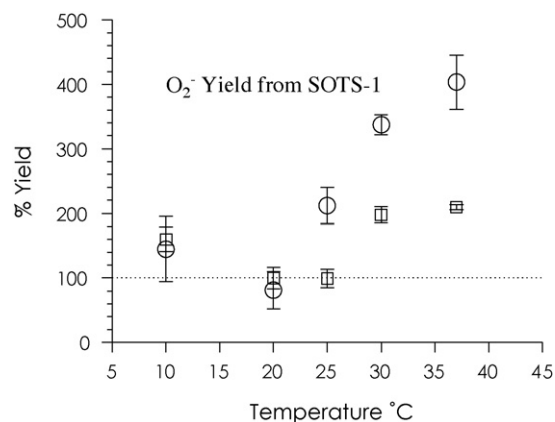


Fig. 5. Apparent O_2^- yield from SOTS-1 in seawater as a function of temperature for both FC (squares) and NBD (circles). The error bars for each symbol represent the 95% confidence intervals for the series of measurements undertaken at each temperature. The effects of thermal production of O_2^- can be clearly seen at 30 °C and above for FC and NBD, where the latter is also apparently affected by hydrolysis reactions. The data at 10 °C was measured over 10 days and may have been affected by light induced reactions.

The apparent overall yield of O_2^- from SOTS-1 using FC (Fig. 5) was close to the anticipated values in the temperature range 20–25 °C, with increased yields observed at both 10 °C and temperatures above 30 °C. Parallel experiments using FC in PBS with SOTS-1 at 25 °C had yields and decay rates that were slightly different from seawater, though not statistically significant ($k(\text{PBS}) = 2.4 \pm 0.3 \times 10^{-5} \text{ s}^{-1}$, $k(\text{SW}) = 2.2 \pm 0.6 \times 10^{-5} \text{ s}^{-1}$; SOTS-1 = 15.14 μM , expected yield 6.06 μM : Yield (PBS) = $5.0 \pm 0.6 \mu\text{M}$ (83 \pm 10%), Yield(SW) = $5.6 \pm 0.9 \mu\text{M}$ (93 \pm 15%). This may indicate that the increased yield with SOTS-1 at temperatures above 25 °C was related to reactions between FC and components of the seawater as experiments in PBS with SOTS-1 do not show any evidence for additional reductants of FC [68].

In the present work we saw no evidence of any influence on the results due to any temperature dependence of the FC reaction with O_2^- . Previous work has shown that the rate constant for the FC reaction with O_2^- varies only slightly [80] over the temperature range used here and thus should not be a factor in the present work. However for NBD-Cl there is only one measurement in the literature presently for the rate of reaction of NBD-Cl with O_2^- ($1.5 \pm 0.3 \times 10^{-5} \text{ M}^{-1} \text{ s}^{-1}$) [97] but the temperature is not specified and thus we have no indication of the temperature dependence of this reaction. However given the reactivity of NBD-Cl with other nucleophiles [126] it is not expected that the rate of this reaction would be an issue but instead the loss of NBD-Cl via hydrolysis may at some point lead to less than 100% trapping of O_2^- by NBD-Cl.

Another potential problem previously identified with the use of FC to determine superoxide fluxes over long time periods is due to the possible underestimation of the actual flux due to the reoxidation of ferrocytochrome to FC by H_2O_2 which may accumulate in the samples over time [127]. This effect may occur but is probably very small in the present work as the major sink for SOTS-1 produced O_2^- would have been the oxidation of O_2^- to O_2 by FC [82], and not the formation of H_2O_2 .

NBD-Cl does have the advantage over FC that the absorbance at the analytical wavelength (470 nm) prior to the addition of an O_2^- source is effectively zero, which allows the use of a long pathlength detection systems. In the case of FC the samples must be diluted before measurement as the absorption by FC itself is considerably when used in a long pathlength system such as employed here. This was the case for the samples run at 10 °C (Fig. 4 and Table 1) which were run over 5 days at low SOTS-1 concentration (3.8 μM) and gave calculated SOTS-1 decay rate and yields (Fig. 5) which were higher than expected with both FC and NBD-Cl. It is likely that the faster rate and higher yield found at 10 °C was due to handling artifacts involved in the dilution of the samples prior to making absorbance measurements.

3.2. Temperature effects on O_2^- production by SOTS-1

3.2.1. Calculation of the activation energy for SOTS-1 in seawater

The temperature dependence on the thermal decomposition of SOTS-1 in seawater from 21.6 to 37.0 °C is shown as an Eyring plot [128] using the FC data in Fig. 6. The data from 10 °C was omitted from this analysis due to the experimental problems noted above in making these measurements. The estimated activation energy (E_A) for the thermal decomposition of SOTS-1 in seawater is $108 \pm 29 \text{ kJ mol}^{-1}$ ($n = 4$, $R^2 = 0.96$, 95% CI). Similarly in PBS ($n = 3$, $R^2 = 0.99$, 95% CI) we calculate a value of $115 \pm 6 \text{ kJ mol}^{-1}$. The two values are not statistically different given the large error in the seawater value and we would expect that the activation energy is the same in both PBS and seawater given the mechanism shown in Fig. 2. The main reason for the large uncertainty in the seawater measurements is due to the methods used for trapping the O_2^- formed upon SOTS-1 decay. We are currently looking into developing a method to directly determine SOTS-1 in seawater in order to

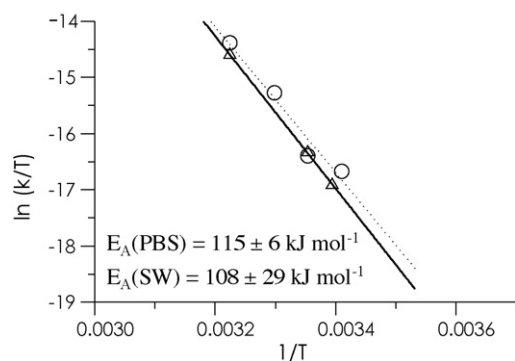


Fig. 6. Eyring plot of the measured thermal dissociation rates of SOTS-1 in seawater (circles) and PBS (triangles). The least squares regression fit to the data is also shown for PBS (solid line) and seawater (dotted line). Only data between 37.0 and 20.0 °C are included here due to the problems described in the text when measuring at lower temperatures.

better improve our estimates of k and E_A in seawater. Our measured values are similar to other data for the thermal decomposition of related azo compounds (112 – 170 kJ mol^{-1}) [129,130].

3.2.2. Non-SOTS-1 thermal production of O_2^- in seawater

The observed increases in the apparent yield of O_2^- from SOTS-1 at elevated temperatures using NBD and FC could also be in part explained by another thermal source of O_2^- in seawater, the presence of which has previously been overlooked. Interestingly a series of studies by Bruskov and coworkers [131–133] has suggested just such a source exists in simple salt solutions leading to the formation of H_2O_2 and other ROS. In their work they found that in organic free NaCl and NaHCO_3 solutions, similar in pH and concentration to seawater, that heating increased H_2O_2 production. Studies in artificial seawater (sea salt dissolved in pure water) revealed H_2O_2 production rates of $\sim 16 \text{ nM h}^{-1}$ at 40 °C with an estimated activation energy of 87 kJ mol^{-1} over the temperature range 40–65 °C [131]. The source of these ROS is suggested to be from the thermal activation of reducing compounds present in seawater [132].

The production of H_2O_2 in weak alkaline solutions from reactions between tannin, pyrogallol or gallic acid with O_2 , presumably via O_2^- as an intermediate, were first described by Schönbein [134] in 1860. Later work has examined both the thermal and photochemical pathways of H_2O_2 formation from these substances [135] revealing that the rate of this reaction increases with increasing pH. An additional source of O_2^- could be from the auto-oxidation of hydroquinones [136] present in seawater from the lysis of bacteria [32] and phytoplankton [137]. Based on this evidence we suggest that the presence of a natural thermal source of superoxide must therefore be considered highly likely in experiments with seawater at elevated temperatures (>25 °C) and in particular when using coastal seawater with high loadings of terrestrial organic material.

3.3. Determination of superoxide concentrations using MCLA

The production of O_2^- from SOTS-1 was also followed by chemiluminescence using MCLA as the detection probe in both seawater and PBS in order to validate our theoretical approach. An example using 7.5 μM in PBS with DTPA at 26 °C is shown in Fig. 7. We found excellent agreement between the data and the predicted concentrations and fluxes (calculated from equations (23) and (24)) over 2 h of measurements.

A further example of a direct comparison for SOTS-1 at 21.6 °C in both PBS and Antarctic seawater is shown in Figs. 8 and 9. Fig. 8 shows the time dependence of the raw count rate from the photon counter over one and half days and clearly shows the initial build

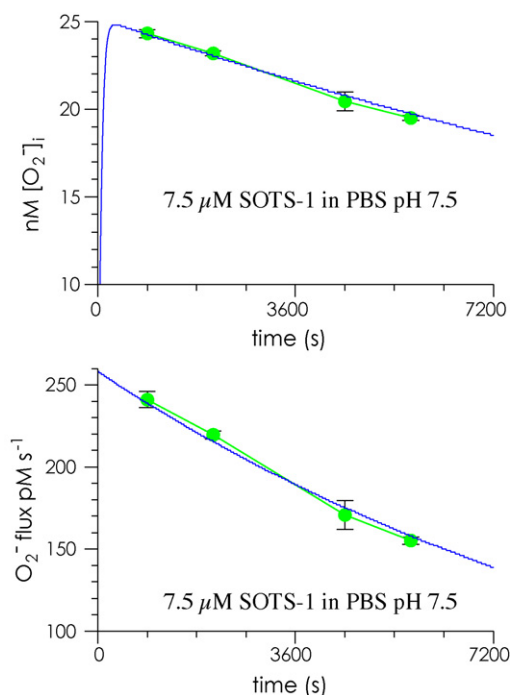


Fig. 7. (top) SOTS-1 in Phosphate Buffer Solution (PBS) with MCLA detection of the instantaneous concentration of superoxide ($[O_2^-]_i$). (bottom) Calculated production rate (green circles) and model estimates (blue) for superoxide from SOTS-1 in PBS. This experiment was performed at 26 °C with O_2^- detected using MCLA chemiluminescence.

up to the maximum concentration and then the slow decay after. To convert the photon counts into $[O_2^-]$ the following conversion is valid for this data: $[O_2^-]$ (nM) = (signal-background)/19600, the sensitivity measured by calibration with KO_2 additions was ~ 19600 counts nM^{-1} in both PBS and Antarctic seawater, while the background counts were ~ 4000 counts in PBS and ~ 6000 counts in the Antarctic seawater. Fig. 9 shows the natural log transformed data from Fig. 8 and it is easy to see the time it takes for the pseudo steady state to be established after which equation (27) can be applied in order to calculate k , the SOTS-1 decay rate. The time to reach the maximum O_2^- was ~ 3000 s in line with that predicted by equation (28).

Additionally from the PBS data we can calculate using equation (24), the value for the second order uncatalyzed dismutation rate for O_2^- , assuming that in the presence of DTPA in PBS there are no other reactions, of $k_2 = 3.0 \pm 0.3 \times 10^5 M^{-1} s^{-1}$ (pH 7.5). This value is very close to the value predicted for pH 7.5, $k_2 = 2.0 \times 10^5 M^{-1} s^{-1}$, from the data compilation ($pK_a = 4.88$,

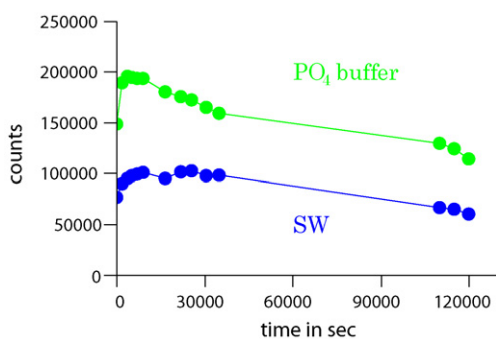


Fig. 8. Raw Chemiluminescence output (counts per 200 ms time period) obtained using as described in the text. For SOTS-1 in PBS (pH 7.4, green) and SW (pH 8.14, blue).

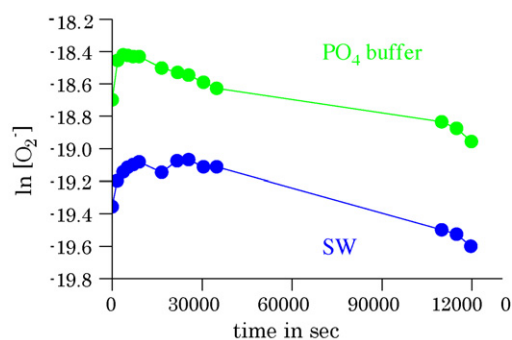


Fig. 9. Natural log of the O_2^- concentration as a function of time for the data shown in Fig. 8. For SOTS-1 at 21.6 °C in PBS (pH 7.4, green) and SW (pH 8.14, blue).

$k_{HO_2/O_2^-} = 8.5 \times 10^7 M^{-1} s^{-1}$, $k_2 = k_{HO_2/O_2^-} \times 10^{-pH} / 10^{-pK_a}$) by Bielski et al. [8]. Similarly for the MCLA measurements made in DTPA amended seawater we calculate using equation (27), a value of $k_{obs} = 0.0020 \pm 0.0001$, for the reaction of O_2^- with DOM. This value is slightly lower than we obtained previously (0.004 to 0.006) in decay experiments with KO_2 [5] on water collected on the same cruise but in different places in the Drake Passage.

During the present work we observed significantly different sensitivities for O_2^- with MCLA kept at different temperatures. This was first observed during a preliminary experiment at 21.5 °C run over 2 days where we kept one aliquot of MCLA at room temperature (21.5 °C) and another aliquot was kept overnight in the fridge (7 °C) to minimize auto-oxidation. Running samples with these two aliquots we observed that the reagent kept in the fridge gave a chemiluminescence signal which was 38% less than the solution maintained at room temperature and this difference decreased as the reagent warmed up. It is therefore important that the same temperature is maintained throughout the analysis to avoid this problem or alternatively, and a much more tedious option, calibration must be performed over a range of temperatures. This is an important factor to consider in regard to the determination of vertical profiles of O_2^- production as *in situ* real time measurements throughout the thermocline would be strongly affected by this phenomenon.

3.4. Can natural O_2^- fluxes be measured in seawater?

So is it possible to measure natural O_2^- fluxes in seawater? The MCLA chemiluminescence technique seems the most promising as it is relatively simple and is already used at sea. Putting this into perspective, estimates of the midday solar flux of O_2^- in surface waters range from 9 to 17 $nM h^{-1}$, which is equivalent to an initial O_2^- flux from ~ 0.25 to 0.5 μM SOTS-1 at 25 °C. The maximum O_2^- level attained in DTPA amended seawater would depend on the value of k_{obs} for the reaction with organic matter ($0.002\text{--}0.030 s^{-1}$) [5,138], concentrations of 83–2350 pM would be anticipated. The lower end of this range is still above the detection limit for O_2^- using MCLA and indicates that *in situ* production of O_2^- could be measured using this approach if an adequate separation between signal and noise can be maintained. In natural seawater k_{obs} is increased due to reactions with trace metals [5], and this would have the effect of lowering $[O_2^-]_i$ closer to the detection limit of the current MCLA system. It would however also shorten the time to achieve pseudo steady state (~ 1 h in DTPA amended seawater). All of the work performed here was carried out in filtered seawater samples. While this would unlikely affect measurements of photochemically produced O_2^- it is still to be determined if these methods will work in the presence of biology and particles. More work is needed on this before biological production rates can be properly assessed.

Spectrophotometric methods may also have a role to play in measuring O_2^- fluxes, and in our work FC appears to be the most suitable reagent for this work. Our data suggests that the minimum O_2^- flux that could be measured with FC using a 100 cm pathlength flow cell is $\sim 1 \text{ pM s}^{-1}$ as some of the gain in sensitivity in using the long pathlength is lost because the sample needs to be diluted to maintain the absorbance of the FC and ferrocyclochrome species in the linear range. The use of NBD-Cl as a reagent for O_2^- is not recommended at present unless a time consuming HPLC step [125] is introduced to separate the different interfering reaction products and most notably the hydrolysis product, NBD-OH.

SOTS-1 is an easy O_2^- source to work with and it has few of the drawbacks that are connected with other commonly used O_2^- sources. We have also found in related work that commercially available SOTS-1 is clean enough to be used directly in seawater without altering the metal concentration or speciation appreciably. Thus we are currently employing and evaluating SOTS-1 as a well defined O_2^- source for studying trace metal redox reactions in seawater.

4. Conclusions

We have shown in this work that through the development of the appropriate mathematical derivations and theory coupled with the use of SOTS-1 as a O_2^- source that analytical detection systems for O_2^- can be calibrated for use in seawater to determine both concentrations and fluxes. The overall goal of such work however is to make such measurements in the ocean *in situ* and this is the logical next step to pursue.

Acknowledgements

Thanks to Mirja Dunker for her help in performing part of the laboratory work. This work was supported by the BMBF Verbundproject SOPRAN (TP 1.2) and forms part of the German contribution to SOLAS (Surface Ocean Lower Atmosphere Studies).

References

- [1] E. Micinski, L.A. Ball, O.C. Zafriou, *J. Geophys. Res. Oceans* 98 (1993) 2299.
- [2] D. Kim, T. Oda, A. Ishimatsu, T. Muramatsu, *Biosci. Biotechnol. Biochem.* 64 (2000) 911.
- [3] J.-A. Marshall, M. Hovenden, T. Oda, G.M. Hallegraeff, *J. Plankton Res.* 24 (2002) 1231.
- [4] O.C. Zafriou, *Marine Chem.* 30 (1990) 31.
- [5] M.I. Heller, P.L. Croot, *Environ. Sci. Technol.* (2009), doi:10.1021/es901766r.
- [6] B.M. Voelker, D.L. Sedlak, *Marine Chem.* 50 (1995) 93.
- [7] B.M. Voelker, D.L. Sedlak, O.C. Zafriou, *Environ. Sci. Technol.* 34 (2000) 1036.
- [8] B.H.J. Bielski, D.E. Cabelli, R.L. Arudi, A.B. Ross, *J. Phys. Chem. Ref. Data* 14 (1985) 1041.
- [9] J.M. McCord, I. Fridovich, *J. Biol. Chem.* 244 (1969) 6049.
- [10] J.V. Goldstone, B.M. Voelker, *Environ. Sci. Technol.* 34 (2000) 1043.
- [11] S.M. Fan, *Marine Chem.* 109 (2008) 152.
- [12] L. Weber, C. Völker, M. Schartau, D.A. Wolf-Gladrow, *Global Biogeochem. Cycles* 19 (2005) GB1019.
- [13] A. Tagliabue, L. Bopp, O. Aumont, K.R. Arrigo, *Global Biogeochem. Cycles* 23 (2009).
- [14] J.W. Moffett, R.G. Zika, *Marine Chem.* 13 (1983) 239.
- [15] P.L. Croot, P. Laan, J. Nishioka, V. Strass, B. Cisewski, M. Boye, K. Timmermans, R. Bellerby, L. Goldson, H.J.W. de Baar, *Marine Chem.* 95 (2005) 65.
- [16] M. Fujii, A.L. Rose, T.D. Waite, T. Omura, *Environ. Sci. Technol.* 40 (2006) 880.
- [17] A.J. Swallow, *Nature* 222 (1969) 369.
- [18] R.G. Petasne, R.G. Zika, *Nature* 325 (1987) 516.
- [19] R.M. Baxter, J.H. Carey, *Nature* 306 (1983) 575.
- [20] F.J. Millero, *Geochim. Cosmochim. Acta* 51 (1987) 351.
- [21] N.V. Blough, O.C. Zafriou, *Inorg. Chem.* 24 (1985) 3502.
- [22] B. Dister, O.C. Zafriou, *J. Geophys. Res. Oceans* 98 (1993) 2341.
- [23] D.W. O'Sullivan, P.J. Neale, R.B. Coffin, J.B. Boyd, C.L. Osburn, *Marine Chem.* 97 (2005) 14.
- [24] B.H. Yocis, D.J. Kieber, K. Mopper, *Deep Sea Res. Part I: Oceanogr. Res.* 47 (6) (2000) 1077.
- [25] I. Obernosterer, P. Ruardij, G.J. Herndl, *Limnol. Oceanogr.* 46 (2001) 632.
- [26] J. Yuan, A.M. Shiller, *Deep-Sea Res. II* 48 (2001) 2947.
- [27] P.L. Croot, K. Bluhm, C. Schlosser, P. Streu, E. Breitbarth, R. Frew, M. Van Ardelan, *Geophys. Res. Lett.* 35 (2008) L19606.
- [28] H. Speisky, M. Gómez, C. Carrasco-Pozo, E. Pastene, C. Lopez-Alarcón, C. Olea-Azar, *Bioorg. Med. Chem.* 16 (2008) 6568.
- [29] N. Kishikawa, N. Ohkubo, K. Ohyama, K. Nakashima, N. Kuroda, *Anal. Bioanal. Chem.* 393 (2009) 1337.
- [30] V.A. Roginsky, L.M. Pisarenko, W. Bors, C. Michel, *J. Chem. Soc. Perkin Trans. 2* (1999) 871.
- [31] R.M. Cory, D.M. McKnight, *Environ. Sci. Technol.* 39 (2005) 8142.
- [32] M. Akagawa-Matsushita, T. Itoh, Y. Katayama, H. Kuraishi, K. Yamasato, *J. Gen. Microbiol.* 138 (1992) 2275.
- [33] J.M. McCord, I. Fridovich, *J. Biol. Chem.* 242 (1967) 5753.
- [34] I. Fridovich, *Ann. Rev. Biochem.* 64 (1995) 97.
- [35] J.A. Marshall, M. de Salas, T. Oda, G. Hallegraeff, *Marine Biol.* 147 (2005) 533.
- [36] J.A. Marshall, T. Ross, S. Pyecroft, G. Hallegraeff, *Marine Biol.* 147 (2005) 541.
- [37] A.L. Rose, T.P. Salmon, T. Lukondeh, B.A. Neilan, T.D. Waite, *Environ. Sci. Technol.* 39 (2005) 3708.
- [38] A.B. Kustka, Y. Shaked, A.J. Milligan, D.W. King, F.M.M. Morel, *Limnol. Oceanogr.* 50 (2005) 1172.
- [39] N.E. Good, C.G. Winget, W. Winter, T.N. Connolly, S. Izawa, R.M.M. Singh, *Biochemistry* 5 (1966) 467.
- [40] J.K. Grady, N.D. Chasteen, D.C. Harris, *Anal. Biochem.* 173 (1988) 111.
- [41] G.H. Zhao, N.D. Chasteen, *Anal. Biochem.* 349 (2006) 262.
- [42] M. Kirsch, E.E. Lomonosova, H.G. Korth, R. Sustmann, H. de Groot, *J. Biol. Chem.* 273 (1998) 12716.
- [43] G.R. Hodges, K.U. Ingold, *Free Radic. Res.* 33 (2000) 547.
- [44] M.S. McDowell, A. Bakac, J.H. Espenson, *Inorg. Chem.* 22 (1983) 847.
- [45] A.L. Rose, T.D. Waite, *Environ. Sci. Technol.* 39 (2005) 2645.
- [46] S. Garg, A.L. Rose, T.D. Waite, *Geochim. Cosmochim. Acta* 71 (2007) 5620.
- [47] V. Feigenbrugel, C. Loew, S. Le Calve, P. Mirabel, *J. Photochem. Photobiol. a-Chem.* 174 (2005) 76.
- [48] H. Görner, *Photochem. Photobiol.* 82 (2006) 801.
- [49] R.A. Holroyd, B.H.J. Bielski, *J. Am. Chem. Soc.* 100 (1978) 5796.
- [50] B.H.J. Bielski, A.O. Allen, *J. Phys. Chem.* 81 (1977) 1048–1050.
- [51] M.E.T. Sillanpää, J.H.P. Ramo, *Environ. Sci. Technol.* 35 (2001) 1379.
- [52] A. Svenson, L. Kaj, H. Björndal, *Chemosphere* 18 (1989) 1805.
- [53] S. Metsärinne, P. Rantanen, R. Aksela, T. Tuhkanen, *Chemosphere* 55 (2004) 379.
- [54] A. Godrant, A.L. Rose, G. Sarthou, T.D. Waite, *Limnol. Oceanogr. Methods* 7 (2009) 682.
- [55] A.L. Rose, J.W. Moffett, T.D. Waite, *Anal. Chem.* 80 (2008) 1215.
- [56] A. Milne, M.S. Davey, P.J. Worsfold, E.P. Achterberg, A.R. Taylor, *Limnol. Oceanogr. Methods* 7 (2009).
- [57] I. Fridovich, *J. Biol. Chem.* 245 (1970) 4053.
- [58] C. Galbusera, P. Orth, D. Fedida, T. Spector, *Biochem. Pharmacol.* 71 (2006) 1747.
- [59] G.R. Hodges, M.J. Young, T. Paul, K.U. Ingold, *Free Radical Biol. Med.* 29 (2000) 434.
- [60] R.V. Lloyd, R.P. Mason, *J. Biol. Chem.* 265 (1990) 16733.
- [61] T.A. Dix, J. Aikens, *Chem. Res. Toxicol.* 6 (1993) 2.
- [62] A.G. Dickson, *Marine Chem.* 44 (1993) 131.
- [63] M.G. Bonini, S. Miyamoto, P.D. Mascio, O. Augusto, *J. Biol. Chem.* 279 (2004) 51836.
- [64] M. Saran, W. Bors, 1991, p. 957.
- [65] S. Goldstein, C. Michel, W. Bors, M. Saran, G. Czapski, *Free Radic. Biol. Med.* 4 (1988) 295.
- [66] B.J. Bolann, R.J. Ulvik, *Clin. Chem.* 37 (1991) 1993.
- [67] J. Weinstein, B.H.J. Bielski, *J. Am. Chem. Soc.* 101 (1979) 58.
- [68] K.U. Ingold, T. Paul, M.J. Young, L. Doiron, *J. Am. Chem. Soc.* 119 (1997) 12364.
- [69] C. Von Sonntag, H.P. Schuchmann, *Angew. Chem. Int. Ed. Eng.* 30 (1991) 1229.
- [70] B.C. Gilbert, R.G.G. Holmes, H.A.H. Laue, R.O.C. Norman, *J. Chem. Soc. Perkin Trans. 2* (1976) 1047.
- [71] T. Paul, *Arch. Biochem. Biophys.* 382 (2000) 253.
- [72] K.G. Konya, T. Paul, S.Q. Lin, J. Lusztyk, K.U. Ingold, *J. Am. Chem. Soc.* 122 (2000) 7518.
- [73] C.H. Fischer, E.J. Hart, A. Henglein, *J. Phys. Chem.* 90 (1986) 1954.
- [74] K. Hyland, C. Auclair, *Biochem. Biophys. Res. Commun.* 102 (1981) 531.
- [75] X.L. Qiao, S.M. Chen, L. Tan, H. Zheng, Y.D. Ding, Z.H. Ping, *Magn. Reson. Chem.* 39 (2001) 207.
- [76] C.Z. Zhang, F.R.F. Fan, A.J. Bard, *J. Am. Chem. Soc.* 131 (2009) 177.
- [77] N. Soh, *Anal. Bioanal. Chem.* 386 (2006) 532.
- [78] G. Bartosz, *Clin. Chim. Acta* 368 (2006) 53.
- [79] E.J. Land, A.J. Swallow, *Arch. Biochem. Biophys.* 145 (1971) 365.
- [80] J. Butler, G.G. Jayson, A.J. Swallow, *Biochim. Biophys. Acta* 408 (1975) 215.
- [81] W.H. Koppenol, K.J.H. Vanbuuren, J. Butler, R. Braams, *Biochim. Biophys. Acta* 449 (1976) 157.
- [82] J.F. Turrens, J.M. McCord, *FEBS Lett.* 227 (1988) 43.
- [83] I. Fridovich, *J. Biol. Chem.* 272 (1997) 18515.
- [84] Y. Ilan, Y.A. Ilan, G. Czapski, *Biochim. Biophys. Acta* 503 (1978) 399.
- [85] W.H. Koppenol, F. Levine, T.L. Hatmaker, J. Epp, J.D. Rush, *Arch. Biochem. Biophys.* 251 (1986) 594.
- [86] M.A. Augustin, J.K. Yandell, *Inorg. Chem.* 18 (1979) 577.
- [87] C. Beauchamp, I. Fridovich, *Anal. Biochem.* 44 (1971) 276.
- [88] B.H.J. Bielski, G.G. Shiue, S. Bajuk, *J. Phys. Chem.* 84 (1980) 830.
- [89] S.I. Liochev, I. Fridovich, *Arch. Biochem. Biophys.* 318 (1995) 408.
- [90] H. Ukedo, S. Maeda, T. Ishii, M. Sawamura, *Anal. Biochem.* 251 (1997) 206.

- [91] S.I. Liochev, I. Batinic-Haberle, I. Fridovich, *Arch. Biochem. Biophys.* 324 (1995) 48.
- [92] R.L. Arudi, A.O. Allen, B.H.J. Bielski, *FEBS Lett.* 135 (1981) 265.
- [93] C. Auclair, M. Torres, J. Hakim, *FEBS Lett.* 89 (1978) 26.
- [94] P.B. Ghosh, M.W. Whitehouse, *Biochem. J.* 108 (1968) 155.
- [95] R.S. Fager, C.B. Kutina, E.W. Abrahamson, *Anal. Biochem.* 53 (1973) 290.
- [96] D.J. Birkett, N.C. Price, G.K. Radda, A.G. Salmon, *FEBS Lett.* 6 (1970) 346.
- [97] R.O. Olojo, R.H. Xia, J.J. Abramson, *Anal. Biochem.* 339 (2005) 338.
- [98] B.S. Baines, G. Allen, K. Brocklehurst, *Biochem. J.* 163 (1977) 189.
- [99] J. Meisenheimer, *Justus Liebigs Ann. Chem.* 323 (1902) 205.
- [100] H. Kobayashi, E. Gil-Guzman, A.M. Mahran, R.K. Sharma, D.R. Nelson, A.J. Thomas, A. Agarwal, *J. Androl.* 22 (2001) 568.
- [101] C. Lu, G. Song, J.M. Lin, *Trac-Trends Anal. Chem.* 25 (2006) 985.
- [102] K. Faulkner, I. Fridovich, *Free Radic. Biol. Med.* 15 (1993) 447.
- [103] H. Gyllenhammar, *J. Immunol. Methods* 97 (1987) 209.
- [104] S.I. Liochev, I. Fridovich, *Arch. Biochem. Biophys.* 337 (1997) 115.
- [105] M. Nakano, K. Sugioaka, Y. Ushijima, T. Goto, *Anal. Biochem.* 159 (1986) 363.
- [106] T. Okajima, K. Tokuda, T. Ohsaka, *Bioelectrochem. Bioenerg.* 41 (1996) 205.
- [107] Y. Kambayashi, K. Ogino, *J. Toxicol. Sci.* 28 (2003) 139.
- [108] K. Fujimori, H. Nakajima, K. Akutsu, M. Mitani, H. Sawada, M. Nakayama, *J. Chem. Soc. Perkin Trans. 2* (1993) 2405.
- [109] K. Fujimori, T. Komiyama, H. Tabata, T. Nojima, K. Ishiguro, Y. Sawaki, H. Tatsuzawa, M. Nakano, *Photochem. Photobiol.* 68 (1998) 143.
- [110] M.M.J. Oosthuizen, M.E. Engelbrecht, H. Lambrechts, D. Greyling, R.D. Levy, *J. Bioluminescence Chemiluminescence* 12 (1997) 277.
- [111] O.C. Zafriou, B.M. Voelker, D.L. Sedlak, *J. Phys. Chem. A* 102 (1998) 5693.
- [112] A.V. Harcourt, W. Esson, *Phil. Trans. R. Soc. Lond.* 156 (1866) 193.
- [113] A.G. Dickson, *Deep Sea Research Part I: Oceanographic Research Papers* 40 (1993) 107.
- [114] F.J. Millero, J.Z. Zhang, S. Fiol, S. Sotolongo, R.N. Roy, K. Lee, S. Mane, 1993, p. 143.
- [115] I. Kruk, T. Michalska, K. Lichstzeld, A. Kladna, H.Y. Aboul-Enein, *Chemosphere* 41 (2000) 1059.
- [116] M. Collinson, E.F. Bowden, *Anal. Chem.* 64 (1992) 1470.
- [117] M. Nakano, *Cell. Mol. Neurobiol.* 18 (1998) 565.
- [118] L. Pronai, H. Nakazawa, K. Ichimori, Y. Sagusa, T. Ohkubo, K. Hiramatsu, S. Arimori, J. Fehrer, *Inflammation* 16 (1992) 437.
- [119] Y. Kambayashi, S. Tero-Kubota, Y. Yamamoto, M. Kato, M. Nakano, K. Yagi, K. Ogino, *J. Biochem.* 134 (2003) 903.
- [120] H. Miyano, T. Toyo'oka, K. Imai, *Anal. Chim. Acta* 170 (1985) 81.
- [121] B. Heyne, S. Ahmed, J.C. Scaiano, *Org. Biomol. Chem.* 6 (2008) 354.
- [122] M.A. Cubillos, E.A. Lissi, E.B. Abuin, *Chem. Phys. Lipids* 104 (2000) 49.
- [123] G.S. Hammond, R.C. Neuman, *J. Am. Chem. Soc.* 85 (1963) 1501.
- [124] A.A. Al-Majed, F. Belal, M.A. Abounassif, N.Y. Khalil, *Microchim. Acta* 141 (2003) 1.
- [125] L. Johnson, S. Lagerkvist, P. Lindroth, M. Ahnoff, K. Martinsson, *Anal. Chem.* 54 (1982) 939.
- [126] N. Latelli, S. Zeroual, N. Ouddai, M. Mokhtari, I. Ciofini, *Chem. Phys. Lett.* 461 (2008) 16.
- [127] P.L. Vandewalle, N.O. Petersen, *FEBS Lett.* 210 (1987) 195.
- [128] H. Eyring, *J. Chem. Phys.* 3 (1935) 107.
- [129] F.M. Lewis, M.S. Matheson, *J. Am. Chem. Soc.* 71 (1949) 747.
- [130] J.R. Shelton, C.K. Liang, P. Kovacic, *J. Am. Chem. Soc.* 90 (1968) 354.
- [131] V.I. Bruskov, A. Chernikov, S.V. Gudkov, Z.K. Massalimov, *Biophysics* 48 (2003) 1022.
- [132] V.I. Bruskov, L.V. Malakhova, Z.K. Masalimov, A.V. Chernikov, *Nucl. Acids Res.* 30 (2002) 1354.
- [133] A. Chernikov, V.I. Bruskov, *Biophysics* 47 (2002) 717.
- [134] C.F. Schönbein, *J. für Praktische Chemie* 81 (1860) 257.
- [135] P.A. Clapp, N. Du, D.F. Evans, *J. Chem. Soc. -Faraday Trans.* 86 (1990) 2587.
- [136] T. Ishii, I. Fridovich, *Free Rad. Biol. Med.* 8 (1990) 21.
- [137] M.P. Miller, D.M. McKnight, S.C. Chapra, *Aquat. Sci.* 71 (2009) 170.
- [138] M.I. Heller, P.L. Croot, *J. Geophys. Res.-Oceans*, submitted for publication.

The kinetics of Superoxide reactions with dissolved organic matter in Tropical Atlantic surface waters near Cape Verde (TENATSO)

Heller, M.I. and Croot, P.L.

The kinetics of Superoxide reactions with dissolved organic matter in Tropical Atlantic surface waters near Cape Verde (TENATSO)

M.I. Heller¹ and P.L. Croot¹.

¹FB2 Marine Biogeochemie, Leibniz-Institut für Meereswissenschaften (IfM-Geomar),
Dienstgebäude Westufer, Düsternbrooker Weg 20, 24105 Kiel, Germany.

Index Terms:

4807 Chemical Speciation and Complexation 4805 Biogeochemical cycles
4851 Oxidation/reduction reactions 4852 Photochemistry
4264 Ocean Optics

Keywords: Tropical Atlantic, Superoxide, CDOM, Hydrogen Peroxide

Revised manuscript submitted to JGR-Oceans

ABSTRACT

The decay kinetics of superoxide (O_2^-) reacting with organic matter was examined in oligotrophic waters at, and nearby, the TENATSO ocean observatory adjacent to the Cape Verde archipelago. Superoxide is the short lived primary photochemical product of colored dissolved organic matter (CDOM) photolysis and also reacts with CDOM or trace metals (Cu, Fe) to form H_2O_2 . In the present work we focused our investigations on reactions between CDOM and superoxide. O_2^- decay kinetics experiments were performed by adding KO_2 to diethylenetriaminepentaacetic acid (DTPA) amended seawater and utilizing an established chemiluminescence technique for the detection of O_2^- at nM levels. In Cape Verdean waters we found a significant reactivity of superoxide with CDOM with maximal rates adjacent to the chlorophyll maximum, presumably from production of new CDOM from bacteria/phytoplankton. This work highlights a poorly understood process which impacts on the biogeochemical cycling of CDOM and trace metals in the open ocean.

1. INTRODUCTION

The superoxide (O_2^-) radical is suspected to be a critically important species involved in the redox cycling of metal ions in natural waters [Heller and Croot, 2009; Rose and Waite, 2006; Voelker *et al.*, 2000]. In sunlit surface waters O_2^- is a major product of the photo-oxidation of colored dissolved organic matter (CDOM) [Micinski *et al.*, 1993; O'Sullivan *et al.*, 2005] and it can also be produced via phytoplankton metabolic processes [Marshall *et al.*, 2005]. Inorganic and organic complexes of Cu(II)/Cu(I) and Fe(II)/Fe(III) can react rapidly with superoxide leading to a catalytic cycle for superoxide decay [Voelker *et al.*, 2000]. The products of superoxide decomposition are H_2O_2 and O_2 , and photochemically produced superoxide is believed to be the major pathway for H_2O_2 formation in the ocean [Croot *et al.*, 2004; O'Sullivan *et al.*, 2005; Yuan and Shiller, 2001]. There is currently a lack of published

data on direct measurements of superoxide production rates from the open ocean, with only a recent study on non-photochemical production [Rose *et al.*, 2008] and an earlier study investigating photoproduction in the Caribbean [Micinski *et al.*, 1993] available. In the absence of direct measurements, H₂O₂ photo-production rates can be used as a reasonable estimate of the major O₂⁻ source in the ocean [Zafiriou, 1990]. A number of reactions have been identified in seawater that affect superoxide decay rates and these include; (i) The 2nd order uncatalysed dismutation reaction of superoxide with its conjugate acid (HO₂) [Zafiriou, 1990], (ii) Reactions with Cu species in seawater [Voelker *et al.*, 2000], (iii) Reactions with Fe species in seawater [Rose and Waite, 2006], and (iv) Reactions with CDOM [Goldstone and Voelker, 2000]. Overall the kinetic reactivity of O₂⁻ is then determined by the following reactions:

$$\frac{\partial[O_2^-]}{\partial t} = 2k_2[O_2^-]^2 + \sum k_M [M]_X [O_2^-] + k_{org} [O_2^-] \quad (1)$$

where k_2 is the 2nd order uncatalysed dismutation rate constant, $[M]_X$ denotes the concentration of different metal species, and (k_M) is the rate constants for the reactions with metals and includes both the Cu(II)/Cu(I) and Fe(III)/Fe(II) redox pairs (see below), the reaction with organic substances is described by the first order rate k_{org} .

$$\sum k_M [M]_X = (k_{Cu(I)}[Cu(I)] + k_{Cu(II)}[Cu(II)] + k_{Fe(II)}[Fe(II)] + k_{Fe(III)}[Fe(III)]) \quad (2)$$

The observed rate of superoxide decay can then be written as follows with only a single term each for the first order and second order rate components

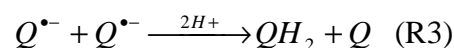
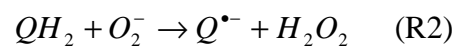
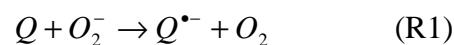
$$\frac{\partial[O_2^-]}{\partial t} = -2k_2[O_2^-]^2 - k_{obs}[O_2^-] \quad (3)$$

where k_{obs} is described as the sum of the first order reaction rates.

$$k_{obs} = \sum k_M [M]_X + k_{org} \quad (4)$$

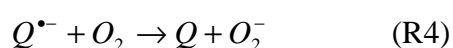
Metal complexes of the chelator diethylenetriaminepentaacetic acid (DTPA) react only very slowly with superoxide and so under the conditions of sufficient DTPA to complex reactive trace metals it can be assumed that $k_{\text{obs}} = k_{\text{org}}$ [Goldstone and Voelker, 2000].

CDOM is the main light absorbing substance in the ocean and represents an important chromophore in the UV region. CDOM plays an important role in light availability for primary productivity [Blough and Del Vecchio, 2002] and for photochemical reactions where it is critical to the production of free radical species [Dister and Zafiriou, 1993]. In the open ocean CDOM is produced by heterotrophic processes in the upper water column [Steinberg *et al.*, 2004] and is destroyed by solar bleaching. Key components identified in CDOM include humic and fulvic acids which can also form complexes with trace metals [Cory and McKnight, 2005]. The redox active fraction of CDOM, which can easily exchange electrons, has been attributed to quinone moieties [Scott *et al.*, 1998]. Quinones can shuttle between three redox states; the fully oxidized quinone (Q), which can undergo a one electron reduction to the semiquinone radical ($Q^{\bullet-}$) and with a further one electron reduction to the hydroquinone (QH_2). Superoxide reacts rapidly with both the quinone and hydroquinone to form the radical semiquinone species [Shkarina *et al.*, 2001], which dismutates to reform the starting quinone and hydroquinone, thus creating a potential catalytic cycle for the decay of superoxide [Goldstone and Voelker, 2000]. H_2O_2 is also produced from the superoxide mediated oxidation of the hydroquinone [Ishii and Fridovich, 1990].



where Q is the quinone, QH_2 is the hydroquinone and $Q^{\bullet-}$ is the semiquinone radical [Eyer, 1991; Roginsky *et al.*, 1999]. It should be noted that for reaction 3 there is no pH dependence as H^+ is not a reactant in the rate limiting step. The initial reaction is to form the quinone and

the unprotonated hydroquinone. The pKa's of hydroquinone are both above pH 8 (pKa₁ = 9.6-10, pKa₂ = 11.4-11.9 [Eyer, 1991]) and thus at seawater pH the hydroquinone is expected to be in the QH₂ form. As pointed out by Meisel [1975] for reaction 3 at pH's below 10 the initially formed Q²⁻ will rapidly protonate to form QH₂ and thus in seawater the influence of pH is not important on this reaction. The pKa for the semiquinone is 4.1 [Eyer, 1991] and thus the deprotonated species dominates at seawater pH. The semiquinone radical however can also generate superoxide by reactions with oxygen [Meisel, 1975].



The overall aim of our study is to assess the role of superoxide in iron redox cycling and its potential for aiding the dissolution of Saharan aerosols deposited in the Tropical Atlantic. In this present work we examine the organic (non-metal) pathways for superoxide decay in seawater in order to better understand other key pathways for superoxide loss in seawater. This is the first study that we are aware of in open ocean waters that focuses on the relationship between CDOM and the organic reactions with superoxide in seawater.

2. METHODOLOGY

2.1 Chemical Analysis

Reagents.

All reagents were prepared using 18MΩ cm resistivity water (hereafter MQ water) supplied by a combination of an ELIX-3 and Synergy 185 water systems (Millipore). MCLA ([2-methyl-6-(4-methoxyphenyl)-3,7-dihydroimidazo[1,2-a]pyrazin-3-one, HCl]), (Fluka) was used as received. A primary 1 mM MCLA standard, was prepared by dissolving 10 mg MCLA in 34.5 mL MQ water. Aliquots (1 mL) of the primary solution were then pipetted into polyethylene vials and frozen at -80°C until required for use. The working MCLA standard, 1 μM, was prepared from a thawed vial of the primary stock by dilution into 1 L

MQ water. This solution was buffered in 0.05 M sodium acetate and adjusted to pH_{NBS} of 6 with quartz distilled 6 M HCl (Q-HCl). A 3.8 mM stock solution of DTPA was made up by dissolving 0.6g in 400 mL MQ water. For each experiment a fresh superoxide stock was provided in a dark glass bottle by adding a specific amount (8-10 mg) of potassium superoxide, KO_2 , to a $\text{pH}_{\text{NBS}} = 13$ NaOH solution. This pH ensured a stable superoxide concentration over the required experiment time. All plasticware used in this work was extensively acid cleaned before use with 0.1 M Q-HCl.

Measurement of Sample pH.

In the present manuscript we report seawater pH values using the total hydrogen scale (pH_{TOT}) [Dickson, 1993] while we use the NBS scale (pH_{NBS}) for pH measurements of buffers and other low ionic strength solutions. All pH measurements during the course of this work were made using a WTW pH meter 330i calibrated with Tris buffers [Millero *et al.*, 1993].

Seawater sampling.

During May 2009 we occupied 3 stations in the vicinity of the island of Sao Vicente in the Cape Verde archipelago (see Figure 1): Station 8 (S8) to the North East on May 17 ($17^\circ 20' \text{ N } 24^\circ 47' \text{ W}$), Station 9 (S9) to the South West on May 23 ($16^\circ 44' \text{ N } 25^\circ 15' \text{ W}$), and Station 10 (S10) on May 30 at the TENATSO time-series observatory ($17^\circ 35' \text{ N } 24^\circ 15' \text{ W}$). At each station we obtained continuous vertical profiles for temperature, salinity and oxygen. Discrete samples were obtained for chlorophyll, CDOM and superoxide decay kinetics (Table 1). Macronutrients and H_2O_2 during May 2009 were only sampled at the TENATSO site, which had also previously been sampled for these parameters in November 2008. Sampling was performed using a CTD-rosette (Seabird) sampling system deployed

from the *RV Islandia* (INDP, Cape Verde). Discrete samples were taken using 8 L Niskin Bottles on the 12 bottle rosette. Samples for macronutrients and chlorophyll were analyzed using standard protocols [Grasshoff *et al.*, 1999].

CDOM measurements.

CDOM measurements were performed using a LWCC-2100 100 cm pathlength liquid waveguide cell (World Precision Instruments, Sarasota, FL, USA) and an Ocean Optics USB4000 UV-VIS spectrophotometer in conjunction with an Ocean Optics DT-MINI-2-GS light source. Samples were syringe filtered through 0.2 μm filters (Sarstedt), the first 10 mL were discarded and the absorbance measured by direct injection into the LWCC. Absorbance measurements were made relative to MQ water and corrected for the refractive index of seawater based on the procedure outlined in Nelson *et al.* [2007]. The resulting dimensionless optical density spectra were converted to absorption coefficient (m^{-1}): $a_{\text{CDOM}(\lambda)} = 2.303 A_{\lambda} / \ell$, where 2.303 converts decadal logarithmic absorbance to base e, and ℓ is the effective optical pathlength of the waveguide (here 103.8 ± 0.5 cm as determined by the manufacturer).

H₂O₂ measurements in surface waters.

Samples for H₂O₂ were analyzed at sea within 1-2 hours of collection using a flow injection chemiluminescence (FIA-CL) reagent injection method [Yuan and Shiller, 1999] as described previously [Croot *et al.*, 2004]. In brief, the chemiluminescence of luminol is catalysed by the reaction of H₂O₂ present in the sample with Co²⁺ at alkaline pH. Samples were analyzed using 5 replicates: typical precision was 2–3% through the concentration range 1–300 nM, the detection limit (3s) is typically 0.2 nM.

Superoxide Measurement Technique and Apparatus.

For this work, we employed a chemiluminescence analysis method for superoxide utilizing MCLA that has been described previously [Heller and Croot, 2009]. Our system utilizes a commercially available FeLume (Wateville Analytical) system, which is comprised of a light tight box equipped with a Plexiglas spiral flow cell mounted below a photon counter (Hamamatsu HC135-01). The photon counter is linked via a Bluetooth serial port to a laptop computer and controlled through a purpose built Labview™ (National Instruments) virtual instrument. The photon counter has a base counting period of 10 ms, for the present work we used average counts of an integration time of 200 ms. Dark background counts for this detector were typically 60–120 counts s⁻¹. For O₂⁻ determination we ran the sample and the MCLA reagent directly into the flow cell using a peristaltic pump (Gilson Minipuls 3, operating at 18 rpm,) with the sample line being pulled through the flow cell as this leads to the smallest amount of dead time in the system (typically 2-3 s). The overall flow rate through the cell was 8.25 mL min⁻¹, comprising 5.0 mL min⁻¹ from the MCLA and 3.25 mL min⁻¹ from the sample. The transit time through the optical cell (300 µL) was therefore 2.18 s.

Field measurements of superoxide reaction rates in seawater.

Our approach is based on measuring the decay rate of known quantities of added O₂⁻ (as KO₂) to seawater. O₂⁻ is detected via its chemiluminescence reaction with MCLA. The experimental setup used here was the same as we had used previously [Heller and Croot, 2009] but in this case consisted of only the sample treatments with DTPA in order to prevent reactions with trace metals from occurring.

For each experiment up to 10 depths from throughout the water column were sampled. From each depth a 60 mL Teflon bottle was filled with 40 mL of the fresh collected filtered seawater and spiked with DTPA (3.8 µM final concentration). Samples with DTPA were left overnight (12 hours) to equilibrate before the addition of superoxide, as we had

previously found that shorter equilibration times did not completely remove the influence of the metal ions. After equilibration 20 μL of a freshly prepared KO_2 solution ($\sim 100 \mu\text{M O}_2^-$) was added to the samples and immediately injected in the flow injection system where the chemiluminescence signal was detected and followed for up to 3 minutes. The superoxide concentrations of the KO_2 standard was checked by UV spectrophotometry with the same 100 cm long path as used for the CDOM measurements (above) and the concentration of superoxide was calculated by solving for both the superoxide and H_2O_2 absorbance for multiple wavelengths in the range 250 – 300 nm. Values for the molar absorptivity for O_2^- [Bielski *et al.*, 1985] and HO_2^- [Bielski and Allen, 1977] at pH 12.5 were obtained from the relevant literature.

Background Chemiluminescence:

MCLA produces chemiluminescence by itself due to auto-oxidation of the conjugate base of MCLA with O_2 [Fujimori *et al.*, 1993]. Auto-oxidation reactions are reduced by using an analytical pH less than the pK_a of MCLA (7.75) [Fujimori *et al.*, 1998] and by reducing the MCLA concentration [Kambayashi and Ogino, 2003]. MCLA also reacts rapidly with singlet oxygen to produce chemiluminescence [Fujimori *et al.*, 1998] however singlet oxygen is present at low pM concentrations as it is efficiently quenched in seawater [Cory *et al.*, 2008]. MCLA also does not appreciably react with H_2O_2 [Kambayashi and Ogino, 2003] to produce chemiluminescence at the concentrations encountered (nM to μM) in the present work. In our study we ran seawater samples without added superoxide to determine the baseline chemiluminescence due to the auto-oxidation reaction of MCLA. The baseline values determined in this manner (range: 7000 – 15000 counts per 200 ms period) were subtracted from the superoxide decay data in order to correctly determine the decay rate (see below). In the present work where we added nM superoxide in order to observe the

decay the baseline corrections were relatively minor with regard to the initial counts (< 1%). At lower concentrations of superoxide baseline correction is more important as is the signal to noise ratio.

Linearity of the MCLA technique:

We have previously shown [Heller and Croot, 2009] that the chemiluminescence response between MCLA and superoxide is linear over the range of superoxide concentrations employed in this work. The assessment of this linear response is of course complicated by the rapid decay of the superoxide. Previously we performed a series of experiments in which seawater samples were spiked with varying amounts of a known concentration of superoxide and then calculated the initial superoxide signal based on the decay curve. For the configuration used in our experiments we found a linear response, for the range 0-90 nM superoxide, as has been shown previously [Mitani *et al.*, 1994; Zheng *et al.*, 2003]. A practical concern however is that with high concentrations of superoxide (> 90 nM) the 1 μ M MCLA is insufficient to prevent uncatalysed dismutation of superoxide in the pH_{NBS} 6 buffer despite the fast reactivity of MCLA with O₂⁻ [Akutsu *et al.*, 1995; Gotoh and Niki, 1990]. An additional check on the linearity of the response was that the calculated rates in DTPA amended seawater [Heller and Croot, 2009] were not significantly different from earlier estimates [Zafiriou, 1990]. This would not have been observed if the response was significantly non-linear.

Precision and Accuracy:

Analysis of replicate samples using near surface water collected from close to Cape Verde, were used to assess the precision of the technique. For this small data set (n=5), $k_{obs} = 0.0245 \pm 0.0016$ (2 σ) indicating a precision of 6.4 % for these samples. The main problem associated with this technique initially was the formation of bubbles in the flow cell which

gave rise to signal spikes, this problem was reduced when seawater samples were given adequate time to come into equilibrium with the laboratory temperature after collection. Care is also needed in mixing the samples thoroughly when adding the superoxide. For the work reported here from Cape Verde samples were run in duplicate.

The accuracy of the MCLA method for the determination of both superoxide concentration and the value of the rate constants k_1 and k_2 are difficult to assess given that the superoxide concentration is transient and there are no standard reference materials available with a certified rate constant. Thus direct comparison with the earlier work by Goldstone and Voelker [Goldstone and Voelker, 2000] on k_{org} ($0.1 - 1.4 \text{ s}^{-1}$) is not possible as we did not measure the same samples as them and their work was performed using samples with significantly higher $a_{CDOM(300)}$ values ($0.5 - 20 \text{ m}^{-1}$) than in our work. From our previous work [Heller and Croot, 2009] performed in the absence of appreciable DOM we found good agreement for the pH dependent value of k_2 (our value: $4.4 \pm 1.6 \times 10^{12} [\text{H}^+] \text{ M}^{-1} \text{ s}^{-1}$; pH_{TOT} scale, $n = 14$, 95% CI) with earlier work by Zafiriou using spectrophotometry [Zafiriou et al., 1998] k_2 ($5 \pm 1 \times 10^{12} [\text{H}^+] \text{ M}^{-1} \text{ s}^{-1}$; pH_{NBS} scale). Recently we have shown that the MCLA technique is highly accurate in seawater when calibrated as described here [Heller and Croot, 2010]. Thus we believe that our method is at least as accurate, if not better, as other available methods including spectrophotometry.

Measurement of impurities in superoxide standards prepared from KO_2 and calibration of the initial superoxide concentration.

(i) Trace Metals: In the last decades KO_2 has not been used widely as a source of superoxide due to the perception, that it was highly contaminated with metals. However it now appears that many of the problems, reported in earlier studies, with KO_2 may have resulted from non trace metal clean equipment, most likely from water supplies which did not utilize final filtration as was alluded to in some earlier works [Weinstein and Bielski, 1979]. In the course

of our work we could find no evidence of any measurements of the trace metal content in KO_2 . Recently [*Heller and Croot, 2009*] we analyzed directly aliquots of KO_2 solutions for Fe and Cu and found that the KO_2 contained 0.7 ± 0.1 ppm Fe (dry weight) and no detectable Cu (less than 0.06 ppm Cu). Thus for the present work, using our standard protocol, we would have added ~ 3 pM Fe (< 0.8 pM Cu) which would provide a maximum additional decay rate of $3 \times 10^{-4} \text{ s}^{-1}$ (using a reaction rate with Fe of $1 \times 10^8 \text{ M}^{-1} \text{ s}^{-1}$) significantly less than our observed rates. Thus the influence of trace metals in the KO_2 in our studies was apparently not significant to affect the results.

(ii) There is a significant amount of H_2O_2 in solutions prepared from KO_2 and this is unavoidable with any superoxide source, including photochemical and enzymatic production pathways. In the course of this work we came across problems with the current spectrophotometric methods used for calibrating O_2^- that was generated photochemically using acetone or benzophenone in 2-propanol/water mixtures following the method of McDowell et al. [1983]. In brief the absorption spectra of acetone [*Feigenbrugel et al., 2005*] and benzophenone [*Bennett and Johnston, 1994*] overlap with that of O_2^- [*Bielski et al., 1985*] and the reaction with benzophenone also produces acetone [*Görner, 2006; 2007*]. Similarly another common system used to generate a flux of O_2^- , Xanthine/Xanthine Oxidase also has been shown to be more complicated than first thought [*Hodges et al., 2000*]. Thus in the present work we chose to use KO_2 as our source for O_2^- in simple pulse chase decay experiments. In this work we always made measurements in order to determine the concentrations of both species in each standard solution prepared by UV spectrophotometry with either a LWCC-2100 100 cm pathlength liquid waveguide cell (World Precision Instruments, Sarasota, FL, USA), or a 10 cm Quartz-cuvette (Hellma), and an Ocean Optics USB4000 UV-VIS spectrophotometer combined with an Ocean Optics DT-MINI-2-GS light source. Concentrations of H_2O_2 and O_2^- were determined by determining the least squares

solution to the measured absorbance, at multiple wavelengths, by using published molar extinction coefficients for H_2O_2 [Bielski and Allen, 1977] and O_2^- [Bielski et al., 1985]. A full description of this method can be found in Heller and Croot [2010]. Mean initial concentrations in the primary KO_2 solution assessed in this way were $900 \pm 50 \mu\text{M}$ for H_2O_2 and $90 \pm 10 \mu\text{M}$ O_2^- . No DTPA or other complexing agents were added to our KO_2 primary solution. H_2O_2 in the final seawater solutions was also assessed on occasion by using the chemiluminescence flow injection method [Yuan and Shiller, 1999] described above.

Effect of KO_2 addition on pH of samples

In earlier works on superoxide kinetics in seawater, authors either did not report which pH scale they used or have used pH_{NBS} , apparently unaware of problems with this scale at high ionic strengths [Dickson, 1993; Millero et al., 1993]. In the present work we are able to calculate the *in situ* and laboratory pH_{TOT} based on temperature, pressure, salinity, nutrient, alkalinity and TCO_2 data, provided by the TENATSO laboratory at the INDP in Cape Verde. Laboratory pH_{TOT} measurements were also made on the samples prior and after the addition of superoxide. In all cases pH_{TOT} increased after the addition of superoxide by approximately 0.08-0.10 pH_{TOT} units. These small increases in pH_{TOT} however did not apparently affect first order decay rates in any significant manner as evidenced by the good precision for k_{obs} found over a range of superoxide additions (see section above on precision) where the maximal pH_{TOT} change was up to 0.20 pH units. It should be noted that a larger pH_{TOT} change was induced by the warming of the samples to the laboratory temperature and these temperature induced changes in superoxide reactivity need to be considered when considering *in situ* rates.

2.2 Calculation of rate data for superoxide.

The raw chemiluminescence signal for the reaction between MCLA and O_2^- recorded by the computer was processed using a specially designed Labview™ VI constructed for this purpose using standard kinetic fitting procedures, incorporating the non-linear Levenberg-Marquardt algorithm [Levenberg, 1944; Marquardt, 1963], to determine both the 1st (in the following k_1 is equivalent to k_{obs}) and 2nd order (k_2) rates simultaneously (equation 3). Previously [Heller and Croot, 2009] we have shown that equation 3 has the general solution:

$$[O_2^-] = \frac{k_1}{\left(\frac{k_1}{[O_2^-]_0} + k_2 \right) e^{k_1 t} - k_2} \quad (5)$$

Note that for the above equation when $k_2 = 0$ (no dismutation) the solution to equation 5 is the same as that for a normal first order reaction. However the equation does not collapse to solely second order when $k_1 = 0$ due to the assumption made in the derivation that $k_1 \neq 0$. Thus in the case of $k_1 = 0$ the normal 2nd order rate equation should be used, for practical purposes in this work this was done when $k_1 < 1 \times 10^{-4} \text{ s}^{-1}$. Using the same reasoning the minimum value for k_1 (k_{obs}) that can be estimated using our approach is $1 \times 10^{-4} \text{ s}^{-1}$.

3. RESULTS AND DISCUSSION

3.1 Vertical profiles of superoxide organic matter kinetics.

Typical results for the O_2^- decay in DTPA amended seawater are shown in figure 2 for two samples from different depths at S9. Both decay curves show the typical rapid decay of superoxide (initially ~100 nM) within the first 10 seconds before the sample has reached the detector. What is most interesting to note however is that the sample from 150 m displays two distinct decay rates (easily seen in the natural log transformed data), a fast initial rate for the first 60 s which is followed by an extremely slow decay, while the sample from 10 m only decays at an essentially constant rate. For the data from 150 m at S9 (Figure 2) we assessed

changes in the first order decay rate (k_{org}) over the course of the experiment, by analyzing the data over different time intervals. Using this approach it indicated that k_{org} in this sample reduced from 0.026 to 0.0046 s^{-1} over the course of the decay experiment. This change in the decay rate suggests either the appearance of a significant back reaction producing superoxide (see below) or alternatively that there were two pools of organic matter reacting with superoxide, a small highly reactive pool which was mostly responsible for the initial fast reaction rate and a larger less reactive group of organic molecules that corresponded to the slower rate observed in the later part of the experiment. This change in the reaction rate with time was seen throughout the mid depth range (60-150 m) at S9, but was not apparent at S8 and S10.

For the vertical profiles at S9 there was a clear maximum in k_{org} in the depth range 60-100 m which was below the mixed layer depth (MLD) but still within the euphotic zone (Figure 3). This maximum was not as distinct in the other two stations where decay rates were relatively uniform. Overall, with the exception of the samples mentioned above from S9, in every experiment the decay of O_2^- in DTPA amended seawater showed constant first order decay kinetics with k_{org} ranging from 0.009 to 0.034 s^{-1} (Table 1), additionally for these samples the decay rate was found to not appreciably vary (less than 5%) as a function of the superoxide concentration (0-20 nM) suggesting that the reaction was not limited by the concentration of DOM or alternatively that a catalytic cycle with components of the DOM had been established.

3.2 Is there a relationship between CDOM and superoxide kinetics?

In the present work we use values of $a_{\text{CDOM}(300)}$ as a proxy for DOM, as unfortunately we do not have any measurements of Dissolved Organic Carbon (DOC) from these stations. Profiles of $a_{\text{CDOM}(300)}$ at S9 and S10 showed distinct maxima at 80 m just below the deep

chlorophyll maxima (DCM) at 60 m (Figure 3) as has been observed previously in the Tropical Atlantic [Kitidis *et al.*, 2006]. At S8 however $a_{\text{CDOM}(300)}$ was relatively uniform throughout the upper 400 m despite a well developed DCM at 60 m. Mixed Layer depths (MLD-calculated as the depth at which σ_θ had increased by 0.05 over the surface value) at the time of sampling ranged from 27 m at S8, 33 m at S9, to 50 m at S10 (Figure 2). For S10 the sampling was in the early morning when the MLD is at its deepest due to night time convective cooling [Brainerd and Gregg, 1995]. Both S8 and S9 represent late afternoon stations when MLD are shallower. At all stations surveyed in May 2009 the DCM was below the MLD.

CDOM is comprised of an unknown number of potential chromophores [Nelson and Siegel, 2002] and forms only a small part of the DOC pool in the ocean, of which it is suggested to be a refractory component [Nelson *et al.*, 2007]. The sources of CDOM are not well described but include zooplankton and protozoan grazing [Steinberg *et al.*, 2004], bacterial production [Nelson *et al.*, 2004] and riverine input [Blough and Del Vecchio, 2002]. There are no major riverine sources in our study region [Cotrim da Cunha *et al.*, 2009] and our data strongly suggests that both the maxima in $a_{\text{CDOM}(300)}$ and k_{org} could be related to the remineralization of organic matter below the DCM via zooplankton grazing and bacterial activity.

Previous work has suggested correlations between $a_{\text{CDOM}(300)}$ and (i) radical production via sunlight irradiation [Dister and Zafiriou, 1993; O'Sullivan *et al.*, 2005] and (ii) superoxide decay in DTPA amended coastal seawater [Goldstone and Voelker, 2000]. The relationship between $a_{\text{CDOM}(300)}$ and radical production we can not assess here directly as we did not examine production rates, however in the earlier study by O'Sullivan and coworkers [2005] the quantum yield of H_2O_2 was determined in the laboratory from photolysis of CDOM in natural water samples, including samples from rivers, estuaries, and both the

coastal and open ocean. These authors found that the H_2O_2 quantum yield measured at 290 nm ranged from 4.2×10^{-4} in freshwater to 2.1×10^{-6} in marine waters and a linear relationship was found between the production of H_2O_2 and the loss of absorbance in the CDOM spectrum due to photobleaching. These authors also observed no significant relationship between H_2O_2 production and the dissolved organic carbon (DOC) concentration. However samples which contained terrigenous carbon in the form of humic substances showed a higher H_2O_2 production. In the context of the present work, Figure 3 indicates that there was potentially photo-bleaching occurring in the surface waters of S8 and S9 as evidenced by small decreases in $a_{\text{CDOM}(300)}$ values from depth towards the surface. No such gradient in $a_{\text{CDOM}(300)}$ is apparent at S10, however diel cycles may be important here, as S10 is the only station which was sampled in the morning after night time convective mixing could have eroded such a feature away.

The correlation between $a_{\text{CDOM}(300)}$ and k_{org} found by Goldstone and Voelker [2000] for DTPA amended coastal seawater samples, predicts for our measured $a_{\text{CDOM}(300)}$ values, $k_{\text{org}} = 0.1\text{-}0.2 \text{ s}^{-1}$, an order of magnitude more than what we observed (Table 1). Unlike the earlier coastal study, we found no statistically significant correlation between $a_{\text{CDOM}(300)}$ and k_{org} at any of the stations we sampled. This result strongly suggests that open ocean CDOM is significantly less reactive with superoxide than coastal waters and this may be related to the lack of riverine and terrestrial derived humic materials in open ocean waters. It also strongly suggests that the organic components reacting with superoxide in seawater make only minor contributions to $a_{\text{CDOM}(300)}$ in open ocean waters. To examine further the influence of CDOM/DOM on superoxide kinetics we routinely made a series of experiments with samples diluted with MQ, but using the same DTPA concentration, to check that the observed reaction was due to components in the seawater. In all cases the observed value of k_{org} varied linearly with the proportion of seawater in the sample (Figure 4), which when coupled with the

assumption that DTPA complexation removed the reaction with trace metals, strongly suggests that it was an organic component of the seawater that was responsible for the observed first order decay of superoxide. In all samples measured in our study we observed superoxide decay rates significantly in excess of that expected solely from the uncatalysed dismutation reaction, the kinetics of which is well described from studies in pure water [Bielski *et al.*, 1985] and seawater [Heller and Croot, 2009; Zafiriou, 1990].

There are only a few open ocean studies of superoxide decay, our earlier study in the Southern Ocean [Heller and Croot, 2009] found no significant organic mediated decay. Higher values ($k_{\text{org}} = 0.02 - 1.4 \text{ s}^{-1}$) were found in coastal waters [Goldstone and Voelker, 2000] where DTPA was allowed to equilibrate with the seawater for several hours before analysis and a photochemical source of superoxide was used. The equilibration time with DTPA is a critical parameter to consider as we had previously observed in Southern Ocean samples [Heller and Croot, 2009] that 2 hours equilibration was insufficient to complex all metal reactions and that 12 hours was optimal. A recent study in the Tropical Pacific [Rose *et al.*, 2008] found values of $9.7 \times 10^{-3} \text{ s}^{-1} > k > 1 \times 10^{-4} \text{ s}^{-1}$, but in this work DTPA was added immediately prior to measurement and an enzymatic source for superoxide was employed. This work is then difficult to compare with as the metal reactions are still included and problems also exist regarding the superoxide source. This is an important difference between our work and Rose *et al.* as enzymatic sources, with constant generation of superoxide, can not be used in a simple pulse chase experiment such as performed in this work and instead must rely on the achievement of steady state conditions in order to calculate the decay rate from a production rate estimate.

3.3 What organic species are reacting with O_2^- ?

In the present work we have examined the relationship between DOM and superoxide decay kinetics with the initial assumption that CDOM is proportional to the reactive organic component. Our results suggest that there is not a clear link between bulk CDOM and superoxide reactivity in open ocean waters. However CDOM is obviously still critical for the photo-production of superoxide [Dister and Zafiriou, 1993; Micinski et al., 1993]. In this section we examine what organic species present in seawater may be responsible for the observed reactions with superoxide. Where rate constants are known for these reactions they are summarized in Table 2.

Quinones are cellular components in bacteria [Akagawa-Matsushita et al., 1992], marine fungi [Bugni et al., 2000; Son et al., 2002] and phytoplankton [Greene et al., 1992; Miller et al., 2009] which can be released to the water upon grazing or cell-lysis. There is currently increased interest in quinone/hydroquinone chemistry in natural waters due to their presence in humic and fulvic substances [Miller et al., 2009; Tossell, 2009], where they may be responsible for much of the humic component in CDOM fluorescence [Cory and McKnight, 2005; Klapper et al., 2002]. The possible impacts on biogeochemical cycles mediated by quinones was recently the subject of a review article [Uchimiya and Stone, 2009]. We could find no reports in the literature for the concentrations of quinones in the dissolved phase in seawater. Quinone like moieties have been detected in marine particles however [Brandes et al., 2004] where they may contribute up to 10% of the particle content. Quinones may also be formed abiotically from reactions between proteins and carbohydrates in seawater [Hedges, 1978].

Quinones react rapidly with superoxide ($k_{R1} 1-9 \times 10^8 \text{ M}^{-1} \text{ s}^{-1}$) [Bielski et al., 1985] and have been suggested previously to be the potential reactants in seawater [Goldstone and Voelker, 2000]. Using published data for the model quinone 1,4-benzoquinone ($k_{R1} = 1 \times 10^9 \text{ M}^{-1} \text{ s}^{-1}$, for reaction with superoxide) [Meisel, 1975], its semiquinone radical ($k_{R3} = 2.3 \times 10^7$

$\text{M}^{-1} \text{s}^{-1}$, self reaction) [Meisel, 1975] and hydroquinone ($k_{\text{R2}} = 1.7 \times 10^7 \text{ M}^{-1} \text{ s}^{-1}$, for reaction with superoxide)[Rao and Hayon, 1975] here we estimate, via simple numerical modeling incorporating the quinone reactions (R1-R4) described above and the uncatalysed dismutation reaction for O_2^- , that a $k_{\text{org}} = 0.03 \text{ s}^{-1}$ would require a total quinone and hydroquinone concentration of $\sim 9 \text{ nM}$ for catalytic cycling under the conditions of our experiments. Note that the reaction between the semiquinone and superoxide is not included here as the reaction rate constant is presently unknown, however previous work suggests that it does not influence the overall reaction kinetics significantly [Ishii and Fridovich, 1990; Roginsky and Barsukova, 2000]. The reaction between the hydroquinone and O_2 is also neglected as it is slow due to it being spin forbidden [Roginsky and Barsukova, 2000].

Figure 5 illustrates the results for a numerical simulation of the reaction between 10 nM of quinone/hydroquinone and 100 nM of superoxide using the reaction rates mentioned above. It is clear from figure 5 that the decay rate is first order over the first 60 seconds but then slows as the production of superoxide from the semiquinone reaction with oxygen begins to become more important when superoxide drops below $\sim 10 \text{ nM}$. The modeled result is similar to what was observed in figure 2 for the sample from S9 at 150 m, hinting that reactions with quinones may have been important there. The critical reactions involved are the rate of regeneration of superoxide from the reaction between oxygen and the semiquinone radical ($k_{\text{R4}} = 5 \times 10^4 \text{ M}^{-1} \text{ s}^{-1}$) [Eyer, 1991] and the dismutation rate of the radical into the quinone and the hydroquinone ($k_{\text{R2}} = 2.3 \times 10^7 \text{ M}^{-1} \text{ s}^{-1}$). This also helps to explain why there was no apparent relationship between k_{org} with CDOM absorbance as at a concentration of 10 nM of the quinone no relationship with CDOM absorbance should be expected as the contribution of the quinone to the CDOM absorbance is on the order of 0.5 to 1 %. Based on a typical molar absorption of $2500 \text{ M}^{-1} \text{ cm}^{-1}$ at 290 nm for the hydroquinone and significantly

less for the quinone, thus with a 1m path length this corresponds to an absorbance of 0.0025 when the overall absorbance is 0.3 to 0.6 as seen in figure 3.

Using our values for k_{org} and compilations of O_2^- reaction rates with organic compounds [Bielski *et al.*, 1985; Shkarina *et al.*, 2001] we can draw up a list of alternative organic compounds that could also be responsible for the observed reaction kinetics (Table 2). Of all the candidate molecules, the quinones as discussed above are still the most likely. Two candidates do stand out as having some small influence on the observed rates. Glutathione and related thiols react rapidly with superoxide ($k = 6.7 \times 10^5 \text{ M}^{-1} \text{ s}^{-1}$) [Asada and Kanematsu, 1976] but so far have been only found at sub nM concentrations in seawater [Dupont *et al.*, 2006]. Catechols ($k = 2.7 \times 10^5 \text{ M}^{-1} \text{ s}^{-1}$) may be present in seawater at low nM levels as siderophores [Butler, 2005] and can be further oxidized to quinones. Currently however there is no information on the concentrations of quinones, catechols or thiols in the waters around Cape Verde and so no firm conclusions can be drawn on the identification of the organic species reacting with superoxide.

3.4 Superoxide kinetics and H₂O₂ production at TENATSO.

At the TENATSO site (S10) surface concentrations of nitrate and phosphate were at trace levels in the mixed layer, below which the nutricline appeared along with a distinct nitrite maximum at 60 m (Figure 6) coincident with the DCM (Figure 3). In both November 2008 and May 2009, H₂O₂ was relatively constant in the upper 50m and decreased rapidly below (Figure 6) consistent with previous data from this region [Croot *et al.*, 2004; Steigenberger and Croot, 2008]. Both the H₂O₂ and nitrite profiles show the importance of photochemistry on the distribution of these species in the water column, but also show the contrast between the species in terms of photo-production (H₂O₂) and photodecay (Nitrite).

Interestingly there was a strong correlation between H_2O_2 concentrations and k_{org} for samples below the MLD ($R^2 = 0.93$, $n=7$, figure 7) away from the main photo-production zone for H_2O_2 . This raises the intriguing possibility that if quinones are determining k_{org} then the relationship to H_2O_2 in deep waters may be due to the back reaction between O_2 and the semiquinone radical producing superoxide (R4) which in turn can react via a number of pathways, including reaction with hydroquinone, to produce H_2O_2 (R2). The reaction scheme outlined is in essence the same as that for the auto-oxidation of hydroquinones [Eyer, 1991; Ishii and Fridovich, 1990] and could be responsible for part of the observed deep water H_2O_2 production that maintains the low concentrations observed there [Yuan and Shiller, 2004]. Repeating the numerical modeling performed above for the O_2^- decay experiments in the presence of quinones, but in the absence of an external O_2^- source, suggests that a constant production rate of 1 nM per day of H_2O_2 can be generated using only the catalytic action of 2 nM hydroquinone and a steady state O_2^- concentration of 0.65 pM resulting from the reaction between O_2 and the semiquinone radical. This model result is however clearly a simplification as reactions with trace metals are most likely also important in the deep waters and they potentially may accelerate reactions forming H_2O_2 directly [Li and Trush, 1993] but also may reduce the O_2^- steady state concentration [Heller and Croot, 2009]. Further work is therefore necessary to elucidate the role of quinones within DOM and their potential role in redox cycling in the ocean. The use of fluorescence techniques to quantify the quinone content of CDOM [Cory and McKnight, 2005] appears a promising method for application to marine studies.

4. CONCLUSIONS

In Tropical Atlantic waters we observed significant reactions for superoxide with organic matter in the upper water column. Vertical profiles of k_{org} were similar to, but not

identical to, profiles of $a_{\text{CDOM}(300)}$. At one station maxima for k_{org} were found just below the chlorophyll maximum, suggesting that this pattern may be due to the production or release of unbleached organic matter. Following up on earlier suggestions that the superoxide reactive component of CDOM may comprise quinone functional groups, exudated from bacteria or phytoplankton, our results indicate that nM concentrations of dissolved quinones could be responsible for the observed k_{org} values. Though there is currently no data on quinones in seawater to confirm this. Our work highlights a poorly understood process which impacts on the biogeochemical cycling of CDOM, H_2O_2 and trace metals in the open ocean.

ACKNOWLEDGEMENTS

The authors would like to express their deep thanks and appreciation to the crew of the *R.V. Islandia* (INDP). Special thanks to Pericles da Silva and Ivanice Monteiro (INDP). Chlorophyll data was courtesy of Wiebke Mohr (IFM-GEOMAR). This work was supported by the BMBF Verbunds project SOPRAN (TP 1.2) and forms part of the German contribution to SOLAS (Surface Ocean Lower Atmosphere Studies).

REFERENCES

- Akagawa-Matsushita, M., T. Itoh, Y. Katayama, H. Kuraishi, and K. Yamasato (1992), Isoprenoid Quinone Composition Of Some Marine Alteromonas, Marinomonas, Deleya, Pseudomonas And Shewanella Species, *Journal Of General Microbiology*, 138, 2275-2281.
- Akutsu, K., H. Nakajima, T. Katoh, S. Kino, and K. Fujimori (1995), Chemiluminescence Of Cipridina Luciferin Analogs .2. Kinetic-Studies On The Reaction Of 2-Methyl-6-Phenylimidazo[1,2-A]Pyrazin-3(7h)-One (Cla) With Superoxide - Hydroperoxyl

- Radical Is An Actual Active Species Used To Initiate The Reaction, *Journal Of The Chemical Society-Perkin Transactions 2*(8), 1699-1706.
- Asada, K., and S. Kanematsu (1976), Reactivity Of Thiols With Superoxide Radicals, *Agricultural And Biological Chemistry*, 40(9), 1891-1892.
- Bennett, G. E., and K. P. Johnston (1994), Uv-Visible Absorbency Spectroscopy Of Organic Probes In Supercritical Water, *Journal Of Physical Chemistry*, 98(2), 441-447.
- Bielski, B. H. J., and A. O. Allen (1977), Mechanism of the disproportionation of superoxide radicals, *J. Phys. Chem.*, 81(11), 1048-1050.
- Bielski, B. H. J., D. E. Cabelli, R. L. Arudi, and A. B. Ross (1985), Reactivity Of HO₂/O₂⁻ Radicals In Aqueous-Solution, *Journal Of Physical And Chemical Reference Data*, 14(4), 1041-1100.
- Blough, N. V., and R. Del Vecchio (2002), Chromophoric DOM in the coastal ocean, in *Biogeochemistry of Marine Dissolved Organic Matter*, edited by D. A. Hansell and C. A. Carlson, pp. 509-546, Academic Press, San Diego.
- Brainerd, K. E., and M. C. Gregg (1995), Surface mixed and mixing layer depths, *Deep Sea Research Part I: Oceanographic Research Papers*, 42, 1521-1543.
- Brandes, J. A., C. Lee, S. Wakeham, M. Peterson, C. Jacobsen, S. Wirick, and G. Cody (2004), Examining marine particulate organic matter at sub-micron scales using scanning transmission X-ray microscopy and carbon X-ray absorption near edge structure spectroscopy, *Marine Chemistry*, 92(1-4), 107-121.
- Bugni, T. S., D. Abbanat, V. S. Bernan, W. M. Maiese, M. Greenstein, R. M. Van Wagoner, and C. M. Ireland (2000), Yanuthones: Novel Metabolites from a Marine Isolate of *Aspergillus niger*, *The Journal of Organic Chemistry*, 65(21), 7195-7200.
- Butler, A. (2005), Marine Siderophores and Microbial Iron Mobilization, *BioMetals*, 18(4), 369.

- Cory, R. M., and D. M. McKnight (2005), Fluorescence Spectroscopy Reveals Ubiquitous Presence of Oxidized and Reduced Quinones in Dissolved Organic Matter, *Environmental Science & Technology*, 39(21), 8142-8149.
- Cory, R. M., J. B. Cotner, and K. McNeill (2008), Quantifying Interactions between Singlet Oxygen and Aquatic Fulvic Acids, *Environmental Science & Technology*, 43(3), 718-723.
- Cotrim da Cunha, L., P. Croot, and J. LaRoche (2009), Influence of river discharge in the tropical and subtropical North Atlantic Ocean, *Limnol. Oceanogr.*, 54(2), 644-648.
- Croot, P. L., P. Streu, I. Peeken, K. Lochte, and A. R. Baker (2004), Influence of the ITCZ on H₂O₂ in near surface waters in the equatorial Atlantic Ocean, *Geophysical Research Letters*, 31, L23S04, doi:10.1029/2004GL020154.
- Dickson, A. G. (1993), pH buffers for sea water media based on the total hydrogen ion concentration scale, *Deep Sea Research Part I: Oceanographic Research Papers*, 40(1), 107-118.
- Dister, B., and O. C. Zafiriou (1993), Photochemical Free-Radical Production-Rates in the Eastern Caribbean, *J. Geophys. Res.-Oceans*, 98(C2), 2341-2352.
- Dupont, C. L., J. W. Moffett, R. R. Bidigare, and B. A. Ahner (2006), Distributions of dissolved and particulate biogenic thiols in the subarctic Pacific Ocean, *Deep-Sea Research Part I-Oceanographic Research Papers*, 53(12), 1961-1974.
- Eyer, P. (1991), Effects of superoxide dismutase on the autoxidation of 1,4-hydroquinone, *Chemico-Biological Interactions*, 80(2), 159.
- Feigenbrugel, V., C. Loew, S. Le Calve, and P. Mirabel (2005), Near-UV molar absorptivities of acetone, alachlor, metolachlor, diazinon and dichlorvos in aqueous solution, *Journal Of Photochemistry And Photobiology A-Chemistry*, 174(1), 76-81.

- Fujimori, K., H. Nakajima, K. Akutsu, M. Mitani, H. Sawada, and M. Nakayama (1993), Chemiluminescence Of Cypridina Luciferin Analogs . Part 1. Effect Of pH On Rates Of Spontaneous Autoxidation Of CLA In Aqueous Buffer Solutions, *Journal Of The Chemical Society-Perkin Transactions 2*(12), 2405-2409.
- Fujimori, K., T. Komiyama, H. Tabata, T. Nojima, K. Ishiguro, Y. Sa-waki, H. Tatsuzawa, and M. Nakano (1998), Chemiluminescence of Cypridina Luciferin Analogs. Part 3. MCLA Chemiluminescence with Singlet Oxygen Generated by the Retro-Diels-Alder Reaction of a Naphthalene Endoperoxide, *Photochemistry and Photobiology*, 68(2), 143-149.
- Goldstone, J. V., and B. M. Voelker (2000), Chemistry of Superoxide Radical in Seawater: CDOM Associated Sink of Superoxide in Coastal Waters, *Environmental Science and Technology*, 34, 1043-1048.
- Görner, H. (2006), Oxygen uptake and involvement of superoxide radicals upon photolysis of ketones in air-saturated aqueous alcohol, formate, amine or ascorbic acid solutions, *Photochemistry And Photobiology*, 82(3), 801-808.
- Görner, H. (2007), Oxygen uptake upon photolysis of 3-benzoylpyridine and 3,3'-dipyridylketone in air-saturated aqueous solution in the presence of formate, ascorbic acid, alcohols and amines, *Journal Of Photochemistry And Photobiology A-Chemistry*, 187(1), 105-112.
- Gotoh, N., and E. Niki (1990), Rate Of Spin-Trapping Of Superoxide As Studied By Chemiluminescence, *Chemistry Letters*(8), 1475-1478.
- Grasshoff, K., K. Kremling, and M. Ehrhardt (1999), *Methods of Seawater analysis*, Wiley-VCH Verlag, Weinheim (FRG).

- Greene, R. M., R. J. Geider, Z. Kolber, and P. G. Falkowski (1992), Iron-Induced Changes in Light Harvesting and Photochemical Energy Conversion Processes in Eukaryotic Marine Algae, *Plant Physiology*, 100, 565-575.
- Hedges, J. I. (1978), The formation and clay mineral reactions of melanoidins, *Geochimica et Cosmochimica Acta*, 42(1), 69-76.
- Heller, M. I., and P. L. Croot (2009), Superoxide Decay Kinetics in the Southern Ocean, *Environmental Science & Technology*, doi: 10.1021/es901766r.
- Heller, M. I., and P. L. Croot (2010), Application of a Superoxide (O_2^-) thermal source (SOTS-1) for the determination and calibration of O_2^- fluxes in seawater, *Analytica Chimica Acta*
- Hodges, G. R., M. J. Young, T. Paul, and K. U. Ingold (2000), How should xanthine oxidase-generated superoxide yields be measured?, *Free Radical Biology and Medicine*, 29(5), 434.
- Ishii, T., and I. Fridovich (1990), Dual Effects Of Superoxide-Dismutase On The Autoxidation Of 1,4-Naphthohydroquinone, *Free Radical Biology and Medicine*, 8(1), 21-24.
- Kambayashi, Y., and K. Ogino (2003), Reestimation of Cypridina Luciferin Analogs (MCLA) as a Chemiluminescence Probe to detect active oxygen species-Cautionary note for use of MCLA, *The Journal of Toxicological Sciences*, 28(3), 139.
- Kitidis, V., A. P. Stubbins, G. Uher, R. C. Upstill Goddard, C. S. Law, and E. M. S. Woodward (2006), Variability of chromophoric organic matter in surface waters of the Atlantic Ocean, *Deep Sea Research Part II: Topical Studies in Oceanography*, 53(14-16), 1666-1684.
- Levenberg, K. (1944), A Method for the Solution of Certain Non-Linear Problems in Least Squares, *The Quarterly of Applied Mathematics*, 2, 164-168.

- Li, Y. B., and M. A. Trush (1993), Oxidation of Hydroquinone by Copper: Chemical Mechanism and Biological Effects, *Archives of Biochemistry and Biophysics*, 300(1), 346-355.
- Marquardt, D. W. (1963), An Algorithm for Least-Squares Estimation of Nonlinear Parameters, *SIAM Journal on Applied Mathematics*, 11(2), 431-441.
- Marshall, J. A., M. de Salas, T. Oda, and G. Hallegraeff (2005), Superoxide production by marine microalgae, *Marine Biology*, 147(2), 533-540.
- McDowell, M. S., A. Bakac, and J. H. Espenson (1983), A convenient route to superoxide ion in aqueous solution, *Inorg. Chem.*, 22(5), 847-848.
- Meisel, D. (1975), Free-Energy Correlation Of Rate Constants For Electron-Transfer Between Organic Systems In Aqueous-Solutions, *Chemical Physics Letters*, 34(2), 263-266.
- Micinski, E., L. A. Ball, and O. C. Zafiriou (1993), Photochemical Oxygen Activation - Superoxide Radical Detection and Production-Rates in the Eastern Caribbean, *Journal of Geophysical Research-Oceans*, 98(C2), 2299-2306.
- Miller, M. P., D. M. McKnight, and S. C. Chapra (2009), Production of microbially-derived fulvic acid from photolysis of quinone-containing extracellular products of phytoplankton, *Aquatic Sciences*, 71(2), 170-178.
- Millero, F. J., J. Z. Zhang, S. Fiol, S. Sotolongo, R. N. Roy, K. Lee, and S. Mane (1993), The Use of Buffers to Measure the pH of Seawater, *Marine Chemistry*, 44(2-4), 143-152.
- Mitani, M., Y. Yokoyama, S. Ichikawa, H. Sawada, T. Matsumoto, K. Fujimori, and M. Kosugi (1994), Determination Of Horseradish-Peroxidase Concentration Using The Chemiluminescence Of Cypridina Luciferin Analog, 2-Methyl-6-(P-Methoxyphenyl)-3,7-Dihydroimidazo[1,2-A]Pyrazin-3-One, *Journal Of Bioluminescence And Chemiluminescence*, 9(6), 355-361.

- Nelson, N. B., and D. A. Siegel (2002), Chromophoric DOM in the open ocean, in *Biogeochemistry of Marine Dissolved Organic Matter*, edited by D. A. Hansell and C. A. Carlson, pp. 547-578, Academic Press, San Diego.
- Nelson, N. B., C. A. Carlson, and D. K. Steinberg (2004), Production of chromophoric dissolved organic matter by Sargasso Sea microbes, *Marine Chemistry*, 89(1-4), 273-287.
- Nelson, N. B., D. A. Siegel, C. A. Carlson, C. Swan, J. W. M. Smethie, and S. Khatiwala (2007), Hydrography of chromophoric dissolved organic matter in the North Atlantic, *Deep Sea Research Part I: Oceanographic Research Papers*, 54(5), 710.
- O'Sullivan, D. W., P. J. Neale, R. B. Coffin, T. J. Boyd, and S. L. Osburn (2005), Photochemical production of hydrogen peroxide and methylhydroperoxide in coastal waters, *Marine Chemistry*, 97(1-2), 14-33.
- Rao, P. S., and E. Hayon (1975), Redox potentials of free radicals. IV. Superoxide and hydroperoxy radicals . O₂⁻ and . HO₂, *J. Phys. Chem.*, 79(4), 397-402.
- Roginsky, V., and T. Barsukova (2000), Kinetics of oxidation of hydroquinones by molecular oxygen. Effect of superoxide dismutase, *J. Chem. Soc., Perkin Trans. 2*, 1575 - 1582.
- Roginsky, V. A., L. M. Pisarenko, W. Bors, and C. Michel (1999), The kinetics and thermodynamics of quinone-semiquinone-hydroquinone systems under physiological conditions, *Journal Of The Chemical Society-Perkin Transactions 2*(4), 871-876.
- Rose, A. L., and D. Waite (2006), Role of superoxide in the photochemical reduction of iron in seawater, *Geochimica Et Cosmochimica Acta*, 70(15), 3869-3882.
- Rose, A. L., E. A. Webb, T. D. Waite, and J. W. Moffett (2008), Measurement and Implications of Nonphotochemically Generated Superoxide in the Equatorial Pacific Ocean, *Environ. Sci. Technol.*, 42(7), 2387-2393.

- Scott, D. T., D. M. McKnight, E. L. Blunt-Harris, S. E. Kolesar, and D. R. Lovley (1998), Quinone moieties act as electron acceptors in the reduction of humic substances by humics-reducing microorganisms, *Environmental Science & Technology*, 32(19), 2984-2989.
- Shkarina, E. I., T. V. Makisimova, I. N. Nikulina, E. L. Lozovskaya, Z. V. Chumakova, V. P. Pakhomov, I. I. Sapezhinskii, and A. P. Azamastsev (2001), Effect of Biologically Active Substances on the Antioxidant Activity of Phytopreparations, *Pharmaceutical Chemistry Journal*, 35, 332-339.
- Son, B., J. Kim, H. Choi, and J. Kang (2002), A radical scavenging Farnesylhydroquinone from a marine-derived fungus *Penicillium* sp, *Archives of Pharmacal Research*, 25(1), 77-79.
- Steigenberger, S., and P. L. Croot (2008), Identifying the processes controlling the Distribution of H₂O₂ in surface waters along a meridional transect in the Eastern Atlantic., *Geophysical Research Letters*, 35, L03616, doi:03610.01029/02007GL032555.
- Steinberg, D. K., N. B. Nelson, C. A. Carlson, and A. C. Prusak (2004), Production of chromophoric dissolved organic matter (CDOM) in the open ocean by zooplankton and the colonial cyanobacterium *Trichodesmium* spp, *Marine Ecology-Progress Series*, 267, 45-56.
- Tossell, J. A. (2009), Quinone-hydroquinone complexes as model components of humic acids: Theoretical studies of their structure, stability and Visible-UV spectra, *Geochimica et Cosmochimica Acta*, 73(7), 2023-2033.
- Uchimiya, M., and A. T. Stone (2009), Reversible redox chemistry of quinones: Impact on biogeochemical cycles, *Chemosphere*, 77(4), 451-458.

- Voelker, B. M., D. L. Sedlak, and O. C. Zafiriou (2000), Chemistry of Superoxide Radical in Seawater: Reactions with Organic Cu Complexes, *Environmental Science and Technology*, *34*, 1036-1042.
- Weinstein, J., and B. H. J. Bielski (1979), Kinetics of the Interaction of HO₂ and O₂⁻ Radicals with Hydrogen Peroxide. The Haber-Weiss Reaction., *Journal of the American Chemical Society*, *101*, 58-62.
- Yuan, J., and A. M. Shiller (1999), Determination of Subnanomolar Levels of Hydrogen Peroxide in Seawater by Reagent-Injection Chemiluminescence Detection, *Analytical Chemistry*, *71*, 1975-1980.
- Yuan, J., and A. M. Shiller (2001), The distribution of hydrogen peroxide in the southern and central Atlantic ocean, *Deep-Sea Research II*, *48*, 2947-2970.
- Yuan, J. C., and A. M. Shiller (2004), Hydrogen peroxide in deep waters of the North Pacific Ocean, *Geophysical Research Letters*, *31*(1).
- Zafiriou, O. C. (1990), Chemistry of superoxide ion (O₂⁻) in seawater. I. pK_{asw}^{*} (HOO) and uncatalysed dismutation kinetics studied by pulse radiolysis, *Marine Chemistry*, *30*, 31-43.
- Zafiriou, O. C., B. M. Voelker, and D. L. Sedlak (1998), Chemistry of the superoxide radical (O₂⁻) in seawater: Reactions with inorganic copper complexes, *Journal of Physical Chemistry A*, *102*(28), 5693-5700.
- Zheng, J., S. R. Springston, and J. Weinstein-Lloyd (2003), Quantitative analysis of hydroperoxyl radical using flow injection analysis with chemiluminescence detection, *Analytical Chemistry*, *75*(17), 4696-4700.

Figure Legends:

Figure 1: Location of the sampling stations referred to in the text. Station 8 (S8) is shown as a green triangle, Station 9 (S9) is a red circle and Station 10 (S10 TENATSO) is depicted as a blue square.

Figure 2: (left) Observed superoxide decay for DTPA amended seawater for 2 samples from Station 9. (right) natural log transformed data of the superoxide decay rate in the left panel.

Figure 3: Vertical profiles of parameters measured in this study for 3 stations in the vicinity of Sao Vicente, Cape Verde. (Top) Observed first order O_2^- decay kinetics in seawater equilibrated with DTPA and CDOM absorbance (300 nm) (Bottom) Vertical profiles of density anomaly (σ_θ) and Chlorophyll. Error bars are shown for the 95% confidence interval.

Figure 4: Variation in measured k_{org} for seawater diluted with Milli-Q from 3 near surface samples collected during the period July 2008 – May 2009.

Figure 5: (left) Variation in the concentrations of quinone species as a function of time for a numerically simulated superoxide (100 nM) addition experiment. (right) Semi-logarithmic plot of the superoxide decay in the same experiment, the initial decay rate is shown as a black line, the overall decay is shown as a purple line. In this experiment the initial conditions were 5 nM quinone plus 5 nM hydroquinone, though experiments initialized with 10 nM quinone or 10 nM hydroquinone gave almost identical results after 5s of simulated reaction time.

Figure 6: (left) H_2O_2 and (right) nitrite vertical profiles from TENATSO (17° 35' N, 24° 15' W). Error bars are shown for the 95% confidence interval.

Figure 7: The linear relationship between k_{org} and H_2O_2 for waters below the mixed layer at the TENATSO site in May 2009.

Table 1: Superoxide decay kinetics and aCDOM(300 nm) measured during this study.

<i>Station</i>	<i>Depth (m)</i>	$k_{org} (s^{-1})^A$	$aCDOM (m^{-1})$
S08	10	-0.0093 ± 0.0002	0.364
S08	20	-0.0158 ± 0.0004	0.391
S08	30	-0.0147 ± 0.0002	0.415
S08	40	-0.0138 ± 0.0002	0.428
S08	60	-0.0134 ± 0.0002	0.433
S08	70	-0.0133 ± 0.0002	0.417
S08	80	-0.0119 ± 0.0003	0.337
S08	100	-0.0125 ± 0.0002	0.444
S08	150	-0.0116 ± 0.0003	0.293
S08	200	-0.0155 ± 0.0004	0.377
S08	300	-0.0137 ± 0.0003	0.368
S08	400	-0.0153 ± 0.0004	0.297
S09	10	-0.0156 ± 0.0002	0.308
S09	20	-0.0133 ± 0.0002	0.158
S09	30	-0.0123 ± 0.0002	0.240
S09	40	-0.0175 ± 0.0002	0.308
S09	60	-0.0190 ± 0.0004 ^B	0.411
S09	70	-0.0342 ± 0.0011 ^B	0.455
S09	80	-0.0321 ± 0.0005 ^B	0.668
S09	100	-0.0325 ± 0.0006 ^B	0.311
S09	150	-0.0256 ± 0.0002 ^B	0.304
S09	200	-0.0266 ± 0.0003	0.277
S09	300	-0.0162 ± 0.0002	0.260
S09	400	-0.0142 ± 0.0002	0.413
S10	5	-0.0147 ± 0.0002	0.497
S10	10	-0.0129 ± 0.0003	0.482
S10	20	-0.0133 ± 0.0004	0.497
S10	30	-0.0130 ± 0.0002	0.495
S10	40	-0.0151 ± 0.0002	0.477
S10	50	-0.0168 ± 0.0002	0.533
S10	60	-0.0199 ± 0.0017	0.581
S10	80	-0.0145 ± 0.0004	0.797
S10	100	-0.0179 ± 0.0002	0.586
S10	120	-0.0151 ± 0.0002	0.553
S10	150	-0.0123 ± 0.0005	0.548
S10	200	-0.0153 ± 0.0015	0.655

^AAll errors are reported to the 95% confidence interval. The error in aCDOM is ±0.004 at the 95% confidence interval.

^BData displayed an initial fast decay rate and a slower secondary rate, the initial rate is reported here.

Table 2: Reaction rates of organic species relevant to seawater involving O_2^-

<i>Reactant</i>	<i>Reaction</i>	<i>Rate $M^{-1} s^{-1}$</i>	<i>Reference</i>
Consumption of Superoxide			
1,4-benzoquinone	$Q + O_2^- \rightarrow Q^{\bullet} + O_2$	8×10^8	[Meisel, 1975]
hydroquinone	$QH_2 + O_2^- \rightarrow Q^{\bullet} + H_2O_2$	1.7×10^7	[Rao and Hayon, 1975]
glutathione	$GSH + O_2^- + H^+ \rightarrow GS^{\bullet} + H_2O_2$	6.7×10^5	[Asada and Kanematsu, 1976]
catechol	$Q(OH)_2 + O_2^- \rightarrow QO_2^{\bullet} + H_2O_2$	2.7×10^5	[Bielski et al., 1985]
Production of Superoxide			
semiquinone radical	$Q^{\bullet} + O_2 \rightarrow Q + O_2^-$	5×10^4	[Eyer, 1991]
Related Quinone/Hydroquinone reactions			
Dismutation	$2Q^{\bullet} \rightarrow Q + Q^{2-}$	2.3×10^7	[Meisel, 1975]

Note: Hydroquinone is a 1,4 diol and catechol is a 1,2 diol, both upon reaction with superoxide form their respective semiquinone radicals. Only compounds with reaction rate constants $> 1 \times 10^5 M^{-1} s^{-1}$ were considered here [Bielski et al., 1985], this then excludes amino acids, sugars, macronutrients and halides, all of which are critical constituents of seawater.

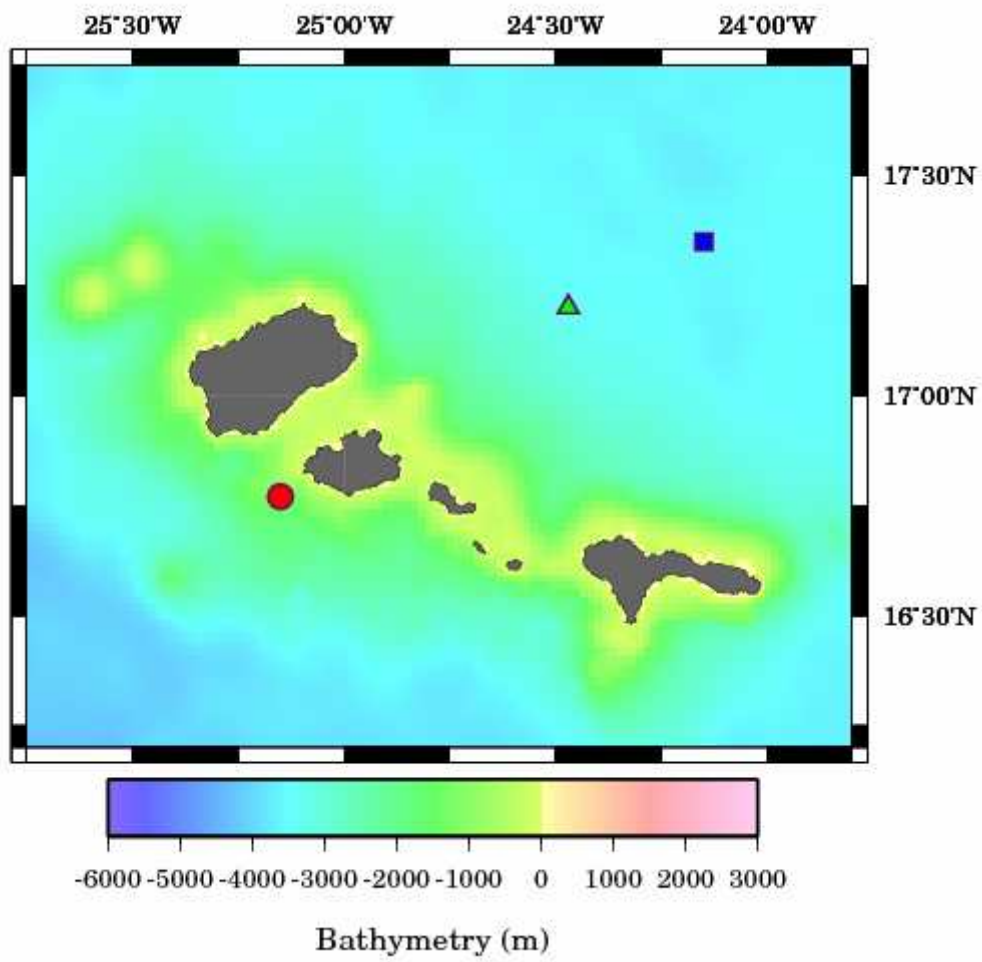


Figure 1:

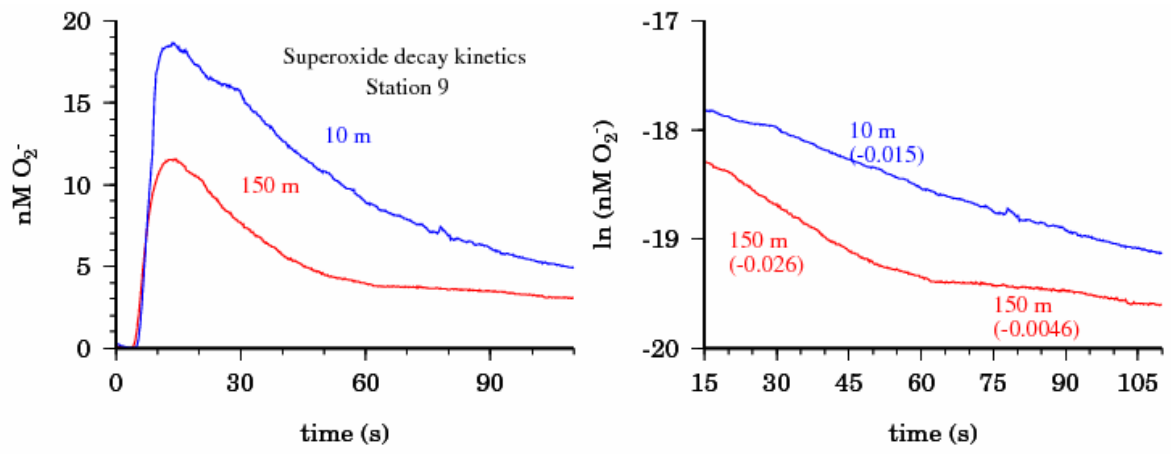


Figure 2:

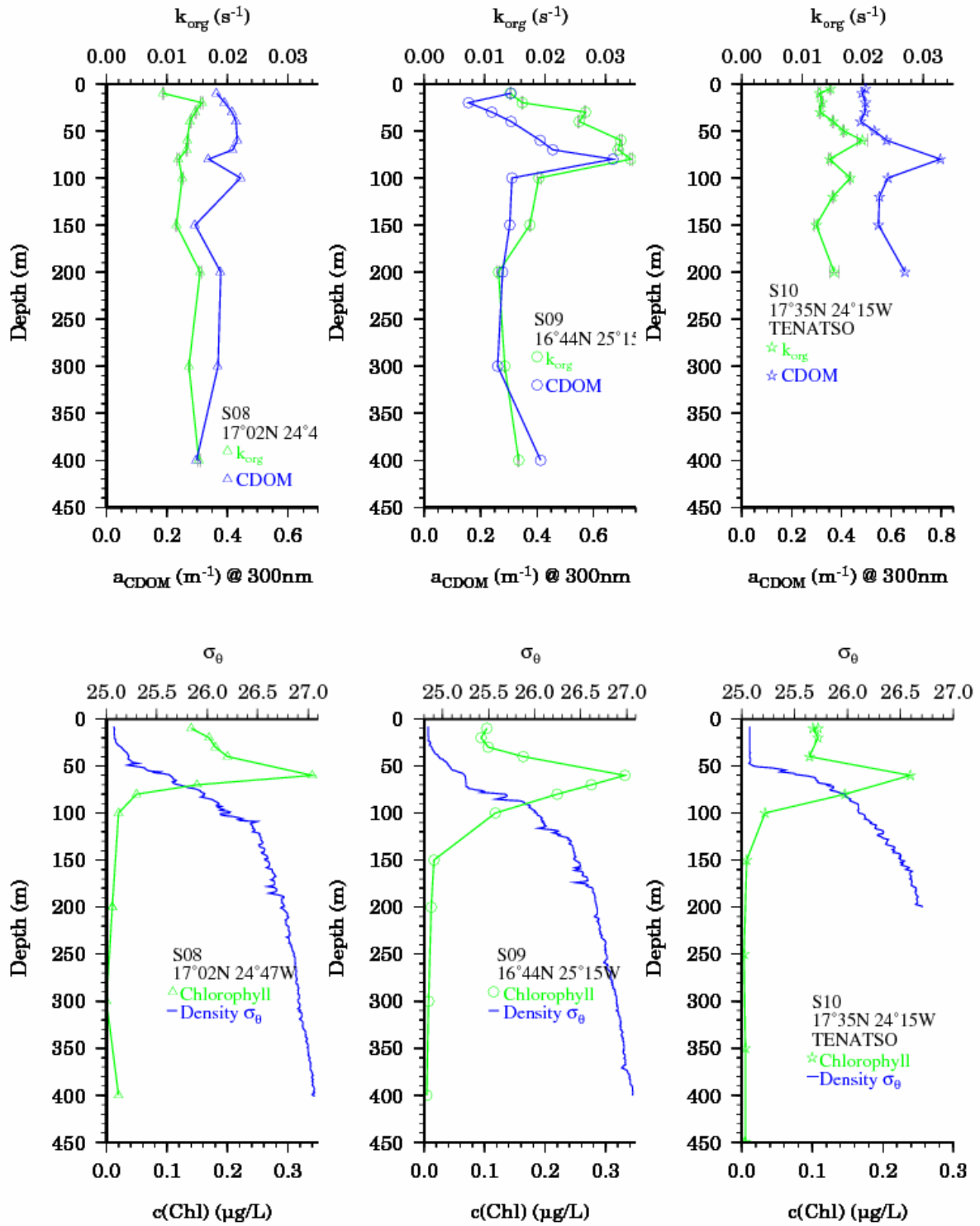


Figure 3:

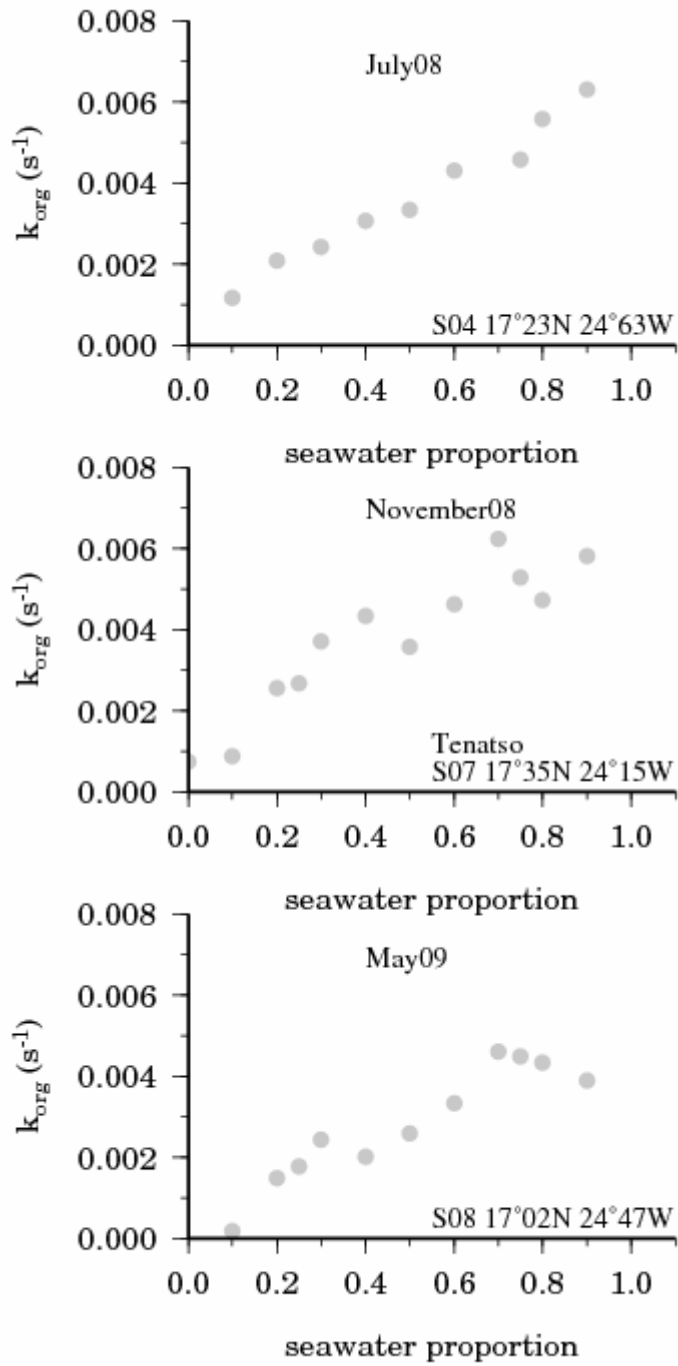


Figure 4:

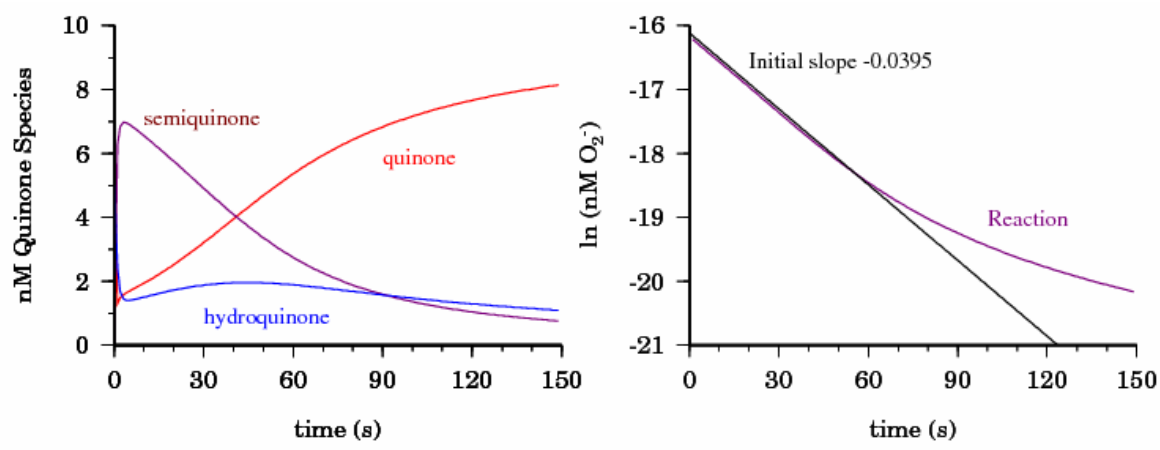


Figure 5:

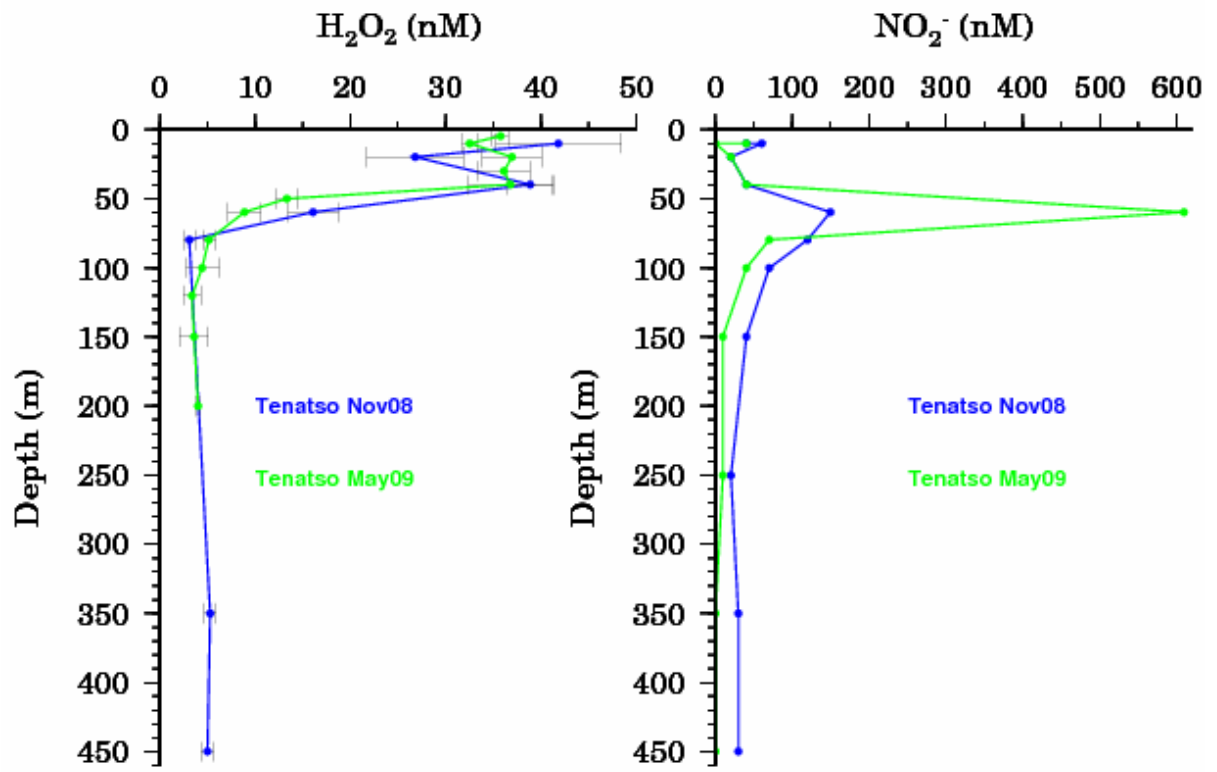


Figure 6:

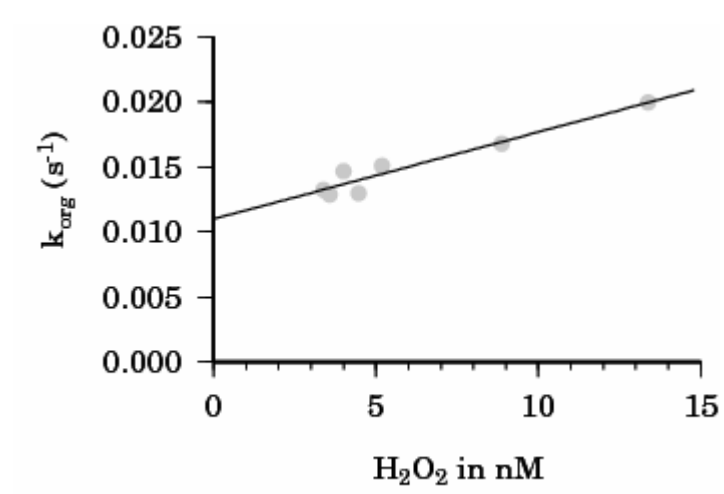


Figure 7:

**Superoxide decay as a probe for speciation changes during
dust dissolution in Tropical Atlantic surface waters near Cape
Verde**

Heller, M.I. and Croot, P.L.

Superoxide decay as a probe for speciation changes during dust dissolution in Tropical Atlantic surface waters near Cape Verde

M.I. Heller and P.L. Croot.*

FB2 Marine Biogeochemie, Leibniz-Institut für Meereswissenschaften (IfM-Geomar),
Dienstgebäude Westufer, Düsternbrooker Weg 20, 24105 Kiel, Germany.

Keywords: Superoxide, Iron, Copper, Tropical Atlantic

Running title: Dust dissolution in Cape Verdean surface waters

*Corresponding author: mheller@ifm-geomar.de

Submitted to Marine Chemistry

ABSTRACT

It is been well demonstrated that the major source of iron (Fe) to the Tropical Atlantic is through aeolian deposition of Saharan dust. However presently we know very little about the dissolution processes of these aerosols in the sunlit productive surface waters of this region. Candidate processes identified as being potentially critical to dust dissolution include thermal dissolution, direct photochemical reduction, ligand induced dissolution and reductive dissolution by superoxide (O_2^-), formed predominantly by photochemical reactions with dissolved organic matter in seawater. O_2^- is short lived (half life: 1-100 s) in seawater as it reacts rapidly with both the (Fe(II)/Fe(III)) and copper (Cu(I)/Cu(II)) redox couples and to a less extent with dissolved organic matter. In the euphotic zone where high fluxes of sunlight and potentially O_2^- exist there exists the possibility of a kinetic controlled reduction of Fe in colloids and particles to the more soluble and bioavailable Fe(II). However, presently no information is available from the open ocean on the rates that this process may be occurring. Here we present data using a new methodological approach to assess trace metal speciation which involves the measurement of O_2^- decay kinetics. Our method allows an assessment of changes in both the organic reactivity with O_2^- simultaneously with apparent changes in the speciation of iron and/or copper. Our approach allows evaluation of the importance of each of the different reaction pathways for O_2^- and thus the factors which control metal redox speciation in seawater. In the present work we applied this technique using seawater collected in the vicinity of the island of Sao Vicente, Cape Verde, to dust incubation experiments to ascertain rapidly if dust dissolution had altered the *in situ* iron speciation in seawater.

1. Introduction

1.1 Importance of dust dissolution to open ocean biogeochemical cycles

1.1.1 Global Importance

The main input of crustal elements (Fe, Mn, Al) to the ocean is through aeolian dust transport from mainly the great deserts of this world. The supply of these elements to surface waters is a major process affecting their distribution and biogeochemistry in the global ocean. This is particularly important in HNLC (high nutrient low chlorophyll) regions, which receive low dust inputs, such as the Southern Ocean and the equatorial Pacific, where iron has been demonstrated to be the key limiting element for phytoplankton growth (Boyd et al., 2000; Coale et al., 1996). While the importance of dust supply as a source of iron to the ocean has been recognized now for some time still very little is known about the biogeochemical processes driving dust dissolution in the surface ocean immediately after dust deposition has occurred.

The total aeolian flux of desert dust to the surface waters of the oceans is relatively well constrained but the fraction which subsequently dissolves, for metals such as iron, and which is then available for the growth of phytoplankton is not well known at present. Global models assume that only 1-2% of the aerosols which are transported to the ocean are converted into dissolved iron in seawater. However field measurements show a much wider range of values depending on the dust loading and source (Baker and Croot, 2008; Baker and Jickells, 2006). Particle size may also be important in determining the aerosol solubility (Baker and Jickells, 2006) and this could result in regional differences as the average particle size decreases with distance from the desert source although some large particles (>20 μm) can be transported over long distances (Mahowald et al., 2005). Studies of Saharan dust have shown that the particle diameter decreased from ~7-28 μm at the coast of West Africa (Stuut et al., 2005) to 1-3 in Caribbean waters (Talbot et al., 1986).

Observations of temporal changes in the concentration of dissolved iron show that the input through dust must be significantly higher than the model results (Sedwick et al., 2007). In the Southern Hemisphere the dust deposition is significantly lower than in the Northern hemisphere due to the lack of land masses to act as source regions. In the tropical Atlantic which receives high dust fluxes, iron is found in relatively high concentrations in the surface waters, and the particle fluxes to the deep waters are also dominated by dust inputs (Croot et al., 2004; Kremling and Streu, 1993).

1.1.2 Saharan dust deposition to the Cape Verde archipelago

The Cape Verdean Islands are located along the main transport pathway for Saharan dust originating from the Saharan and Sahel zones of the West African continent. In a key early study Chiapello (1995) reported results from an aerosol monitoring station on the north eastern most island of Sal in the Cape Verde group between December 1991 and December 1994. This study found a distinct seasonal pattern which showed maximum dust input during the winter months of December and January. The meteorological analysis of this season suggested that the dust transport occurred in the trade winds and at low altitudes. This is in contrast to the seasonal signal at Miami and Barbados (Prospero, 1999) which has a clear maximum in the summer months of June and July. The reason for this seasonal difference lies in the different mechanisms of dust plume generation operating at these times and in particular in the summer when Saharan dust outbreaks are formed by the uplifting of hot dry air which entrains aerosols and is subsequently transported westward in the Saharan air layer (SAL) (Karyampudi et al., 1999). The westward passage of the SAL during summer sees the dust pass high over the Eastern Atlantic and Cape Verde but as the air mass cools and sinks the dust is deposited in the Western Atlantic.

Charles Darwin was one of the first to describe the reddish brown dust that covered ships as they sailed through this region (Darwin, 1846). This main component of the dust is hematite probably mixed with goethite (Balsam et al., 1995). It was also shown that hematite has a northerly Saharan source while goethite originates from the Sahel. The quantity of iron-stained quartz differs depending from where it originates. South Saharan and Sahelian dust was found to contain 57%, whereas the dust from the central and North Saharan had only a content of 5-15% of iron-stained quartz. This is important as iron-stained quartz is typical for the winter dust plume which has its origin in Senegal whereas the summer dust bloom has clearly lower iron-stained quartz content. The summer dust blooms extent north from Senegal in Mauritania and in the Western Sahara. Moreover it was found that the dust of the winter bloom is richer in kaolinite but the dust mostly transported in summer has a higher content of carbonate, illite, chlorite and feldspar (Balsam et al., 1995). The iron oxides have been found to be transported 3300 km from the African coast whereas the transportation distance of quartz decreased rapidly from the coast (Kolla et al., 1979) most probably due to the coarser grain size compared to the iron oxides.

Primary productivity in the oligotrophic eastern tropical Atlantic around the Cape Verde islands is strongly limited by the availability of fixed nitrogen (Michaels et al., 1996). Much of the primary productivity of the oligotrophic North East Atlantic is apparently driven

by nitrogen fixing cyanobacteria (Voss et al., 2004), including the well known species *Trichodesmium* (Tyrrell et al., 2003), which utilize the enzyme nitrogenase (Chen et al., 1998). Indeed recent work has shown that the *nifH* gene, which can be used as marker for nitrogenase using species, is widespread in this region (Langlois et al., 2005). Nitrogen fixation in this area has been shown via bioassay experiments to be limited by phosphorous (Sañudo-Wilhelmy et al., 2001), iron (Moore et al., 2009) and a combination of iron and phosphorous (Mills et al., 2004).

1.2 Processes potentially affecting dust dissolution in the open ocean

There are several identified processes that are potentially key to the dissolution of dust or aerosol recently deposited to the surface ocean. Figure 1 summarizes the main reaction pathways that are known presently and in the following text they are in turn briefly discussed.

1.2.1 Iron solubility and redox speciation

Fe(III) is the thermodynamically favored form of iron under oxygenated seawater conditions but undergoes rapid precipitation or particle scavenging in the formation of various Fe(III)-oxyhydroxide phases with differing chemical reactivities (Kuma et al., 1996). In seawater dissolved Fe(III) has been shown to be complexed by strong ligands (Croot and Johansson, 2000; Rue and Bruland, 1995), presumably produced by bacteria or phytoplankton, a consequence of which is to increase the solubility of iron in seawater (Liu and Millero, 2002).

Fe(II), the more bioavailable form, is presently viewed as a reactive intermediate in iron cycling, primarily generated by photochemical processes (Johnson et al., 1994), and existing at extremely low concentrations (pM or less) in oxic-seawater because of rapid oxidation by O₂ and H₂O₂ (Millero and Sotolongo, 1989; Millero et al., 1987). The reduction of Fe(III) to Fe(II) by photochemical, or biological processes, is a possible mechanism to access soluble Fe(II) in seawater (Croot and Laan, 2002). Organic complexation of Fe(II) in seawater is suspected, based on slower Fe(II) oxidation rates (Croot et al., 2007), but no definitive evidence has been presented yet.

1.2.2 Dust dissolution via organic complexation of Iron

It is well known that siderophores play an important role in the acquisition of iron (Neilands, 1995). Siderophores employ functional groups such as hydroxamate or catecholate but also include α -hydroxycarboxylate and carboxylate functionalities to bind iron (Sayyed

and Chincholkar, 2006). The concentration of siderophores in most natural waters is low and it has been calculated that the production by marine cyanobacteria is a costly strategy in terms of cellular nutrient and energy budgets (Volker and Wolf-Gladrow, 1999). The most well studied siderophore is Desferrioxamine-B (DFO) which is produced by terrestrial bacteria, but has also been identified in marine bacterial cultures (Gledhill et al., 2004). Other identified marine siderophores were found to contain α -hydroxycarboxylic acid moieties, in the form of β -hydroxyaspartic acid or citric acid (Barbeau et al., 2001), with a further class proposed to be amphiphilic siderophores which contain a peptide headgroup appended by a series of fatty acids (Martinez et al., 2000). In samples from the Atlantic Ocean, two hydroxamate siderophores related to DFO, were identified at low pM concentrations (Mawji et al., 2008).

Siderophores have a distinct effect on the dissolution of iron containing minerals via a proton- or ligand- promoted surface dissolution mechanism (Carrasco et al., 2007; Kraemer et al., 2005). The absorption of the siderophore on the mineral surface is the first necessary step, but this also lowers the concentration of siderophores in the solution, which may therefore decrease the effect on iron solubility. Borer et al. (2007; 2009a) showed that more iron was dissolved when a combination of siderophore and oxalate was used. The addition of surface-active agents (surfactants), which may be produced by bacteria, has also been shown to enhance dissolution of iron oxides (Carrasco et al., 2007).

Other organic complexes can also convert particulate Fe(III) into soluble forms via photoreductive mechanisms. Observations of persistent Fe(II) concentrations in oxic surface seawater during spring bloom in Funka Bay (Kuma et al., 1992) coincident with high concentrations of the oxidation products of glucose (e.g. gluconic- and glucuronic- acid) spurred laboratory studies into testing various dissolved organic substances which may be released from phytoplankton. It was found that Fe(III) is easily photoreduced by sunlight in the presence of hydroxycarboxylic acids like glyceric, gluconic, glucuronic, glucaric and tartaric acids which are all oxidation products of sugars (Kuma et al., 1995). Similarly the photoreduction of Fe(III)-fulvic acid and citrate has also been considered, but while Fe(III)-humate and Fe(III)-oxalate complexes are easily photoreduced in acidic natural waters the effect was minimal at seawater pH (Voelker et al., 1997; Voelker and Sulzberger, 1996).

1.3 Possible role of Superoxide (O_2^-) in the dissolution of Saharan dust

The O_2^- radical is potentially an important species involved in the redox cycling of metal ions in natural waters (Goldstone and Voelker, 2000; Rose and Waite, 2006; Voelker and Sedlak, 1995; Zafiriou et al., 1998). Inorganic complexes of Cu(II)/Cu(I) and

Fe(II)/Fe(III) can react rapidly with O_2^- leading to a catalytic cycle for O_2^- decay (Voelker et al., 2000).

1.3.1 Production of O_2^- in the surface ocean

The existence of O_2^- in seawater was first proposed by Swallow (1969) who suggested that O_2^- could be formed by reactions of the hydrated electron with oxygen in seawater and from photochemical production from phenolic compounds present in dissolved organic matter (DOM). It was some time later before qualitative or indirect evidences were found for the photochemical production of O_2^- in aqueous solutions with the assumption that its decomposition is the major source for H_2O_2 (Baxter and Carey, 1983; Petasne and Zika, 1987). The first measurements of superoxide fluxes in seawater were obtained from Caribbean waters (Micinski et al., 1993) which were illuminated in the laboratory with a solar simulator and the fluxes determined by using isotopically labelled ^{15}NO gas to react with O_2^- to form peroxyxynitrite (Blough and Zafiriou, 1985) which rearranges to form nitrate. Using this approach photochemical production rates for O_2^- in surface waters followed a seasonal cycle with $0.1-6 \text{ nM min}^{-1} \text{ sun}^{-1}$ (where sun^{-1} is the intensity of the solar simulator used (Dister and Zafiriou, 1993)) in spring- and $0.2-8 \text{ nM min}^{-1} \text{ sun}^{-1}$ in the autumn. Overall it was found that approximately 35% of the total radical flux was present as O_2^- .

The main mechanism for the production of O_2^- is thought to be from the absorption of a photon by DOM which excites this molecule into a triplet state which subsequently reacts with O_2 (naturally occurring in the triplet state) to form O_2^- and a carbocation (O'Sullivan et al., 2005). Direct measurements of the apparent quantum yield for O_2^- are not available, however related data does exist for the formation of the reaction product H_2O_2 (O'Sullivan et al., 2005; Yocis et al., 2000) and indicates that UV wavelengths, 300 to 400 nm, are the major source of O_2^- in seawater. Photochemical production of O_2^- in seawater based on measurements of H_2O_2 *in situ* formation fluxes (Obernosterer et al., 2001; Yocis et al., 2000; Yuan and Shiller, 2001) indicate rates in surface waters of 9 (Antarctic) to 17 nM h^{-1} (Tropical Atlantic), assuming the rate of O_2^- production is twice that of H_2O_2 . Superoxide can also be produced by metabolic processes in phytoplankton (Marshall et al., 2005).

1.3.2 Uncatalysed dismutation and organic reactions of O_2^-

The bimolecular dismutation reaction of O_2^- with its conjugated acid HO_2 is relatively slow under seawater conditions and concentrations, where it mostly present as the radical form O_2^- at the pH of 8.1 (Zafiriou, 1990). DOM present in seawater has been found to have a

pseudo-first order decay nonmetallic sink for O_2^- (Goldstone and Voelker, 2000), through experiments treated with Diethylenetriaminepentaacetic acid (DTPA) which removes metal reactions through complexation. The reaction of O_2^- with DOM was found to be a significant reaction pathway for O_2^- when the reaction with metals does not dominate.

Key components identified in CDOM are humic and fulvic acids which are also known to form complexes with trace metals (Cory and McKnight, 2005). The redox active fraction of CDOM, which are able to easily exchange electrons, has been attributed to quinone moieties (Scott et al., 1998). Quinones can shuttle between three redox states; the fully oxidized quinone, which can undergo a one electron reduction to the semiquinone radical and with a further one electron reduction to the hydroquinone. Superoxide reacts rapidly with both the quinone and hydroquinone to form the radical semiquinone species (Ilan et al., 1976; Shkarina et al., 2001), which dismutates to reform the starting quinone and hydroquinone thus creating a potential catalytic cycle for the decay of superoxide (Goldstone and Voelker, 2000).

1.3.3 The reactivity of O_2^- with Cu

Copper is also an essential micronutrient in the ocean but is also toxic for most marine phytoplankton (Brand et al., 1986). In seawater dissolved copper is strongly complexed by organic ligands (Moffett and Brand, 1996; Moffett and Dupont, 2007). Two classes of copper complexing ligands are typically described according to their conditional stability constants. Strong ligands, L1, with $\log K \sim 12-14$ and weaker ligands, L2, $\log K \sim 9-11$, which are most likely produced by phytoplankton or bacteria (Croot et al., 2000). It was found that ligands of the L1 type were produced from *Synechococcus* cultures when grown under Cu-stress (Moffett and Brand, 1996). The reduced form of Cu, Cu(I) is only found at low pM concentrations in surface waters (Moffett and Zika, 1988) and is believed to be produced predominantly via photochemical processes.

Superoxide reacts rapidly with inorganic Cu(I) and Cu(II) in seawater at close to the diffusion rate (Zafiriou et al., 1998), while reactions with natural Cu organic complexes in seawater are reduced ($k = 3-8 \times 10^8 \text{ M}^{-1} \text{ s}^{-1}$) (Voelker et al., 2000). Voelker et al. investigated the reaction of O_2^- with the Cu complexes formed in Cu stressed *Synechococcus* cultures and found there was still an appreciable reaction with O_2^- ($k = 5 \pm 3 \times 10^7 \text{ M}^{-1} \text{ s}^{-1}$). It was suggested by these authors that the high reactivity of the Cu complexes from *Synechococcus* was due to exchangeable water in the complex which allowed the O_2^- entry. Recently it was

shown that despite strong organic complexation, Cu was the dominant sink for O_2^- in the Southern Ocean (Heller and Croot, 2009).

1.3.4 The reactivity of O_2^- with Fe and other metals

Both inorganic Fe(II), $k \sim 0.1-7 \times 10^8 \text{ M}^{-1} \text{ s}^{-1}$, and Fe(III), $k \sim 1.5-1.8 \times 10^8 \text{ M}^{-1} \text{ s}^{-1}$, react rapidly with O_2^- (Bielski et al., 1985; Matthews, 1983; Voelker and Sedlak, 1995). It was first suggested by Voelker and Sedlak (1995) that the reduction of inorganic Fe(III) by photochemically produced O_2^- in sunlit surface waters may be producing significant fluxes of Fe(II). Other workers have also suggested that O_2^- could play a role in maintaining a significant concentration of Fe(II) in seawater (Croot et al., 2005; Fujii et al., 2008; Rose and Waite, 2002) by reduction of inorganic or organically complexed iron. Superoxide has also recently been proposed to dissolve Fe containing minerals and particles in seawater (Fujii et al., 2006). Experiments using Fe(III)-organic complexes indicate that they are generally less reactive with O_2^- (Bielski et al., 1985; Garg et al., 2007b; Sedlak and Hoigne, 1993). Indeed measurements of the Fe complex with DFO, $k = 9.3 \pm 0.2 \times 10^3 \text{ M}^{-1} \text{ s}^{-1}$, show that this species is relatively inert to O_2^- (Rose and Waite, 2005).

The importance of O_2^- reactions with other metals under seawater conditions are not clarified up to now. While Mn(II) reacts with both HO_2 and O_2^- in a pH-dependent rate (Cabelli and Bielski, 1984), it is not clear if the reactions in seawater are significantly fast enough to influence the overall decay of O_2^- in seawater.

1.3.5 Dust dissolution by O_2^-

The suggestion that O_2^- can dissolve terrigenous sources of iron or iron oxides, is currently under debate. Voelker and Sedlak (1995) found in their pulse radiolysis studies that O_2^- did not react with colloidal Fe(III). They observed that at pH values greater than 6 the Fe(II) concentration decreased due to formation of unreactive amorphous $Fe(OH)_3$. Earlier Rush and Bielski observed similarly in their pulse radiolysis experiments that O_2^- disappeared at a rate virtually independent of the amount of colloidal iron present at a pH of 7.2 (Rush and Bielski, 1985). At a pH of 8 they observed no reaction between Fe(II)/Fe(III) and O_2^- since oxygen and Fe(II) had reacted during the mixing process and colloidal iron had precipitated before the solution could be pulsed.

An earlier study however investigated whether O_2^- can release iron from Ferritin (Bolann and Ulvik, 1990), a large spherical protein (450 kDa) that is used for storing Fe, as a ferrihydrite like crystal, in cells. This study found that the amount of the iron released

depends on the size of the iron core, but not on the iron content of the protein shell of ferritin. It was evident that O_2^- can only remove a few Fe(II) atoms from the surface of the center iron core of ferritin. However more recently Fujii and coworkers suggested from their work that O_2^- can reduce Fe(III) present in amorphous ferric oxides (Fujii et al., 2006). However they left it open if this process affects the bioavailability of iron to organisms as it is still dependent on the presence of Fe binding ligands and how quickly the produced Fe(II) is reoxidized.

1.5 Superoxide sources employed in this work

Previously KO_2 was widely used to examine the reactivity of O_2^- . The use of KO_2 was found to have several advantages as a cheap direct source of O_2^- . The main problem with the use of KO_2 is the relatively low yield (Bolann and Ulvik, 1991), typically 15% or so, and the high concentration of H_2O_2 present which for calibration work needs to be corrected for (see below). KO_2 was for a long time perceived to be highly contaminated with metals based on work performed during the 1970s and 80s. However it appears that in much of the earlier work performed with KO_2 problems were caused by the use of non trace metal free equipment and water supplies which did not use final filtration (Weinstein and Bielski, 1979). Recently we reexamined the metal content of commercial KO_2 and discovered that trace metal impurities were low and KO_2 could be successfully used as a calibration source for superoxide in decay experiments in seawater (Heller and Croot, 2009). Due to the nature of KO_2 it can only be used for pulse experiments and not as a source for flux measurements.

Xanthine oxidase (XO) catalyzes the oxidation of xanthine (X) or hypoxanthine (HX) in the presence of O_2 to form uric acid with the production of O_2^- or H_2O_2 . This method is commonly used due to the commercial availability of the reactants and the ease of use, indeed several papers have been published using XO/X as a O_2^- source in seawater (Godrant et al., 2009; Kustka et al., 2005; Milne et al., 2009; Rose et al., 2008). The flux of O_2^- varies as a function of pH and other conditions, but at a pH of 7 there is believed to be a production of 20% O_2^- and 80% H_2O_2 (Fridovich, 1970). The flux of the univalent pathway to O_2^- increases at alkaline pH, up to approximately pH 8, and under high pO_2 or low substrate conditions (Fridovich, 1970; Galbusera et al., 2006). For quantitative work and in particularly when a steady rate of O_2^- formation is required, the X/XO system has been found to be unsuitable as XO becomes deactivated during its turnover, which decreases the O_2^- formation, even in an experiment duration of less than one hour (Hodges et al., 2000). Many researchers have also observed that commercial XO preparations are contaminated with iron or other trace metals

(Dix and Aikens, 1993; Hodges et al., 2000; Lloyd and Mason, 1990). This limits the use of XO to experiments where the trace metals are buffered with the use of DTPA or DFO and reactions between trace metals in seawater and O_2^- can therefore not be studied. Calibration of the XO/X source is complicated in seawater by the need to accurately control and measure the pH during the experiment, something which is not a trivial task (Dickson, 1993). The XO/X system does not only produce O_2^- as recent work suggests that it also produced carbonate radicals (Bonini et al., 2004) which may be important under seawater conditions. XO also requires an organic substrate to produce O_2^- which may interfere in the processes being examined in seawater. In the present work we used the XO/X system for comparative purposes only.

Current methods which generate O_2^- in relative high concentrations will favor the uncatalysed dismutation resulting in a high H_2O_2 production also. To order to mimic the in vivo situation where O_2^- is produced very slowly but continuously over a long duration, Ingold et al. (1997) synthesized a series of suitable azo compounds (superoxide thermal sources - SOTS) which decompose thermally to yield either directly or indirectly electron rich carbon-centered radicals. Many of those primary radicals are known to react with O_2 to yield carbocations and O_2^- (Von Sonntag and Schuchmann, 1991). We recently (Heller and Croot, 2010b) have developed methods in seawater for using SOTS-1 as a O_2^- source, where the first order thermal decomposition of the reagent permits the calculation of the time dependence of the concentration of SOTS-1 under conditions of constant temperature:

$$[SOTS]_t = [SOTS]_0 e^{-kt} \quad (1)$$

where k is the temperature dependent decay rate of the SOTS-1. In the absence of other superoxide sources the instantaneous O_2^- production rate (P) from SOTS-1 can be described as follows, assuming a 0.4 stoichiometry for the reactions between the SOTS-1 radical and O_2 (Ingold et al., 1997):

$$P = 0.4k[SOTS]_t \quad (2)$$

1.6 Objectives of this study

The focus of this paper is on processes affecting the dissolution of Saharan dust and the possible role that O_2^- has on this in the ocean around Cape Verde. The Cape Verde site was chosen due to its location under the Saharan dust plume and the logistical support that is available there through the Tropical Eastern North Atlantic Time Series Observatory (TENATSO) located near the island of Sao Vicente. There were two main objectives of the present work:

- (1) To determine if the reduction of Fe by O_2^- was an important process in the dissolution of Saharan dust suspended in seawater.
- (2) To quantify the decay rate of O_2^- in seawater and determine the key reaction pathways in order to constrain the lifetime of this molecule in seawater and its potential influence on trace metal redox cycles.

2. Methods

2.1. pH measurements

In the present work we report seawater pH values using the total hydrogen scale (pH_{TOT}) while we use the NBS scale, pH_{NBS} , for pH measurements of buffers and other low ionic strength solutions. All pH measurements were made using a WTW pH meter 330i calibrated with Tris buffers (Millero et al., 1993). In the present manuscript we report seawater pH values using the total hydrogen scale (pH_{TOT}) (Dickson, 1993)

2.2 Reagents

2.2.1 General Reagents

All reagents were prepared using 18M Ω cm resistivity water (hereafter referred to as MQ water) supplied by a combination of an ELIX-3 and Synergy 185 water systems (Millipore). High purity HCl (6 M, hereafter abbreviated to Q-HCl) was made by redistillation of Merck trace-metal grade acids in a quartz sub-boiling still (Kuehnen et al., 1972). A primary 2-methy-6-(p-methoxyphenyl)3-7-dihydroimidazol[1,2- α]pyrazin-3-one (MCLA) standard, 1mM MCLA, was prepared by dissolving 10 mg of MCLA in 34.5 mL of MQ water; 1-mL aliquots of this solution were then pipetted into polyethylene vials and frozen at -80 °C until required for use. The working MCLA standard, 1 μ M, was prepared from a thawed vial of the primary stock by dilution into 1 L of MQ water. This solution was buffered in 0.05 M sodium acetate and adjusted to pH_{NBS} of 6 with Q-HCl. A 3.8 mM stock solution of Diethylenetriaminepentaacetic acid (DTPA) was prepared up by dissolving 0.6 g in 400 mL MQ water. All plasticware used in this work was extensively acid cleaned before use. A secondary Cu standard (0.1 ppm, 1.54 μ M) was prepared by serial dilution of the primary (1000 ppm, 15.4 mM) (Merck) in MQ water. A 10mM Fe(III) stock solution was prepared from $FeCl_3 \cdot 6H_2O$ (Sigma) in 1% Q-HCl followed by the preparation of a working iron standard solution (1 μ M) and acidified to pH 2 with Q-HCl. In the experiments a 1mM stock solution of k-D-Gluconic acid (GluAc) and a 100 μ M solution of Desferrioxamine-B (DFO) were used. A 0.1 M Ferrozine (FZ) (Sigma-Aldrich) was prepared by dissolving 4.92g in

100mL MQ water. Also a 1.2 M Neocuproine stock was prepared by dissolving 5g in 20mL Methanol.

2.2.2 Description of the application of the O_2^- sources employed in this work

In the present work we principally used KO_2 as O_2^- source to determine the O_2^- decay rates as described previously (Heller and Croot, 2009). In brief, a small amount of KO_2 (8-10 mg) was weighed out in an acid washed brown glass bottle, 2 mL of 1 M NaOH was then added and then the solution was diluted with MQ to a final volume of 15 mL. UV spectrophotometry was performed on the sample using either a 1 m LWCC-2100 100 cm pathlength liquid waveguide cell (World Precision Instruments, Sarasota, FL, USA), or a 10 cm Quartz-cuvette (Hellma), coupled to an Ocean Optics USB4000 UV-VIS spectrophotometer in combination with an Ocean Optics DT-MINI-2-GS light source. The concentration of both O_2^- and HO_2^- in the standard solution were determined by least squares solution to the measured absorbance, at multiple wavelengths, using published molar extinction coefficients for the conjugate base of hydrogen peroxide (Baxendale and Wilson, 1957; Taylor and Cross, 1949), HO_2^- which predominates at this pH, and O_2^- (Bielski et al., 1985). Mean initial concentrations in the primary KO_2 solution assessed in this way were $900 \pm 50 \mu\text{M}$ for H_2O_2 and $90 \pm 10 \mu\text{M}$ O_2^- .

In this work we also employed the enzymatic reaction between xanthine (X) and xanthine oxidase (XO) to produce O_2^- which has found to be useable in several buffered solutions (pH 6.5-8.5) as well as in seawater (Milne et al., 2009; Rose et al., 2008). A primary 3.29 mM xanthine stock was prepared in 0.05 M NaOH solution which was subsequently adjusted to a pH of 9 after the xanthine had completely dissolved. A final concentration of 50 μM was used in the experiments. Primary XO stocks of 1 unit mL^{-1} were prepared by dissolving 3.2 mg ($7.7 \text{ units mg}^{-1}$) in 24.64 mL and individual 1 mL stocks were stored at -80°C until required for use. In all experiments performed here a concentration of 1 unit/L of XO was used.

500 μg aliquots of SOTS-1 (di(4-carboxybenzyl)hyponitrite) (Molecular weight 330.3 g mol^{-1}) was used as received (Cayman Chemicals) and stored at -80°C until use. Immediately prior to the start of any experiment the 500 μg SOTS-1 aliquots were dissolved in 200 μL DMSO (Fluka, puriss p.a. $\geq 99.9\%$) before further dilution in either pH 7 phosphate buffer or seawater. Typical final concentrations for SOTS-1 in this study were between 1.9 to 15.1 μM .

2.3 Seawater sampling

Sampling was performed in the vicinity of Sao Vicente in Cape Verde (Figure 2 and Table 1) from the research vessel *RV Islandia* belonging to the Instituto Nacional para Desenvolvimento das Pescas (INDP), Mindelo, Sao Vicente, Cape Verde. Surface seawater was pumped into the 10' research container that is located on the trawl deck of the *Islandia* through tubing attached to a towed fish. Contamination from the ship was minimized by towing the fish at ~ 5m distance alongside the ship with the crane arm of a hydrographic winch (J-frame), keeping it outside the ship's wake as far as possible. The towed fish is a 1m long solid stainless steel, epoxy coated torpedo of 50 kg with three fins at the tail. The sample tubing consisted of 15m of Bev-a-line IV (Excelon) tubing (1/2 inch outside diameter) which was connected to the fish at one end and to an Almatec A-15 Teflon diaphragm pump at the other. The diaphragm pump was driven by compressed air supplied by a Jun-Air 300 compressor. The walls of the research container were lined with clean plastic bags in order to turn it into a pseudo clean room as no HEPA filtered laminar flow cabinets are available onboard the *Islandia*. The tubing was attached with tape and tie-wraps to the fish and the stainless steel hydrowire deployed from the J-frame. Prior to deployment the tubing had been extensively cleaned with 0.1M HCl and rinsed with MQ water. Filtered seawater was obtained in-line at a flow rate of 2-3 L min⁻¹ through a Sartorius Sartobran PH filter cartridge (0.4µm prefilter and 0.2 µm final filter). Unfiltered seawater was obtained directly from the outlet of the diaphragm pump. Discrete deeper samples for total metal analysis were taken using a MITESS sampler (Bell et al., 2002) deployed on a Kevlar wire. Samples from both the fish and the MITESS were drawn into acid cleaned low density polyethylene bottles for later analysis for total metals (acidified onboard with Q-HCl, 2mL/L) in the laboratory in Kiel. Samples for macronutrients and chlorophyll were analyzed using standard protocols (Grasshoff et al., 1999)

2.4 Measurement Technique and Apparatus.

All experiments involving trace metals and O₂⁻ were conducted in an over pressurized trace metal clean laboratory (Class 5) belonging to the IFM-GEOMAR deployed in Cape Verde during the course of this work. Measurements of the surface seawater collected during this work ranged from 8.06 - 8.08 pH_{TOT} and did not change appreciably during the experiments.

2.4.1 Superoxide decay kinetics

For chemiluminescence measurements of O_2^- we recently adapted (Heller and Croot, 2009) existing flow injection methods for O_2^- which utilize the reagent MCLA (Nakano, 1998; Oosthuizen et al., 1997; Pronai et al., 1992). The mechanism and specificity for the reaction of MCLA and O_2^- is well described (Kambayashi et al., 2003). This system comprises a light tight box equipped with a Plexiglas spiral flow cell mounted below a photon counter (Hamamatsu HC-135-01) linked to a laptop computer via a Bluetooth connection controlled through a purpose built Labview™ (National Instruments) virtual instrument. For O_2^- determination we ran the sample and the MCLA reagent directly into the flow cell using a peristaltic pump (Gilson Minipuls 3, operating at 18 rpm,) with the sample line being pulled through the flow cell as this leads to the smallest amount of dead time in the system (typically 2-3 s). The overall flow rate through the cell was 8.25 mL min^{-1} , comprising 5.0 mL min^{-1} from the MCLA and 3.25 mL min^{-1} from the sample. The transit time through the optical cell ($300 \mu\text{L}$) was therefore 2.18 s.

In the present work we examine the reactivity of superoxide in seawater in a series of experiments designed to elucidate the contributions of the key reaction pathways as described in our earlier work (Heller and Croot, 2009). Briefly our reaction scheme is based on previous work that assumes the reactivity of O_2^- in seawater is controlled by 3 possible reaction mechanisms: (1) The second order uncatalyzed dismutation reaction (k_D) between HO_2 and O_2^- (Bielski and Allen, 1977) that has been previously described (Zafiriou, 1990) in seawater. (2) A reaction between O_2^- and coloured dissolved organic matter (CDOM) (Goldstone and Voelker, 2000). (3) The catalytic reaction between O_2^- and redox sensitive trace metals which can be further separated into the two most likely metal species based on a compilation of the available kinetics data (Bielski et al., 1985). Chiefly rapid reactions between O_2^- and the redox couple Cu(I)/Cu(II) this also includes reactions with organic Cu species (Voelker et al., 2000; Zafiriou et al., 1998). Finally O_2^- reactions with the redox couple Fe(II)/Fe(III) (Fujii et al., 2008; Garg et al., 2007a; Garg et al., 2007b; Rose and Waite, 2006; Voelker and Sedlak, 1995).

Based on the previous research on O_2^- reactions in seawater described above workers in this field have developed the following reactivity scheme for O_2^- :

$$\frac{\partial[O_2^-]}{\partial t} = 2k_D[O_2^-]^2 + \sum k_M[M]_X[O_2^-] + k_{org}[O_2^-] \quad (3)$$

where the metal reactions (k_M) include both the Cu(II)/Cu(I) and Fe(III)/Fe(II) redox pairs (equation 4), the reaction with organic substances is described by the first order rate k_{org} .

$$\sum k_M [M]_X = (k_{Cu(I)}[Cu(I)] + k_{Cu(II)}[Cu(II)] + k_{Fe(II)}[Fe(II)] + k_{Fe(III)}[Fe(III)]) \quad (4)$$

The observed rate of superoxide decay can then be written as follows with only a single term each for the first order and second order rate components

$$\frac{\partial[O_2^-]}{\partial t} = 2k_D [O_2^-]^2 + k_{obs} [O_2^-] \quad (5)$$

where k_{obs} is described as the sum of the first order reaction rates.

$$k_{obs} = \sum k_M [M]_X + k_{org} \quad (6)$$

If the complexing agent DTPA is added to the sample to complex all the trace metals in solution then $k_{obs} = k_{org}$ (Goldstone and Voelker, 2000). In the present work we employed a final DTPA concentration of 3.8 μ M and an equilibration time of 12 hours to ensure that the trace metals were fully complexed (Heller and Croot, 2009; Heller and Croot, 2010b). Though for the experiment from station 8, a shorter 2 hour equilibration time was used in order to observe any possible effects.

Our overall approach is based on measuring the decay rate of known quantities of added O_2^- (as KO_2) to seawater. O_2^- is detected via its chemiluminescence reaction with MCLA (see above). For the present work an experimental setup similar to that used in nutrient bioassay experiments (Mills et al., 2004) was adopted by which a number of experimental treatments are utilized (Figure 3): (i) Control – reaction with unmodified seawater. (ii) Metal free reaction – this is achieved by complexation of trace metals in solution with DTPA, this reactivity measured here then only corresponds to reactions mechanism 1 and 2 shown above. (iii & iv) Addition of 0.78 nM and 1.57nM Cu(II) to the seawater to form a titration series with the control, this approach was also used in a previous study (Voelker et al., 2000). (v & vi) Addition of 0.5nM Fe and 1nM Fe(III) to the seawater to form a titration series with the control. Apparent reaction rates for Cu (k_{Cu}) and Fe (k_{Fe}) with O_2^- were calculated via linear regression of k_{obs} versus the total metal added. Using our experimental setup the minimum values for k_{Cu} and k_{Fe} that were measurable is estimated at $1 \times 10^6 \text{ M s}^{-1}$.

2.4.2 Iron solubility measurements using ^{55}Fe

The radioisotope ^{55}Fe is a weak beta emitter with a half-life of 2.7 years. Fe solubility measurements were performed using the radioisotope, ^{55}Fe (Hartmann Analytics, Braunschweig, Germany). The experimental setup was the same as described previously (Schlosser and Croot, 2009) and was itself adapted from earlier work (Kuma et al., 1996; Nakabayashi et al., 2002). The ^{55}Fe isotope had a specific activity of 157.6 MBq/mg Fe, a

total activity of 75MBq, and was dissolved in 0.1 M HCl. ^{55}Fe dilution standards were produced with MQ water and acidified with Q-HCl to a $\text{pH} < 2$.

After the addition of ^{55}Fe ($t_0 = 0\text{h}$; total Fe $\text{Fe}_T = 20 \text{ nmol L}^{-1}$; $\text{pH} 7.9$) to each sample, a small subsample was immediately filtered through a $0.02 \mu\text{m}$ Anotop syringe filter (Whatman) and acidified with Q-HCl, to keep the Fe from adsorbing to the bottle walls (Fischer et al., 2007; Schlosser and Croot, 2008). Duplicates of the unfiltered and $0.02 \mu\text{m}$ filtered samples ($400 \mu\text{L}$) were transferred into 6 mL vials to which 4.5 mL of scintillation fluid (Lumagel Plus[®]) were then added. This procedure was repeated for subsamples taken at later times. Sample storage, treatment and measurement were performed at room temperature (20°C). The activity of the ^{55}Fe solutions were determined by scintillation counting (Packard, Tri-Carb 2900TR) and then converted to soluble Fe concentrations, taking into account the activity of the added isotope solution and the *in-situ* dissolved Fe concentration of each sample.

2.4.3 Determination of Fe(II)

Dissolved Fe(II) was determined by complexation with FZ (Gibbs, 1976; Stookey, 1970) with subsequent determination of the absorbance of the $\text{Fe}(\text{FZ})_3$ complex at 562 nm by spectrophotometry using a 1 m LWCC-2100 100 cm pathlength liquid waveguide cell (World Precision Instruments, Sarasota, FL, USA) coupled to an Ocean Optics USB4000 UV-VIS spectrophotometer in combination with an Ocean Optics DT-MINI-2-GS light source. For the experiments with dust described here a final concentration of 1 mM FZ in the samples was used throughout. The detection limit using this approach was estimated to be 0.7 nM based on the analysis of replicate blank samples prepared in seawater.

2.4.4 Determination of dissolved Iron by chemiluminescence flow injection analysis

The total dissolvable Fe (TDFe) concentration was measured in the laboratory in Kiel with an established luminol chemiluminescence flow injection analysis (FIA) method (de Jong et al., 2000; Obata et al., 1993). Discrete samples for TDFe were taken in 100 mL clean polyethylene bottles (Kartell) and acidified to $\text{pH} 1.8$ with triple quartz distilled (3QD) concentrated hydrochloric acid (1 ml L^{-1}).

2.4.5 Determination of Trace Metals by Graphite Furnace Atomic Absorption Spectrophotometry (GFAA)

Samples were analyzed according to the method described in Grasshoff (1999) and Kremling and Streu (2001). For the analysis of Cd, Co, Cu, Fe, Ni, Pb and Zn, 300–500 g portions of the samples were subjected to a simultaneous dithiocarbamate–freon extraction modified from the procedure by Danielsson et al. (1978) implying maximum concentration factors of 500. The final extracts with the metals were measured by electrothermal atomic absorption spectrometry with Zeeman background correction (ETAAS; Perkin-Elmer Model 4100 ZL). Accuracy and precision was evaluated using both the certified reference material NASS-5 or the SAFe intercalibration sample (Johnson et al., 2007).

2.5 Dust dissolution experiments

2.5.1 Source of the dust used in this work

The dust used in these experiments was Saharan dust that had accumulated on the side of a volcanic cone near the Cape Verde Atmospheric Observatory at the NW of Sao Vicente (16.848° N, 24.871° W). The sample was sieved through a 100 µm net prior to use in our experiments. Preliminary analysis of the composition of the dust showed that it was similar to that described previously for loess collected from the nearby island of Sal (Chiapello et al., 1997). As all the Cape Verdean islands, including Sao Vicente, have a volcanic origin the area around the Atmospheric Observatory is dominated by recent (picrobasalts and basanites) and intermediate (nephelinites) black volcanic material (Jørgensen and Holm, 2002). The Saharan dust deposits on Sao Vicente are easy to recognize due to their bright yellow-red color while the volcanic rocks/soils are significantly darker. Rognon and coworkers (1996) found that ~80-95% of the aeolian silts deposited on the Cape Verdean islands have a Saharan origin and are transported through the strong Harmattan winds as it blows across the Cape Verdean islands. The main sources of the Saharan dust to Cape Verde are from Mali, Niger, Chad and southern Algeria (d'Almeida, 1987).

In the present work our dust was simply stored in trace metal clean plastic bags after sieving. Our main objective was to have a large homogenized sample that was suitable for repeat experiments. One critical issue we came across in the early design of these experiments was related to the issue of whether to use collected aerosols or loess deposits. In the end we chose loess deposits as this allowed a large sample to be collected. Additional issues regarding storage (e.g. frozen or unfrozen, humidity control) and removing the aerosol from the filter further complicated the use of collected aerosols.

2.5.2 Rationale behind our experimental design

In order to assess the impact and possible role of O_2^- in the dissolution of iron oxides contained in Saharan dust we designed a series of abiotic incubation experiments in order to simulate a number of possible scenarios (Figure 3). Due to sampling limitations only selected combinations of different scenarios were performed during the same sampling period.

- (1) *Seawater only* – this forms the basis for the control experiment.
- (2) *Seawater + Dust* – in part to mimic a natural dust deposition event (though the dust is retained in the bottle unlike in the natural world where it would sink through the mixed layer and be lost eventually).
- (3) *Seawater + different amounts of DFO*- DFO is a terrestrial siderophore and a strong chelator for Fe(III) (Schwarzenbach and Schwarzenbach, 1963).
- (4) *Seawater + Dust + DFO*- DFO will also promote dissolution of solid iron phases as was now shown in several studies (Carrasco et al., 2007; Kraemer et al., 2005). The DFO Fe(III) complex is also by itself not photo-reducible (Kunkely and Vogler, 2001) and is known to inhibit the formation of ROS by some phytoplankton (Kawano et al., 1996).
- (5) *Seawater + Dust + Gluconic acid*- Gluconic acid is formed from the oxidation of glucose and is a relatively weak Fe(III) chelator (Escandar et al., 1990; Escandar et al., 1996) but can apparently undergo photoreduction in seawater to form Fe(II) (Kuma et al., 1995; Öztürk et al., 2004).

2.5.3 Setup of the Incubation Experiments

Prior to the initiation of each experiment filtered surface seawater was collected from an offshore stations (Figure 2 and Table 1) as described above. Incubation experiments were performed in 4.5 L polycarbonate bottles according to the scheme found above (for details on each individual experiment see Table 1). During July 2008 the same four different treatments (Figure 3) were applied in duplicate to all experiments with 0.2 μ m filtered seawater; an unmodified control and 3 treatments with added dust (8.0 ± 0.1 mg of the dust - see above) including one treatment supplemented with DFO (1 nM) and another with GluAc (1 μ M). Experiments performed in May 2009 (Table 1) focused on the impact of DFO alone (Station 8 - no dust additions) and on different amounts of dust and light/dark cycles (Station 9). For the incubation all 8 of the 4.5L bottles were placed into incubators located at the INDP through which seawater was constantly pumped to maintain a relatively constant temperature ($28 \pm 1^\circ$ C) in the bottles over the experimental run. These same incubators had previously been used in shipboard experiments (Mills et al., 2004). Light was attenuated to 20% of incident surface

values with blue filters (Lagoon Blue, Lee Filters #172). It should be noted however that the polycarbonate bottles used in this study do not transmit UV light appreciably. At specific times sub-samples were taken from the bottles for TDFe and for O_2^- decay kinetics (Figure 3).

3. Results and Discussion

3.1 Investigation into the reactivity of iron and copper with O_2^- in seawater

3.1.1 ^{55}Fe solubility experiments with O_2^- sources

Initial laboratory work focused on the effect of O_2^- and/or siderophores on iron solubility and was assessed over a 24 hour time period by the addition of 20 nM of ^{55}Fe to surface seawater which had been collected earlier from the Tropical Eastern Atlantic during Meteor expedition M68-3 (Schlosser and Croot, 2009). As expected after 24 hours soluble iron levels (Figure 4), in the presence of 2 nM of the siderophore DFO, were increased (2370 ± 450 pM) over that of the natural seawater (1480 ± 30 pM). However, in the presence of the enzymatic O_2^- source, X/XO, soluble iron values actually decreased (1080 ± 300 pM), as did a control experiment in the presence of only xanthine (1150 ± 170 pM). The combination of DFO and X/XO was initially lower than for the case of only DFO was present but was similar (2270 ± 250 pM) by the end of the 24 hour time period (Figure 4).

It appears then from these preliminary data using amorphous Fe colloids formed upon direct addition of Fe to seawater that in the presence of the X/XO system there was no increase in soluble Fe as might be expected if colloidal iron was reduced to more soluble forms via O_2^- reduction. However the unexpected effect of lower soluble Fe in the presence of xanthine itself raised issues in the use of this O_2^- source for seawater experiments involving an assessment of iron solubility and so we did not pursue work with X/XO further in the present work.

3.1.2 Fe(II) formation from Saharan dust in seawater

We examined the formation of Fe(II) (Figure 5) from our Saharan dust sample (see section 2.5.1) in the presence and absence of the thermal O_2^- source SOTS-1 (Heller and Croot, 2010a; Ingold et al., 1997) by using 1 mM FZ in order to prevent the reoxidation of Fe(II) that was formed (Lin and Kester, 1992; Thompsen and Mottola, 1984). In the absence of SOTS-1 we observed essentially no change in Fe(II) over the first 4 hours of the experiment and only a small change at later times. In the presence of SOTS-1, 7 nM of Fe(II) was formed instantaneously and then the concentration proceeded to increase over time (Figure 5). After 24 hours at which point the SOTS-1 had completely decayed the Fe(II)

concentration had increased to 26 ± 2 nM in the presence of SOTS-1 and to 9 ± 1 nM in the sample without SOTS-1. The formation of some Fe(II) in the sample without SOTS-1 is consistent with earlier work in seawater where a significant thermal reaction was also observed (Croot and Hunter, 2000).

The initial instantaneous formation in the presence of SOTS-1 of 7 nM Fe(II) probably represents highly labile Fe from the dust or seawater and the subsequent slower formation of Fe(II) was due to reactions where the release of Fe from the dust was the rate determining step. This is consistent with the mechanism proposed by Fujii et al (2006) by which Fe must dissociate from the surface first before reduction by O_2^- and that as the iron colloid ages it undergoes transformations that decrease the dissociation rate. This phenomenon has also been seen in the iron solubility work of Kuma and coworkers (Kuma et al., 2000; 1996). Saharan dust is undoubtedly a mix of crystalline iron phases and amorphous aged iron oxides and it is the latter that we suppose to be the source of the exchangeable iron that transferred into dissolved phase in seawater.

If it is assumed that the time dependence of the observed Fe(II) signal in the presence of SOTS-1 is due to the reaction with O_2^- produced from the decay of SOTS-1, the following time dependence can be proposed (Heller and Croot, 2010a) for the Fe(II) concentration (A) :

$$A_t = A_{max} (1 - e^{-kt}) + A_0 \quad (7)$$

Where k is the thermal decay constant for SOTS-1 at the temperature of the experiment (21.6 °C), A_t is the concentration of A at time t , A_0 is the concentration of A at time $t=0$ and A_{max} is the maximum yield of A when the SOTS-1 has completely reacted. This equation can be rearranged to solve for k as a function of t .

$$-kt = \ln \left(1 - \frac{(A_t - A_0)}{A_{SOTS}} \right) \quad (8)$$

Application of equation 8 (Figure 5) reveals a linear decrease in kt with time as expected with $k = 2.5 \pm 0.4 \times 10^{-5} \text{ s}^{-1}$ consistent with other estimates of the decay rate of SOTS-1 in seawater (Heller and Croot, 2010a). As the SOTS-1 concentration in this experiment was initially 2.5 μM then this would represent a total O_2^- supply of 1 μM over the course of the experiment, based on the 40 mol% conversion of SOTS-1 into O_2^- (Ingold et al., 1997). Thus if O_2^- was the limiting reagent, as the Fe in the dust was in excess, then this represents an overall yield of 2.5% for Fe(II). Based on the mechanism proposed by Fujii et al. (2006) we can speculate that this value represents the exchangeable iron in the sample and as such may be comparable to solubility estimates for Saharan dust obtained by other methods (Baker et al., 2006; Buck et al., 2006).

3.1.3 Influence of Fe(II) or Cu(I) chelators on the decay of O₂⁻ in seawater

An important aspect of the interpretation of the O₂⁻ decay rate is whether the reaction with metals such as Cu and Fe forms a truly catalytic redox reaction where cycling between two redox states occurs. To assess this we performed experiments in the presence of strong Fe(II) or Cu (I) chelators, in seawater collected from station 8 (Table 1). For each metal two titration sets were prepared by adding the appropriate higher oxidation state of the metal (Fe(III) or Cu(II)), to one series with added chelators and one series without. The chelators used were the Fe(II) chelator FZ (160 μM) and the Cu(I) chelator Neocuproine (380 μM).

It can be clearly seen in Figure 6 that in the presence of FZ that k_{obs} was essentially constant, while in the absence of FZ k_{obs} increased linearly with increasing addition of Fe(III). A value of $\log k_{\text{Fe}} = 7.11 \pm 0.12 \text{ M}^{-1} \text{ s}^{-1}$ (95% CI) can be obtained by linear regression of k_{obs} against the added Fe concentration ($R^2 = 0.93$, $n=6$) in the absence of FZ. In the case of Cu(II) additions to the seawater, in the presence of Neocuproine k_{obs} varies little. However in the absence of Neocuproine k_{obs} was too fast for our measurement system when Cu concentrations exceeded 1.6 nM. For the Cu concentrations where kinetic measurements were possible we calculate a value of $\log k_{\text{Cu}} = 7.99 \pm 0.16 \text{ M}^{-1} \text{ s}^{-1}$ (95% CI) via linear regression of k_{obs} against the added Cu concentration ($R^2 = 0.97$, $n=3$) in the absence of Neocuproine.

The data in figure 6 clearly indicates that the observed reaction is catalytic over the concentration range we examined and thus our modeling approach is apparently valid under these conditions. It should be remembered that this requires fast reactions between O₂⁻ and both the oxidized (Mⁿ⁺¹) and reduced (Mⁿ⁺) form of the redox couple, with the observed rate related to the individual rates by the following equation (Voelker et al., 2000):

$$k_M = \frac{2k_{M^{n+}}k_{M^{n+1}}}{k_{M^{n+}} + k_{M^{n+1}}} \quad (9)$$

Comparison of our calculated values for k_{Cu} were intermediate to that found previously for the strong L1 Cu complex produced by *Synechococcus* ($k_{\text{Cu}} = 5 \pm 3 \times 10^7 \text{ M}^{-1} \text{ s}^{-1}$) and the weaker L2 Cu complexes ($k_{\text{Cu}} = 3\text{-}8 \times 10^8 \text{ M}^{-1} \text{ s}^{-1}$) found in coastal seawater (Voelker et al., 2000). This was most likely due in the present case to the complete titration of any L1 complexes present (Moffett and Brand, 1996) resulting in the observed k_{Cu} being an average of the entire pool of Cu organic complexes. In our earlier study in the Southern Ocean (Heller and Croot, 2009) we found k_{Cu} to vary systematically through the water column with lowest values found at the chlorophyll maxima. Below that k_{Cu} became relatively constant ($\log k_{\text{Cu}} = 7.6 - 7.9$) in the intermediate and deep waters.

Similarly the value calculated here for k_{Fe} in the seawater from station 8 is in the range of values we previously measured in the Southern Ocean (Heller and Croot, 2009). However our values are considerably higher than recent laboratory measurements in which high concentrations of Fe(III), 200 nM, were complexed with model ligands (4 μM) and natural organic matter ($k_{\text{Fe}} = 2.3 \pm 0.1 \times 10^5 \text{ M}^{-1} \text{ s}^{-1}$) in bicarbonate solutions using XO/X as a O_2^- source (Rose and Waite, 2005). It is likely however that in our samples that the added Fe was weakly complexed as the strong iron chelators were saturated and this may have led to the high reactivity.

3.1.4 Influence of DFO on the decay of O_2^- in seawater

Using water from station 8 we conducted an experiment using the strong Fe chelator DFO in order to examine the influence of Fe(III) complexation on the decay of O_2^- in seawater and in particular the values of k_{Fe} and k_{Cu} obtained by titration. As can be seen in figure 7, the addition of DFO had little or no effect when Cu was added to the seawater samples and values for k_{Cu} were similar for all 3 treatments. However for Fe the values of k_{obs} did not apparently vary as a function of the added Fe as would be expected when they are strongly chelated. This also implies that the Fe in the control sample was also apparently inert to O_2^- up to an addition of 2 nM suggesting that an excess of strong iron ligand was already present in this sample.

3.2 Dust dissolution experiments

3.2.1 Existing conditions before sampling

One aspect that is critical to our understanding of the processes that are occurring during dust deposition relates to the prehistory of the water being examined. Recent work from the Mediterranean (Wagener et al., 2008) and the Tropical Atlantic (Rijkenberg et al., 2008) point to the importance of the seasonal effects and to the time between dust events in how the system, here including biology, responds to the input of dust or aerosol. However unless there is continuous monitoring in a Lagrangian fashion (e.g. FeCycle (Boyd et al., 2005)) it is impossible to know anything about the prehistory of the water before initiating an experiment. In the present work we have used the available satellite tools to assess the sampling location prior to occupation (<http://disc.sci.gsfc.nasa.gov/giovanni>).

Ocean color observations from satellite (MODIS AQUA and SeaWiFs) indicated no major changes in chlorophyll concentrations (0.1 – 0.3 $\mu\text{g L}^{-1}$) during the sampling periods in either July 2008 or May 2009. Satellite measurements of aerosol optical depth (AOD) from

MODIS Terra indicate that significant dust storms passed over the sampling sites in July 2008, on the 11th, 13th, 18th, 25th and 29th of July. During each sampling cruise (Figure 2) we also made AOD measurements using a pre-calibrated Microtops instrument (Porter et al., 2001) borrowed from NASA (contact: Alexander Smirnov. See the webpage for more details http://aeronet.gsfc.nasa.gov/new_web/maritime_aerosol_network.html) as part of their Maritime Aerosol Network (MAN) (Smirnov et al., 2009). These measurements complement and enhance the satellite data as they reveal information on the aerosol load at the time of sampling. Station 1 (AOD(500 nm) = 0.34 ± 0.04) had the lowest values of all, while station 2 (AOD(500 nm) = 0.55 ± 0.03) elevated. The major dust outbreak of July 24 and 25 was clearly captured in the Microtops data obtained during the sampling of station 3 (AOD(500 nm) = 0.79 ± 0.19). While a smaller outbreak was seen at the final station (Station 4 AOD(500 nm) = 0.41 ± 0.07). For the experiments performed in May 2009, there were some major dust outbreaks to the southeast of Sao Vicente but none passed directly over our study sites. It should however be remembered that during the summer in Cape Verde most of the dust passes directly overhead in the SAL (Karyampudi et al., 1999) and that AOD may not be representative of the actual deposition to the ocean.

3.2.2 Dust dissolution in the experimental assays

The time variation in TDFe over time for the treatments from stations 1-4 in July 2008 are shown in figure 8. Dealing first with the controls it is clear that all the concentrations decreased with time in these bottles suggesting that adsorption to the polycarbonate bottle walls was an issue here, though the data set is too small to provide adequate statistical confirmation of this trend. Polycarbonate bottles have been preferred to glass and other plastics for trace metal work for their low adsorption properties but more as noted in the original work (Fitzwater et al., 1982) Fe adsorption will increase over time. In the present work the loss of Fe from solution, presumably to the walls, will also represent the precipitation of iron from an oversaturated solution due to recent dust deposition. Interestingly the concentration of TDFe after 48 hours was similar in experiments 2-4 (0.26 ± 0.02 nM), and only slightly more in experiment 1 (0.40 ± 0.11 nM), possibly indicating a natural equilibrium value for iron in solution related to the soluble iron only. The polycarbonate bottles were thoroughly cleaned in between use, by rinsing with 1% HCl, and it is possible that frequent cleaning may create adsorption sites on the bottle. Whatever the reason for the loss of iron from the solution is, be it a natural process or an artifact of the experiment, it is clearly something that needs to be directly addressed in future work.

For all 4 stations the treatments with the dust additions, but without added chelators, were significantly higher than the controls at both 24 hours (2 way ANOVA: $p = 0.04$) and 48 hours ($p = 0.006$) as would be expected. The treatment with dust and DFO was also significantly higher from the control after 48 hours ($p = 0.02$) but not after 24 hours. The dust and Gluconic acid treatment however was only weakly statistically significant from the control ($p = 0.07$) after 24 hours and not significantly different at all after 48 hours. There was no statistically significant trend found between the various dust treatments. The differences between station 2 and 3 are most intriguing as these stations were closely spaced in location and time (4 days apart) and the differences may be related to the large dust storm that was passing overhead at the time of sampling station 3 (see above).

Much of the variability in the data appeared to be related to apparent differences between the stations as the variability between replicate samples was small in comparison. For instance at station 1 the 3 dust treatments do not appear to change between 24 and 48 hours and the Gluconic acid treatment gave the highest Fe values. However at no other stations did the Gluconic acid treatment give the maximum Fe values, indeed at station 4 they were the lowest next to the control. Similar apparently contradictory data is seen with the DFO treatments where at stations 2 and 4 the values decrease with time, while at station 3 they increase. However in this case it should also be noted that only 1 nM of DFO was added in each case and thus much of the variation can not be explained by simply complexation by DFO alone.

As the ferric-gluconate complex is light sensitive (Kuma et al., 1995), differences in the sunlight during the time that each incubation was performed are a possible cause for the variability found in that treatment. Indeed analysis of spectral irradiation data (not shown) from the nearby TENATSO Atmospheric Observatory (Personal communication: Nidia Martinez, University of Hamburg) indicate that light levels were much reduced during the period of incubation for station 4 where the lowest values were observed. Similarly the reduction seen for the Gluconic acid and dust treatment during experiment 2 coincides with lower light levels on the 2nd day of incubation. However more incubation data is needed over the diel cycle in order to truly assess the role of light in these experiments.

Borer (2009b) found that light has only a weak effect on the dissolution of ferrihydrite and ferric oxides in the presence of DFO. They proposed that with increasing thermodynamic stability of the Fe(III) hydroxides the release of lattice surface Fe(II) may be outcompeted by reoxidation by oxygen and/or ROS (Sulzberger, 1995; Sulzberger and Laubscher, 1995). A

further important point to consider here in the context of the DFO experiment is if the DFO was itself scavenged by the dust particles and removed from the soluble phase.

In our work the apparent fractional solubility of the dust would be estimated as $0.14 \pm 0.04\%$. This calculation is based on ~ 1.04 mmol of Fe per gram of dust using data for the composition of dust from the Northern Sahara and Sahel regions (Chiapello et al., 1997). However as pointed out in Baker and Croot (2008) this approach clearly underestimates the true solubility of the dust as the seawater is saturated and no more iron can dissolve from the dust.

3.2.3 Variation in k_{obs} during dust dissolution assays

In the present work we measured directly the decay rate of O_2^- in the seawater samples to examine whether changes in metal speciation, and hence reactivity with O_2^- , were occurring on the addition of dust to the seawater. Figure 9 shows the time variation in k_{obs} for the samples with added dust during July 2008. It appears that for stations 1 and 2 there was a decrease in k_{obs} from initially high values to lower values and this may indicate the scavenging of soluble components from the seawater, either onto the dust or onto the bottle walls (see above). Contrastingly for stations 3 and 4, k_{obs} shows a small increase over time possibly indicating the release of substances from the dust. At first approximation we could assume that the changes in k_{obs} are related to changes in Fe speciation, and this does apparently fit the TDFe data seen in figure 8 where the same trends are seen although the magnitude of response varies between the stations. If colloidal iron truly does not react with O_2^- then the k_{obs} data would be dependent on only the soluble reactive species and this would partly explain the differences in the response between the TDFe, which would be mostly colloidal particles, and the k_{obs} results.

We are assuming here that there is minimal dissolution of Cu from the dust. This is probably a valid assumption as work by Desboeufs et al. (1999) indicate that only 0.07 % of the Cu from Saharan dust is soluble which would lead to a contribution of ~ 0.5 pM to our incubation samples, which is analytically insignificant. A further possible explanation of the data in Figure 9 is the scavenging of O_2^- reactive copper complexes onto the dust particles but this is also probably unlikely as previous work has shown most marine Cu organic complexes to be principally hydrophilic (Donat et al., 1986).

In May 2009 with seawater from station 9 we examined the influence of both dust amount and light/dark on the value of k_{obs} (Figure 10). In this experiment there was considerable variation between treatments after only 4 hours with the highest values found for

the dark treatment. However after 24 hours the samples appeared to have reached stable values with the 2 x dust treatment giving the highest values, while both 1 x dust treatments gave identical responses but this was below the control without dust (Figure 10). The results from July 2008 when viewed in the context of figure 10 may therefore indicate that the seawater from stations 1 and 2 were undersaturated and after the large dust event that passed by while station 3 was being sampled (see above) the subsequent stations 3 and 4 responded in a similar manner to the 2 x dust treatment in Figure 10. However this interpretation hinges on systematic variations in the colloidal Fe which was not measured in this work. Although other workers have suggested that most of the variation in dissolved concentrations is due to the colloidal fraction (Bergquist et al., 2007; Wu et al., 2001).

During experiments 1-4, k_{Cu} showed no appreciable variation in any of the treatments (data not shown), indicating that there were no apparent changes in Cu speciation occurring during this time. This is not unexpected as in the absence of biology and little UV light it is unlikely that the speciation would be altered. Commonly the Cu speciation in seawater is assessed by voltammetric methods and while direct comparison with the present work would be useful, it was not practical given the water requirements and the long analysis time required for the voltammetric methods. Titration data from station 9 shown in figure 11 as the k_{Fe} and k_{Cu} values indicated that during this time and with the dust treatments there was little apparent change in the reactivity of the Cu complexes with O_2^- . The only exception was for the single time point obtained in the dark, where all the dust treatments were significantly lower than the control. We can think of no logical explanation for this result, however it will spur us on to undertake more diel cycle studies to see if it occurs again.

In the control sample at station 9 there was no apparent response to the addition of Fe throughout the duration of the experiment suggesting that there was a least a 1 nM excess of a strong iron chelator present at this time. However all the dust treatments gave a linear response to iron additions indicating that there was no strong complexation occurring anymore and that iron released from the dust had complexed with the ligand that was apparent in the control samples. During July 2008 there was a trend towards increasing k_{Fe} in the initial controls at each station (data not shown), from essentially no response at station 1, $\log k_{\text{Fe}} = 7.57 \pm 0.11$ at station 2, $\log k_{\text{Fe}} = 7.60 \pm 0.12$ at station 3 and finally $\log k_{\text{Fe}} = 7.80 \pm 0.12$ at station 4. This may represent an increase in the concentration of weakly complexed soluble iron over time, if it is assumed that the colloidal iron does not react with O_2^- , but in the absence of soluble iron measurements it is difficult to prove. In comparison to our earlier Southern Ocean work (Heller and Croot, 2009) where we observed lower k_{Fe} values in general

and frequently more values below our detection limit consistent with an under saturated system with respect to iron.

The data collected from station 9 indicate a complex dose response curve for the addition of dust. The first 8 mg apparently caused scavenging of O_2^- reactive components while a second 8 mg led to a net release of O_2^- reactive components. The additions we applied here need to be put into the context of dust deposition estimated for the Cape Verde region of the order of $20 \text{ g m}^{-2} \text{ y}^{-1}$ (Jickells et al., 2005). To put our experiments in perspective we added 8 mg in 4.5 L, which when scaled up to 20 m^3 for a 20 m mixed layer would be equivalent to 35.6 g m^{-2} . Working with smaller amounts of dust is difficult due to the problems of accurately weighing out μg amounts. Clearly future experiments need to use lower dust to seawater ratios in order to examine the dose response at more realistic levels for the open ocean.

3.2.4 Variation in k_{org} during dust dissolution assays

The experimental approach used in this work allows us also to follow changes in the apparent reactivity of organic matter with O_2^- in each of the treatments. Figure 12 shows the time course of k_{org} for stations 1 and 4 during July 2008. The striking feature is that for the first 24 hours all of the treatments are apparently similar and only diverge after 48 hours. While the trends differ between stations 1 and 4 they are consistent with the same patterns seen for these stations for k_{obs} for the dust treatment (Figure 9). A further observation is that by the end of 48 hours there is little difference between the values at each station for the respective treatments. Additionally after 48 hours it is the DFO + dust treatment which has the highest value. This could indicate the removal of Fe bound to DOM by DFO with the subsequent release of this DOM to react with O_2^- , as might be expected with humic type functional groups.

In the experiment from station 9 there was no significant difference seen between the dust treatments for k_{org} (Figure 13), though they were all significantly lower than the dust free control. This indicates that the addition of dust can remove some portion of the O_2^- reactive DOM either by the reverse of the mechanism suggested above, where by Fe from the dust chelates the DOM making an O_2^- inert complex, or by adsorption onto particles where it is presumably the more hydrophobic fraction which is scavenged. This is an interesting result as it may have implications for the residence time of some components of DOM under the Saharan dust plume

Overall k_{org} was a minor but significant contributor to the overall O_2^- decay in all the treatments as was seen also in vertical profiles from the nearby TENATSO station (Heller and Croot, 2010b). Further work is needed to elucidate the functional groups that are responsible for the reactions with O_2^- .

3.3 Implications for Biogeochemistry

3.3.1 Implications for the dissolution of dust by O_2^-

That O_2^- can reduce Fe from dust was clearly shown in Figure 5, however this was in the presence of 1 mM of the strong Fe(II) chelators FZ. In the open ocean the Fe(II) produced from reactions between O_2^- and dust would be most likely rapidly oxidized by O_2 or H_2O_2 and so only a small fraction might eventually be stabilized by any natural Fe(II) chelators (Croot et al., 2007). Furthermore the data here strongly suggests that major sink for O_2^- in the Eastern Tropical Atlantic is with Cu organic complexes and to a lesser extent DOM. Similarly we might also expect a low encounter rate between dust particles and O_2^- . Combining all these factors together it suggests that O_2^- is not a significant pathway for the dissolution of dust in the ocean.

3.3.2 Implications for O_2^- , Fe(II) and Cu(I) in the Tropical Ocean

Based on the values of k_{Cu} and k_{Fe} measured in the present work we can estimate that the major sink for O_2^- in these waters was through reactions with Cu. It is also clear from our experiments that Fe could be important when concentrations increase after dust events as relatively little Cu is supplied via the dust. However it is still unclear what the contribution of colloidal iron or weakly complexed iron is to the k_{Fe} signal and this remains a missing piece of the puzzle. Superoxide reactions with DOM are a minor sink but potentially important for altering the chemical composition of the DOM.

Reactions between O_2^- and Fe(III) have been previously suggested to be an important source of Fe(II) in seawater (Voelker and Sedlak, 1995). Using the same approach as we did previously (Heller and Croot, 2009) we can use the k_{Fe} values, along with equation 9, to estimate the maximum ratio of Fe(II) to Fe(III) present in seawater under steady state conditions as ~45 pM Fe(II) per nM Fe(III). The caveat here is that it appears that the calculation should be made with the truly soluble Fe and not the colloidal Fe however we can not categorically rule colloidal Fe out as a source yet. This means that O_2^- could be a significant source of Fe(II) in the waters under the Saharan dust plume in the Tropical Eastern Atlantic but it crucially depends on determining if nanomolar colloidal Fe reacts with O_2^- .

Measurements of Cu(I) (Moffett and Zika, 1988) in the subtropical Atlantic indicated that Cu(I) is 5-10 % of the total copper in the euphotic zone, which is slightly more than we estimate here 20-40 pM, based on our k_{Cu} values, 1 nM dissolved Cu and assuming that reactions with Cu(II) organic complexes are the slower step (see equation 9) and that the Cu(I) reaction rate is the same as for inorganic Cu(I) (Heller and Croot, 2009). This suggests that there is probably an additional contribution from the direct photoreduction of Cu complexes, or less likely, that there may possibly be Cu(I) complexes inert to O_2^- in seawater.

4. Conclusions

Our use of superoxide decay measurements, in conjunction with a multiple treatment experimental design, shows promise as a probe for detecting changes in metal speciation in seawater. This method also supplies information relevant to determining the turnover time for O_2^- and helps to constrain estimates of Fe(II) and Cu(I) in the ocean. Using this approach for the first time in dust dissolution experiments has shown that the principle of the idea works. However both the approach and measurements need to be refined more for this to become a more useful tool in oceanographic studies. Further work is already planned with single treatment, large volume, high sampling frequency experiments where sufficient sample exists to obtain ultrafiltration samples and comparative voltammetric measurements of the *in situ* speciation.

In the present work we applied an experimental assay approach to the question of what processes control dust dissolution in seawater. Our results indicate that while ligand promoted and thermal dissolution appeared to be clearly important, our experiments in natural waters were highly variable and most of this variability was apparently related to dynamic factors associated with changes in surface seawater chemistry occurring over both spatial and temporal scales. Key amongst these factors is most likely the abundance of colloidal metal species and ligands. Thus it is crucial that future work needs to examine simultaneously both the soluble and colloidal size ranges and focuses on the relationship between k_{obs} and soluble copper and iron species in order to better constrain the key processes occurring during the dissolution of aeolian dust in seawater.

Acknowledgements

The authors would like particularly to express their deep thanks and appreciation to the crew of the *R.V. Islandia* (INDP). Special thanks go to Pericles da Silva and Ivanice Monteiro (INDP) for all their patience and help with our work in Cape Verde. Thanks also to members of the trace metal speciation group at IFM-GEOMAR who helped directly with this project: Kathrin Wuttig, Peter Streu, Anna Dammshäuser, Thibaut Wagener and Mirja Dunker. Thanks also to our bioassay colleagues from IFM-GEOMAR (Wiebke Mohr, Philipp Raab and Julie La Roche) and IOW (Nicola Wannicke) who provided logistical support and encouragement during this work. This work was supported by the BMBF Verbunds project SOPRAN (TP 1.2) and forms part of the German contribution to SOLAS (Surface Ocean Lower Atmosphere Studies).

References:

- Baker, A.R. and Croot, P.L., 2008. Atmospheric and marine controls on aerosol iron solubility in seawater. *Marine Chemistry*: doi:10.1016/j.marchem.2008.09.003.
- Baker, A.R. and Jickells, T.D., 2006. Mineral particle size as a control on aerosol iron solubility. *Geophysical Research Letters*, 33(17).
- Baker, A.R., Jickells, T.D., Witt, M. and Linge, K.L., 2006. Trends in the solubility of iron, aluminium, manganese and phosphorus in aerosol collected over the Atlantic Ocean. *Marine Chemistry*, 98(1): 43-58.
- Balsam, W.L., Ottobliesner, B.L. and Deaton, B.C., 1995. Modern and Last Glacial Maximum Eolian Sedimentation Patterns in the Atlantic-Ocean Interpreted from Sediment Iron-Oxide Content. *Paleoceanography*, 10(3): 493-507.
- Barbeau, K., Rue, E.L., Bruland, K.W. and Butler, A., 2001. Photochemical cycling of iron in the surface ocean mediated by microbial iron(III)-binding ligands. *Nature*, 413(6854): 409-413.
- Baxendale, J.H. and Wilson, J.A., 1957. The photolysis of hydrogen peroxide at high light intensities. *Transactions of the Faraday Society*, 53: 344-356.
- Baxter, R.M. and Carey, J.H., 1983. Evidence for Photochemical Generation of Superoxide Ion in Humic Waters. *Nature*, 306(5943): 575-576.
- Bell, J., Betts, J. and Boyle, E., 2002. MITESS: a moored in situ trace element serial sampler for deep-sea moorings. *Deep-Sea Research Part I-Oceanographic Research Papers*, 49(11): 2103-2118.
- Bergquist, B.A., Wu, J. and Boyle, E.A., 2007. Variability in oceanic dissolved iron is dominated by the colloidal fraction. *Geochimica et Cosmochimica Acta*, 71(12): 2960-2974.
- Bielski, B.H.J. and Allen, A.O., 1977. Mechanism of the disproportionation of superoxide radicals. *J. Phys. Chem.*, 81(11): 1048-1050.
- Bielski, B.H.J., Cabelli, D.E., Arudi, R.L. and Ross, A.B., 1985. Reactivity of HO_2/O_2^- Radicals in Aqueous-Solution. *Journal of Physical and Chemical Reference Data*, 14(4): 1041-1100.
- Blough, N.V. and Zafiriou, O.C., 1985. Reaction of Superoxide with Nitric Oxide to Form Peroxonitrite in Alkaline Aqueous Solution. *Inorganic Chemistry*, 24: 3502-3504.
- Bolann, B.J. and Ulvik, R.J., 1990. On the limited ability of superoxide to release iron from ferritin. *Eur. J. Biochem.*, 193: 899-904

- Bolann, B.J. and Ulvik, R.J., 1991. Improvement of a Direct Spectrophotometric Assay for Routine Determination of Superoxide-Dismutase Activity. *Clinical Chemistry*, 37(11): 1993-1999.
- Bonini, M.G., Miyamoto, S., Mascio, P.D. and Augusto, O., 2004. Production of the Carbonate Radical Anion during Xanthine Oxidase Turnover in the Presence of Bicarbonate. *J. Biol. Chem.*, 279(50): 51836-51843.
- Borer, P., Hug, S.J., Sulzberger, B., Kraemer, S.M. and Kretzschmar, R., 2007. Photolysis of citrate on the surface of lepidocrocite: An in situ attenuated total reflection infrared spectroscopy study. *Journal of Physical Chemistry C*, 111(28): 10560-10569.
- Borer, P., Kraemer, S.M., Sulzberger, B., Hug, S.J. and Kretzschmar, R., 2009a. Photodissolution of lepidocrocite (γ -FeOOH) in the presence of desferrioxamine B and aerobactin. *Geochimica Et Cosmochimica Acta*, 73(16): 4673-4687.
- Borer, P., Sulzberger, B., Hug, S.J., Kraemer, S.M. and Kretzschmar, R., 2009b. Photoreductive Dissolution of Iron(III) (Hydr)oxides in the Absence and Presence of Organic ligands: Experimental Studies and Kinetic Modeling. *Environmental Science & Technology*, 43(6): 1864-1870.
- Boyd, P.W. et al., 2005. FeCycle: Attempting an iron biogeochemical budget from a mesoscale SF6 tracer experiment in unperturbed low iron waters. *Global Biogeochemical Cycles* 19: GB4S20, 10.1029/2005GB002494.
- Boyd, P.W. et al., 2000. Mesoscale iron fertilisation elevates phytoplankton stocks in the polar Southern Ocean. *Nature*, 407: 695-702.
- Brand, L.E., Sunda, W.G. and Guillard, R.R.L., 1986. Reduction of Marine Phytoplankton Reproduction Rates by Copper and Cadmium. *Journal of Experimental Marine Biology and Ecology*, 96: 225-250.
- Buck, C.S., Landing, W.M., Resing, J.A. and Lebon, G.T., 2006. Aerosol iron and aluminum solubility in the northwest Pacific Ocean: Results from the 2002 IOC cruise. *Geochemistry Geophysics Geosystems*, 7.
- Cabelli, D.E. and Bielski, B.H.J., 1984. Pulse-Radiolysis Study of the Kinetics and Mechanisms of the Reactions between Manganese(II) Complexes and HO_2/O_2^- Radicals .2. the Phosphate Complex and an Overview. *Journal of Physical Chemistry*, 88(25): 6291-6294.
- Carrasco, N., Kretzschmar, R., Pesch, M.L. and Kraemer, S.M., 2007. Low concentrations of surfactants enhance siderophore-promoted dissolution of goethite. *Environmental Science & Technology*, 41(10): 3633-3638.

- Chen, Y.-B., Dominic, B., Mellon, M.T. and Zehr, J.P., 1998. Circadian Rhythm of Nitrogenase Gene Expression in the Diazotrophic Filamentous Nonheterocystous Cyanobacterium *Trichodesmium* sp. Strain IMS 101. *J. Bacteriol.*, 180(14): 3598-3605.
- Chiapello, I. et al., 1997. Origins of African dust transported over the northeastern tropical Atlantic. *Journal of Geophysical Research-Atmospheres*, 102(D12): 13701-13709.
- Chiapello, I. et al., 1995. An Additional Low Layer Transport of Sahelian and Saharan Dust over the North-Eastern Tropical Atlantic. *Geophysical Research Letters*, 22(23): 3191-3194.
- Coale, K.H. et al., 1996. A massive phytoplankton bloom induced by an ecosystem-scale iron fertilization experiment in the equatorial Pacific Ocean. *Nature*, 383(6600): 495-501.
- Cory, R.M. and McKnight, D.M., 2005. Fluorescence spectroscopy reveals ubiquitous presence of oxidized and reduced quinones in dissolved organic matter. *Environmental Science & Technology*, 39(21): 8142-8149.
- Croot, P.L. et al., 2007. The effects of physical forcing on iron chemistry and speciation during the FeCycle experiment in the South West Pacific. *Journal of Geophysical Research - Oceans*, 112: C06015, doi:10.1029/2006JC003748.
- Croot, P.L. and Hunter, K.A., 2000. Labile forms of iron in coastal seawater: Otago Harbour, New Zealand. *Marine Freshwater Research*, 51: 193-203.
- Croot, P.L. and Johansson, M., 2000. Determination of iron speciation by cathodic stripping voltammetry in seawater using the competing ligand 2-(2-Thiazolylazo)-p-cresol (TAC). *Electroanalysis*, 12(8): 565-576.
- Croot, P.L. and Laan, P., 2002. Continuous shipboard determination of Fe(II) in Polar waters using flow injection analysis with chemiluminescence detection. *Analytica Chimica Acta*, 466: 261-273.
- Croot, P.L. et al., 2005. Spatial and Temporal distribution of Fe(II) and H₂O₂ during EISENEX, an open ocean mesoscale iron enrichment. *Marine Chemistry* 95: 65-88.
- Croot, P.L., Moffett, J.W. and Brand, L., 2000. Production of extracellular Cu complexing ligands by eucaryotic phytoplankton in response to Cu stress. *Limnology and Oceanography*, 45: 619-627.
- Croot, P.L., Streu, P. and Baker, A.R., 2004. Short residence time for iron in surface seawater impacted by atmospheric dry deposition from Saharan dust events. *Geophysical Research Letters*, 31(23): 4.

- d'Almeida, G.A., 1987. On the Variability of Desert Aerosol Radiative Characteristics. *Journal of Geophysical Research-Atmospheres*, 92(D3): 3017-3026.
- Danielsson, L.G., Magnusson, B. and Westerlund, S., 1978. Improved Metal Extraction Procedure for Determination of Trace-Metals in Sea-Water by Atomic-Absorption Spectrometry with Electrothermal Atomization. *Analytica Chimica Acta*, 98(1): 47-57.
- Darwin, C., 1846. An account of the Fine Dust which often falls on Vessels in the Atlantic Ocean. *Quarterly Journal of the Geological Society*, 2(1-2): 26-30.
- de Jong, J.T.M., Boye, M., Schoemann, V., Nolting, R.F. and de Baar, H.J.W., 2000. Shipboard techniques based on flow injection analysis for measuring dissolved Fe, Mn and Al in seawater *J. Environ. Monit.*, 2: 496-502.
- Desboeufs, K.V., Losno, R., Vimeux, F. and Cholbi, S., 1999. The pH-dependent dissolution of wind-transported Saharan dust. *Journal of Geophysical Research-Atmospheres*, 104(D17): 21287-21299.
- Dickson, A.G., 1993. The Measurement of Seawater pH. *Marine Chemistry*, 44(2-4): 131-142.
- Dister, B. and Zafiriou, O.C., 1993. Photochemical Free-Radical Production-Rates in the Eastern Caribbean. *Journal of Geophysical Research-Oceans*, 98(C2): 2341-2352.
- Dix, T.A. and Aikens, J., 1993. Mechanisms and biological relevance of lipid peroxidation initiation. *Chemical Research in Toxicology*, 6(1): 2-18.
- Donat, J.R., Statham, P.J. and Bruland, K.W., 1986. An evaluation of a C-18 solid phase extraction technique for isolating metal-organic complexes from central North Pacific Ocean waters. *Marine Chemistry*, 18: 85-99.
- Escandar, G.M., Gandolfo, F.H. and Sala, L.F., 1990. Complex Formation between Aldonic and Uronic acids and Ferric Ion in Aqueous Solution. *Anal. Asoc. Quim. Argent.*, 78: 37-48.
- Escandar, G.M. et al., 1996. Interaction of Divalent Metal Ions with D-Gluconic Acid in the Solid Phase and Aqueous Solution. *Polyhedron*, 15: 2251-2261.
- Fischer, A.C., Kroon, J.J., Verburg, T.G., Teunissen, T. and Wolterbeek, H.T., 2007. On the relevance of iron adsorption to container materials in small-volume experiments on iron marine chemistry: ⁵⁵Fe-aided assessment of capacity, affinity and kinetics. *marchem*, 107(4): 533-546.
- Fitzwater, S.E., Knauer, G.A. and Martin, J.H., 1982. Metal contamination and its effect on primary production measurements. *Limnology and Oceanography*, 27: 544-551.

- Fridovich, I., 1970. Quantitative Aspects of Production of Superoxide Anion Radical by Milk Xanthine Oxidase*. *The Journal of Biological Chemistry*, 245(16): 4053-4057.
- Fujii, M., Ito, H., Rose, A.L., Waite, T.D. and Omura, T., 2008. Superoxide-mediated Fe(II) formation from organically complexed Fe(III) in coastal waters. *Geochimica et Cosmochimica Acta*, 72(24): 6079-6089.
- Fujii, M., Rose, A.L., Waite, T.D. and Omura, T., 2006. Superoxide-Mediated Dissolution of Amorphous Ferric Oxyhydroxide in Seawater. *Environ. Sci. Technol.*, 40: 880-887.
- Galbusera, C., Orth, P., Fedida, D. and Spector, T., 2006. Superoxide radical production by allopurinol and xanthine oxidase. *Biochemical Pharmacology*, 71(12): 1747-1752.
- Garg, S., Rose, A.L. and Waite, T.D., 2007a. Superoxide-mediated reduction of organically complexed iron(III): Impact of pH and competing cations (Ca^{2+}). *Geochimica Et Cosmochimica Acta*, 71(23): 5620-5634.
- Garg, S., Rose, A.L. and Waite, T.D., 2007b. Superoxide mediated reduction of organically complexed Iron(III): Comparison of non-dissociative and dissociative reduction pathways. *Environmental Science & Technology*, 41(9): 3205-3212.
- Gibbs, C.R., 1976. Characterization and Application of FerroZine Iron Reagent as a Ferrous Iron Indicator. *Analytical Chemistry*, 48: 1197-1201.
- Gledhill, M. et al., 2004. Production of siderophore type chelates by mixed bacterioplankton populations in nutrient enriched seawater incubations. *Marine Chemistry*, 88(1-2): 75-83.
- Godrant, A., Rose, A.L., Sarthou, G. and Waite, T.D., 2009. New method for the determination of extracellular production of superoxide by marine phytoplankton using the chemiluminescence probes MCLA and red-CLA. *Limnol. Oceanogr. Methods* 7: 682-692.
- Goldstone, J.V. and Voelker, B.M., 2000. Chemistry of superoxide radical in seawater: CDOM associated sink of superoxide in coastal waters. *Environmental Science & Technology*, 34(6): 1043-1048.
- Grasshoff, K., Kremling, K. and Ehrhardt, M., 1999. *Methods of Seawater analysis*. Wiley-VCH Verlag, Weinheim (FRG).
- Heller, M.I. and Croot, P.L., 2009. Superoxide Decay Kinetics in the Southern Ocean. *Environmental Science & Technology*: doi: 10.1021/es901766r.
- Heller, M.I. and Croot, P.L., 2010a. Application of a Superoxide (O_2^-) thermal source (SOTS-1) for the determination and calibration of O_2^- fluxes in seawater. submitted to *Analytica Chimica Acta*.

- Heller, M.I. and Croot, P.I., 2010b. The kinetics of Superoxide reactions with dissolved organic matter in Tropical Atlantic surface waters near Cape Verde (TENATSO). submitted to *Journal of Geophysical Research – Oceans*.
- Hodges, G.R., Young, M.J., Paul, T. and Ingold, K.U., 2000. How should xanthine oxidase-generated superoxide yields be measured? *Free Radical Biology and Medicine*, 29(5): 434-441.
- Ilan, Y.A., Czapski, G. and Meisel, D., 1976. One-Electron Transfer Redox Potentials Of Free-Radicals .1. Oxygen-Superoxide System. *Biochimica Et Biophysica Acta*, 430(2): 209-224.
- Ingold, K.U., Paul, T., Young, M.J. and Doiron, L., 1997. Invention of the first azo compound to serve as a superoxide thermal source under physiological conditions: Concept, synthesis, and chemical properties. *Journal of the American Chemical Society*, 119(50): 12364-12365.
- Jickells, T.D. et al., 2005. Global Iron Connections Between Desert Dust, Ocean Biogeochemistry, and Climate. *SCIENCE*, 309: 67-71.
- Johnson, K.S. et al., 2007. Developing Standards for Dissolved Iron in Seawater. *EOS, Transactions of the American Geophysical Union*, 88(11): 131-132.
- Johnson, K.S., Coale, K.H., Elrod, V.A. and Tindale, N.W., 1994. Iron photochemistry in seawater from the equatorial Pacific. *Marine Chemistry*, 46: 319-334.
- Jørgensen, J.Ø. and Holm, P.M., 2002. Temporal variation and carbonate contamination in primitive ocean island volcanics from São Vicente, Cape Verde Islands. *Chemical Geology*, 192(3-4): 249-267.
- Kambayashi, Y. et al., 2003. Formation of Superoxide Anion during Ferrous Ion-Induced Decomposition of Linoleic Acid Hydroperoxide under Aerobic Conditions. *J Biochem*, 134(6): 903-909.
- Karyampudi, V.M. et al., 1999. Validation of the Saharan dust plume conceptual model using lidar, Meteosat, and ECMWF data. *Bulletin of the American Meteorological Society*, 80(6): 1045-1075.
- Kawano, I., Oda, T., Ishimatsu, A. and Muramatsu, T., 1996. Inhibitory effect of the iron chelator Desferrioxamine (Desferal) on the generation of activated oxygen species by *Chattonella marina*. *Marine Biology*, 126: 765-771.
- Kolla, V., Biscaye, P.E. and Hanley, A.F., 1979. Distribution of Quartz in Late Quaternary Atlantic Sediments in Relation to Climate. *Quaternary Research*, 11(2): 261-277.

- Kraemer, S.M., Butler, A., Borer, P. and Cervini-Silva, J., 2005. Siderophores and the dissolution of iron-bearing minerals in marine systems, *Molecular Geomicrobiology. Reviews In Mineralogy & Geochemistry*, pp. 53-84.
- Kremling, K. and Streu, P., 1993. Saharan Dust Influenced Trace-Element Fluxes in Deep North-Atlantic Subtropical Waters. *Deep-Sea Research Part I-Oceanographic Research Papers*, 40(6): 1155-1168.
- Kremling, K. and Streu, P., 2001. The behaviour of dissolved Cd, Co, Zn, and Pb in North Atlantic near-surface waters (30 degrees N/60 degrees W-60 degrees N/2 degrees W). *Deep-Sea Research Part I-Oceanographic Research Papers*, 48(12): 2541-2567.
- Kuehnen, E.C., Alvarez, R., Paulson, P.J. and Murphy, T.J., 1972. Production and analysis of special high purity acids purified by sub-boiling distillation. *Analytical Chemistry*, 44: 2050-2056.
- Kuma, K., Katsumoto, A., Shiga, N., Sawabe, T. and Matsunaga, K., 2000. Variation of size-fractionated Fe concentrations and Fe(III) hydroxide solubilities during a spring phytoplankton bloom in Funka Bay (Japan). *Marine Chemistry*, 71(1-2): 111-123.
- Kuma, K., Nakabayashi, S. and Matsunaga, K., 1995. Photoreduction of Fe(III) by Hydroxycarboxylic acids in seawater. *Water Research*, 29: 1559-1569.
- Kuma, K., Nakabayashi, S., Suzuki, Y., Kudo, I. and Matsunaga, K., 1992. Photo-reduction of Fe (III) by dissolved organic substances and existence of Fe (II) in seawater during spring blooms. *Marine Chemistry*, 37: 15-27.
- Kuma, K., Nishioka, J. and Matsunaga, K., 1996. Controls on iron(III) hydroxide solubility in seawater: The influence of pH and natural organic chelators. *Limnology and Oceanography*, 41(3): 396-407.
- Kunkely, H. and Vogler, A., 2001. Photoreduction of aqueous ferrioxamine B by oxalate induced by outer-sphere charge transfer excitation. *Inorganic Chemistry Communications*, 4(4): 215-217.
- Kustka, A.B., Shaked, Y., Milligan, A.J., King, D.W. and Morel, F.M.M., 2005. Extracellular production of superoxide by marine diatoms: Contrasting effects on iron redox chemistry and bioavailability. *Limnology and Oceanography*, 50(4): 1172-1180.
- Langlois, R.J., LaRoche, J. and Raab, P.A., 2005. Diazotrophic Diversity and Distribution in the Tropical and Subtropical Atlantic Ocean. *Appl. Environ. Microbiol.*, 71(12): 7910-7919.
- Lin, J. and Kester, D.R., 1992. The kinetics of Fe(II) complexation by Ferrozine in seawater. *Marine Chemistry*, 38: 283-301.

- Liu, X. and Millero, F.J., 2002. The solubility of iron in seawater. *Marine Chemistry*, 77: 43-54.
- Lloyd, R.V. and Mason, R.P., 1990. Evidence against Transition Metal-Independent Hydroxyl Radical Generation by Xanthine-Oxidase. *Journal of Biological Chemistry*, 265(28): 16733-16736.
- Mahowald, N.M. et al., 2005. Atmospheric global dust cycle and iron inputs to the ocean. *Global Biogeochemical Cycles*, 19(4): 17.
- Marshall, J.A., de Salas, M., Oda, T. and Hallegraeff, G., 2005. Superoxide production by marine microalgae. *Marine Biology*, 147(2): 533-540.
- Martinez, J.S. et al., 2000. Self-assembling amphiphilic siderophores from marine bacteria. *Science*, 287(5456): 1245-1247.
- Matthews, R.W., 1983. The radiation chemistry of aqueous ferrous sulfate solutions at natural pH. *Australian Journal of Chemistry*, 36: 1305-1317.
- Mawji, E. et al., 2008. Hydroxamate Siderophores: Occurrence and Importance in the Atlantic Ocean. *Environmental Science & Technology*, 42(23): 8675-8680.
- Michaels, A.F. et al., 1996. Inputs, losses and transformations of nitrogen and phosphorus in the pelagic North Atlantic Ocean. *Kluwer Academic Publ*, pp. 181-226.
- Micinski, E., Ball, L.A. and Zafiriou, O.C., 1993. Photochemical Oxygen Activation - Superoxide Radical Detection and Production-Rates in the Eastern Caribbean. *Journal of Geophysical Research-Oceans*, 98(C2): 2299-2306.
- Millero, F.J. and Sotolongo, S., 1989. The oxidation of Fe(II) with H₂O₂ in seawater. *Geochimica et Cosmochimica Acta*, 53: 1867-1873.
- Millero, F.J., Sotolongo, S. and Izaguirre, M., 1987. The oxidation kinetics of Fe(II) in seawater. *Geochimica et Cosmochimica Acta*, 51: 793-801.
- Millero, F.J. et al., 1993. The Use of Buffers to Measure the pH of Seawater, pp. 143-152.
- Mills, M.M., Ridame, C., Davey, M., La Roche, J. and Geider, R.J., 2004. Iron and phosphorus co-limit nitrogen fixation in the eastern tropical North Atlantic. *Nature*, 429(6989): 292-294.
- Milne, A., Davey, M.S., Worsfold, P.J., Achterberg, E.P. and Taylor, A.R., 2009. Real-time detection of reactive oxygen species generation by marine phytoplankton using flow injection-chemiluminescence. *Limnology and Oceanography-Methods*, 7: 706-715.
- Moffett, J.W. and Brand, L.E., 1996. Production of strong, extracellular Cu chelators by marine cyanobacteria in response to Cu stress. *Limnology and Oceanography*, 41(3): 388-395.

- Moffett, J.W. and Dupont, C., 2007. Cu complexation by organic ligands in the sub-arctic NW Pacific and Bering Sea. *Deep-Sea Research Part I-Oceanographic Research Papers*, 54(4): 586-595.
- Moffett, J.W. and Zika, R.G., 1988. Measurement of Copper(I) in Surface Waters of the Sub-Tropical Atlantic and Gulf of Mexico. *Geochimica Et Cosmochimica Acta*, 52(7): 1849-1857.
- Moore, M.C. et al., 2009. Large-scale distribution of Atlantic nitrogen fixation controlled by iron availability. *Nature Geosci*, advance online publication.
- Nakabayashi, S. et al., 2002. Variation in iron(III) solubility and iron concentration in the northwestern North Pacific Ocean. *Limnology and Oceanography*, 47(3): 885-892.
- Nakano, M., 1998. Detection of active oxygen species in biological systems. *Cellular And Molecular Neurobiology*, 18(6): 565-579.
- Neilands, J.B., 1995. Siderophores - Structure And Function Of Microbial Iron Transport Compounds. *Journal Of Biological Chemistry*, 270(45): 26723-26726.
- O'Sullivan, D.W., Neale, P.J., Coffin, R.B., Boyd, J.B. and Osburn, C.L., 2005. Photochemical production of hydrogen peroxide and methylhydroperoxide in coastal waters. *Marine Chemistry*, 97: 14-33.
- Obata, H., Karatani, H. and Nakayama, E., 1993. Automated Determination of Iron in Seawater by Chelating Resin Concentration and Chemiluminescence Detection. *Anal. Chem.*, 65: 1524-1528.
- Obernosterer, I., Ruardij, P. and Herndl, G.J., 2001. Spatial and diurnal dynamics of dissolved organic matter (DOM) fluorescence and H₂O₂ and the photochemical oxygen demand of surface water DOM across the subtropical Atlantic Ocean. *Limnology and Oceanography*, 46(3): 632-643.
- Oosthuizen, M.M.J., Engelbrecht, M.E., Lambrechts, H., Greyling, D. and Levy, R.D., 1997. The effect of pH on chemiluminescence of different probes exposed to superoxide and singlet oxygen generators. *Journal of Bioluminescence and Chemiluminescence*, 12(6): 277-284.
- Öztürk, M. et al., 2004. Iron enrichment and photoreduction of iron under PAR and UV in the presence of hydrocarboxylic acid: Implications for phytoplankton growth in the Southern Ocean. *Deep-Sea Research II*, 51(22-24): 2841-2856.
- Petasne, R.G. and Zika, R.G., 1987. Fate of Superoxide in Coastal Sea-Water. *Nature*, 325(6104): 516-518.

- Porter, J.N., Miller, M., Pietras, C. and Motell, C., 2001. Ship-Based Sun Photometer Measurements Using Microtops Sun Photometers. *Journal of Atmospheric and Oceanic Technology*, 18: 765-774.
- Pronai, L. et al., 1992. Time Course Of Superoxide Generation By Leukocytes-The MCLA Chemiluminescence System. *Inflammation*, 16(5): 437-449.
- Prospero, J.M., 1999. Long-range transport of mineral dust in the global atmosphere: Impact of African dust on the environment of the southeastern United States. *Proceedings of the National Academy of Sciences of the United States of America*, 96(7): 3396-3403.
- Rijkenberg, M.J.A. et al., 2008. Changes in iron speciation following a Saharan dust event in the tropical North Atlantic Ocean. *Marine Chemistry*, 110(1-2): 56-67.
- Rognon, P., CoudeGaussen, G., Revel, M., Grousset, F.E. and Pedemay, P., 1996. Holocene Saharan dust deposition on the Cape Verde islands: Sedimentological and Nd-Sr isotopic evidence. *Sedimentology*, 43(2): 359-366.
- Rose, A.L., Moffett, J.W. and Waite, T.D., 2008. Determination of Superoxide in Seawater Using 2-Methyl-6-(4-methoxyphenyl)-3,7- dihydroimidazo[1,2-a]pyrazin-3(7H)-one Chemiluminescence. *Anal. Chem.*, 80(4): 1215-1227.
- Rose, A.L. and Waite, D., 2006. Role of superoxide in the photochemical reduction of iron in seawater. *Geochimica et Cosmochimica Acta*, 70(15): 3869-3882.
- Rose, A.L. and Waite, T.D., 2002. Kinetic Model for Fe(II) Oxidation in Seawater in the Absence and Presence of Natural Organic Matter. *Environmental Science and Technology*, 36: 433-444.
- Rose, A.L. and Waite, T.D., 2005. Reduction of organically complexed ferric iron by superoxide in a simulated natural water. *Environmental Science & Technology*, 39(8): 2645-2650.
- Rue, E.L. and Bruland, K.W., 1995. Complexation of iron(III) by natural organic ligands in the Central North Pacific as determined by a new competitive ligand equilibration/adsorptive cathodic stripping voltammetric method. *Marine Chemistry* 50: 117-138.
- Rush, J.D. and Bielski, B.H.J., 1985. Pulse Radiolytic Studies of the Reactions of HO_2/O_2^- with Fe(II)/Fe(III) Ions - the Reactivity of HO_2/O_2^- with Ferric Ions and Its Implication on the Occurrence of the Haber-Weiss Reaction. *Journal of Physical Chemistry*, 89(23): 5062-5066.
- Sañudo-Wilhelmy, S.A. et al., 2001. Phosphorus limitation of nitrogen fixation by *Trichodesmium* in the central Atlantic Ocean. *Nature*, 411(6833): 66-69.

- Sayed, R.Z. and Chincholkar, S.B., 2006. Purification of siderophores of *Alcaligenes faecalis* on amberlite XAD. *Bioresource Technology*, 97(8): 1026-1029.
- Schlosser, C. and Croot, P., 2009. Controls on seawater Fe(III) solubility in the Mauritanian upwelling zone. *Geophys. Res. Lett.*, 36: L18606, doi:10.1029/2009GL038963.
- Schlosser, C. and Croot, P.L., 2008. Application of cross-flow filtration for determining the solubility of iron species in open ocean seawater. *Limnology and Oceanography-Methods*, 6: 630-642.
- Schwarzenbach, G. and Schwarzenbach, K., 1963. Hydroxamatkomplexe I. Die Stabilität der Eisen(III)-Komplexe einfacher Hydroxamsäuren und des Ferrioxamins B. *Helvetica Chimica Acta*, 46: 1390-1401.
- Scott, D.T., McKnight, D.M., Blunt-Harris, E.L., Kolesar, S.E. and Lovley, D.R., 1998. Quinone moieties act as electron acceptors in the reduction of humic substances by humics-reducing microorganisms. *Environmental Science & Technology*, 32(19): 2984-2989.
- Sedlak, D.L. and Hoigne, J., 1993. The Role of Copper and Oxalate in the Redox Cycling of Iron in Atmospheric Waters. *Atmospheric Environment Part a-General Topics*, 27(14): 2173-2185.
- Sedwick, P.N., Sholkovitz, E.R. and Church, T.M., 2007. Impact of anthropogenic combustion emissions on the fractional solubility of aerosol iron: Evidence from the Sargasso Sea. *Geochemistry Geophysics Geosystems*, 8: 21.
- Shkarina, E.I. et al., 2001. Effect of Biologically Active Substances on the Antioxidant Activity of Phytopreparations. *Pharmaceutical Chemistry Journal*, 35: 332-339.
- Smirnov, A. et al., 2009. Maritime Aerosol Network (MAN) as a component of AERONET. *Journal of Geophysical Research*, 114: D06204, doi:10.1029/2008JD011257.
- Stookey, L.L., 1970. Ferrozine - A New Spectrophotometric Reagent for Iron. *Analytical Chemistry*, 42: 779-781.
- Stuut, J.B. et al., 2005. Provenance of present-day eolian dust collected off NW Africa. *Journal of Geophysical Research-Atmospheres*, 110(D4): 14.
- Sulzberger, B., 1995. Roles of Photochemically Formed Fe(II) as a Reductant. *Abstracts of Papers of the American Chemical Society*, 210: 47-ENVR.
- Sulzberger, B. and Laubscher, H., 1995. Reactivity of Various Types of Iron(III) (Hydr)Oxides Towards Light-Induced Dissolution. *Marine Chemistry*, 50(1-4): 103-115.
- Swallow, A.J., 1969. Hydrated electrons in seawater. *Nature*, 222: 369-370.

- Talbot, R.W. et al., 1986. Distribution and Geochemistry of Aerosols in the Tropical North-Atlantic Troposphere - Relationship to Saharan Dust. *Journal of Geophysical Research-Atmospheres*, 91(D4): 5173-5182.
- Taylor, R.C. and Cross, P.C., 1949. Light Absorption of Aqueous Hydrogen Peroxide Solutions in the Near Ultraviolet Region'. *Journal of the American Chemical Society*, 71(6): 2266-2268.
- Thompsen, J.C. and Mottola, H.A., 1984. Kinetics of the Complexation of Iron(II) with Ferrozine. *Analytical Chemistry*, 56: 755-757.
- Tyrrell, T. et al., 2003. Large-scale latitudinal distribution of *Trichodesmium* spp. in the Atlantic Ocean. *J. Plankton Res.*, 25(4): 405-416.
- Voelker, B.M., Morel, F.M.M. and Sulzberger, B., 1997. Iron redox cycling in surface waters: Effects of humic substances and light. *Environmental Science & Technology*, 31(4): 1004-1011.
- Voelker, B.M. and Sedlak, D.L., 1995. Iron Reduction by Photoproduced Superoxide in Seawater. *Marine Chemistry*, 50(1-4): 93-102.
- Voelker, B.M., Sedlak, D.L. and Zafiriou, O.C., 2000. Chemistry of Superoxide Radical in Seawater: Reactions with Organic Cu Complexes. *Environmental Science and Technology*, 34: 1036-1042.
- Voelker, B.M. and Sulzberger, B., 1996. Effects of fulvic acid on Fe(II) oxidation by hydrogen peroxide. *Environmental Science & Technology*, 30(4): 1106-1114.
- Volker, C. and Wolf-Gladrow, D.A., 1999. Physical limits on iron uptake mediated by siderophores or surface reductases. *Marine Chemistry*, 65(3-4): 227-244.
- Von Sonntag, C. and Schuchmann, H.P., 1991. The Elucidation of Peroxyl Radical Reactions in Aqueous-Solution with the Help of Radiation-Chemical Methods. *Angewandte Chemie-International Edition in English*, 30(10): 1229-1253.
- Voss, M., Croot, P., Lochte, K., Mills, M. and Peeken, I., 2004. Patterns of Nitrogen Fixation along 10°N in the Tropical Atlantic. *Geophysical Research Letters*, 31: L23S09, doi:10.1029/2004GL020127.
- Wagener, T., Pulido-Villena, E. and Guieu, C., 2008. Dust iron dissolution in seawater: Results from a one-year time-series in the Mediterranean Sea. *Geophysical Research Letters*, 35(16).
- Weinstein, J. and Bielski, B.H.J., 1979. Kinetics of the Interaction of HO₂ and O₂-Radicals with Hydrogen-Peroxide - Haber-Weiss Reaction. *Journal of the American Chemical Society*, 101(1): 58-62.

- Wu, J., Boyle, E., Sunda, W. and Wen, L.-S., 2001. Soluble and Colloidal Iron in the Oligotrophic North Atlantic and North Pacific. *Science*, 293: 847-849.
- Yocis, B.H., Kieber, D.J. and Mopper, K., 2000. Photochemical production of hydrogen peroxide in Antarctic Waters,. *Deep Sea Research Part I : Oceanographic Research*, 47(6): 1077-1099.
- Yuan, J. and Shiller, A.M., 2001. The distribution of hydrogen peroxide in the southern and central Atlantic ocean. *Deep-Sea Research II*, 48: 2947-2970.
- Zafiriou, O.C., 1990. Chemistry of Superoxide Ion-Radical (O_2^-) in Seawater .I. $pK^*_{a_{sw}}(HOO)$ and Uncatalyzed Dismutation Kinetics Studied by Pulse-Radiolysis. *Marine Chemistry*, 30(1-3): 31-43.
- Zafiriou, O.C., Voelker, B.M. and Sedlak, D.L., 1998. Chemistry of the superoxide radical (O_2^-) in seawater: Reactions with inorganic copper complexes. *Journal Of Physical Chemistry A*, 102(28): 5693-5700.

Figure legends.

Figure 1: Schematic of proposed reaction pathways for the dissolution of Saharan dust in surface seawater, incorporating the ligand promoted dissolution of iron from the dust and including reactions between superoxide with dust and Fe.

Figure 2: Location of the sampling stations occupied during this work in the vicinity of the Cape Verde archipelago. The location of the TENATSO ocean observatory (orange hexagon) is also shown for reference.

Figure 3: Sampling methodology used in the incubation experiments for assessing the impact of dust dissolution on the decay kinetics of O_2^- .

Figure 4: Iron solubility experiments (0.02 μm Anotop 25) conducted in seawater (collected during M68-3 in the Eastern Tropical Atlantic) with the radioisotope ^{55}Fe . (top left) Concentration of soluble iron as a function of time in the presence of 2 nM of the strong Fe complexing siderophore DFO. (top right) Soluble iron in the presence of 2 nM DFO with O_2^- produced enzymatically with the xanthine/xanthine oxidase system (50 μM Xanthine and 1 unit L^{-1} Xanthine Oxidase). (bottom right) Soluble iron in the presence of O_2^- but without DFO. (bottom left) Control experiment in the presence of 50 μM xanthine only.

Figure 5: Laboratory dust dissolution experiment utilizing O_2^- production with the superoxide thermal source SOTS-1. (left) Fe(II) formation from the added dust (8 mg in 1 L) in the presence (red circles) or absence (blue triangles) of SOTS-1. The Fe(II) was trapped with 1 mM Ferrozine (Fz) and detected spectrophotometrically. (right) Log transformed data showing the relationship between the decay rate of SOTS-1 and the Fe(II) formation rate.

Figure 6: (left) Comparison between Fe titrations of seawater and seawater with Ferrozine (160 μM). (right) Comparison between Cu titrations of seawater and seawater with Neocuproine (380 μM). The experiments in seawater without chelator could only be followed until a Cu content of 1.57nM as with higher Cu additions the reaction was too fast to be determined.

Figure 7: Titration data for Cu and Fe from experiment 8 after 24 hours incubation showing the influence of the iron chelator DFO on k_{obs} . Data from the 3 experimental treatments are

shown: Seawater samples with no DFO (circles), seawater with 2.5 nM DFO added (triangles) and seawater with 5 nM DFO (diamonds). The DTPA amended samples are also shown in each figure as the value at a metal concentration 0. (left) Cu titration data. The least squares regression fit to the non-DTPA amended data are also shown. In all cases $R^2 > 0.95$ and the corresponding k_{Cu} is displayed. (right) Fe titration data. The least squares regression fit to the non-DTPA amended data are also shown for comparison only as the fits were poor in all cases ($R^2 < 0.4$).

Figure 8: Total dissolvable iron concentrations in the 4 experiments performed in July 2008 in the different sample treatments after 24 (green bars) and 48 hours (blue bars). For a full description of the experimental setup please refer to the text.

Figure 9: (left) Time variation in k_{obs} for the seawater plus dust treatment from experiments 1 (circles) and 2 (triangles) performed in July 2008. (right) Time variation in k_{obs} for the seawater plus dust treatment from experiments 3 (diamonds) and 4 (squares) also performed in July 2008. The error bars to the values of k_{obs} are contained within the size of the symbol. The data presented here is for the seawater only samples, no DTPA or metals added.

Figure 10: Time course of k_{obs} for all of the treatments in experiment 9 performed in May 2009. Treatments included: A no dust addition control (circles), a +8 mg dust addition (triangles), a +16 mg dust addition (diamonds), and a +8 mg dust addition that was kept in the dark for the duration of the experiment (squares). The error bars to the values of k_{obs} are contained within the size of the symbol. The gray vertical bars indicate the night hours during the experiment.

Figure 11: Time course for calculated values of k_{Cu} and k_{Fe} from experiment 9 showing evidence for the presence of natural Fe chelators that did not react with O_2^- . Treatments included: A no dust addition control (circles), a +8 mg dust addition (triangles), a +16 mg dust addition (diamonds), and a +8 mg dust addition that was kept in the dark for the duration of the experiment (squares). (left) $\log k_{Fe}$ values calculated during experiment 9 (right). $\log k_{Cu}$ values calculated during experiment 9. Note that the minimum value determinable in our work for k_{Cu} and k_{Fe} is $10^6 M^{-1} s^{-1}$ and this is shown as a dotted line in the figure. The gray vertical bars indicate the night hours during the experiment.

Figure 12: Time course showing the variation in k_{org} , the organic reaction with O_2^- measured using DTPA amended seawater samples, for all treatments (control – circles, dust addition – triangles, dust addition with 1 nM desferrioxamine B – diamonds, dust addition with 1 μM Gluconic acid - squares) from (left) Station 1 and (right) Station 4. The error bars to the values of k_{org} are contained within the size of the symbol.

Figure 13: Time course showing the variation in k_{org} , the organic reaction with O_2^- measured using DTPA amended seawater samples, from experiment 9. Treatments included: A no dust addition control (circles), a +8 mg dust addition (triangles), a +16 mg dust addition (diamonds), and a +8 mg dust addition that was kept in the dark for the duration of the experiment (squares). The error bars to the values of k_{org} are contained within the size of the symbol. The gray vertical bars indicate the night hours during the experiment.

Table 1: Date and location of the filtered (0.2 μm) surface seawater samples used in this study for incubation experiments. All samples were obtained in the vicinity of Sao Vicente, Cape Verde with the R.V. *Islandia*. All treatments were run in duplicate.

Date ¹	Station/		Cu ² nM	Fe ³ nM	Treatment Bottle 1	Treatment Bottle 2	Treatment Bottle 3	Treatment Bottle 4	
	Experiment	Latitude N							Longitude W
15.07.08	1	16°46'	25°70'	0.90	4.62	SW	SW+Dust	SW+Dust +1nM DFO	SW+Dust+1 μM GluAc
20.07.08	2	17°04'	24°51'	2.12	2.94	SW	SW+Dust	SW+Dust +1nM DFO	SW+Dust+1 μM GluAc
24.07.08	3	17°04'	24°49'	1.81	2.11	SW	SW+Dust	SW+Dust +1nM DFO	SW+Dust+1 μM GluAc
29.07.08	4	17°14'	24°38'	1.15	1.10	SW	SW+Dust	SW+Dust +1nM DFO	SW+Dust+1 μM GluAc
19.05.09	8	17°12'	24°28'	-	-	SW	SW+2.5nM DFO	SW+5nM DFO	-
23.05.09	9	16°46'	25°09'	0.87	1.20	SW	SW+Dust	SW++Dus t ⁴	SW+Dust (Dark) ⁵

Notes: ¹Samples were collected at sea on this date in the early evening, returned to the INDP in Mindelo and the experimental treatments placed in the incubators pre dawn on the following day. The experiment then ran for 48 hours. ²Dissolved Cu concentration measured in the initial sample. ³Dissolved Fe concentration measured in the initial sample. ⁴Dust additions were with 8.0 ± 0.1 mg per 4.5 L seawater, with the exception of experiment 9 were treatment 3 consisted of 16.0 ± 0.1 mg per 4.5 L seawater. ⁵Samples in this treatment were kept in the dark throughout the experiment.

Fe Redox cycling in the Tropical Atlantic: Saharan Dust impacts

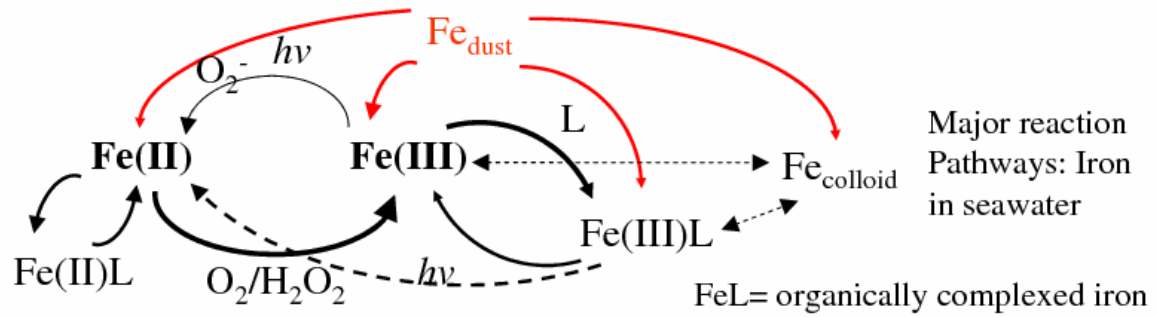


Figure 1: Schematic of proposed reaction pathways for the dissolution of Saharan dust in surface seawater, incorporating the ligand promoted dissolution of iron from the dust and including reactions between superoxide with dust and Fe.

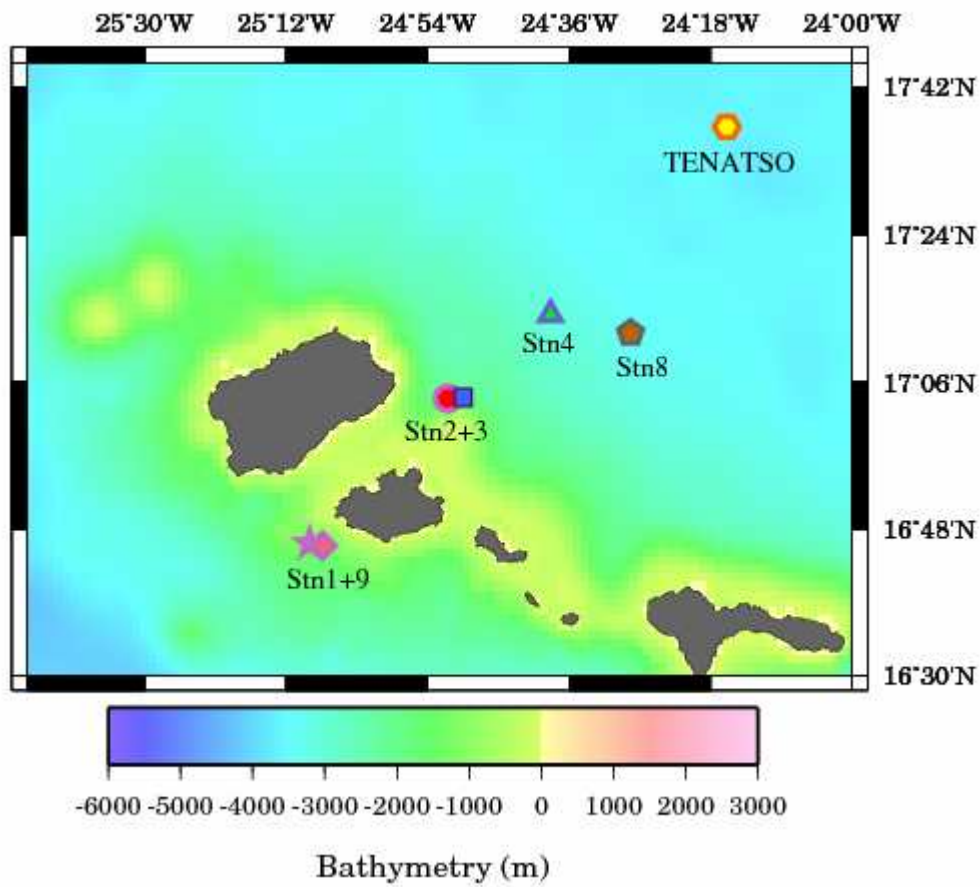


Figure 2: Location of the sampling stations occupied during this work in the vicinity of the Cape Verde archipelago. The location of the TENATSO ocean observatory (orange hexagon) is also shown for reference.

Sampling Methodology: Superoxide Kinetic Reactivity Cape Verde

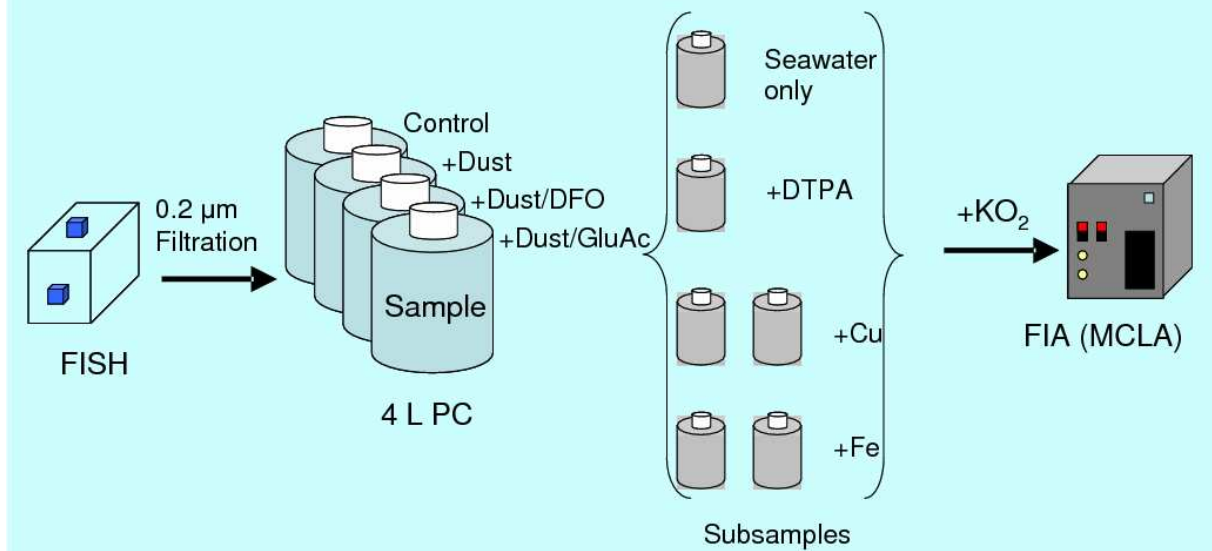


Figure 3: Sampling methodology used in the incubation experiments for assessing the impact of dust dissolution on the decay kinetics of O₂⁻.

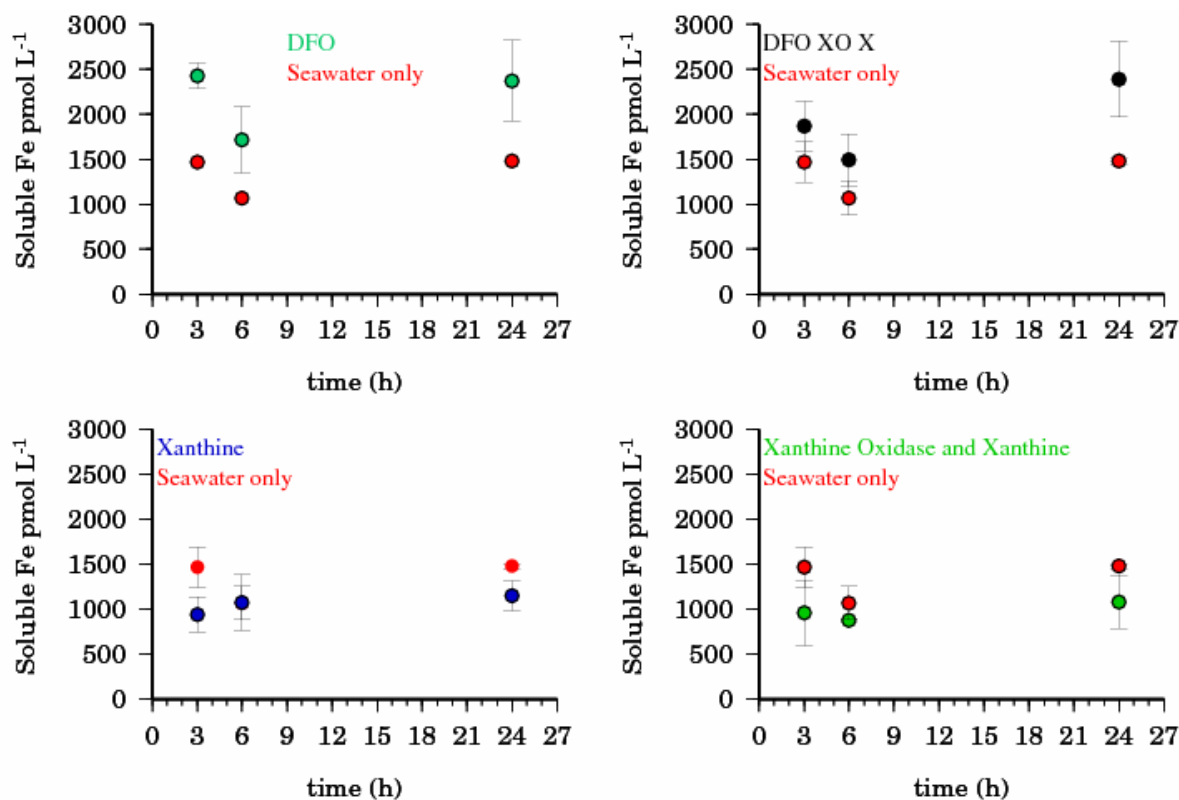


Figure 4: Iron solubility experiments (0.02 μm Anotop 25) conducted in seawater (collected during M68-3 in the Eastern Tropical Atlantic) with the radioisotope ⁵⁵Fe. (top left) Concentration of soluble iron as a function of time in the presence of 2 nM of the strong Fe complexing siderophore DFO. (top right) Soluble iron in the presence of 2 nM DFO with O₂⁻ produced enzymatically with the xanthine/xanthine oxidase system (50 μM Xanthine and 1 unit L⁻¹ Xanthine Oxidase). (bottom right) Soluble iron in the presence of O₂⁻ but without DFO. (bottom left) Control experiment in the presence of 50 μM xanthine only.

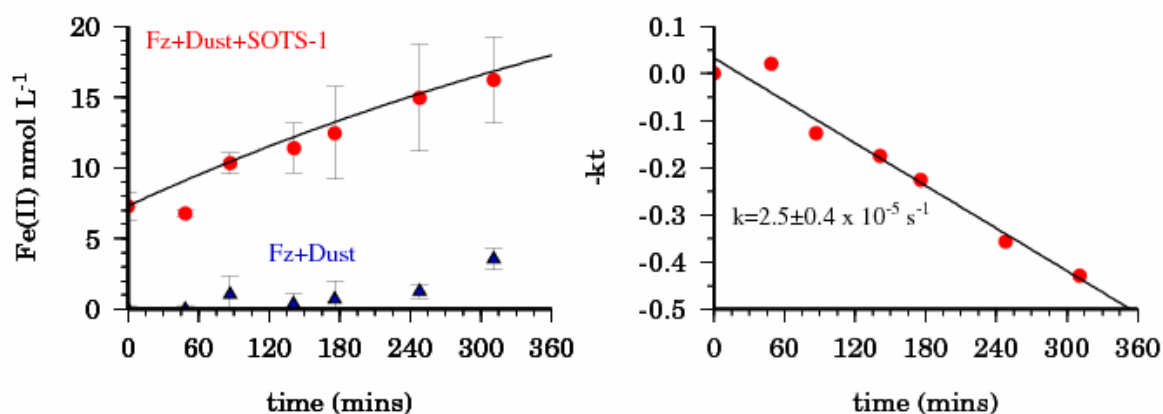


Figure 5: Laboratory dust dissolution experiment utilizing O_2^- production with the superoxide thermal source SOTS-1. (left) Fe(II) formation from the added dust (8 mg in 1 L) in the presence (red circles) or absence (blue triangles) of SOTS-1. The Fe(II) was trapped with 1 mM Ferrozine (Fz) and detected spectrophotometrically. (right) Log transformed data showing the relationship between the decay rate of SOTS-1 and the Fe(II) formation rate.

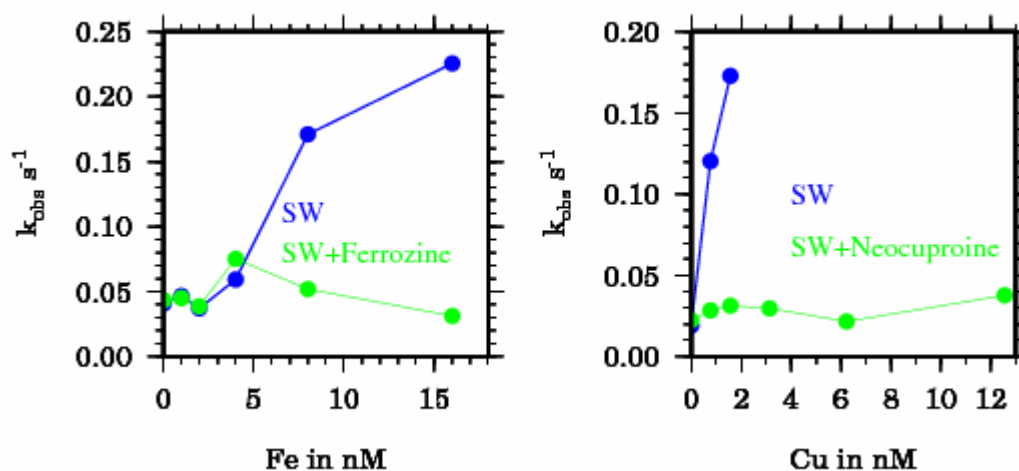


Figure 6: (left) Comparison between Fe titrations of seawater and seawater with Ferrozine (160 μ M). (right) Comparison between Cu titrations of seawater and seawater with Neocuproine (380 μ M). The experiments in seawater without chelator could only be followed until a Cu content of 1.57nM as with higher Cu additions the reaction was too fast to be determined.

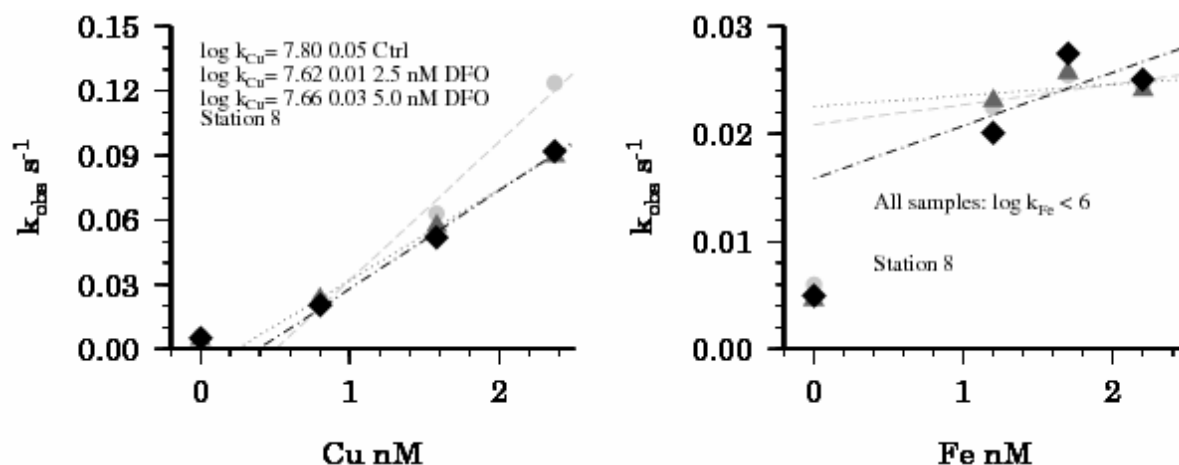


Figure 7: Titration data for Cu and Fe from experiment 8 after 24 hours incubation showing the influence of the iron chelator DFO on k_{obs} . Data from the 3 experimental treatments are shown: Seawater samples with no DFO (circles), seawater with 2.5 nM DFO added (triangles) and seawater with 5 nM DFO (diamonds). The DTPA amended samples are also shown in each figure as the value at a metal concentration 0. (left) Cu titration data. The least squares regression fit to the non-DTPA amended data are also shown. In all cases $R^2 > 0.95$ and the corresponding k_{Cu} is displayed. (right) Fe titration data. The least squares regression fit to the non-DTPA amended data are also shown for comparison only as the fits were poor in all cases ($R^2 < 0.4$).

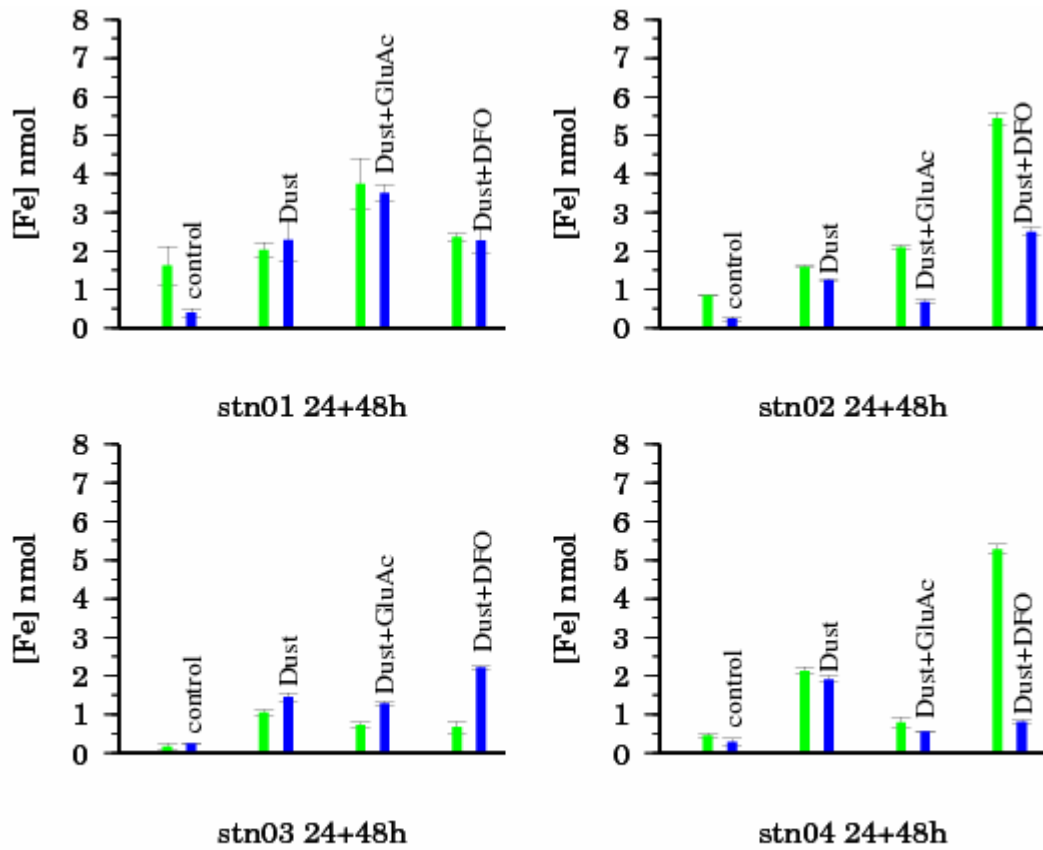


Figure 8: Total dissolvable iron concentrations in the 4 experiments performed in July 2008 in the different sample treatments after 24 (green bars) and 48 hours (blue bars). For a full description of the experimental setup please refer to the text.

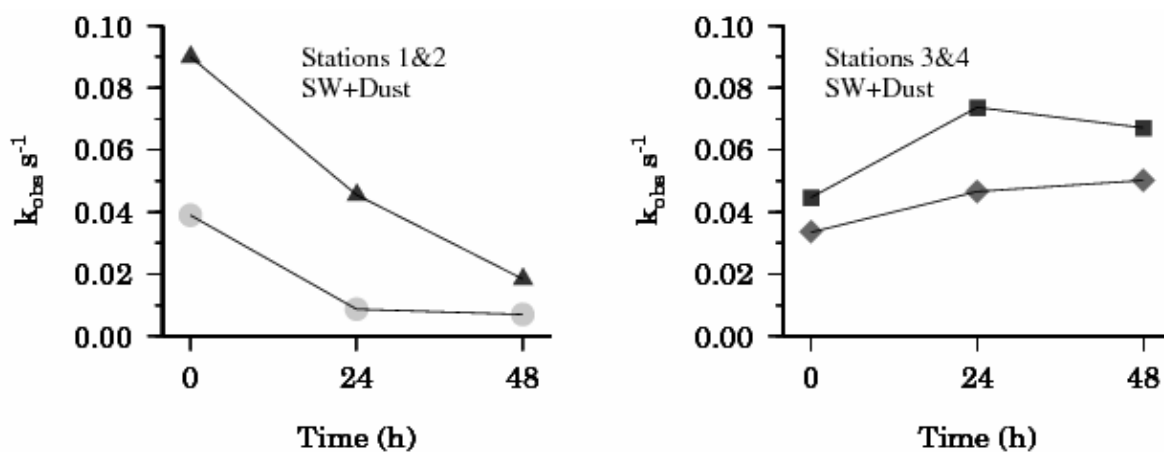


Figure 9: (left) Time variation in k_{obs} for the seawater plus dust treatment from experiments 1 (circles) and 2 (triangles) performed in July 2008. (right) Time variation in k_{obs} for the seawater plus dust treatment from experiments 3 (diamonds) and 4 (squares) also performed in July 2008. The error bars to the values of k_{obs} are contained within the size of the symbol. The data presented here is for the seawater only samples, no DTPA or metals added.

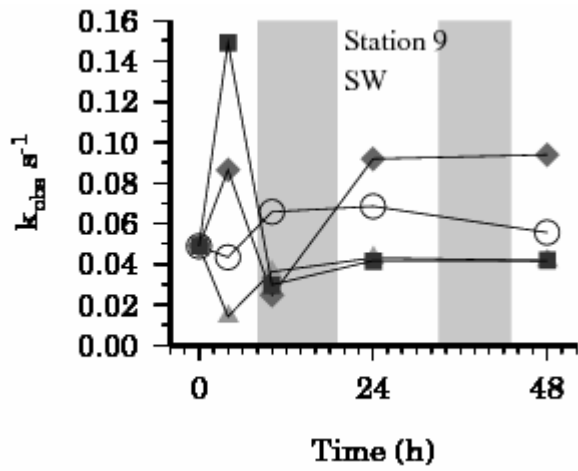


Figure 10: Time course of k_{obs} for all of the treatments in experiment 9 performed in May 2009. Treatments included: A no dust addition control (circles), a +8 mg dust addition (triangles), a +16 mg dust addition (diamonds), and a +8 mg dust addition that was kept in the dark for the duration of the experiment (squares). The error bars to the values of k_{obs} are contained within the size of the symbol. The gray vertical bars indicate the night hours during the experiment.

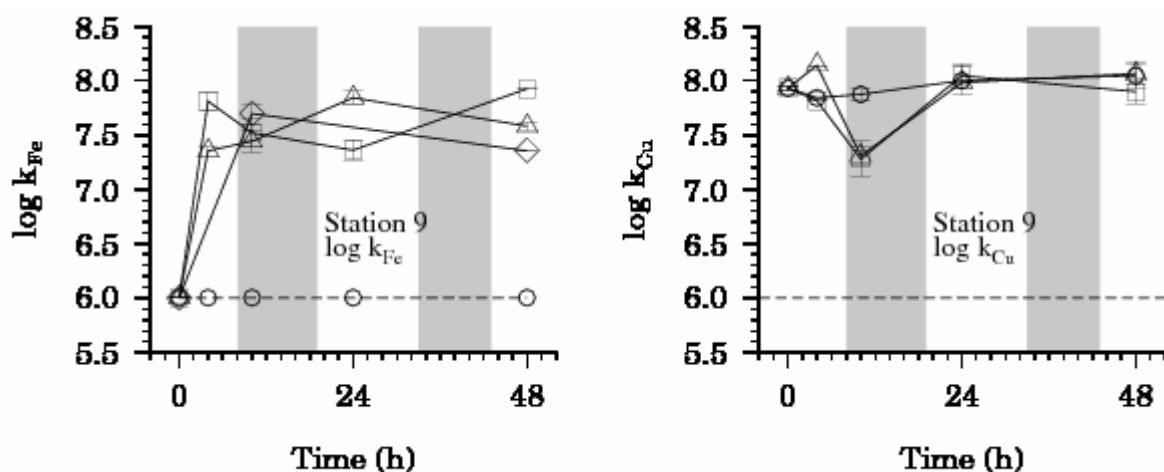


Figure 11: Time course for calculated values of k_{Cu} and k_{Fe} from experiment 9 showing evidence for the presence of natural Fe chelators that did not react with O_2^- . Treatments included: A no dust addition control (circles), a +8 mg dust addition (triangles), a +16 mg dust addition (diamonds), and a +8 mg dust addition that was kept in the dark for the duration of the experiment (squares). (left) $\log k_{Fe}$ values calculated during experiment 9 (right). Log k_{Cu} values calculated during experiment 9. Note that the minimum value determinable in our work for k_{Cu} and k_{Fe} is $10^6 M^{-1} s^{-1}$ and this is shown as a dotted line in the figure. The gray vertical bars indicate the night hours during the experiment.

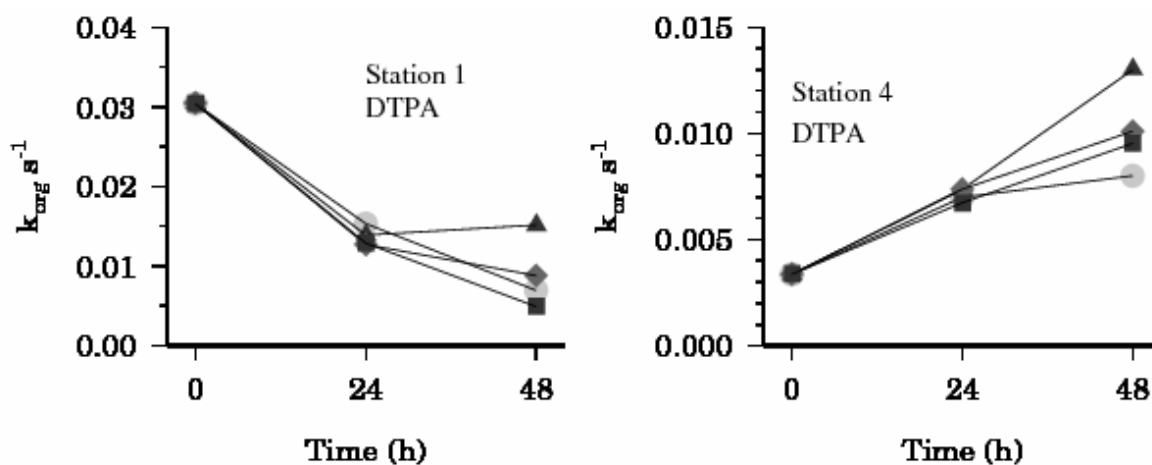


Figure 12: Time course showing the variation in k_{org} , the organic reaction with O_2^- measured using DTPA amended seawater samples, for all treatments (control – circles, dust addition – triangles, dust addition with 1 nM desferrioxamine B – diamonds, dust addition with 1 μM Gluconic acid - squares) from (left) Station 1 and (right) Station 4. The error bars to the values of k_{org} are contained within the size of the symbol.

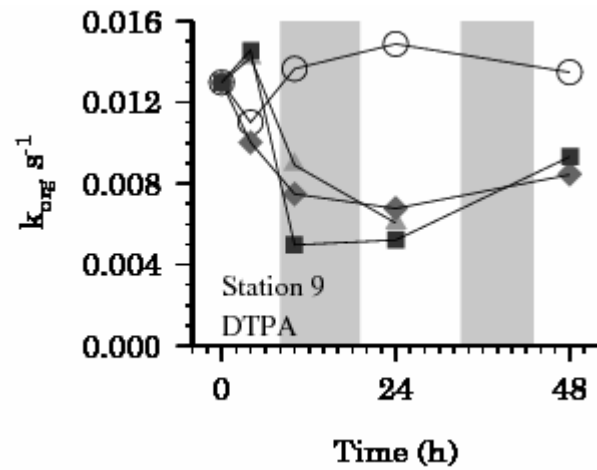


Figure 13: Time course showing the variation in k_{org} , the organic reaction with O_2^- measured using DTPA amended seawater samples, from experiment 9. Treatments included: A no dust addition control (circles), a +8 mg dust addition (triangles), a +16 mg dust addition (diamonds), and a +8 mg dust addition that was kept in the dark for the duration of the experiment (squares). The error bars to the values of k_{org} are contained within the size of the symbol. The gray vertical bars indicate the night hours during the experiment.

Superoxide Decay Kinetics in the Southern Ocean

Heller, M.I. and Croot, P.L.

Superoxide Decay Kinetics in the Southern Ocean

MAIJA I. HELLER AND PETER L. CROOT*

FB2 Marine Biogeochemistry, Chemical Oceanography,
Leibniz Institut für Meereswissenschaften (IFM-GEOMAR),
Kiel D-24105, Germany

Received June 17, 2009. Revised manuscript received
September 27, 2009. Accepted September 30, 2009.

Measurements of superoxide (O_2^-) reaction kinetics were made during a transect with the research icebreaker Polarstern (ANT24-3) in the Antarctic through the Drake Passage in austral autumn 2008. Our sampling strategy was designed to investigate the sinks of superoxide in Polar waters; principally through reactions with dissolved organic matter (DOM) or metals (copper and iron). We modified an existing chemiluminescence flow injection system using methyl *Cypridina* luciferin analog (MCLA) for the detection of O_2^- and added O_2^- using KO_2 as the source. Our results indicate that O_2^- in ambient seawater had a half-life ranging from 9.3 to 194 s. DTPA additions to seawater, to remove the effects of reactions with metals, revealed O_2^- decay rates consistent with a second order reaction, indicating that the dismutation reaction dominated and that reactions with DOM were not significant. Titrations of seawater by the addition of nanomolar amounts of iron or copper revealed the importance of organic chelation of Fe and/or Cu in controlling the reactivity with O_2^- . Throughout the water column reactions with Cu appeared to be the major sink for superoxide in the Southern Ocean. This new strategy suggests an alternative approach for speciation measurements of Fe and Cu in seawater.

Introduction

The superoxide (O_2^-) radical is potentially an important species involved in the redox cycling of metal ions in natural waters (1–4). In sunlit surface waters O_2^- is a major product of the photo-oxidation of colored dissolved organic matter (CDOM) (5) and can also be produced by metabolic processes in phytoplankton (6, 7). Inorganic complexes of Cu(II)/Cu(I) and Fe(II)/Fe(III) can react rapidly with superoxide (Table S1 Supporting Information) leading to a catalytic cycle for superoxide decay (2).

To assess the effect of superoxide on metal redox cycling it is necessary to understand both the rates of production and destruction. There are few direct measurements of superoxide production rates from the open ocean, with single studies published on photoproduction (5) and nonphotochemical production (8). However, studies of H_2O_2 photoproduction are available and provide a reasonable estimate of the major O_2^- source in the ocean (9). Several reactions have been identified in seawater that could control superoxide decay rates and these principally include the following: (i) the second-order uncatalyzed dismutation reaction of superoxide with its conjugate acid (9); (ii) reactions with Cu species in seawater (2, 3); (iii) reactions with Fe species in

seawater (1, 4, 10); and (iv) reactions with CDOM or other organic matter (11). These pathways for superoxide decay are summarized in Figure S1.

Earlier work by Voelker and colleagues (1–3, 11) found that organically complexed Cu was a far more important sink for superoxide than the dismutation reaction and that reactions with Cu complexes could represent a significant source of Cu(I). Other workers have also suggested that superoxide could play a role in maintaining a significant concentration of Fe(II) in seawater (10, 12, 13) by reduction of inorganic or organically complexed iron.

The aim of the present work was to measure the decay kinetics of superoxide in Antarctic seawater from the Drake Passage to assess the sinks for superoxide and related effects on metal speciation in these waters. We examined here the role of natural Fe and Cu complexes in open ocean seawater to act as catalytic O_2^- sinks by relating the decay rate of O_2^- to Cu and Fe concentrations and speciation. O_2^- was added as KO_2 to ambient, DTPA-complexed, and trace-metal-amended seawater samples from a range of depths throughout the water column and the decay of O_2^- was followed by a chemiluminescence technique.

Experimental Section

Complete descriptions of the experimental methods can be found in the Supporting Information (SI) accompanying this manuscript.

pH Measurements. In the present work we report seawater pH values using the total hydrogen scale (pH_{TOT}) (14) while we use the NBS scale, pH_{NBS} , for pH measurements of buffers and other low ionic strength solutions. All pH measurements were made using a WTW pH meter 330i calibrated with Tris buffers (15).

Reagents. All reagents were prepared using 18M Ω cm resistivity water (hereafter MQ water) supplied by a combination of an ELIX-3 and Synergy 185 water systems (Millipore). High-purity HCl (6 M, hereafter abbreviated to Q-HCl) was made by redistillation of Merck trace-metal grade acids in a quartz sub-boiling still (16). MCLA ([2-methyl-6-(4-methoxyphenyl)-3,7-dihydroimidazo[1,2-a]pyrazin-3-one, HCl]) (Fluka) was used as received. A primary MCLA standard, 1 mM MCLA, was prepared by dissolving 10 mg of MCLA in 34.5 mL of MQ water; 1-mL aliquots of this solution were then pipetted into polyethylene vials and frozen at -80°C until required for use. The working MCLA standard, 1 μM , was prepared from a thawed vial of the primary stock by dilution into 1 L of MQ water. This solution was buffered in 0.05 M sodium acetate and adjusted to pH_{NBS} of 6 with Q-HCl. A 3.8 mM stock solution of diethylenetriaminepentaacetic acid (DTPA) was made up by dissolving 0.6 g in 400 mL of MQ water. A working Cu(II) standard (0.1 ppm) was prepared by serial dilution of the primary (1000 ppm) in MQ water with 1% 6 M Q-HCl. A 10 mM Fe(III) primary stock solution was prepared from $FeCl_3 \cdot 6H_2O$ (Sigma) in MQ water with 1% 6 M Q-HCl. A working iron standard solution (1 μM) was prepared from the primary stock solution, diluted with MQ water, and acidified with 1% 6 M Q-HCl. For each experiment a fresh superoxide stock was prepared in a trace-metal-clean dark glass bottle by adding a specific amount (8–10 mg) of potassium superoxide, KO_2 , to a 0.05 M NaOH solution (CAUTION: KO_2 is explosive and must be handled with care). This pH ensured a relatively stable superoxide source concentration over the time frame of the experiment (half-life approximately 3 h). In the present manuscript we report seawater pH values using the total hydrogen scale (pH_{TOT})

* Corresponding author e-mail: pcroot@ifm-geomar.de.

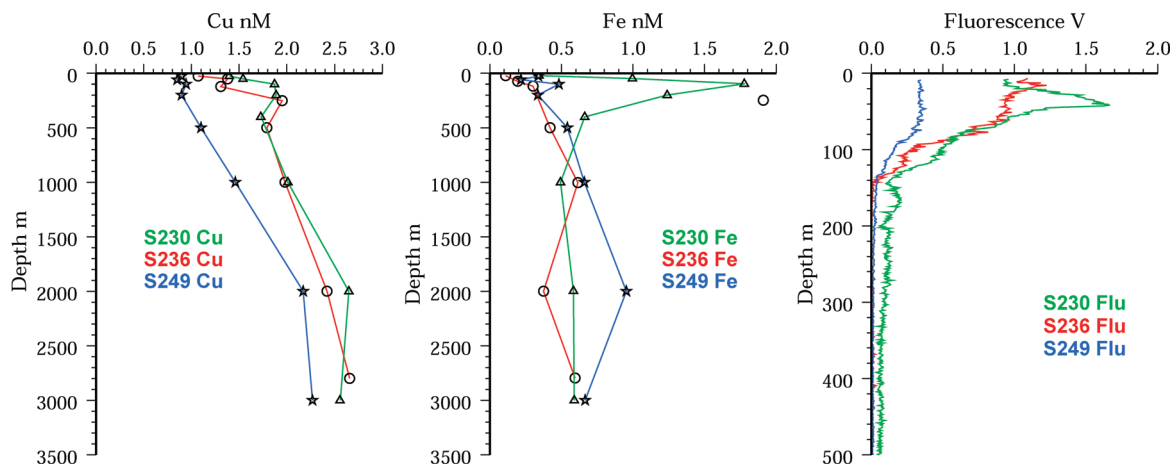


FIGURE 1. Dissolved metal data from stations in the Drake Passage: (left) copper, (center) iron, and (right) arbitrary chlorophyll fluorescence (volts).

(14) All plasticware used in this work was extensively acid cleaned before use.

Superoxide Measurement Technique and Apparatus. For this work, we adapted an existing chemiluminescence analysis method for superoxide which utilizes the reagent MCLA (17–20). The mechanism and specificity for the reaction of MCLA and O_2^- is well described (21). Our method is not substantially different from that recently published by Rose et al. (22) in which they also used a commercially available flow injection system (FeLume - developed by Whitney King at Colby College, Waterville, ME). All measurements were performed onboard the research icebreaker Polarstern in a Class 100 Clean Container at 23 °C. For full details of this method the reader is referred to the SI.

Reaction Kinetics. Our experimental design was based on previous research on superoxide reactions with Cu complexes (2) and organic matter (11) with the inclusion of reactions with Fe (23, 24). In this scheme the reactivity of O_2^- is determined by the following reactions:

$$\frac{\partial [O_2^-]}{\partial t} = 2k_2[O_2^-]^2 + \sum k_M[M]_X[O_2^-] + k_{org}[O_2^-] \quad (1)$$

where k_2 is the second-order uncatalyzed dismutation rate constant and the rate constant for the metal reactions (k_M) includes both the Cu(II)/Cu(I) and Fe(III)/Fe(II) redox pairs, the reaction with organic substances is described by the first order rate k_{org} .

$$\sum k_M[M]_X = (k_{Cu(I)}[Cu(I)] + k_{Cu(II)}[Cu(II)] + k_{Fe(II)}[Fe(II)] + k_{Fe(III)}[Fe(III)]) \quad (2)$$

The observed rate of superoxide decay can then be written as follows with only a single term each for the first-order and second-order rate components

$$\frac{\partial [O_2^-]}{\partial t} = -2k_2[O_2^-]^2 - k_{obs}[O_2^-] \quad (3)$$

where k_{obs} is described as the sum of the first order reaction rates.

$$k_{obs} = \sum k_M[M]_X + k_{org} \quad (4)$$

In the samples with added DTPA it is assumed that $k_{obs} = k_{org}$ (11). For full details of the numerical methods used to solve k_2 and k_{obs} simultaneously see the SI.

Field Measurements of Superoxide Reaction Rates in Seawater. Our approach is based on measuring the decay rate of known quantities of added O_2^- (as KO_2) to seawater. O_2^- is detected via its chemiluminescence reaction with MCLA (see above). The experimental setup consists of a minimum of 6 experimental treatments: (i) control, reaction with unmodified seawater; (ii) metal-free reaction, achieved by complexation of trace metals in solution with DTPA, this reactivity measured here then only corresponds to reactions mechanism 1 and 2 shown above; (iii and iv) addition of Cu(II) to the seawater to form a titration series with the control, this approach was also used in a previous study (2); (v and vi) addition of Fe(III) to the seawater to form a titration series with the control (see Figure S3).

For each experiment 6 depths from throughout the water column were sampled. From each depth six 60-mL Teflon bottles were filled with 40 mL of the fresh collected seawater. One was spiked with DTPA (3.8 μ M), two were spiked with Cu (0.85 nM, 1.7 nM), two were spiked with Fe (1 nM, 2 nM), and one was left with seawater only. Metal additions were left to equilibrate for 3 h, while DTPA samples were left overnight (12 h). After equilibration, 20 μ L of a freshly prepared KO_2 solution ($\sim 100 \mu$ M O_2^- as checked by UV spectrophotometry and corrected for H_2O_2 absorbance) was added to the samples and immediately injected in the flow injection system where the chemiluminescence signal was detected and followed for up to 5 min. Full details of the data analysis methods used can be found in the SI.

Results

Measurements of total dissolved Cu and Fe and the chlorophyll fluorescence at the stations occupied in the Drake Passage are shown in Figure 1. Dissolved Cu increased monotonically with depth as has been seen previously in this region (25). Profiles of dissolved Fe also increased with depth with the exception of station 230 where an iron-rich plume originating from the Antarctic Peninsula could be clearly observed from the surface to 500 m. This iron rich plume was coincident with enhanced chlorophyll with the highest levels found closest to the Antarctic Peninsula (Figure 1) at station 230.

In all experiments the decay of O_2^- in natural seawater was predominantly first order with k_{obs} ranging from 0.004 to 0.074 s^{-1} (Tables S3–S4). In the vertical profiles there was a clear minimum in k_{obs} in the depth range 50–75 m which was the lower part of the mixed layer but still within the euphotic zone (Figure 1). For samples with added DTPA, the observed decay was strongly second-order and did not fit a

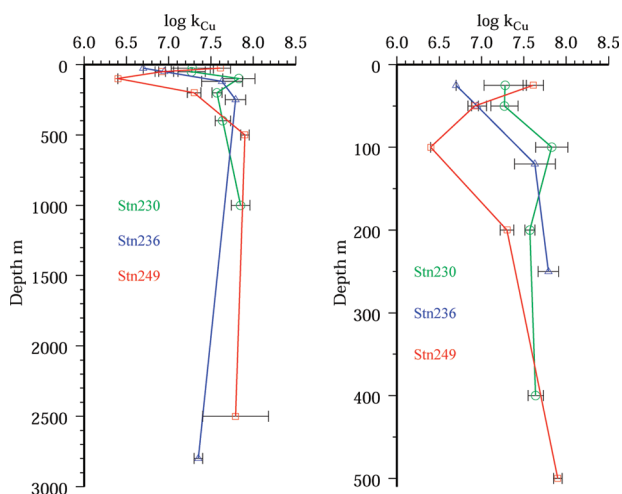


FIGURE 2. Calculated Cu reaction rates (k_{Cu} , $\text{M}^{-1} \text{s}^{-1}$) with superoxide in the Drake Passage, Station 230 (green, circles), Station 236 (blue, triangles), and Station 249 (red, squares): (left) full depth range; (right) top 500 m of the profile. Error bars represent the 95% confidence intervals.

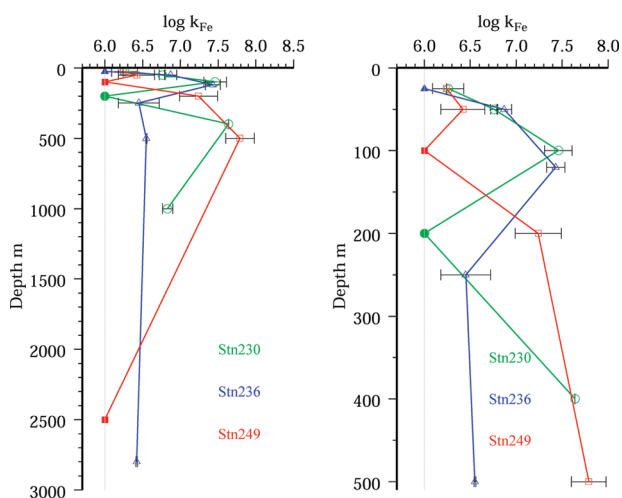


FIGURE 3. Calculated Fe reaction rates (k_{Fe} , $\text{M}^{-1} \text{s}^{-1}$) with superoxide in the Drake Passage, Station 230 (green, circles), Station 236 (blue, triangles), and Station 249 (red, squares): (left) full depth range; (right) top 500 m of the profile. Closed symbols indicate the value was below the detection limit of $\log k_{\text{Fe}} = 6$. Error bars represent the 95% confidence intervals.

first-order decay curve. Second-order rate constants were fitted by simultaneous estimation of the MCLA sensitivity and rate data (see SI) for each experimental run (Tables S3–S4). In only a few DTPA-amended samples, from intermediate depths (200–500 m) and from the near surface close to the Antarctic Peninsula (Station 230), were significant first-order components detectable.

The addition of Cu and Fe to seawater increased the rate of superoxide decay (Figure S7); in general this effect was more pronounced below 500 m and with added Cu. For many samples from the euphotic zone (0–120 m) the addition of Cu or Fe did not appreciably change the rate of superoxide decay, most likely indicating an excess of strong superoxide inert organic chelators in the sample. Estimates of $\log k_{\text{Cu}}$ are shown in Figure 2 and varied from 6.4 to 7.9 with a clear minimum at station 249 at 100 m. Values of $\log k_{\text{Cu}}$ were relatively constant below 200 m at all stations. Estimates of $\log k_{\text{Fe}}$ are displayed in Figure 3 and varied from below detection (<6) to 7.9 and tended toward maximal rates in mid-depth waters (100–500 m) with lowest values in the upper 200 m.

Discussion

Superoxide Decay Rates in Seawater. Measurements of superoxide decay in open ocean waters are limited, with earlier results being undetectable ($<1.5 \text{ s}^{-1}$) using spectrophotometry (9), while recent results in the Tropical Pacific using a chemiluminescence approach similar to ours (8) found values of $9.7 \times 10^{-3} \text{ s}^{-1} > k > 1 \times 10^{-4} \text{ s}^{-1}$. Higher values have been found in coastal waters (3, 11, 26). The kinetics of the dismutation reaction has been extensively examined in pure water (27, 28) and Zafriou (9) made the first direct measurements of K_{HO_2} in seawater ($\text{p}K_{\text{a}}^* = 4.60 \pm 0.15$) and measured the dismutation rate constant k_2 ($5 \pm 1 \times 10^{12} [\text{H}^+] \text{ M}^{-1} \text{ s}^{-1}$) on the pH_{NBS} scale. In the present work from the experiments performed with DTPA and seawater we measured the dismutation rate using pH_{TOT} as $4.4 \pm 1.6 \times 10^{12} [\text{H}^+] \text{ M}^{-1} \text{ s}^{-1}$ ($n = 14$, 95% CI), in reasonably good agreement with the earlier data of Zafriou (9) given the differences in the pH scales used and that Zafriou did not state at what temperature his work was conducted.

A recent study in the Tropical Pacific by Rose et al. (8) observed first-order rates with DTPA-amended seawater and these authors suggested it was from reactions with organic species or strong metal organic species that did not react with DTPA rapidly. There is a significant difference between our study and theirs with regard to the experimental setup as in their work they added DTPA immediately before measuring the superoxide decay while in the present study we equilibrated the DTPA with the seawater for a minimum of 12 h before the addition of superoxide. The longer equilibration time used in our work was based on the findings of Hering and Morel (29) and experiments in our own lab which indicated a minimum of 1 h was required. We suggest here that the addition of DTPA immediately before measurement does not prevent trace metal reactions with superoxide and thus work performed in this manner needs to be interpreted carefully.

Importance of Nonmetal (Organic) Reactions with Superoxide. Previous work by Goldstone and Voelker (11) found a significant reaction between superoxide and DOM. In the present work we found this reaction pathway to be minor as we observed in DTPA-amended samples reaction rates that were distinctly second order and similar to the rate of the dismutation reaction in seawater (9). However closer examination at stations close to the Antarctic Peninsula (Station 230) suggests that there were small contributions from DOM, most noticeably in the productive surface waters (25 m: $k_{\text{obs}} = 0.006 \pm 0.001$) and in the region of the nutricline (200 m: $k_{\text{obs}} = 0.004 \pm 0.001$). The observed pattern in our work is partially consistent with the production of new organic matter in the surface waters by phytoplankton and the remineralization of organic matter at depth via zooplankton grazing and bacterial activity.

Goldstone and Voelker (11) found a correlation between CDOM absorption at 300 nm and k_{org} for DTPA-amended coastal seawater samples. Unfortunately during our cruise no measurements of CDOM absorption were made, however a previous photochemical study in the same region (30) found values of $\sim 0.25 \text{ m}^{-1}$ for surface water CDOM absorption at 300 nm which would suggest a value of $k_{\text{org}} = 0.1 \text{ s}^{-1}$ based on the work of Goldstone and Voelker. The much lower values for k_{org} found here suggest that open ocean CDOM is significantly less reactive with superoxide than coastal waters and this may be related to the lack of riverine humic materials.

Half Life and Steady State Concentration for O_2^- . In the present study we observed half-lives for superoxide in ambient seawater ranging from 9.3 to 193.6 s (mean 43.5 s, $n = 27$). In general the slowest rates were found around 50–75 m in the euphotic zone, though there was no statistically significant trend with depth. Earlier estimates for seawater were significantly longer; 5–20 min (26) based solely on the

dismutation reaction indicating the importance of including reactions with metals in estimating superoxide lifetimes.

Previous workers (2, 8, 11) have utilized the concept of a pseudo-steady-state concentration of O_2^- in seawater based on equal production and decay terms:

$$[O_2^-]_{ss}(2k_2[O_2^-]_{ss} + k_{obs}) = \text{production} \quad (5)$$

Estimates of the steady-state concentration can be obtained by solving eq 5 as a quadratic equation. For Antarctic waters we can find no published values for superoxide formation but we can estimate an upper limit of 9 nM h^{-1} by using H_2O_2 production rates (31) of 4.5 nM h^{-1} for sunlit surface waters at midday in the vicinity of the Antarctic Peninsula. Using this approach we estimate $[O_2^-]_{ss} \approx 116 \pm 28 \text{ pM}$ ($n = 3$, 95% CI) for samples in the Drake Passage at 25 m depth. Our estimate is similar to that suggested by Voelker and colleagues based on midday photoproduction in coastal and open ocean waters of $[O_2^-]_{ss} \sim 10\text{--}200 \text{ pM}$ (2, 11).

Implications for Steady-State Deep Water H_2O_2 Concentrations. Measurements of H_2O_2 in deep waters in the Drake Passage ranged from 2 to 6 nM (Croot et al. in preparation) similar to other deep waters (32). Yuan and Shiller (32) suggested a 12-day residence time in the deep North Pacific for H_2O_2 based on the assumption of a 0.01 nM h^{-1} biological production rate and an extrapolation of measured biological decay rates (0.009 nM h^{-1}) for H_2O_2 . If we apply the same deep water production rate here to the decay constants we determined it suggests a O_2^- production rate of 20 pM h^{-1} resulting in a $[O_2^-]_{ss}$ for deep water (>500 m) of $0.26 \pm 0.24 \text{ pM}$ (95% CI: range $0.15\text{--}0.46 \text{ pM}$, $n = 7$). This contrasts sharply with recent data from intermediate waters in the Tropical Pacific (8) which indicated $[O_2^-]_{ss}$ of $20\text{--}150 \text{ pM}$ with superoxide first order decay rates of $0.001\text{--}0.01 \text{ s}^{-1}$. Such high $[O_2^-]_{ss}$ would indicate elevated deepwater H_2O_2 production ($0.08\text{--}0.6 \text{ nM h}^{-1}$) and concentrations ($8\text{--}61 \text{ nM}$, assuming a 4 day residence time for H_2O_2 (33)) which have currently not been observed in the field. Alternative pathways for H_2O_2 production that do not involve superoxide (34) would further suggest that the $[O_2^-]_{ss}$ are pM or less in deep waters as our study suggests.

Effect of O_2^- on Metal Speciation in Seawater. The significant decreases observed in our study for the decay rate of superoxide in DTPA-amended seawater indicate that for ambient seawater, reactions with metals must be the dominant superoxide decay process. For a $[O_2^-]_{ss} = 100 \text{ pM}$ our study predicts that the dismutation reaction would represent less than 1% of the loss of superoxide in all samples without DTPA. Under the higher concentrations of superoxide used in the decay experiments we performed the uncatalyzed-dismutation pathway represents $78 \pm 24\%$ ($n = 27$, 95% CI, range $42\text{--}94\%$) of the initial loss rate (Figure S6). Thus it is necessary to include the uncatalyzed dismutation pathway for our experiments but it is clearly a minor pathway in the open ocean.

Superoxide reacts rapidly with inorganic Cu species in seawater (3) and also with organic Cu complexes (2) despite their apparent strong complexation. In the present study we also saw evidence for a fast reaction between organic Cu species and superoxide, as voltammetric speciation measurements for Cu (Heller and Croot, manuscript in preparation) indicated free metal concentrations for Cu below 10^{-13} M throughout the water column. Such low values of free copper would not be sufficient to generate the values of $\log k_{Cu}$ we observed and thus the reaction must involve organically complexed Cu also. This is consistent with the work of Voelker et al. (2) who found that the strong Cu organic chelators produced by *Synechococcus* reacted rapidly with superoxide and suggested that this may be related to an exchangeable water coordinated to the chelated copper.

Fast reactions with Cu(I) resulting from the reduction of Cu(II) would help to catalyze the decay of superoxide. The impact of superoxide reactions on the Cu redox cycle can be estimated by using the observed value of $\log k_{Cu}$ and its relationship to $k_{Cu(I)}$ and $k_{Cu(II)}$ (2).

$$k_M = \frac{2k_{M^{n+}}k_{M^{n+1}}}{k_{M^{n+}} + k_{M^{n+1}}} \quad (6)$$

Assuming that $k_{Cu(I)} = 1 \times 10^9 \text{ M}^{-1} \text{ s}^{-1}$, which is simply the reaction with inorganic Cu(I) as there is insufficient time to form organic complexes, and that the reactions with superoxide are much faster than the oxidation of Cu(I) by O_2 (3), then eq 6 can be solved for $k_{Cu(II)}$ and the steady state ratio of Cu(I) can be calculated from the following:

$$\frac{[M^{n+}]}{[M^{n+1}]} = \frac{k_{M^{n+1}}}{k_{M^{n+}}} \quad (7)$$

Using this approach we can estimate for our study that Cu(I) under steady state conditions made up between 0.1 and 4% of the total copper pool. For samples from the sunlit upper 100 m in our study this we estimate $1\text{--}63 \text{ pM Cu(I)}$ which is on the limit of current analytical detection schemes (35). Actual measurements of Cu(I) in the subtropical Atlantic indicate that Cu(I) is 5–10% of the total copper (35) in the euphotic zone, suggesting an additional contribution from direct photoreduction of Cu complexes.

Additions of Fe to seawater in this study saw only small increases in superoxide decay rates when compared to copper (Figure S7). For many water samples from the upper water column the addition of iron saw almost no change in the decay kinetics (Figures 2 and 3) suggesting strong organic complexation of iron by chelators in excess of the ambient iron concentration in agreement with previous observations in the Southern Ocean (36, 37). Estimation of the reaction rates of Fe(II) ($k_{Fe(II)}$) and Fe(III) ($k_{Fe(III)}$) with superoxide using k_{Fe} via the same approach as for Cu as above is problematic, if we assume that the reaction is only due to free Fe(II), then the usual value used in the literature, $k_{Fe(II)} = 1 \times 10^7 \text{ M}^{-1} \text{ s}^{-1}$ (Table S1), is inconsistent with the observed values of k_{Fe} (eq 6) in many cases. This suggests that $k_{Fe(II)}$ under seawater conditions may represent faster reactions with superoxide than with free Fe(II). There is precedence for this as studies on Fe(II)-EDTA suggest faster reaction rates with superoxide ($k_{Fe(II)} = 1.2 \times 10^8 \text{ M}^{-1} \text{ s}^{-1}$) (38) and model findings where reactions with Fe(II) species that predominate in ambient seawater ($Fe(OH)^+$, $Fe(OH)_2$, $Fe(CO_3)_2^{2-}$) were suggested to react faster than free Fe(II), though these model results are currently in dispute (39). Using a higher estimate for $k_{Fe(II)} = 5 \times 10^7 \text{ M}^{-1} \text{ s}^{-1}$ (1) we then estimate that under steady-state conditions Fe(II) made up only 0.05–4% of the total iron in our experiment resulting in $<1 \text{ pM Fe(II)}$ from superoxide in the euphotic zone in the Drake Passage. Thus the elevated levels of Fe(II) in Southern Ocean waters seen during a diel cycle must be produced via a direct photoreduction pathway (40).

If iron in our samples is organic complexed then the reduction of the naturally occurring Fe(III) complexes by superoxide is significantly faster than for model siderophores such as ferrioxamine B (Table S1), and is more consistent with reactions with inorganic or weakly complexed iron (1, 24). It may also indicate the importance of rapid superoxide reactions with the reduced form Fe(II) where organic complexation may occur on a slower time scale (41). Recent ultrafiltration studies (42) found that much of the Fe that passed through an $0.2\text{-}\mu\text{m}$ filter did not pass through a 10- or 200-kDa ultrafilter indicating that much of the dissolved Fe is colloidal in nature though still possibly bound to an organic matrix. Thus in the present work we suggest that

where we observed elevated k_{Fe} values it is suggestive of iron weakly bound to soluble complexes or labile sites on organic colloids. Observations of $\log k_{Fe} < 6.5$ are indicative of strong soluble complexes such as siderophores which are relatively unreactive to superoxide.

An important consideration in the present work is whether the presence of up to 500 nM of H_2O_2 derived from the KO_2 source may influence the results for Cu and Fe. We believe this was not the case for Cu based on two lines of reasoning: (1) the reaction of Cu(I) with H_2O_2 is very slow $7 \times 10^3 M^{-1} s^{-1}$ (43) and O_2 would remain the major pathway for Cu(I) oxidation (44); and (2) similarly the reaction of Cu(II) with H_2O_2 is also a minor pathway under seawater conditions (44). As the oxidation of Fe(II) is sensitive to H_2O_2 concentrations (45) in our experiments Fe(II) oxidation would be influenced by H_2O_2 . However the rate-determining step for the superoxide loss was still the reduction of Fe(III) and thus faster oxidation of Fe(II) would not give rise to an acceleration of the overall loss rate of superoxide.

Environmental Significance: Superoxide decay and Biogeochemical Cycles. The concept of "Oceanographic Consistency" was first applied to dissolved trace metal data by Boyle and Edmond (46) and should also be applicable to redox data such as we present here. However the criteria must be extended to include both the effects of fast kinetics and physical mixing processes which can strongly determine the shape of a vertical profile in sunlit waters (41) and to include consistency between production and decay terms. Thus superoxide data should be consistent with both H_2O_2 data and trace metal redox speciation data. In the current study it appears that superoxide decay kinetics in ambient seawater are related to other biogeochemical processes through the reactions with the Cu and Fe species present. Changes in Cu and Fe speciation within the water column caused by release/exudation of chelators by phytoplankton/bacteria in the photic zone and remineralization of metals by zooplankton grazing at intermediate depths are all plausible interpretations of the changes in superoxide decay we observed here. It is apparent here that Cu, based on both the higher concentrations and faster reaction rates than Fe, is the major pathway for superoxide decay in Southern Ocean waters. These reactions occur despite the Cu being strongly organically complexed and has clear implications for both Cu redox cycling and superoxide lifetimes.

Acknowledgments

We gratefully acknowledge the officers and crew of the *P.S. Polarstern* whose help and cooperation made this work possible. Special thanks also to the chief scientist Prof. Eberhard Fahrbach (AWI) for making our participation possible. Shipboard work was only possible with the help of the onboard NIOZ team led by Hein de Baar, and our IFM-GEOMAR colleagues Oliver Baars and Katrin Bluhm. Thanks also to Peter Streu (IFM-GEOMAR) for the laboratory analysis in Kiel. The comments of Dr. Andrew Rose and two anonymous reviewers are gratefully appreciated in helping to improve this manuscript. This work is a contribution to IPY GEOTRACES and was financed by the DFG Antarctic Program (SPP 1158) via a grant to P.C. (CR145/10-1).

Supporting Information Available

Full details of station locations and the experimental setup and related analysis methods; the cruise track and stations locations (Figure S2); experimental set up (Figure S3) and design (Figure S1); and an example of the signal data from the FeLume (Figure S4). This information is available free of charge via the Internet at <http://pubs.acs.org>.

Literature Cited

- Voelker, B. M.; Sedlak, D. L. Iron reduction by photoproduced superoxide in seawater. *Mar. Chem.* **1995**, *50*, 93–102.

- Voelker, B. M.; Sedlak, D. L.; Zafriou, O. C. Chemistry of Superoxide Radical in Seawater: Reactions with Organic Cu Complexes. *Environ. Sci. Technol.* **2000**, *34*, 1036–1042.
- Zafriou, O. C.; Voelker, B. M.; Sedlak, D. L. Chemistry of the superoxide radical (O_2^-) in seawater: Reactions with inorganic copper complexes. *J. Phys. Chem. A* **1998**, *102* (28), 5693–5700.
- Rose, A. L.; Waite, D. Role of superoxide in the photochemical reduction of iron in seawater. *Geochim. Cosmochim. Acta* **2006**, *70* (15), 3869–3882.
- Micinski, E.; Ball, L. A.; Zafriou, O. C. Photochemical Oxygen Activation - Superoxide Radical Detection and Production-Rates in the Eastern Caribbean. *J. Geophys. Res.-Oceans* **1993**, *98* (C2), 2299–2306.
- Marshall, J.-A.; Hovenden, M.; Oda, T.; Hallegraef, G. M. Photosynthesis does influence superoxide production in the ichthyotoxic alga *Chattonella marina* (Raphidophyceae). *J. Plankton Res.* **2002**, *24* (11), 1231–1236.
- Kim, D.; Oda, T.; Ishimatsu, A.; Muramatsu, T. Galacturonic acid-induced Increase of Superoxide Production in Red Tide Phytoplankton *Chattonella marina* and *Heterosigma akashiwo*. *Biosci. Biotechnol. Biochem.* **2000**, *64*, 911–914.
- Rose, A. L.; Webb, E. A.; Waite, T. D.; Moffett, J. W. Measurement and Implications of Nonphotochemically Generated Superoxide in the Equatorial Pacific Ocean. *Environ. Sci. Technol.* **2008**, *42* (7), 2387–2393.
- Zafriou, O. C. Chemistry of superoxide ion (O_2^-) in seawater. I. pK_{asw}^* (HOO) and uncatalysed dismutation kinetics studied by pulse radiolysis. *Mar. Chem.* **1990**, *30*, 31–43.
- Fujii, M.; Ito, H.; Rose, A. L.; Waite, T. D.; Omura, T. Superoxide-mediated Fe(II) formation from organically complexed Fe(III) in coastal waters. *Geochim. Cosmochim. Acta* **2008**, *72* (24), 6079–6089.
- Goldstone, J. V.; Voelker, B. M. Chemistry of Superoxide Radical in Seawater: CDOM Associated Sink of Superoxide in Coastal Waters. *Environ. Sci. Technol.* **2000**, *34*, 1043–1048.
- Croot, P. L.; Laan, P.; Nishioka, J.; Strass, V.; Cisewski, B.; Boye, M.; Timmermans, K.; Bellerby, R.; Goldson, L.; de Baar, H. J. W. Spatial and Temporal distribution of Fe(II) and H_2O_2 during EISENEX, an open ocean mesoscale iron enrichment. *Mar. Chem.* **2005**, *95*, 65–88.
- Rose, A. L.; Waite, T. D. Kinetic Model for Fe(II) Oxidation in Seawater in the Absence and Presence of Natural Organic Matter. *Environ. Sci. Technol.* **2002**, *36*, 433–444.
- Dickson, A. G. pH buffers for sea water media based on the total hydrogen ion concentration scale. *Deep Sea Res. Part I* **1993**, *40* (1), 107–118.
- Millero, F. J.; Zhang, J. Z.; Fiol, S.; Sotolongo, S.; Roy, R. N.; Lee, K.; Mane, S. The Use of Buffers to Measure the pH of Seawater. *Mar. Chem.* **1993**, *44* (2–4), 143–152.
- Kuehnen, E. C.; Alvarez, R.; Paulson, P. J.; Murphy, T. J. Production and analysis of special high purity acids purified by sub-boiling distillation. *Anal. Chem.* **1972**, *44*, 2050–2056.
- Nakano, M. Detection of active oxygen species in biological systems. *Cell. Mol. Neurobiol.* **1998**, *18* (6), 565–579.
- Oosthuizen, M. M. J.; Engelbrecht, M. E.; Lambrechts, H.; Greyling, D.; Levy, R. D. The effect of pH on chemiluminescence of different probes exposed to superoxide and singlet oxygen generators. *J. Biolumin. Chemilumin.* **1997**, *12* (6), 277–284.
- Tampo, Y.; Tsukamoto, M.; Yonaha, M. The antioxidant action of 2-methyl-6-(p-methoxyphenyl)-3,7-dihydroimidazo[1,2-alpha]pyrazin-3-one (MCLA), a chemiluminescence probe to detect superoxide anions. *FEBS Lett.* **1998**, *430* (3), 348–352.
- Pronai, L.; Nakazawa, H.; Ichimori, K.; Saigusa, Y.; Ohkubo, T.; Hiramatsu, K.; Arimori, S.; Feher, J. Time Course Of Superoxide Generation By Leukocytes - The MCLA Chemiluminescence System. *Inflammation* **1992**, *16* (5), 437–450.
- Kambayashi, Y.; Tero-Kubota, S.; Yamamoto, Y.; Kato, M.; Nakano, M.; Yagi, K.; Ogino, K. Formation of Superoxide Anion during Ferrous Ion-Induced Decomposition of Linoleic Acid Hydroperoxide under Aerobic Conditions. *J. Biochem.* **2003**, *134* (6), 903–909.
- Rose, A. L.; Moffett, J. W.; Waite, T. D. Determination of Superoxide in Seawater Using 2-Methyl-6-(4-methoxyphenyl)-3,7-dihydroimidazo[1,2-a]pyrazin-3(7H)-one Chemiluminescence. *Anal. Chem.* **2008**, *80* (4), 1215–1227.
- Garg, S.; Rose, A. L.; Waite, T. D. Superoxide mediated reduction of organically complexed Iron(III): Comparison of non-dissociative and dissociative reduction pathways. *Environ. Sci. Technol.* **2007**, *41* (9), 3205–3212.

- (24) Fujii, M.; Rose, A. L.; Waite, T. D.; Omura, T. Superoxide-mediated dissolution of amorphous ferric oxyhydroxide in seawater. *Environ. Sci. Technol.* **2006**, *40* (3), 880–887.
- (25) Martin, J. H.; Gordon, R. M.; Fitzwater, S. E. Iron in Antarctic waters. *Nature* **1990**, *345*, 156–158.
- (26) Petasne, R. G.; Zika, R. G. Fate of superoxide in coastal sea water. *Nature* **1987**, *325*, 516–518.
- (27) Christensen, H.; Sehested, K. Hydroperoxo and oxygen(1-) radicals at elevated temperatures. *J. Phys. Chem.* **1988**, *92* (10), 3007–3011.
- (28) Bielski, B. H. J.; Cabelli, D. E.; Arudi, R. L.; Ross, A. B. Reactivity Of HO₂/O₂⁻ Radicals In Aqueous-Solution. *J. Phys. Chem. Ref. Data* **1985**, *14* (4), 1041–1100.
- (29) Hering, J. G.; Morel, F. M. M. Kinetics of Trace Metal Complexation: Role of Alkaline-Earth Metals. *Environ. Sci. Technol.* **1988**, *22*, 1469–1478.
- (30) Qian, J. G.; Mopper, K.; Kieber, D. J. Photochemical production of the hydroxyl radical in Antarctic waters. *Deep-Sea Res. Part I* **2001**, *48* (3), 741–759.
- (31) Yocis, B. H.; Kieber, D. J.; Mopper, K. Photochemical production of hydrogen peroxide in Antarctic Waters. *Deep Sea Res. Part I* **2000**, *47* (6), 1077–1099.
- (32) Yuan, J. C.; Shiller, A. M. Hydrogen peroxide in deep waters of the North Pacific Ocean. *Geophys. Res. Lett.* **2004**, *31*, (1).
- (33) Petasne, R. G.; Zika, R. G. Hydrogen peroxide lifetimes in south Florida coastal and offshore waters. *Mar. Chem.* **1997**, *56* (3–4), 215–225.
- (34) Palenik, B.; Morel, F. M. M. Dark production of H₂O₂ in the Sargasso Sea. *Limnol. Oceanogr.* **1988**, *33*, 1606–1611.
- (35) Moffett, J. W.; Zika, R. G. Measurement of copper(I) in surface waters of the subtropical Atlantic and Gulf of Mexico. *Geochim. Cosmochim. Acta* **1988**, *52*, 1849–1857.
- (36) Croot, P. L.; Bowie, A. R.; Frew, R. D.; Maldonado, M.; Hall, J. A.; Safi, K. A.; La Roche, J.; Boyd, P. W.; Law, C. S. Retention of dissolved iron and Fe^{II} in an iron induced Southern Ocean phytoplankton bloom. *Geophys. Res. Lett.* **2001**, *28*, 3425–3428.
- (37) Boye, M.; van den Berg, C. M. G.; de Jong, J. T. M.; Leach, H.; Croot, P. L.; de Baar, H. J. W. Organic complexation of iron in the Southern Ocean. *Deep Sea Res.* **2001**, *48*, 1477–1497.
- (38) Brown, E. R.; Mazzarella, J. D. Mechanism of oxidation of ferrous polydentate complexes by dioxygen. *J. Electroanal. Chem.* **1987**, *222* (1–2), 173.
- (39) Pham, A. N.; Waite, T. D. Oxygenation of Fe(II) in natural waters revisited: Kinetic modeling approaches, rate constant estimation and the importance of various reaction pathways. *Geochim. Cosmochim. Acta* **2008**, *72* (15), 3616–3630.
- (40) Croot, P. L.; Bluhm, K.; Schlosser, C.; Streu, P.; Breitbarth, E.; Frew, R.; Van Ardelan, M. Regeneration of Fe(II) during EIfEX and SOFeX. *Geophys. Res. Lett.* **2008**, *35* (19), L19606, DOI: 10.1029/2008GL035063.
- (41) Croot, P. L.; Frew, R. D.; Hunter, K. A.; Sander, S.; Ellwood, M. J.; Abraham, E. R.; Law, C. S.; Smith, M. J.; Boyd, P. W. The effects of physical forcing on iron chemistry and speciation during the FeCycle experiment in the South West Pacific. *J. Geophys. Res. - Oceans* **2007**, *112*, C06015; doi:10.1029/2006JC003748.
- (42) Schlosser, C.; Croot, P. L. Application of cross-flow filtration for determining the solubility of iron species in open ocean seawater. *Limnol. Oceanogr.: Methods* **2008**, *6*, 630–642.
- (43) Berdnikov, M. Catalytic Activity Of Hydrated Copper Ion During Hydrogen-Peroxide Decomposition. *Zh. Fiz. Khim.* **1973**, *47* (7), 1879–1881.
- (44) Moffett, J. W.; Zika, R. G. Reaction Kinetics of Hydrogen Peroxide with Copper and Iron in Seawater. *Environ. Sci. Technol.* **1987**, *21*, 804–810.
- (45) Santana-Casiano, J. M.; Gonzalez-Davila, M.; Millero, F. J. The role of Fe(II) species on the oxidation of Fe(II) in natural waters in the presence of O₂ and H₂O₂. *Mar. Chem.* **2006**, *99* (1–4), 70–82.
- (46) Boyle, E.; Edmond, J. M. Copper in surface waters south of New Zealand. *Nature* **1975**, *253*, 107–109.

ES901766R

Supporting Information

To accompany the manuscript entitled

Superoxide decay kinetics in the Southern Ocean.

Maija I. Heller and Peter L. Croot

Comprising :

26 Pages

4 Tables

7 Figures

Supplementary Information: Seawater sampling and Kinetic Modelling

Sampling Stations. The location of the sampling stations used in this study can be found in Table S2 and Figure S2. Samples were collected during the GEOTRACES cruise ANT24-3 (Capetown-Punta Arenas), from 6 February- 16 April 2008 on board the German research vessel RV Polarstern. Three stations were occupied in the Drake Passage (Data in Table S3). Data from two stations from the Weddell Sea (Data in Table S4) are also included, but here no total metal data is available.

Water Sampling. Seawater samples were obtained using the TITAN trace metal clean rosette system belonging to the NIOZ [1]. In brief this sampling system consists of a rectangular Titanium rosette fitted with a standard Seabird CTD and 24 modified 12 L Teflon coated GO-FLO bottles (General Oceanics, Miami, FL, USA). The rosette was deployed on a specially made trace metal clean Kevlar wire (17.7 mm) complete with conducting cable. Sample bottles were tripped on the upcast using standard Seabird CTD software. Upon recovery of the rosette the complete rosette was carefully moved into a Class 100 clean room container specially built for sampling from this system. Care and maintenance of the GO-FLO bottles was performed by NIOZ technicians using established protocols [2]. In the sampling clean room, filtered water samples were collected using slight N₂ overpressure and filtration through pre-cleaned 0.2 µm filter cartridges (Sartorius) from the relevant GO-FLO into 1 L trace metal clean Teflon bottles for shipboard superoxide experiments, a replicate 1 L sample was also drawn into low density polyethylene bottles for later analysis for total metals (acidified onboard with Q-HCl, 1mL/L) in the laboratory in Kiel. Analytical work at sea was performed at 23° C in an over-pressurized class 5 clean air container belonging to the IFM-GEOMAR.

Total Dissolved Copper and Iron determination. Samples were analyzed in the laboratory by graphite furnace atomic absorption (ETAAS: Perkin-Elmer Model 4100 ZL) after pre-concentration by simultaneous dithiocarbamate-freon extraction, from seawater (250-500 g) [2-3]. The accuracy of the analytical procedure was evaluated by measurement of the certified seawater standard NASS-5 (National Research Council of Canada) and the SAFe intercomparison standard [4]. Our values for NASS 5 agree within the stated values for NASS 5 and our SAFe data (SAFe S: 0.395 ± 0.025 nM Cu, 0.112 ± 0.013 nM Fe, SAFe D2: 1.480 ± 0.481 nM Cu, 0.829 ± 0.127 nM Fe) are close to the average consensus values for Fe. There is currently no consensus value for Cu for the SAFe samples but are consistent with published data for the same samples [5-6]. The precision for replicate analysis was between 3-5% at the concentrations found in this study. The procedural (analytical) blank was $0.041 \pm 0.024(\sigma_{bl})$ nM (Fe) and < 1 pM (Cu).

Measurement of impurities in superoxide standards prepared from KO₂ and calibration of the initial superoxide concentration.

(i) Trace Metals: Previously KO₂ has not been used widely as a source of superoxide due to the perception from work in the period 1970-1980 that it was highly contaminated with metals. However it appears that many of the earlier problems found with KO₂ resulted from non trace metal clean equipment and in particular water supplies which did not utilize final filtration as was alluded to in some earlier works [7]. Interestingly given the development in chemical preparations and trace metal analysis we could find no evidence of any direct measurements in KO₂ having been made. For the present work we analyzed directly aliquots of KO₂ solutions for Fe and

Cu, prepared as described below, and found that the KO_2 contained 0.7 ± 0.1 ppm Fe (dry weight) and no detectable Cu (less than 0.06 ppm Cu). Thus using our standard protocol we would have added ~ 3 pM Fe (< 0.8 pM Cu) which would provide a maximum additional decay rate of $3 \times 10^{-4} \text{ s}^{-1}$ (using a reaction rate with Fe of $1 \times 10^8 \text{ M}^{-1} \text{ s}^{-1}$ – see Table S1) significantly less than our observed rates. Thus the influence of trace metals in the KO_2 in our studies was apparently not significant to affect the results.

(ii) There is a significant amount of H_2O_2 in solutions prepared from KO_2 and this is unavoidable with any superoxide source, including photochemical and enzymatic production pathways. In the course of this work we came across problems with the current spectrophotometric methods used for calibrating O_2^- that was generated photochemically using acetone or benzophenone in 2-propanol/water mixtures following the method of McDowell et al. [8]. In brief the absorption spectra of acetone [9] and benzophenone [10] overlap with that of O_2^- [11] and the reaction with benzophenone also produces acetone [12-13]. Similarly another common system used to generate a flux of O_2^- , Xanthine/Xanthine Oxidase also has been shown to be more complicated than first thought [14]. Thus in the present work we chose to use KO_2 as our source for O_2^- in simple pulse chase decay experiments. In the present work we routinely made measurements of both species in each standard solution prepared by UV spectrophotometry with either a 1 m LWCC-2100 100 cm pathlength liquid waveguide cell (World Precision Instruments, Sarasota, FL, USA), or a 10 cm Quartz-cuvette (Hellma), and an Ocean Optics USB4000 UV-VIS spectrophotometer in combination with an Ocean Optics DT-MINI-2-GS light source. Concentrations of H_2O_2 and O_2^- were determined by determining the least squares solution to the

measured absorbance, at multiple wavelengths, by using published molar extinction coefficients for H_2O_2 [15-16] and O_2^- [11]. Mean initial concentrations in the primary KO_2 solution assessed in this way were $900 \pm 50 \mu\text{M}$ for H_2O_2 and $90 \pm 10 \mu\text{M}$ O_2^- . No DTPA or other complexing agents were added to our KO_2 primary solution. H_2O_2 in the final seawater solutions was also assessed on occasion by a chemiluminescence flow injection method [17] and the results agreed well with the concentrations determined by direct spectrophotometry. A review paper on specific calibration issues for O_2^- will be submitted shortly (Heller and Croot, manuscript in preparation).

Overview of the FeLume chemiluminescence system: This system comprises a light tight box equipped with a Plexiglas spiral flow cell mounted below a photon counter (Hamamatsu HC-135-01) linked to a laptop computer via a Bluetooth connection controlled through a purpose built LabviewTM (National Instruments) virtual instrument. For O_2^- determination we ran the sample and the MCLA reagent directly into the flow cell using a peristaltic pump (Gilson Minipuls 3, operating at 18 rpm,) with the sample line being pulled through the flow cell as this leads to the smallest amount of dead time in the system (typically 2-3 s). The overall flow rate through the cell was 8.25 mL min^{-1} , comprising 5.0 mL min^{-1} from the MCLA and 3.25 mL min^{-1} from the sample. The transit time through the optical cell ($300 \mu\text{L}$) was therefore 2.18 s.

Back ground Chemiluminescence: MCLA produces chemiluminescence by itself due to auto-oxidation of the conjugate base of MCLA with O_2 [18]. Auto-oxidation reactions are reduced by using an analytical pH less than the pK_a of MCLA (7.75) [19] and by reducing the MCLA concentration [20]. MCLA also reacts rapidly with

singlet oxygen to produce chemiluminescence [19] however singlet oxygen is present at low pM concentrations as it is efficiently quenched in seawater [21]. MCLA also does not appreciably react with H_2O_2 to produce chemiluminescence at the concentrations encountered in the present work [20]. In our study we ran seawater samples without added superoxide and to determine the baseline chemiluminescence due to the auto-oxidation reaction of MCLA. The baseline values determined in this fashion (range: 7000 – 15000 counts per 200 ms period) were subtracted from the superoxide decay data in order to correctly determine the decay rate (see below). In the present work where we added nM superoxide in order to observe the decay the baseline corrections were relatively minor with regard to the initial counts (< 1%). At lower concentrations of superoxide baseline correction is more important as is the signal to noise ratio.

Linearity of the MCLA technique: The linearity of the chemiluminescence response between MCLA and superoxide was assumed in the method of Rose et al. [22] but as was pointed out by reviewers of this work was not demonstrated. The assessment of this linear response is of course complicated by the rapid decay of the superoxide. Thus in the present work we performed a series of experiments in which seawater samples were spiked with varying amounts of a known concentration of superoxide. Using the observed counts as a function of time from the chemiluminescence reaction we were then able to back calculate the initial superoxide signal. For the configuration used in our experiments we found a linear response, for the range 0-90 nM superoxide, (see figure S5) as has been shown previously [23-24]. A practical concern however is that with high concentrations of superoxide (> 90 nM) the 1 μM MCLA is insufficient to prevent uncatalysed dismutation of superoxide in the pH_{NBS} 6 buffer

despite the fast reactivity of MCLA with O_2^- [25-26]. An additional check on the linearity of the response was that the calculated rates in DTPA amended seawater were not significantly different from earlier estimates [27], this would not have been observed if the response was significantly non-linear.

Precision and Accuracy: As this was the first time this approach had been applied we performed an initial experiment using water collected from close to Cape Verde, which was run repeatedly ($n=5$), $k_{obs} = 0.0245 \pm 0.0016$ (2σ) indicating a precision of 6.4 % for these samples. The main problem associated with this technique initially was the formation of bubbles in the flow cell which gave rise to signal spikes, this problem was reduced when seawater samples were given adequate time to come into equilibrium with the laboratory temperature after collection. Care is also needed in mixing the samples thoroughly when adding the superoxide. For the work reported here from the Drake Passage samples were run in duplicate.

The accuracy of the MCLA method for the determination of both superoxide concentration and the value of the rate constants k_1 and k_2 are difficult to assess given that the superoxide concentration is transient and there are no standard reference materials available with a certified rate constant. However by comparison with previous data using spectrophotometry [28-30], which our data compare well with, we believe that this method is at least as accurate, if not better, as other available methods.

Measurement of Sample pH. In the present manuscript we report seawater pH values using the total hydrogen scale (pH_{TOT}) [31] while we use the NBS scale for pH, pH_{NBS} , for pH measurements of buffers and other low ionic strength solutions. All pH measurements during the course of this work were made using a WTW pH meter 330i

calibrated with Tris buffers [32]. In earlier works on superoxide kinetics in seawater, authors either did not report which pH scale they used or have used pH_{NBS} , apparently unaware of problems with this scale at high ionic strengths [31-32]. In particular the work of Zafiriou [27] on the uncatalyzed dismutation superoxide reaction in seawater was apparently made with the pH_{NBS} scale, the exact pH scale is not specified, and a precise conversion to the pH_{TOT} scale is not possible as some of the relevant information was not supplied in that work (i.e. Temperature, Alkalinity or TCO_2). In our work we are able to calculate the in situ and laboratory pH_{TOT} based on temperature, pressure, salinity, nutrient, alkalinity and TCO_2 data, provided by the shipboard party (NIOZ). Laboratory pH_{TOT} measurements were also made on the samples prior and after the addition of superoxide. In all cases pH_{TOT} increased after the addition of superoxide by approximately 0.08-0.10 pH_{TOT} units. These small increases in pH_{TOT} however did not apparently affect first order decay rates in any significant manner as evidenced by the good precision for k_{obs} found over a range of superoxide additions (see section above on precision) where the maximal pH_{TOT} change was up to 0.20 pH units. It should be noted that a larger pH_{TOT} change was induced by the warming of the samples to the laboratory temperature (see Tables S3 and S4) and these temperature induced changes in superoxide reactivity need to be considered when considering *in situ* rates.

Calculation of rate data for superoxide. The raw chemiluminescence signal for the reaction between MCLA and O_2^- recorded by the computer was processed using a specially designed LabviewTM VI constructed for this purpose using standard kinetic fitting procedures to determine both the 1st (k_{obs}) and 2nd order (k_2) rates simultaneously. The photon counter has a base counting period of 10 ms, for the

present work we used average counts of an integration time of 200 ms. Dark background counts for this detector were typically 60–120 counts s⁻¹. Apparent reaction rates for Cu (k_{Cu}) and Fe (k_{Fe}) with O₂⁻ were calculated via linear regression of k_{obs} versus the total metal added [29]. Using our experimental setup the minimum values for k_{Cu} and k_{Fe} that were measurable is estimated at 1x10⁶ M s⁻¹.

Model Calculations for O₂⁻ kinetics. Numerical modeling of O₂⁻ reactions in seawater was performed using a fully explicit model written in C++ updated from an earlier version [33] to include Cu chemistry. Rate constants for the key reactions involved were compiled from those already published in the literature (see Table S2).

Supplementary Information on the Fitting Procedures:

The following rate equation is assumed:

$$\frac{\partial[\text{O}_2^-]}{\partial t} = -k_1[\text{O}_2^-] - k_2[\text{O}_2^-]^2 \quad (1)$$

Where k_1 (units: s⁻¹) is a first order rate constant and can be considered as the sum of all first order reactions with superoxide, k_2 is the second order dismutation rate (units: M⁻¹ s⁻¹) which has previously been described by Zafiriou [27].

Rearranging equation 1 above gives the following:

$$\frac{\partial[\text{O}_2^-]}{(-k_1[\text{O}_2^-] - k_2[\text{O}_2^-]^2)} = \partial t \quad (2)$$

Integrating both sides yields:

$$\int \frac{\partial[\text{O}_2^-]}{(-k_1[\text{O}_2^-] - k_2[\text{O}_2^-]^2)} = \int \partial t \quad (3a)$$

Which is equivalent to the following:

$$- \int \frac{\partial[O_2^-]}{([O_2^-](k_1 + k_2[O_2^-]))} = \int \partial t \quad (3b)$$

Which can be separated by partial fractions:

$$- \int \frac{\partial[O_2^-]}{([O_2^-]k_1)} + \int \frac{k_2 \partial[O_2^-]}{(k_1(k_1 + k_2[O_2^-]))} = \int \partial t \quad (4)$$

Using u substitution with $u = (k_1 + k_2[O_2^-])$ leads to:

$$- \frac{1}{k_1} \ln|[O_2^-]| + \frac{1}{k_1} \ln|(k_1 + k_2[O_2^-])| = t + \beta \quad (5)$$

where β is a constant, and the equation can be rearranged to give:

$$\frac{\ln|(k_1 + k_2[O_2^-])| - \ln|[O_2^-]|}{k_1} = t + \beta \quad (6)$$

$$\frac{\ln\left(\frac{k_1}{[O_2^-]} + k_2\right)}{k_1} = t + \beta \quad (7)$$

$$\ln\left(\frac{k_1}{[O_2^-]} + k_2\right) = k_1 t + \beta' \quad (8)$$

Solving at $t = 0$ for β yields:

$$\beta = \frac{k_1}{[O_2^-]_0} + k_2 \quad (9)$$

where $[O_2^-]_0$ = the initial concentration of superoxide

$$\frac{k_1}{[O_2^-]} + k_2 = \left(\frac{k_1}{[O_2^-]_0} + k_2\right) e^{k_1 t} \quad (10)$$

Thus upon rearranging equation 10 above gives a final solution for the concentration of superoxide as a function of time and the initial superoxide concentration.

$$[O_2^-] = \frac{k_1}{\left(\frac{k_1}{[O_2^-]_0} + k_2\right) e^{k_1 t} - k_2} \quad (11a)$$

Similarly if it is assumed that the MCLA response to O_2^- is linear then a sensitivity factor S can be calculated as a function of the O_2^- concentration and the count rate:

$$S = \frac{C}{[O_2^-]} \quad (12)$$

Substituting S/C for $[O_2^-]$ in equation 1 above and solving as for the case shown above then yields the following equation just in terms of the observed count rates:

$$C = \frac{k_1}{\left(\frac{k_1}{C_0} + \frac{k_2}{S}\right) e^{k_1 t} - \frac{k_2}{S}} \quad (11b)$$

Note that for the above equation when $k_2 = 0$ (no dismutation) the solution to equation 11 is the same as that for a normal first order reaction. However the equation does not collapse to solely second order when $k_1 = 0$ as then step 4 above would involve division by 0. Thus in the case of $k_1 = 0$ the normal 2nd order rate equation should be used, for practical purposes in this work this was done when $k_1 < 1 \times 10^{-4} \text{ s}^{-1}$.

In the present work we constructed a LabviewTM VI to solve both the first and second order reaction rates simultaneously.

Table S1: 2nd Order Reaction Rate Constants (M⁻¹ s⁻¹) for Metal species with O₂⁻

Species	HO ₂	O ₂ ⁻
Cu(I)	$> 1*10^9$ (a)	$\sim 1*10^{10}$ (a)
	-	$9.4\pm 0.8*10^9$ (b)
	-	$1.98\pm 0.05*10^9$ (c)
Cu(II)	$1.2*10^8$ (d)	$1.1*10^{10}$ (d)
	-	$6.63 \pm 0.71*10^8$ (c)
Fe(II)	$1.2\pm 0.5*10^6$ (e)	$7.2*10^8$ (f)
	$1.2\pm 0.2*10^6$ (g)	$1.0\pm 0.1*10^7$ (g)
Fe(III)	-	$1.8*10^8$ (g)
	$3.1*10^5$ (h)	$1.5\pm 0.2*10^8$ (i)
HO ₂	$8.3\pm 0.7*10^5$ (j)	$9.7\pm 0.6*10^7$ (j)
Cu(II)L	-	$2.9-8.1*10^8$ (k)
	-	$5\pm 3*10^7$ (l)
Fe(III)L	-	$9.3\pm 0.2*10^3$ (m)
	-	$2.3\pm 0.1*10^5$ (n)

Notes: The reader is also referred to the compilation of Bielski et al. [11]. In describing the experimental setup used in each work we use the following abbreviations: pulse radiolysis (p.r.), flash photolysis (f.p.), γ irradiation (γ -r), optical detection of superoxide (opt) and chemical detection of superoxide or equivalent (chem.). The pKa for HO₂ is 4.60 ± 0.15 [27]. All experiments are in the range 20-25° C.

(a) Cu⁺, pH 5.3, p.r. opt. [34]. (b) Cu⁺, p.r. opt. [35]. (c) Cu⁺ and Cu⁺⁺ in seawater, p.r. opt. [30]. (d) Cu²⁺ and Cu²⁺-arginine, p.r, opt.[36]. (e) Fe²⁺, pH 1, p.r, opt.[37]. (f) Fe²⁺ and Fe³⁺, p.r., opt [38]. (g) Fe²⁺ species, pH 1-7, p.r, opt [39]. (h) Fe³⁺ species, pH 2.74, p.r., opt [40]. (i) Fe(OH)²⁺ species, pH 1-7, p.r, opt [39]. (j) As summarized in Bielski et al. [11]. (k) Natural seawater with Cu complexing ligands [29]. (l) Copper complexing ligands produced by *Synechococcus* [29]. (m) Fe(III) complexed with desferrioxamine B in bicarbonate buffered solution [41]. (n) Fe(III) complexed with natural organic matter in bicarbonate buffered solution [41].

Table S2: Location of sampling stations in the Weddell Sea and Drakes Passage.

Station	Date/Time UTC	Max depth	Latitude	Longitude
Weddell Sea				
204	23.03.08 12:40	4600 m	64° 48.0 S	42° 53.2 W
216	27.03.08 21:04		63° 42.1 S	50° 50.6 W
Drake Passage				
230	03.04.08 01:20	2450 m	60° 06.0 S	55° 16.2 W
236	05.04.08 16:31	3420 m	58° 58.3 S	58° 07.9 W
249	10.04.08 19:47	4250 m	56° 07.3 S	63° 45.4 W

Table S3: Compilation of rate data from the O₂⁻ decay experiments performed in the Drake Passage.

Station	Depth (m)	^a pH _{TOT} (<i>in situ</i>)	^b pH _{TOT} (<i>lab</i>)	DTPA <i>k</i> ₂ M ⁻¹ s ⁻¹	SW <i>k</i> ₁ s ⁻¹	log <i>k</i> _{Fe}	Fe intercept M ⁻¹ s ⁻¹	R ²	log <i>k</i> _{Cu}	Cu intercept M ⁻¹ s ⁻¹	R ²
230-6	25	8.07	7.77	^c 2.00±0.02 x10 ⁵	19.3±0.4 x10 ⁻³	6.26±0.35	18±2 x10 ⁻³	0.86	7.28±0.51	14±24 x10 ⁻³	0.75
230-6	50	8.03	7.73	9.36±0.1 x10 ⁴	13.22±0.3 x10 ⁻³	6.76±0.08	7±2 x10 ⁻³	0.99	7.27±0.33	10±16 x10 ⁻³	0.87
230-6	100	8.03	7.72	7.79±0.03 x10 ⁴	35.9±0.6 x10 ⁻³	7.46±0.3	9±58 x10 ⁻³	0.89	7.83±0.38	50±64 x10 ⁻³	0.84
230-6	200	8.00	7.67	^c 2.44±0.03 x10 ⁵	33.5±0.6 x10 ⁻³	^d < 6	34±2 x10 ⁻³	0.63	7.57±0.11	31±10 x10 ⁻³	0.98
230-6	400	7.90	7.63	4.80±0.02 x10 ⁴	13.6±0.2 x10 ⁻³	7.64±0	25±88 x10 ⁻³	0.02	7.64±0.18	9±20 x10 ⁻³	0.96
230-6	1000	7.92	7.67	4.51±.06 x10 ⁴	41.1±0.5 x10 ⁻³	6.83±0.14	7±4 x10 ⁻³	0.97	7.85±0.22	50±38 x10 ⁻³	0.94
236-5	25	-	7.83	1.77±0.06 x10 ⁵	24.7±0.7 x10 ⁻³	^d < 6	25±2 x10 ⁻³	0.97	6.70±0	27x10 ⁻³	1.00
236-5	50	-	7.83	6.82±0.05 x10 ⁴	7.6± 0.1 x10 ⁻³	6.87±0.16	7±4 x10 ⁻³	0.97	6.95±0.21	6±4 x10 ⁻³	0.94
236-5	120	-	7.81	1.44±0.07 x10 ⁴	22.5±0.3 x10 ⁻³	7.43±0.2	18±20 x10 ⁻³	0.95	7.63±0.47	34±52 x10 ⁻³	0.77
236-5	250	-	7.70	7.21±0.03 x10 ⁴	37.1±0.7 x10 ⁻³	6.45±0.54	31±10 x10 ⁻³	0.72	7.79±0.24	29±38 x10 ⁻³	0.93
236-5	500	-	7.66	1.02±0.03 x10 ⁴	16.8±0.2 x10 ⁻³	6.55±0.01	15 x10 ⁻³	1.00	^d < 6	-	-
236-5	2800	-	7.68	6.64±0.04 x10 ⁴	16.6±0.2 x10 ⁻³	6.42±0.02	15 x10 ⁻³	1.00	7.35±0.1	18±6 x10 ⁻³	0.99
249-3	25	8.08	7.83	6.12±0.02 x10 ⁴	21.2±0.4 x10 ⁻³	^d < 6	30±52 x10 ⁻³	0.01	7.61±0.24	16±24 x10 ⁻³	0.93
249-3	50	8.08	7.83	4.02± 0.03 x10 ⁴	9.0 ± 0.8 x10 ⁻³	6.42±0.5	9±4 x10 ⁻³	0.76	6.92±0.07	9±2 x10 ⁻³	0.99
249-3	100	8.06	7.81	2.38± 0.02 x10 ⁴	17.5 ± 0.3 x10 ⁻³	^d < 6	18±4 x10 ⁻³	0.88	6.40±0	12±0.1 x10 ⁻³	1.00
249-3	200	8.03	7.76	4.46± 0.02 x10 ⁴	11.6 ± 0.2 x10 ⁻³	7.24±0.51	12±32 x10 ⁻³	0.74	7.30±0.16	13±8 x10 ⁻³	0.97
249-3	400	7.94	7.68	6.56± 0.02 x10 ⁴	21.2 ± 0.7 x10 ⁻³	7.79±0.39	4±96 x10 ⁻³	0.83	7.90±0.11	17±22 x10 ⁻³	0.99
249-3	2500	7.87	7.68	1.17± 0.04 x10 ⁵	12.2 ± 0.1 x10 ⁻³	^d < 6	12±2 x10 ⁻³	0.33	7.79±0.78	39±120 x10 ⁻³	0.56

Note: ^apH_{TOT} estimated using the MATLAB program CO2SYS [42], no estimates are possible for Station 236-5 due to a lack of alkalinity data. ^bpH_{TOT} as determined by measurement (±0.01) prior to superoxide addition, after superoxide addition pH_{TOT} is ~0.1 pH units higher. ^cSmall first order component also identified in this rate. ^dThe value is below the minimum detectable rate for the experimental design used (1 x 10⁶ M s⁻¹). Error estimates are for 2σ (95% confidence interval). n.d. denotes no data available as the total dissolved Cu and Fe data were not measured.

Table S4: Compilation of rate data from the O₂⁻ decay experiments performed in the Weddell Sea.

Station	Depth (m)	DTPA k_2 M ⁻¹ s ⁻¹	SW k_1 s ⁻¹
204-2	50	3.47 ± 0.04 x10 ⁴	7.3 ± 0.4 x10 ⁻³
204-2	100	3.52 ± 0.05x10 ⁴	29.7 ± 0.6 x10 ⁻³
204-2	1000	3.61 ± 0.02 x10 ⁴	36.3 ± 1.1x10 ⁻³
216-1	25	6.07 ± 0.02 x10 ⁴	74.5 ± 1.9x10 ⁻³
216-1	75	3.00 ± 0.01 x10 ⁴	3.6 ± 0.9 x10 ⁻³
216-1	100	6.37 ± 0.05 x10 ⁴	36.7 ± 1.2 x10 ⁻³
216-1	200	3.75 ± 0.02 x10 ⁴	36.5 ± 1.2 x10 ⁻³
216-1	750	8.40 ± 0.04 x10 ⁴	22.6 ± 0.6 x10 ⁻³
216-1	2000	3.46 ± 0.07 x10 ⁴	34.4 ± 0.7 x10 ⁻³

Note: Error estimates are for 2σ (95% confidence interval). No total dissolved Cu and Fe data were measured from these samples in the Weddell Sea.

Sampling Strategy: Superoxide Kinetic Reactivity

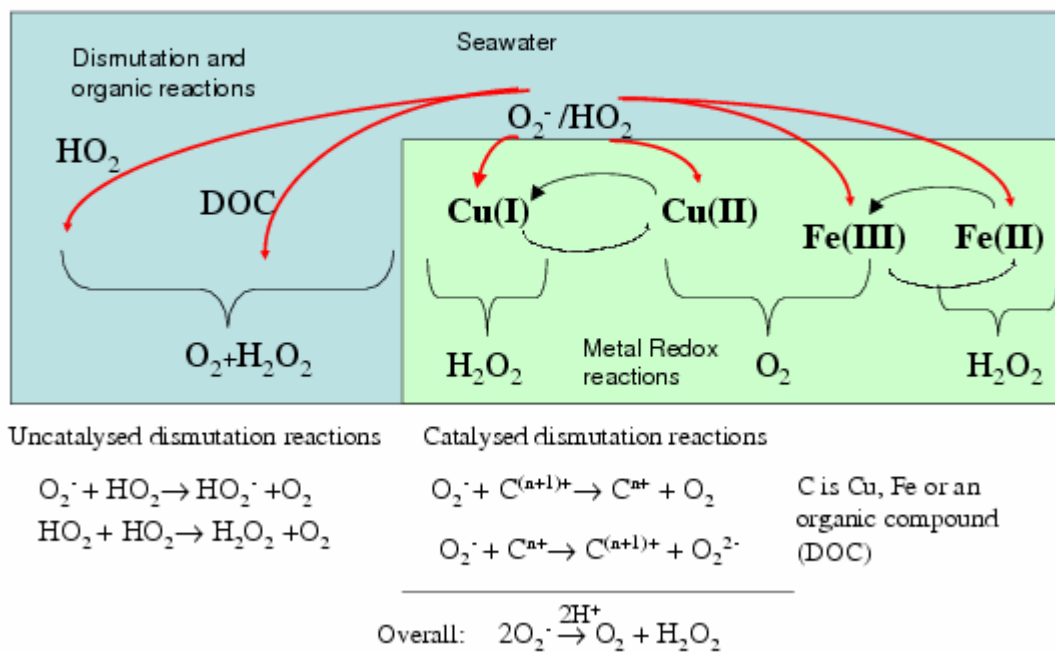


Figure S1: Sampling strategy and main reactions considered for superoxide in seawater in this work.

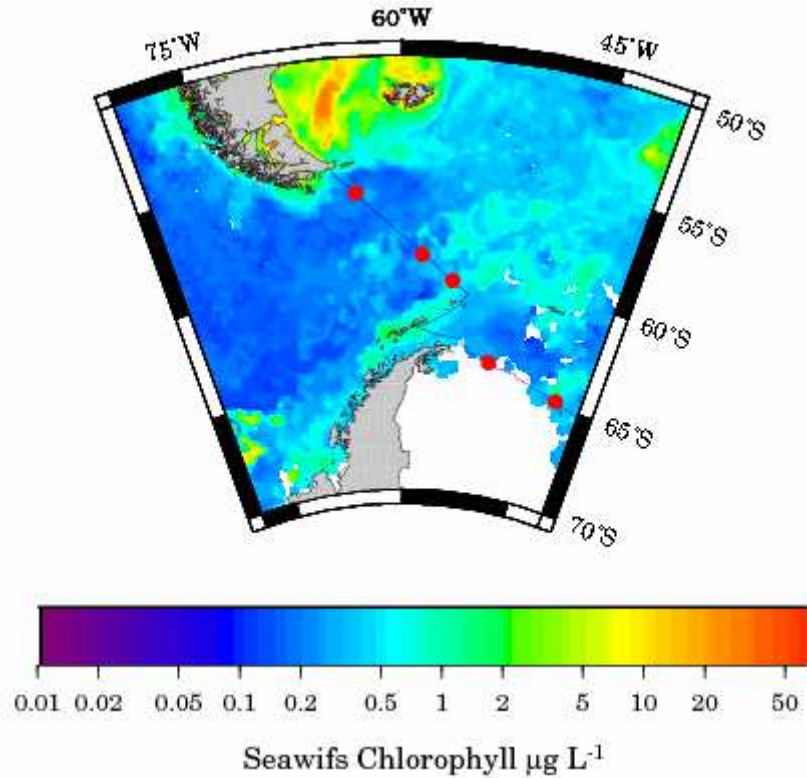


Figure S2: Satellite Chlorophyll data (monthly composite MODISAQUA) for the Weddell Sea and Drake Passage in March 2008. The cruise track (blue line) and location of Stations (red dots) in this work are also shown. Satellite Chlorophyll data was obtained from OBPG MODISAqua Monthly Global 9km Products via GIOVANNI (<http://reason.gsfc.nasa.gov/Giovanni/>) using the Ocean Color TimeSeries Online Visualization and Analysis platform. Analyses and visualizations used in this paper were produced with the Giovanni online data system, developed and maintained by the NASA Goddard Earth Sciences (GES) Data and Information Services Center (DISC). We also acknowledge the MODIS mission scientists and associated NASA personnel for the production of the data used in this research effort. All satellite images are finally displayed as postscript images using the Generic Mapping Tools (GMT) software [43].

Sampling Methodology: Superoxide Kinetic Reactivity

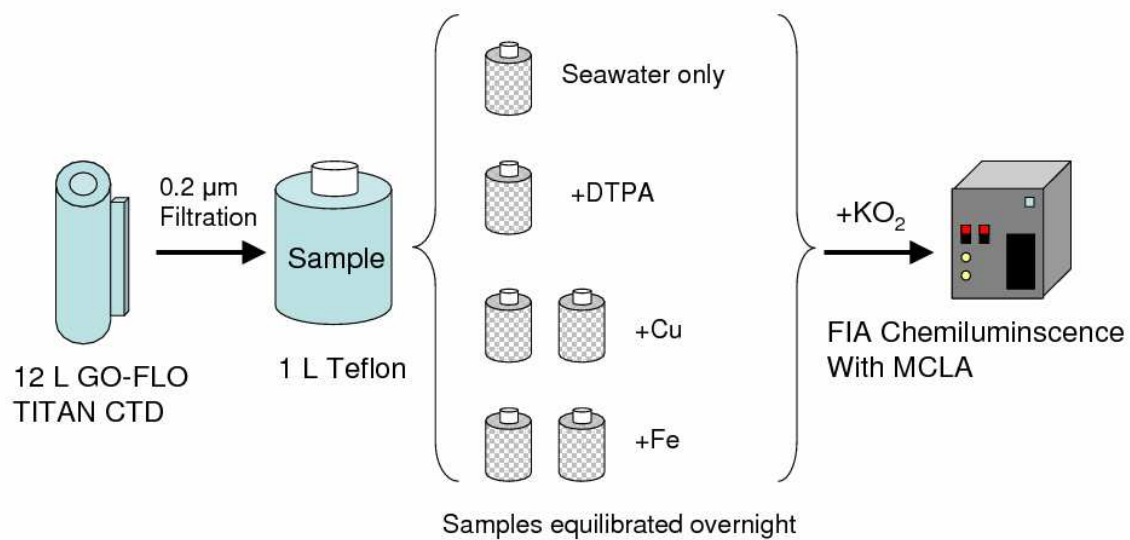


Figure S3: Description of the sampling protocol employed in this work.

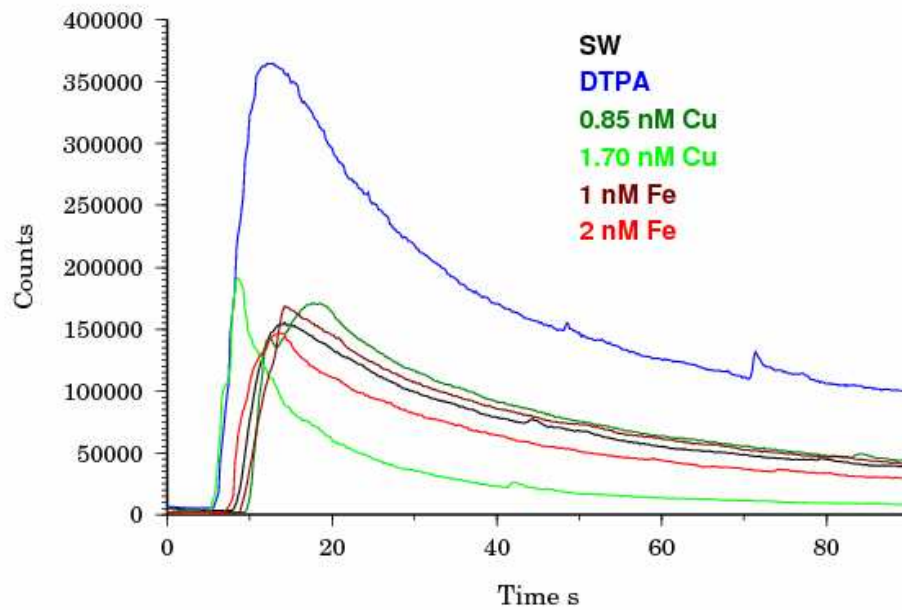


Figure S4: Example chemiluminescence output as observed in this study. The water samples are from 25 m at Station 230 in the Drake Passage.

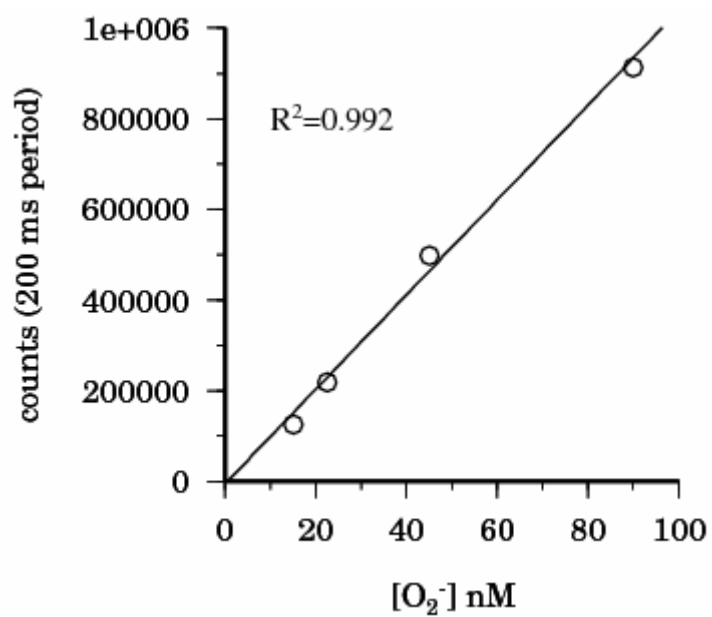


Figure S5: Calculated initial count at $t=0$ from a series of O_2^- additions (circles) to DTPA amended seawater using the conditions employed in this study. Counts were corrected for the baseline due to MCLA auto-oxidation (10,000 counts). The apparent sensitivity is then 10500 ± 500 (1σ) counts (200 ms period) nM^{-1} .

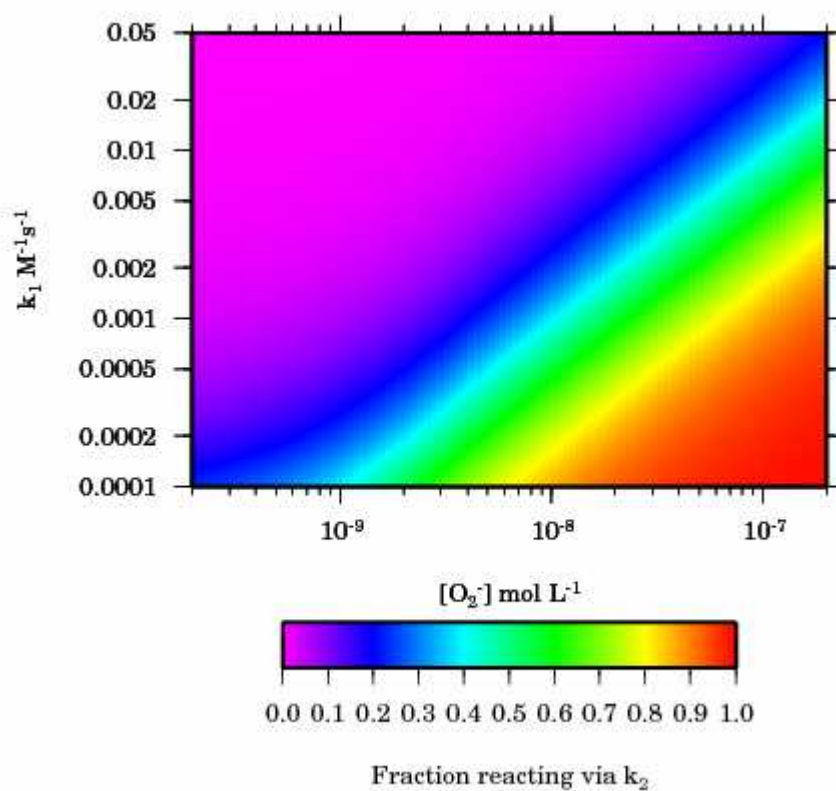


Figure S6: 2D figure showing the instantaneous fraction of superoxide reacting via the uncatalyzed dismutation reaction (k_2) as a function of the superoxide concentration and the first order catalyzed dismutation rate (k_1).

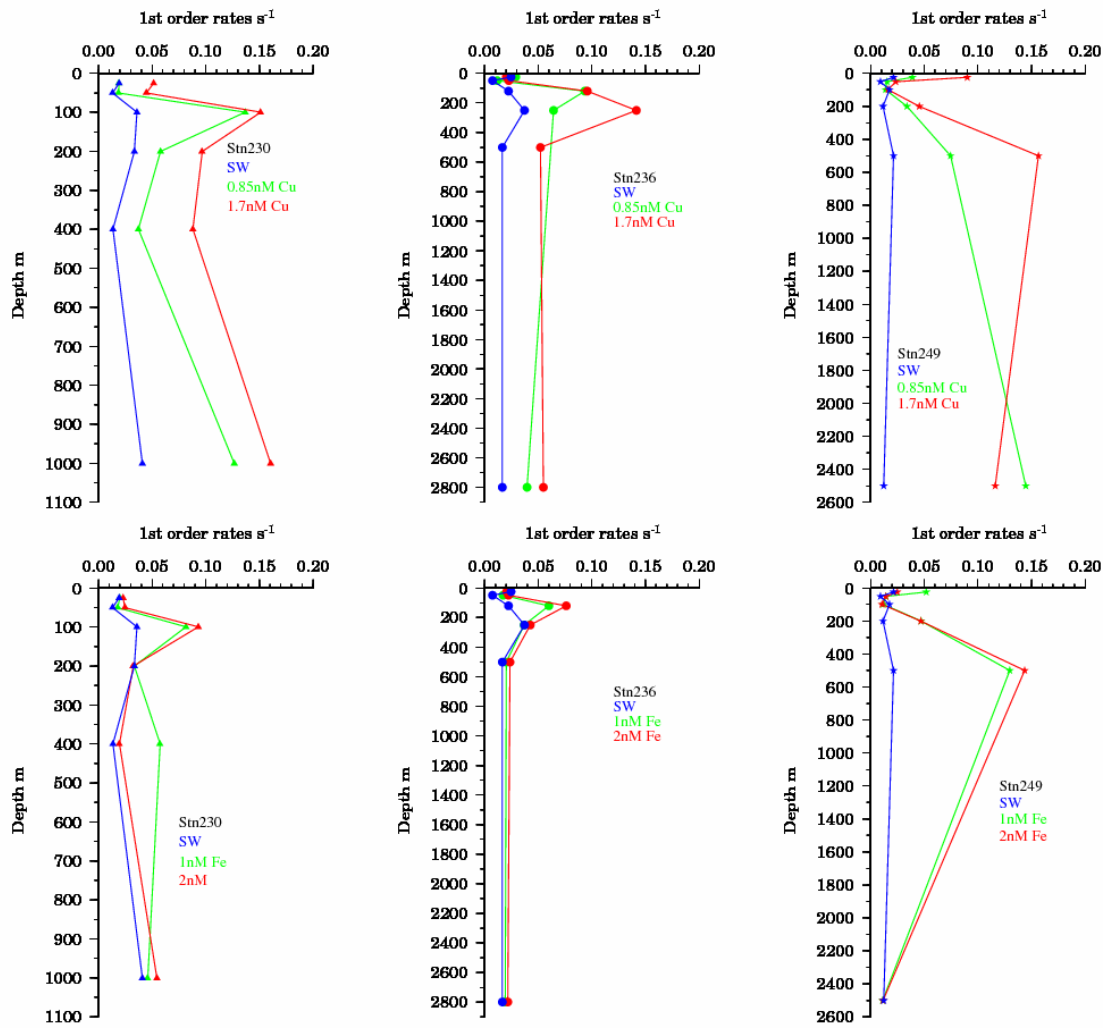


Figure S7: Drake Passage – Influence of Cu and Fe additions on the superoxide reactivity rate (k_{obs}) in seawater. (Top 3 panels) Cu additions to seawater. (Bottom 3 panels) Fe additions to seawater. Data for each station are plotted above and below each other. Values of k_{Cu} and k_{Fe} were determined by least squares linear regression of these data (Table S3).

References:

1. de Baar, H. J. W.; Timmermans, K. R.; Laan, P.; De Porto, H. H.; Ober, S.; Blom, J. J.; Bakker, M. C.; Schilling, J.; Sarthou, G.; Smit, M. G.; Klunder, M., Titan: A new facility for ultraclean sampling of trace elements and isotopes in the deep oceans in the international Geotraces program. *Marine Chemistry* **2008**, *111*, (1-2), 4-21.
2. Bruland, K. W.; Franks, R. P.; Knauer, G. A.; Martin, J. H., Sampling and analytical methods for the determination of copper, cadmium, zinc and nickel at the nanogram per liter level in seawater. *Analytica Chimica Acta* **1979**, *105*, 233-245.
3. Danielsson, L.-G.; Magnusson, B.; Westerlund, S., An improved metal extraction procedure for the determination of trace metals in sea water by atomic absorption spectrometry with electrothermal atomisation. *Analytica Chimica Acta* **1978**, *98*, 47-57.
4. Johnson, K. S.; Boyle, E.; Bruland, K.; Coale, K.; Measures, C.; Moffett, J.; Aguilar-islas, A.; Barbeau, K.; Berquist, B.; Bowie, A.; Buck, K.; Cai, Y.; Chase, Z.; Cullen, J.; Doi, T.; Elrod, V.; Fitzwater, S.; Gordon, M.; King, A.; Laan, P.; Laglera-Baquer, L.; Landing, W.; Lohan, M.; Mendez, J.; Milne, A.; Obata, H.; Ossiander, L.; Plant, J.; Sarthou, G.; Sedwick, P.; Smith, G. J.; Sohst, B.; Tanner, S.; Berg, S. v. d.; Wu, J., Developing Standards for Dissolved Iron in Seawater. *EOS, Transactions of the American Geophysical Union* **2007**, *88*, (11), 131-132.
5. Ellwood, M. J., Wintertime trace metal (Zn, Cu, Ni, Cd, Pb and Co) and nutrient distributions in the Subantarctic Zone between 40-52°S; 155-160°E. *Marine Chemistry* **2008**, *112*, (1-2), 107.
6. Sohrin, Y.; Urushihara, S.; Nakatsuka, S.; Kono, T.; Higo, E.; Minami, T.; Norisuye, K.; Umetani, S., Multielemental Determination of GEOTRACES Key Trace Metals in Seawater by ICPMS after Preconcentration Using an Ethylenediaminetriacetic Acid Chelating Resin. *Analytical Chemistry* **2008**, *80*, (16), 6267-6273.
7. Weinstein, J.; Bielski, B. H. J., Kinetics of the Interaction of HO₂ and O₂⁻ Radicals with Hydrogen Peroxide. The Haber-Weiss Reaction. *Journal of the American Chemical Society* **1979**, *101*, 58-62.
8. McDowell, M. S.; Bakac, A.; Espenson, J. H., A convenient route to superoxide ion in aqueous solution. *Inorg. Chem.* **1983**, *22*, (5), 847-848.
9. Feigenbrugel, V.; Loew, C.; Le Calve, S.; Mirabel, P., Near-UV molar absorptivities of acetone, alachlor, metolachlor, diazinon and dichlorvos in aqueous solution. *Journal Of Photochemistry And Photobiology A-Chemistry* **2005**, *174*, (1), 76-81.
10. Bennett, G. E.; Johnston, K. P., Uv-Visible Absorbency Spectroscopy Of Organic Probes In Supercritical Water. *Journal Of Physical Chemistry* **1994**, *98*, (2), 441-447.
11. Bielski, B. H. J.; Cabelli, D. E.; Arudi, R. L.; Ross, A. B., Reactivity Of HO₂/O₂⁻ Radicals In Aqueous-Solution. *Journal Of Physical And Chemical Reference Data* **1985**, *14*, (4), 1041-1100.
12. Görner, H., Oxygen uptake and involvement of superoxide radicals upon photolysis of ketones in air-saturated aqueous alcohol, formate, amine or ascorbic acid solutions. *Photochemistry And Photobiology* **2006**, *82*, (3), 801-808.
13. Görner, H., Oxygen uptake upon photolysis of 3-benzoylpyridine and 3,3'-dipyridylketone in air-saturated aqueous solution in the presence of formate, ascorbic

acid, alcohols and amines. *Journal Of Photochemistry And Photobiology A-Chemistry* **2007**, *187*, (1), 105-112.

14. Hodges, G. R.; Young, M. J.; Paul, T.; Ingold, K. U., How should xanthine oxidase-generated superoxide yields be measured? *Free Radical Biology and Medicine* **2000**, *29*, (5), 434.
15. Taylor, R. C.; Cross, P. C., Light Absorption of Aqueous Hydrogen Peroxide Solutions in the Near Ultraviolet Region. *Journal of the American Chemical Society* **1949**, *71*, (6), 2266-2268.
16. Baxendale, J. H.; Wilson, J. A., The photolysis of hydrogen peroxide at high light intensities. *Transactions of the Faraday Society* **1957**, *53*, 344-356.
17. Yuan, J.; Shiller, A. M., Determination of Subnanomolar Levels of Hydrogen Peroxide in Seawater by Reagent-Injection Chemiluminescence Detection. *Analytical Chemistry* **1999**, *71*, 1975-1980.
18. Fujimori, K.; Nakajima, H.; Akutsu, K.; Mitani, M.; Sawada, H.; Nakayama, M., Chemiluminescence Of Cypridina Luciferin Analogs .1. Effect Of pH On Rates Of Spontaneous Autoxidation Of CLA In Aqueous Buffer Solutions. *Journal Of The Chemical Society-Perkin Transactions 2* **1993**, (12), 2405-2409.
19. Fujimori, K.; Komiyama, T.; Tabata, H.; Nojima, T.; Ishiguro, K.; Sa-waki, Y.; Tatsuzawa, H.; Nakano, M., Chemiluminescence of Cypridina Luciferin Analogs. Part 3. MCLA Chemiluminescence with Singlet Oxygen Generated by the Retro-Diels-Alder Reaction of a Naphthalene Endoperoxide. *Photochemistry and Photobiology* **1998**, *68*, (2), 143-149.
20. Kambayashi, Y.; Ogino, K., REESTIMATION OF CYPRIDINA LUCIFERIN ANALOGS (MCLA) AS A CHEMILUMINESCENCE PROBE TO DETECT ACTIVE OXYGEN SPECIES-CAUTIONARY NOTE FOR USE OF MCLA. *The Journal of Toxicological Sciences* **2003**, *28*, (3), 139.
21. Cory, R. M.; Cotner, J. B.; McNeill, K., Quantifying Interactions between Singlet Oxygen and Aquatic Fulvic Acids. *Environmental Science & Technology* **2008**, *43*, (3), 718-723.
22. Rose, A. L.; Moffett, J. W.; Waite, T. D., Determination of Superoxide in Seawater Using 2-Methyl-6-(4-methoxyphenyl)-3,7-dihydroimidazo[1,2-a]pyrazin-3(7H)-one Chemiluminescence. *Anal. Chem.* **2008**, *80*, (4), 1215-1227.
23. Zheng, J.; Springston, S. R.; Weinstein-Lloyd, J., Quantitative analysis of hydroperoxyl radical using flow injection analysis with chemiluminescence detection. *Analytical Chemistry* **2003**, *75*, (17), 4696-4700.
24. Mitani, M.; Yokoyama, Y.; Ichikawa, S.; Sawada, H.; Matsumoto, T.; Fujimori, K.; Kosugi, M., Determination Of Horseradish-Peroxidase Concentration Using The Chemiluminescence Of Cypridina Luciferin Analog, 2-Methyl-6-(P-Methoxyphenyl)-3,7-Dihydroimidazo[1,2-A]Pyrazin-3-One. *Journal Of Bioluminescence And Chemiluminescence* **1994**, *9*, (6), 355-361.
25. Akutsu, K.; Nakajima, H.; Katoh, T.; Kino, S.; Fujimori, K., Chemiluminescence Of Cipridina Luciferin Analogs .2. Kinetic-Studies On The Reaction Of 2-Methyl-6-Phenylimidazo[1,2-A]Pyrazin-3(7h)-One (Cla) With Superoxide - Hydroperoxyl Radical Is An Actual Active Species Used To Initiate The Reaction. *Journal Of The Chemical Society-Perkin Transactions 2* **1995**, (8), 1699-1706.
26. Gotoh, N.; Niki, E., Rate Of Spin-Trapping Of Superoxide As Studied By Chemiluminescence. *Chemistry Letters* **1990**, (8), 1475-1478.

27. Zafiriou, O. C., Chemistry of superoxide ion (O_2^-) in seawater. I. pK_{asw}^* (HOO) and uncatalysed dismutation kinetics studied by pulse radiolysis. *Marine Chemistry* **1990**, *30*, 31-43.
28. Voelker, B. M.; Sedlak, D. L., Iron reduction by photoproduced superoxide in seawater. *Marine Chemistry* **1995**, *50*, 93-102.
29. Voelker, B. M.; Sedlak, D. L.; Zafiriou, O. C., Chemistry of Superoxide Radical in Seawater: Reactions with Organic Cu Complexes. *Environmental Science and Technology* **2000**, *34*, 1036-1042.
30. Zafiriou, O. C.; Voelker, B. M.; Sedlak, D. L., Chemistry of the superoxide radical (O_2^-) in seawater: Reactions with inorganic copper complexes. *Journal of Physical Chemistry A* **1998**, *102*, (28), 5693-5700.
31. Dickson, A. G., pH buffers for sea water media based on the total hydrogen ion concentration scale. *Deep Sea Research Part I: Oceanographic Research Papers* **1993**, *40*, (1), 107-118.
32. Millero, F. J.; Zhang, J. Z.; Fiol, S.; Sotolongo, S.; Roy, R. N.; Lee, K.; Mane, S., The Use of Buffers to Measure the pH of Seawater. *Marine Chemistry* **1993**, *44*, (2-4), 143-152.
33. Croot, P. L.; Laan, P.; Nishioka, J.; Strass, V.; Cisewski, B.; Boye, M.; Timmermans, K.; Bellerby, R.; Goldson, L.; de Baar, H. J. W., Spatial and Temporal distribution of Fe(II) and H_2O_2 during EISENEX, an open ocean mesoscale iron enrichment. *Marine Chemistry* **2005**, *95*, 65-88.
34. Rabani, J.; Klug-Roth, D.; Lilie, J., Pulse radiolytic investigations of the catalyzed disproportionation of peroxy radicals. Aqueous cupric ions. *The Journal of Physical Chemistry* **1973**, *77*, (9), 1169-1175.
35. Piechowski von, M.; Nauser, T.; Hoigné, J.; Bühler, R., O_2^- decay catalyzed by Cu^{2+} and Cu^+ ions in aqueous solutions: a pulse radiolysis study for atmospheric chemistry. *Ber. Bunsenges. Phys. Chem.* **1993**, *6*, 762-771.
36. Cabelli, D. E.; Bielski, B. H. J.; Holcman, J., Interaction between Copper(II)-Arginine Complexes and HO_2/O_2^- Radicals, a Pulse Radiolysis Study. *Journal of the American Chemical Society* **1987**, *109*, 3665-3669.
37. Jayson, G. G.; Parsons, B. J.; Swallow, A. J., Oxidation Of Ferrous Ions By Perhydroxyl Radicals. *Journal Of The Chemical Society-Faraday Transactions I* **1973**, *69*, (1), 236-242.
38. Matthews, R. W., The radiation chemistry of aqueous ferrous sulfate solutions at natural pH. *Australian Journal of Chemistry* **1983**, *36*, 1305-1317.
39. Rush, J. D.; Bielski, B. H. J., Pulse Radiolytic Studies of HO_2/O_2^- with Fe(II)/Fe(III) Ions. The reactivity of HO_2/O_2^- with Ferric Ions and Its Implication on the Occurrence of the Haber-Weiss Reaction. *Journal of Physical Chemistry* **1985**, *89*, 5062-5066.
40. Sehested, K.; Bjergbakke, E.; Rasmussen, O. L.; Fricke, H., Reactions of H_2O_3 in the Pulse γ -Irradiated Fe(II)- O_2 System. *The Journal of Chemical Physics* **1969**, *51*, (8), 3159-3166.
41. Rose, A. L.; Waite, T. D., Reduction of organically complexed ferric iron by superoxide in a simulated natural water. *Environmental Science & Technology* **2005**, *39*, (8), 2645-2650.
42. van Heuven, S.; Pierrot, D.; Lewis, E.; .., D. W. R. W. *CO2SYS_calc_MATLAB: MATLAB Program Developed for CO2 System Calculations*, ORNL/CDIAC-105b. ; Carbon Dioxide Information Analysis Center, Oak Ridge National Laboratory, U.S. Department of Energy, Oak Ridge, Tennessee. : 2009.

43. Wessel, P.; Smith, W. H. F., New improved version of the Generic Mapping Tools released. *EOS Trans. AGU* **1998**, 79, 579.

Redox effects of superoxide in polar waters

The oceans constitute 70% of the surface area of the biosphere, and the fertility of the sea's "soil" depends in large part on the micro-nutrients available therein: dissolved organic matter, metal ions, and the like. Light, which arrives on a regular schedule frequently interrupted by weather, serves as a macro-nutrient for photosynthesis, but it also has other effects—its reaction with colored dissolved organic matter, for example, generates superoxide (O_2^-) in the sea as deep as the sun can penetrate. As Peter Croot and Maija Heller of the Leibniz Institute of Marine Sciences (Germany) show in a recent

ES&T paper (2009, DOI 10.1021/es901766r), the fate of superoxide is intimately connected to the oxidation state (and thus the bio-availability) of dissolved metal ions in Antarctica's surrounding Southern Ocean—and in some surprising ways.

The effects of superoxide in ocean-like environments have been studied in detail in the laboratory, but available field data are sparse. This new study "takes maximal advantage of prior work to design and implement a fairly complex experimental design," says Oliver Zafiriou of the Woods Hole Oceanographic Institution.

Seawater was collected at a variety of depths throughout the voyage of the German research vessel *Polarstern* (as a contribution to the International Polar Year GEOTRACES program) through the Weddell Sea and into the Drake Passage. Concentrations of Cu and Fe were determined, giving a depth profile of the dissolved metal ions. Then, decomposition kinetics of added superoxide were analyzed on-ship through a well-characterized

chemiluminescent reaction with the reagent MCLA. By comparing the decay kinetics of superoxide in control seawater with samples "spiked" with Fe, Cu, or the metal chelator DTPA (which, by experimental design, binds metal ions to prevent their reaction with su-

peroxide) is important when their data are compared with data acquired by otherwise very similar experimental methods.

"An important question that this study raises—but does not fully answer—is whether Cu reactions compete with and minimize

Fe reduction to more bio-available forms in the surface ocean," says Zafiriou.

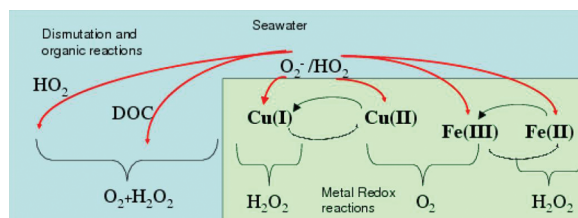
"The fate of the superoxide itself is not as important as its role as a redox agent," agrees Croot. Iron cycles between Fe(II) and Fe(III), and copper cycles between Cu(I) and Cu(II). "These chemical species have very different bioavailabilities and reactivities—and in the

case of Fe, solubilities."

Croot and Heller apply "oceanographic consistency" throughout their discussion of the kinetic data. In chemical oceanography, open ocean water column data should be "smooth and readily related to species with similar chemistries or processes," says Croot. "In this way, it provides a check on whether the data you have are 'consistent' with the processes we know occur in the ocean—including vertical mixing, light penetration, metal complexation, and O_2 or H_2O_2 concentrations, for instance." These internal checks for self-consistency bolster the wealth of new field data that the study provides.

"The Southern Ocean is of considerable interest as a focus of conservation of marine biota, as well as a site where we expect climate change to impact first," says Gustaaf Hallegraeff of the University of Tasmania (Australia). "This work raises new ideas about the bioavailability of Fe, linked to little-studied Cu, in relation to superoxide decay kinetics."

—STEVEN C. POWELL



Superoxide produced in seawater by sunlight has important effects on the redox state—and thus the solubility and bioavailability—of Cu and Fe ions and their complexes.

peroxide), Croot and Heller were able to assess the importance of various contributors to the decomposition of superoxide.

"We went back to using an older source of superoxide, solid KO_2 ," which hadn't been used for years because of a belief that it was contaminated with trace metals, Croot explains. "However, we found that commercial KO_2 supplies were now clean enough for this work—and most importantly without the use of a chelating agent, such as DTPA, in the superoxide source."

Despite being strongly organically complexed in the open ocean, "Cu was apparently the major sink" for superoxide, says Croot. "Fe was a minor sink, and somewhat surprisingly, given earlier coastal work, reactions with organic matter were almost non-existent."

A noteworthy experimental variation was a designated incubation time for DTPA. On the basis of an earlier publication and their own observations, Croot and Heller specifically equilibrated DTPA with seawater samples for a minimum of 12 hours. This re-

Conclusions and Future Outlook

Conclusions and future outlook

The importance of photochemically formed ROS to the biogeochemical and biological processes in the open ocean is now clear but we still have only a poor understanding of the exact mechanisms and critically the rates and fluxes of these compounds. As both superoxide (O_2^-) and hydrogen peroxide (H_2O_2) can act as oxidants and reductants with trace metals they have an important influence on trace metal redox cycling. Presently we have only a little information on the formation rates of O_2^- and H_2O_2 from direct photochemical production in the ocean and their relative reactivity with different metal or organic species present in seawater. This study emphasises the important role of O_2^- in mediating redox changes between various chemical species and in particular with the bio-relevant trace metals Fe and Cu. Typically reactions with metal species of Cu and Fe are extremely fast and only a small amount of metal is required to catalyse O_2^- dismutation.

The initial ideas for this thesis were based on the then available literature regarding the sources and detection methods for O_2^- . However at the beginning of experimental work to setup a detection system for O_2^- in our laboratory, it became soon clear that the previous published methods had either overlooked or ignored problematic issues concerning the production and detection of O_2^- . Due to this reason it became necessary to develop a new detection system using a reliable source of O_2^- , KO_2 , which had been not used for a long time due to supposed trace metal impurities. However we were able to confirm in test analysis that this impurities in modern commercial KO_2 were actually minimal. This source is because of its simplicity free from many of the side effects which are found for example in the enzymatic production of O_2 . A general problem with O_2^- detection systems at the pH of natural water or seawater is the production of hydrogen peroxide which interferes in the detection of O_2^- . H_2O_2 is either produced direct by the O_2^- producing system or it is formed by the uncatalysed dismutation reaction of O_2^- to H_2O_2 and O_2 .

However in ongoing research work we found after an extensive search in the available literature a further source of O_2^- which produces the radical species through thermal decomposition of an azo compound (SOTS-1). This thermal decomposition, which produces superoxide at a relatively low but constant rate, could be successfully tested in seawater. The thermal decomposition of SOTS-1 was evaluated over a range of seawater temperatures using both a flux based detection scheme developed using two spectrophotometric methods or a concentration based detection scheme using a chemiluminescence flow injection system. In this work it is demonstrated that through the development of the appropriate mathematical derivations and theory coupled with the use of SOTS-1 as an O_2^- source that analytical

detection systems for O_2^- can be calibrated for use in seawater to determine both concentrations and fluxes.

For the field expeditions involved in this work different sampling strategies were developed to follow superoxide decay kinetics in either the tropical waters of the North Eastern Atlantic or the Southern Ocean. In the experiments which were conducted close to the Cape Verdean island the focus was also directed on the ability of O_2^- to play a role in dust dissolution processes. The solubility of iron in seawater has important implications for the formation of colloidal and particulate iron and on the bioavailability of iron to phytoplankton. Presently there is little information available on the influence of superoxide on the solubility of iron in seawater. However this process has been suggested to influence the dissolution of dust, iron rich nano-particles and colloids, but no direct assessment has yet been made. Our method described in this thesis allows an assessment of changes in both the organic reactivity with superoxide simultaneously with changes in the free metal speciation of iron and/or copper. This is an important breakthrough as it allows the evaluation of the importance of the different reaction pathways for superoxide and thus the factors which control metal redox speciation in seawater. Through this approach we can ascertain rapidly whether dust dissolution has altered the *in situ* iron speciation in seawater. Furthermore our results indicate that while ligand promoted and thermal dissolution appeared to be clearly important, our experiments in natural waters were highly variable and most of this variability was apparently related to dynamic factors associated with changes in surface seawater chemistry occurring over both spatial and temporal scales. Key amongst these factors is most likely the abundance of colloidal metal species and ligands.

Coloured dissolved organic matter (CDOM) is the main light absorbing substance in the ocean and represents an important chromophore in the UV region. CDOM plays an important role in light availability for primary productivity and for photochemical reactions where it is critical to the production of free radical species. The reaction of O_2^- with organic material, which was previously proposed to be an important reaction pathway in coastal waters, I found in the Open Ocean waters close to Cape Verde to be a small but significant reaction pathway. Similarly in the Southern Ocean the reaction with organic material could only be detected in a few samples close to the Antarctic Peninsula indicating that this reaction in Polar waters is a minor pathway. Thus under metal free conditions the uncatalysed dismutation reaction would form here the major sink of superoxide.

However both of these sinks are not relevant when trace metals, like iron or copper are present. In both study regions, the Southern Ocean and the North Eastern Tropical Atlantic,

the reaction with copper was the dominant sink for O_2^- . The results obtained in polar waters strongly indicate that superoxide reacts directly with organic complexes of copper as the estimated concentration of free copper present, based on voltammetric measurements, is insufficient to be the source of the fast reaction rates observed experimentally. Similarly in tropical waters when seawater was titrated with Cu, the rates were often found to be too quick for the analytical system to measure. There was also a significant reaction between Fe and O_2^- but at reduced rates compared to Cu and the results from my polar study showed that Fe in these waters was strongly complexed by organic ligands and inert to O_2^- .

A clear opportunity for future work is in the application, to *in situ* field measurements of the fluxes of O_2^- in the water column, of the analytical detection system for O_2^- using the superoxide thermal source SOTS-1 described in this thesis. This is the logical next step to pursue in this work and was the reason this work was undertaken. However as it took the duration of this thesis to develop this method there was unfortunately no more opportunities in the field to test it.

The solubility of iron in seawater is an important parameter in determining the formation of colloidal and particulate Fe and in turn in controlling the bioavailability of Fe, a key essential nutrient for phytoplankton growth. Clearly more work is needed to examine iron solubility under ambient conditions. However as iron has a low solubility in seawater, in the absence of organic binding ligands this could be as low as 20 pmol L^{-1} , present analytical methods are not sensitive enough for the accuracy and precision that is required. Only by using radioactive isotopes do we have a significantly low enough detection limit for determining soluble iron, and more measurements are urgently needed. A challenging aspect of this is to try and combine radioisotopes with dust dissolution experiments similar to those conducted during the present thesis. The problem here is to design an experiment so that the radioisotope can be in equilibrium with the cold iron in the dust or perhaps more simply look at the rate of exchange between solution and dust. These experiments could be combined with the superoxide approach developed here but on a larger scale with more frequent sampling. Thus future work at Cape Verde should be planned around these types of experiments.

The redox active fraction of CDOM, which can easily exchange electrons, has been attributed to quinone moieties. Quinones can shuttle between different redox states involving rapid reactions with O_2^- thus creating a potential catalytic cycle for the decay of superoxide. The second manuscript of this thesis presents the first study we are aware of in the open ocean which focused on the relationship between CDOM and the organic reactions with superoxide in seawater and further laboratory work on this certainly would help to improve the

understanding of this processes which is potentially important for the cycling and oxidation of organic matter.

The question of whether other metals react with O_2^- is still open, and the most likely candidate is Manganese (Mn). Mn is a key metal for photosynthesis due to its unique role in photosystem II and it is also used in further redox enzymes like superoxide dismutase. Photochemical processes are of critical importance to both H_2O_2 formation and Mn redox cycling and there exists a strong solar driven diel cycle for both H_2O_2 and Mn^{2+} . Additional diel cycles in the biomass and cell division of pico-phytoplankton and bacterial may create further diel effects relating to Mn adsorption due to changes in particle numbers and surface areas. Thus Mn redox chemistry should be examined in detail to completely understand what controls the lifetime of O_2^- in seawater.

The field work of this thesis was conducted in the North East Atlantic Ocean and the Southern Ocean and there I found different reaction kinetics for O_2^- in these diverse water masses. Up to now only a few field studies for O_2^- chemistry have been conducted in coastal areas and the Pacific Ocean and broader studies will surely help to clarify the key pathways for superoxide production and loss in seawater. This thesis utilized a suite of different reaction conditions and sampling strategies in order to elucidate O_2^- reactions in seawater. This new approach has already borne fruit in studies on the speciation and biogeochemical cycling of the important trace metals Fe and Cu and should be developed further.

Acknowledgements

I would like to thank Dr. Peter Croot for all his knowledge and help in handling and interpreting the data obtained in this thesis and his indefatigable motivation to understand environmental processes in all their detail. Also I would like to thank him for helping me make my first (and maybe single) trip to the Antarctica possible, which I always will remember as something fascinating and wonderful.

I also would like to thank Prof. Dr. Arne Körtzinger and Prof. Dr. Douglas W. R. Wallace who made it possible for me to work in the SOPRAN project in the Cape Verde archipelago which was a great opportunity to learn about the combination of cultural and scientific issues which must be considered if work is planned to be done at a environmental interesting but up to now, for science, not fully accessible area. At this I also want to thank Ivanice Monteiro and especially Pericles Silva, our direct cooperation colleagues at the INDP in Cape Verde, for all their kind help to organize the logistics, their help with the seawater sampling and their experimental work for the expeditions, which made science there finally successful.

Furthermore I want to say thanks to Wiebke who always was a nice and very dependable partner in planning and conducting several field expeditions. Further thanks goes to both K's in our laboratory, Katrin and Kathrin, who also were nice working partners and I especially thank Kathrin here for her quick understanding what needs to be done next during our common work. For the support and the useful comments with all kinds of computer and writing problems I would like to mention Tini, but these are only two out of a lot of examples which made her help so special as she also was great to discuss things with. The analytical support and advice from Peter Streu was a big help in interpreting the results gathered in this work. A further gratitude goes to the FB2-CH as it is a nice and interesting set of people to work together with in Kiel and during the field expeditions and also it was always fun to do things with members of this group outside of work.

Last but not least I would like to thank my friends and family who always supported and tried to accompany me during my PhD journey and reminded me frequently to work on something they believed to fit to my interests.

Eidesstattliche Versicherung

Ich versichere an Eides statt, dass ich die von mir vorgelegte Dissertation – abgesehen von der Beratung durch meinen Betreuer – selbstständig und ohne unerlaubte Hilfe angefertigt habe und alle benutzten Quellen und Hilfsmittel vollständig angegeben habe. Die Zusammenarbeit mit anderen Wissenschaftlern habe ich kenntlich gemacht. Die Arbeit ist unter Einhaltung der Regeln guter wissenschaftlicher Praxis der Deutschen Forschungsgemeinschaft entstanden. Ferner habe ich weder diese noch eine ähnliche Arbeit an einer anderen Abteilung oder Hochschule im Rahmen eines Prüfungsverfahrens vorgelegt, veröffentlicht oder zur Veröffentlichung vorgelegt.

Kiel, 17.Dezember, 2009

(Maija Heller)

WISSENSCHAFTLICHER WERDEGANG

Maija Heller

Geboren am 26.11.1980 in Erlangen

Staatsangehörigkeit: deutsch

2000	Abitur, Hardenberg Gymnasium, Fürth
2000-2006	Studium der Chemie an der Bayerischen Julius-Maximilians-Universität, Würzburg
April 2006	Diplom in Chemie
Mai-Aug. 2006	Forschungsaufenthalt an der Bayerischen Julius-Maximilians-Universität, Würzburg
Aug.-Dez.2006	Wissenschaftliche Angestellte, Meereschemie, Leibniz-Institut für Meereswissenschaften, Kiel
Ab Jan.2007	Promotionsstudium im Fachbereich Marine Biogeochemie am Leibniz-Institut für Meereswissenschaften, Kiel, Betreuer: Prof. Dr. Douglas W.R. Wallace, Dr. Peter Croot
10.12.-11.12.2007	Teilnahme am TRACES Workshop (PIK, Potsdam)
18.01-04.02.2007	Teilnahme an der METEOR Expedition 71/3 in das östliche Mittelmeer
26.02.-02.03.2007	Erfolgreiche Teilnahme an einem Strahlenschutzkurs mit den Inhalten der Module GH und OG
09.07.-23.07.2007	Feldexpedition auf die Kap Verdischen Inseln (Mindelo, Sao Vicente)
19.08.-24.08.2007	Teilnahme and der Goldschmidt Konferenz (Köln)
10.09.-11.09.2007	Teilnahme an einem GOTM Modellierungskurs
20.10.-03.11.2007	Teilnahme an der SOLAS Summer School (Cargese, Korsika, Frankreich)
06.01.-10.01.2008	Gebrauchsunterweisung und Übernahme von 2 MITESS (M oored I n-situ T race E lement S erial S ampler) Geräten zur Wasserprobennahme (MIT, Boston, USA) und Besuch der Woods Hole Oceanographic Institution
03.02.-01.05.2008	Teilnahme an der IPY-GEOTRACES Polarstern Expedition, ANTXXIV-3
01.07.-04.08.2008	Feldexpedition auf die Kap Verdischen Inseln (Mindelo, Sao Vicente)
06.11.-24.11.2008	Feldexpedition auf die Kap Verdischen Inseln (Mindelo, Sao Vicente)

- 22.02.-25.02.2009 Teilnahme am wissenschaftlichem EU COST 735 Workshop „Iron solubility“ (University of East Anglia, Norwich, UK)
- 14.05.-01.6.2009 Feldexpedition auf die Kap Verdischen Inseln (Mindelo, Sao Vicente)
- Oct.2009 The Publikation “Superoxide decay Kinetics in the Southern Ocean” (ES&T, 2010, 44, 191–196) wird als Sonderartikel ausgewählt
- 15.11.-19.11.2009 Teilnahme and der SOLAS Open Science Conference (Barcelona, Spanien)
- 01.02.-02.02.2010 co Organisation des EU COST 735 Workshops “Iron Bioavailability in the Surface Ocean” (IFM-GEOMAR, Kiel, Germany)
- 20.02.-28.02.2010 Teilnahme an dem Ocean Science Meeting 2010 (Portland, Oregon, USA)
- März 2010 Die Publikation “Application of a Superoxide (O_2^-) thermal source (SOTS-1) for the determination and calibration of O_2^- fluxes in seawater” (Analytica Chimica Acta, 667 (2010) 1–13) wird als Sonderartikel ausgewählt
- 07.04.-17.05.2010 Teilnahme an der OCEANET Polarstern Expedition ANTXXVI-4

Publikationen:

- Heller, M.I. and Croot, P.L., 2009d. Superoxide decay as a probe for speciation changes during dust dissolution in Tropical Atlantic surface waters near Cape Verde. Submitted to: Marine Chemistry.
- Heller, M.I. and Croot, P.L., 2009c. The kinetics of Superoxide reactions with dissolved organic matter in Tropical Atlantic surface waters near Cape Verde (TENATSO). Revised submitted to: Journal of Geophysical Research – Oceans.
- Heller, M.I. and Croot, P.L., 2009b. Application of a Superoxide (O_2^-) thermal source (SOTS-1) for the determination and calibration of O_2^- fluxes in seawater. Analytica Chimica Acta 667 (2010) 1–13.
- Heller, M.I. and Croot, P.L., 2009a. Superoxide Decay Kinetics in the Southern Ocean. Environ. Sci. Technol. 2010, 44, 191–196.
- Schmuck, C. and Heller, M., 2007. Solid phase synthesis of a new biomimetic receptor for anionic carbohydrates. Org. Biomol. Chem. 2007, 5, 787-791.